A SIMPLIFIED PROCEDURE FOR ASSESSING FAILURE PROBABILITIES OF REINFORCED CONCRETE FRAME BUILDINGS UNDER EARTHQUAKE LOADING

A thesis

submitted in partial fulfilment

of the requirements

for the Degree of

Doctor of Philosophy in Civil Engineering

at the

University of Canterbury

New Zealand

BY

SACHIO OGAWA

1988

ABSTRACT

The thesis argues the need for a more rational structural code, and as a major step in its attainment describes the development of a simplified technique for assessing the probability of failure of structures due to earthquake effects.

Previous approaches to the development of a rational code are discussed critically and their limitations are described. A major problem is shown to be the difficulty of assessing failure probabilities for complete structures, even using the simplified First-Order Second-Moment approach. The difficulty is illustrated by applying the First-Order Second-Moment method to a simple portal frame structure.

A consistent approach to the analysis of seismic failure probabilities of complete structures is then developed. Cumulative plastic strain energy is used as an overall damage measure, with an interstorey drift limit as a failure criterion. The relationship of the two is established using three separate analyses for estimating:

(1) the total cumulative plastic strain energy absorbed by an entire structure;

(2) the proportion of total energy absorbed by each storey; and

(3) the maximum interstorey drift induced by the energy in each storey.

Finally, a First-Order Second-Moment approach is used for obtaining probabilities of failure. The technique is developed in detail only for reinforced concrete frame structures, though the approach is more universally applicable.

The analysis is relatively complex, but it nevertheless involves a number of simplifying assumptions. These are discussed, and are also the subject of sensitivity analyses.

The analysis is applied to various trial structures. It is tentatively concluded that the seismic reliability implied by New Zealand codes is a little low, compared with results obtained elsewhere.

ACKNOWLEDGEMENTS

The research reported herein was carried out in the Department of Civil Engineering, University of Canterbury, under the overall guidance of its head, Professor R. Park.

I wish to acknowledge the great debt of gratitude I owe to Professor D.G. Elms for first suggesting this topic, and for his encouragement, guidance and help during the investigation, and in many other facets of my stay in Christchurch.

Special thanks are due to Professor T. Paulay for his tireless assistance and many helpful and lively discussions.

I wish to take this opportunity to express my appreciation for the assistance given by Shimizu Corporation, Tokyo, Japan. In particular, my special acknowledgements are given to Mr S. Honjyo, Mr T. Kuroda and Mr M. Takeda (Nuclear Power Department), Mr H. Matsuzawa, Mr S. Katayama and Mr M. Sakamoto (Training and Career Development Department), Dr T. Ohta and Mr S. Suzuki (Educational Committee for Overseas Study), Dr Y. Inada (Research Institute) and Mr K. Saida (STH Project).

The generous financial support provided by the Building Research Association of New Zealand is gratefully

acknowledged. Grateful acknowledgement is also made of the information given to me by Mr R.G. Wilkinson and Mr B. O'Toole of Holmes Consulting Group.

I wish to acknowledge the continuous help by Professor S. Kokusho, Tokyo Institute of Technology since I graduated from the Institute.

My thanks are extended to Japanese Professors and friends who shared wonderful times in Christchurch with my family.

I also wish to register my gratitude to Miss L.K. Anderson for typing the manuscript, Mrs V.J. Grey for her draughting work and Miss R. Groom for typing the Tables.

Lastly, my special thanks to my wife, Masako, my daughter, Ina, and also to our parents in Tokyo for their endless support, understanding and encouragement throughout the year.

TABLE OF CONTENTS

NOTATION

Unless stated otherwise in the text, definitions of the notations used in the thesis are as follows:

C = coefficient for connecting resistance damage energy E_R with the static monotonic plastic strain energy $E_{R(static)}$

$[C]$ = damping matrix

C_d = base shear coefficient ($=C_{d_1}$)

C_{d_i} = the ratio of yield shear strength V_{y_i} for the ith storey to weight sustained by the ith storey ($= V_{y_i} / \sum_{j=i}^{n} w_j$; where n = total number of storeys)

E_D = cumulative energy consumed by the damping mechanism

$E_{d_{(i)}}$ = cumulative plastic strain energy or simply damage energy (absorbed by the ith storey)

E_{d_T} = total cumulative plastic strain energy absorbed by a whole structure

E_{d_T}/w_t = standard damage energy (mm)

$E_{E_{(i)}}$ = cumulative elastic strain energy (absorbed by ith storey)

$E_{e_{(i)}}$ = maximum elastic strain energy ($=\frac{1}{2}V_y\delta_y$) (for ith storey)

E_K = kinetic energy when an earthquake motion vanishes

$E_{R_{(i)}}$ = resistance damage energy (for ith storey)

E_T = total energy input by an earthquake ($=E_K+E_D+E_E+E_d$)

E_{T_j} = total energy for jth mode of a M.D.O.F. system

$^eE_{d_{(i)}}$ = damage energy approximated by an elastic analysis (absorbed by ith storey)

$_{e}E_{d_T}$ = total damage energy approximated by an elastic analysis ($=\sum_{i=1}^{n} {}_{e}E_{d_i}$; where n = total number of storeys)

$_{s}E_{d_j}$ = cumulative plastic strain energy absorbed by S.D.O.F. system with unit mass corresponding to the jth mode of a M.D.O.F. system

$_{s}E_{T_j}$ = total energy absorbed by a S.D.O.F. system with unit mass corresponding to the jth mode of a M.D.O.F. system

F_e = effective dynamic force

F_y = yield force of a spring (kN)

$G_r(\omega)$ = response spectral-density function

g = acceleration of gravity (=9810 mm/sec^2)

$g_{(i)}$ = performance function (for ith storey)

$H(\Omega_k)$ = frequency response function for a circular frequency Ω_k

h = critical damping ratio

$k_e(t)$ = effective dynamic stiffness

$k_{(i)}$ = initial stiffness (of ith storey) (kN/mm)

$[K]$ = stiffness matrix

$l_{(i)}$ = storey height (of ith storey) (mm)

M_T = total mass of a structure

$M_{cap.}$ = moment capacity

$M_{P\Delta}$ = additional moment due to P-Δ effect

$m_{(i)}$ = mass (of ith storey)

$_{ef.}M_j$ = effective mass of jth mode of a M.D.O.F. system

$[M]$ = mass matrix

n_s = sample size for earthquake records with regard to the shape function S

n_α = sample size for earthquake records with regard to the maximum ground acceleration α_{max}

$P[E]$ = probability of occurrence of the event E

$P[E_1|E_2]$ = conditional probability of E_1 assuming E_2 ($= P[E_1 \cap E_2]/P[E_2]$)

$P[F|EQ_{ij}]$ = probability of failure given that an earthquake with the maximum ground acceleration $\alpha_{max} = \alpha_i$ and the shape function $S = s_j$ occurs

P_f = failure probability

$P_{f|EQ}$ = conditional failure probability of an entire structure given an earthquake

$P_{f_i|EQ}$ = conditional failure probability of the ith storey of a structure given an earthquake

q_j = time function of the jth mode for a M.D.O.F. system

${}_s q_j$ = response displacement of a S.D.O.F. system with the same resonant period and critical damping ratio as for the jth mode of a M.D.O.F. system

R = structural resistance variables, such as initial stiffness, yield strength and so on

R_i = the ratio of the damage energy absorbed by the ith storey to that for the entire structure, calculated by an elastic analysis $({}_e E_{d_i}/{}_e E_{d_T})$

S = strong motion duration (sec) or shape functions of spectrum with regard to period and the intensity envelope with regard to time of an earthquake

T = period (sec)

t = time (sec)

$\{U_j\}$ = modal shape for the jth mode of a M.D.O.F. system

V_i = shear force applied to ith storey (kN)

$V_{y_{(i)}}$ = yield shear strength (of ith storey) (kN)

w_i = weight of ith storey (kN)

w_t = total weight of structure ($=M_T \cdot g$)

$w_{t \text{ above}_i}$ = weight of a structure sustained by ith storey (kN)

x_i = horizontal displacement of the ith mass relative to the ground (mm)

$\dot{x}_i$ = horizontal velocity of the ith mass relative to the ground (mm/sec)

$\ddot{x}_i$ = horizontal acceleration of the ith mass relative to the ground (mm/sec^2)

$\ddot{Y}(\Omega_k)$ = Fourier amplitude of input earthquake acceleration for the circular frequency of Ω_k

y = horizontal displacement of the ground (mm)

$\ddot{y}$ = horizontal acceleration of the ground (mm/sec^2)

$\alpha_{(i)}$ = the ratio of second stiffness to initial stiffness (of ith storey)

α_{max} = maximum ground acceleration (mm/sec^2)

β_j = modal participation factor for jth mode of a M.D.O.F. system

γ_i = ith load factor

$\gamma_{max_{(i)}}$ = maximum storey deflection angle (of the ith storey)

γ_u = ultimate storey deflection angle

δ_i = interstorey drift of ith storey (mm)

$\dot{\delta}_i$ = velocity of the ith mass relative to the (i-1)th mass (mm)

$\delta_{max_{(i)}}$ = maximum interstorey drift during an earthquake (of ith storey)

$\zeta_{(\alpha_i)}$ = a parameter of a log-normal distribution (for E_{d_T}/w_t corresponding to $\alpha_{max} = \alpha_i$)

η_{I_i} = dimensionless damage energy input for ith storey

η_{R_i} = dimensionless resistance energy capacity for ith storey

$\lambda_{(\alpha_i)}$ = a parameter of a log-normal distribution (for E_{d_T}/w_t corresponding to $\alpha_{max} = \alpha_i$)

$\lambda_{i,r}$ = ith moment of response spectral-density function

λ_{i,δ_j} = ith moment of spectral-density function with regard to a interstorey drift of jth storey

$\mu_{(i)}$ = maximum ductility factor (of ith storey (= $\delta_{max_i}/\delta_{y_i}$)

μ_{u_i} = ultimate ductility factor (= $l_i \cdot \gamma_u/\delta_{y_i}$)

ν_b = mean crossing rate of a level b

$\nu_b^+(\nu_b^-)$ = mean crossing rate of up (down) crossing

Σ = denotes "sum of"

σ_{δ_i} = zero-order moment of $G_{\delta_i}(\omega)$ $(=\sqrt{\lambda_{0,\delta_i}})$ (mm)

Φ = cumulative distribution function of the standard normal variable

ϕ = resistance factor

ϕ_k = phase angle of kth circular frequency

Ω_{δ_i} = $\sqrt{\lambda_{2,\delta_i}/\lambda_{0,\delta_i}}$ (1/sec)

$\omega_{(j)}$ = circular frequency of a S.D.O.F. system (corresponding to jth mode of a M.D.O.F. system)

U = union ($E_1 U E_2$ means the occurrence of E_1 or E_2, or both)

$\cap$ = intersection ($E_1 \cap E_2$ means the joint occurrence of E_1 and E_2)

CHAPTER 1

INTRODUCTION

"To win a battle, know your enemy and know yourself". This saying from the old Japanese Field Service Code is equally applicable today in the matter of plotting strategies for ensuring structural safety. Present day structural codes exist to enables structures to survive "battles" against the forces of nature and attack by earthquake, wind, snow and so on. The analogy holds well; to avoid disaster we should know the enemy, the forces of nature, and we should thoroughly know and understand the behaviour of structures we design. However, generally we possess incomplete information for both forces and structure. In spite of having only limited information, engineers are expected to develop rational and workable codes. The mismatch between need for and capability of predicting safety is a major source of difficulty in the development of codes.

A structural code must ensure minimum safety levels for all structures. This is the major objective of the code. The required safety levels are probably determined from social acceptance by seeking to minimise the total cost of a structure including the expected consequential losses averaged over the design life. For most structures, the most important consequential loss is loss of life. However,

for some structures such as hospitals or art galleries, loss of functionality or contents become important. The larger the expected consequential losses, the higher the safety required, which demands a greater initial cost. Therefore, the required safety levels depend on occupancies and types of structures and on different loading types. Identical incidental losses are not generally expected. Even though the available information is insufficient, engineers have directed their efforts to develop structural codes in an attempt to satisfy the basic objective.

In order to assess whether the objective is being met in a rational way, it is necessary to know and to quantify the safety levels implied by a structural code. Historically, the assessment has been based on examining real earthquake damage of structures. A survey of damage enables us to establish whether a structural code developed, using limited information, meets the demand of society. At the present time, it appears that this is the only way to be able to assess the overall safety implied by a code. However, we cannot merely wait for uncontrollable experiments. Although the information is limited, it is helpful to quantify safety levels, using available data, for this will at least lead to a somewhat more rational code, and hence to a more soundly-based design procedure.

What a rational code should offer in terms of structural safety therefore is important. In developing recent structural codes, engineers must have recognised that discrimination in required safety levels among different

structures should be made. This leads to so called risk factors in codes so that structures whose failure results in more serious consequences possess higher safety. Moreover, though the loss consequences due to different loadings can be expected to be different, appropriate differences in required safety levels have not been discussed as yet. A code which reflects such considerations may be called a "balanced code". The final aim of which the present study is a part is to establish such a balanced code.

A balanced code is a code for which the lowest level of safety, or highest expected loss, is the same for all loading types. Thus, in such a code, the earthquake load provisions will be no more and no less severe than, say, the wind load provisions from the viewpoint of the least safety level.

To achieve a balanced code, it is imperative to estimate the safety levels or conversely failure probabilities of structures designed in accordance with such a code. The primary cause of failure could be excessive gravity load, extreme wind gust or excessive earthquake motions. These depend on the types of structure and their locations. It is therefore necessary to establish analytical methods for defining failure probabilities for different loadings.

In the case of earthquakes the selection of an appropriate model is considerably more difficult than for other load cases. Firstly, an earthquake manifests itself in ground motions and not in a clearly defined load applied to a

structure. Accordingly, not only its intensity but other characteristics, such as frequency contents, of an earthquake may affect structural behaviour. Ground motions induce time dependent cyclic displacements and hence resistance demands. Moreover, the entire system of a structure may react to earthquake accelerations, whereas for, say, live loading inadequate resistance may arise locally in only one element. Because of these difficulties a satisfactory model for predicting failure probabilities for earthquake loads has not yet been established.

As a contribution to the development of a balanced code, this report presents a simple and rational way to determine failure probabilities for multi storey frame buildings subjected to an earthquake. In the development of an appropriate model the following problems have had to be taken into account.

As failure is being considered, the chosen model must lend itself to quantification of structural damage based on dynamic behaviour. The damage is related to dynamic responses, which are time dependent. So one problem emerges; how can structural damage be related to time dependent dynamic response? Dynamic response is markedly affected by numerous parameters related to characteristics of the structure as well as others describing the earthquake. These make a mathematical model unduly complicated. To avoid such complexity, it is desirable that damage should be represented by a specific quantity which is insensitive to the dynamic parameters involved.

Another difficulty relates to the definition of failure. Since a strength design code is considered, failure is defined as collapse. Thus, the relationship between the damage-specifying quantity and failure represents another problem.

In developing an analytical procedure for failure probabilities with the use of a model, much attention must be paid to consistency throughout the procedure in terms of uncertainty. The uncertainty which exists in the prediction of earthquake characteristics is very large. It dominates the total uncertainty in the procedure. This could mean that although the precision of models and other data might increase, the quality of the results would not improve. It is desirable to avoid unnecessary complexity, yet it is important to make the procedure consistent with the degree of uncertainty involved.

Economic consequences are not taken into account in this study and safety is the sole consideration.

The topics are presented in the following order; Chapter 2 summarises previous literature regarding basic techniques of reliability analysis, reliability assessment of complicated structures, and code calibration procedures. Chapter 3 describes the contribution of failure probabilities to the development of a balanced code, so setting the scope of the present report. Chapter 4 illustrates several of the problems involved by considering a thorough probabilistic

analysis of a simple reinforced concrete portal frame. Chapter 5 discusses strategies for quantification of earthquake damage and proposes a definition of failure based on maximum storey deflecton angle. Chapter 6 develops a deterministic equation for predicting maximum storey drift for multi storey buildings in terms of cumulative plastic strain energy. Chapter 7 describes a procedure for obtaining failure probabilities using the deterministic drift-prediction equation as a performance function. This involves sensitivity studies of the effect of some items on failure probability. Finally, Chapter 8 summarises the work and outlines problems remaining.

CHAPTER 2

REVIEW OF PREVIOUS WORK ON STRUCTURAL RELIABILITY ANALYSIS

2.1 INTRODUCTION

Engineering decisions must be made in the presence of uncertainties arising from inherent randomness in many design parameters, imprecise data, and drastic modelling assumptions. Thus, it is important to evaluate the significance of uncertainty.

The idea that uncertainty must be considered in design is not new. In allowable stress design, the uncertainties are taken into account by restricting the stress in each member of a system subjected to specified loads to a sufficiently low intensity. The ratio of failure or yield stress to the allowable stress defines the safety factor. However, the variances of many other factors involved are not considered in this definition of the safety factor. Therefore its relationship to the precise probability of failure is obscure.

Probabilistic methods are fashionable at present. They are considered to lead to failure probabilities and to the development of more rational systems. Many attempts have

been made to find a way to predict failure probability by taking account of random variables using these techniques to solve structural reliability problems. The purpose of this chapter is to describe an outline of previous work on structural reliability analysis.

Firstly, some basic techniques for calculating failure probability are presented, namely direct integration, automatic numerical integration, Monte Carlo simulation and the so-called advanced First-Order Second-Moment method. As the latter two methods are widely used in reliability problems, the details will be explained for cases where basic random variables are both uncorrelated and correlated.

Secondly, reliability analyses of redundant structures are discussed. Since multiple failure modes are expected for a redundant structure and they make the precise calculation of failure probability difficult. Thus, bounding operations are usually used to estimate a range of total failure probability. These are some of the basic tools in probability analyses. However, such an analytical model does not appear to be appropriate for the present study. Thus some reservation from a viewpoint of understanding total seismic structural behaviour, is warranted.

Thirdly, the probabilistic risk assessment of nuclear power plants is discussed. At present, this seems to be the most thorough and systematic approach. It demands a great amount of work to achieve acceptable results for a particular plant at a specified site. In contrast, for code development a

simple prediction method applicable to different structures and structural types is desired. The difference in these aims will be examined.

Finally, a code calibration method using the advanced First-Order Second-Moment method is described. The numerical values of load and performance factors for a strength design code are optimised, assuming that the total format of the code is appropriate. However, the customary assumptions relevant to earthquake provisions are irrational. To assess questionable assumptions as well as the difficulties involved, these assumptions are also reviewed.

2.2 BASIC TECHNIQUES FOR EVALUATING PROBABILITY OF FAILURE

The reliability of an engineering system may generally be defined as the probability of it satisfactorily performing its intended function or mission. The level of performance of a system will, among other factors, depend on the properties of the system. In this context and for the purpose of a generalised formulation, a performance function (1) may be defined as:

$$g(\mathbf{X}) = g(X_1, X_2, \ldots, X_n) \qquad (2.2.1)$$

where: $\mathbf{X} = (X_1, X_2, \ldots, X_n)$ (a vector of basic variables of the system)

$g(\mathbf{X})$ = performance of the system

Accordingly, the limiting performance requirement may be defined as $g(\mathbf{X})=0$, which represents the "limit state" of the system. This is often called the "failure surface". On one side of the failure surface is the failure state, $g(\mathbf{X}) < 0$. Thus the probability of failure p_f is:

$$p_f = P[g(\mathbf{X}) < 0] \tag{2.2.2}$$

$$= \int_{g(\mathbf{X})<0} f_{\mathbf{X}}(\mathbf{X})d\mathbf{X} \tag{2.2.3}$$

where: $f_{\mathbf{X}}(\mathbf{X})$ = the joint probability density function of $\mathbf{X}$

For the simple case where only two random variables, such as resistant capacity R and load demand L are concerned, the formulation is schematically shown in Fig. 2.2.1. When the basic variables are statistically independent, the failure probability p_f is given by:

$$p_f = \int\cdots\int_{g(\mathbf{X})<0} f_{X_1}(x_1)\cdot f_{X_2}(x_2)\cdot \ldots f_{X_n}(x_n)dx_1dx_2\ldots dx_n \tag{2.2.4}$$

in which:

$f_{X_1}(x_1), f_{X_2}(x_2), \ldots, f_{X_n}(x_n)$ = probability density functions of $x_1, x_2, \ldots, x_n$ respectively

Mathematical direct integration is generally impossible, because many of the probability density functions, even for normal distribution, are not integrable, and also because

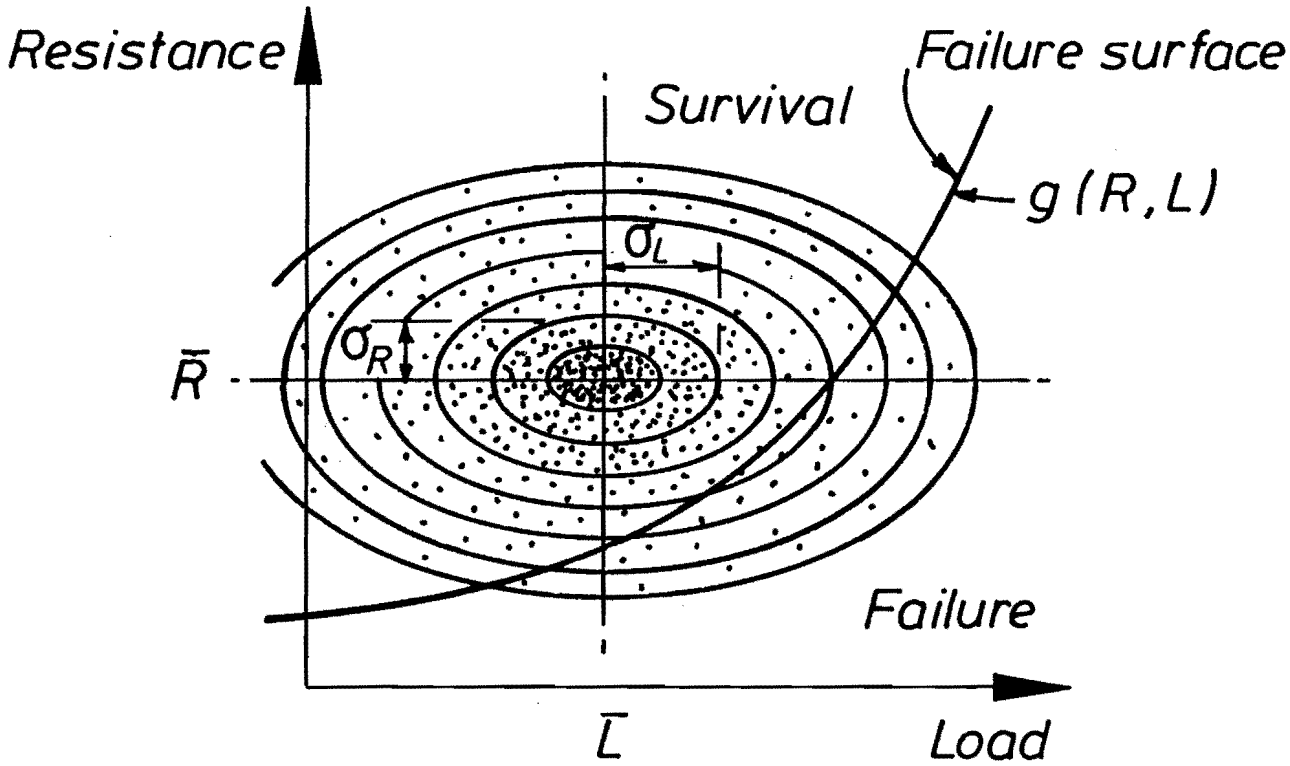

$$p_f = P[g(R,L)<0]$$

$$= \int\int_{g<0} f_{R,L}(r,\ell)\,dr\,d\ell$$

f = Joint Probability Density Function

Fig. 2.2.1 Formulation of reliability analysis

the performance function g is not always a simple relationship.

Automatic numerical integration (2,3) can only be applied to simple cases and therefore is generally restricted to the case of two random variables. In the application, a step function h(g) or indicator function, shown in Fig. 2.2.2, is used. For example, Eq. (2.2.3) can be transformed to:

$$p_f = \int_{-\infty}^{\infty} f_{\mathbf{X}}(\mathbf{X}) \cdot h(g) \cdot d\mathbf{X} \qquad (2.2.5)$$

As the number of variables increases, the numerical integration generally does not converge, and the method is not applicable.

For practical purposes, alternative methods of evaluating p_f are necessary. For the rest of this section, Monte Carlo simulation and the advanced First-Order Second-Moment method are briefly summarised, which are the techniques commonly adopted for the evaluation of the failure probability.

2.2.1 Monte Carlo Simulation

Monte Carlo simulation may be thought of either as a series of deterministic experiments whose results can be investigated statistically, or as a means of numerical integration in a random rather than a systematic fashion. The basic theory is well known. By repeating a simulation process, a set of values of g in Eq. (2.2.2) is obtained, using in each simulation a particular set of values of the

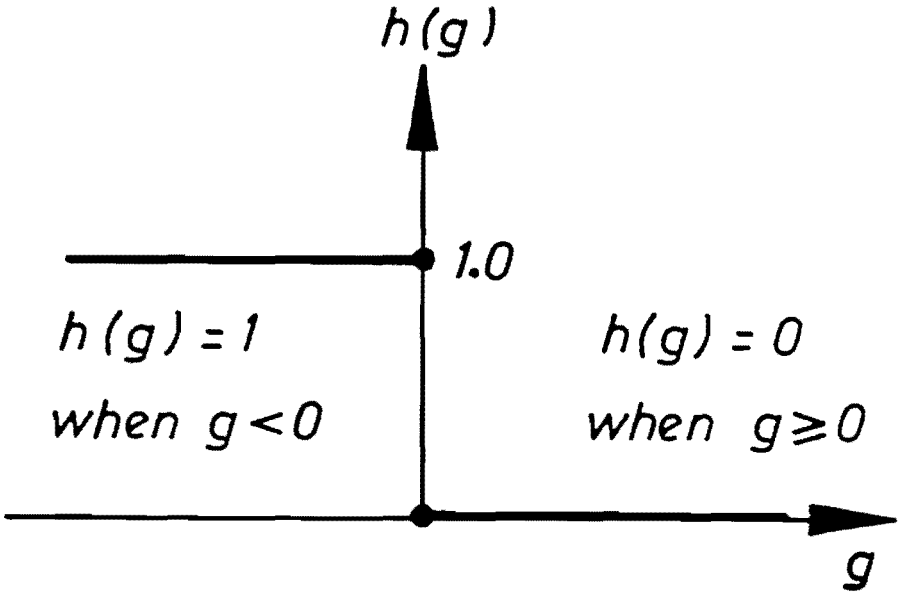

Fig. 2.2.2 Step function h(g)

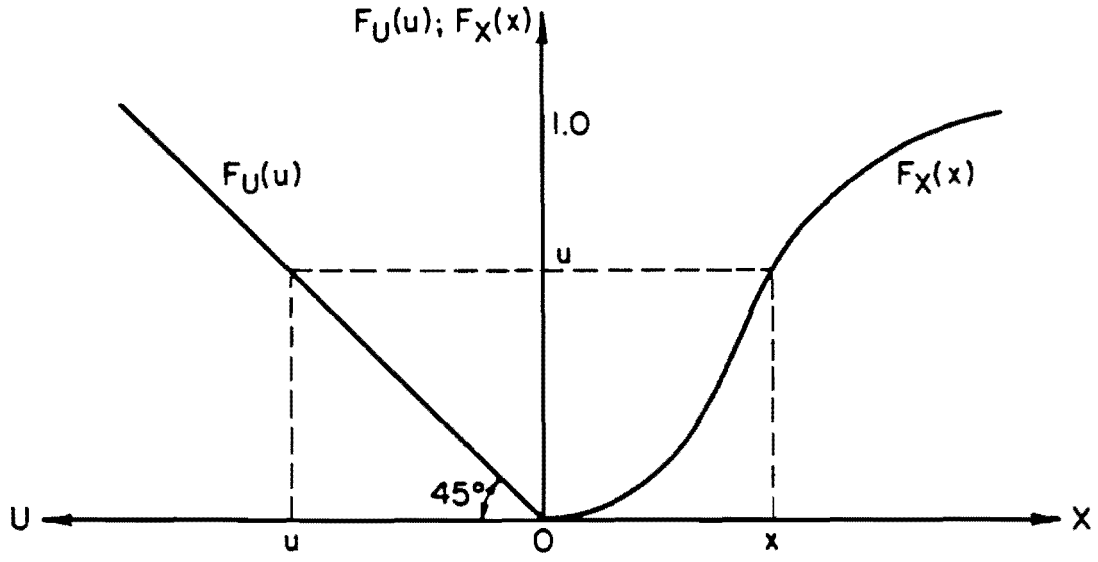

Fig. 2.2.3 Relation between the standard uniform variable u and the random variable x

random variables **X**, generated in accordance with the corresponding probability distributions. Therefore, p_f is expressed by the ratio of the number of negative values of g relative to the total sample size.

A key task in the application of Monte Carlo simulation is the generation of the appropriate values of the random variables in accordance with the respective prescribed probability distributions. The generation of uniformly distributed random numbers between 0 and 1, which are values of the standard unit for variables U, contributes to this. For example, assume a random variable X with cumulative distribution function (CDF) $F_X(x)$. Then at a given cumulative probability $F_X(x) = u$, the value of X is (1):

$$x = F_X^{-1}(u) \tag{2.2.6}$$

The relationship between x and u is shown in Fig. 2.2.3. To generate standard uniform variables, an installed computer subroutine which is usually called a random number generator, is generally available. Alternatively one can readily write a routine (1). Thus, when the inverse of the CDF of the random variable X can be obtained, a random value x is easily generated using Eq. (2.2.6). If the inverse form cannot be analytically expressed, some other methods to generate x which are available must be used. For example, a pair of independent random numbers x_1 and x_2 from a normal distribution $N(\mu,\sigma)$ may be generated by (1):

$$\begin{aligned} x_1 &= \mu + \sigma \sqrt{-2 \ln u_1} \cos 2\pi u_2 \\ x_2 &= \mu + \sigma \sqrt{-2 \ln u_1} \sin 2\pi u_2 \end{aligned} \tag{2.2.7}$$

where: u_1 and u_2 = independent numbers of the standard uniform variables

μ = mean value

σ = standard deviation

When the set of random variables $X_1, X_2, \ldots, X_n$ are dependent, the joint probability density function (PDF) may be expressed as (1):

$$f_{\mathbf{X}}(\mathbf{X}) = f_{X_1}(x_1) \cdot f_{X_2}(x_2|x_1) \cdot \ldots f_{X_n}(x_n|x_1, x_2, \ldots, x_{n-1}) \tag{2.2.8}$$

where $f_{X_1}(x_1)$ = the marginal PDF of X_1

$f_{X_k}(x_k|x_1, x_2, \ldots, x_{k-1})$ = the conditional PDF of X_k given $X_1 = x_1, X_2, \ldots, X_{k=1} = x_{k-1}$

The corresponding joint CDF is:

$$F_{\mathbf{X}}(\mathbf{X}) = F_{X_1}(x_1) \cdot F_{X_2}(x_2|x_1) \cdot \ldots F_{X_n}(x_n|x_1, x_2, \ldots, x_{n-1}) \tag{2.2.9}$$

In the case of dependent random variables, the required random numbers cannot be generated independently for each variable. However, with Eq. (2.2.9), the following provides a basis for generating the required set of dependent random numbers. Suppose a set of uniformly distributed random numbers $(u_1, u_2, \ldots, u_n)$ has been generated. Then a value x_1

may be determined independently as:

$$x_1 = F_{X_1}^{-1}(u_1) \tag{2.2.10a}$$

With this value of x_1, a value of x_2 may be determined from:

$$x_2 = F_{X_2}^{-1}(u_2|x_1) \tag{2.2.10b}$$

Similarly, using the values $x_1, x_2, \ldots x_{n-1}$ already obtained, we can determine the value x_n as:

$$x_n = F_{X_n}^{-1}(u_n|x_1, x_2, \ldots, x_{n-1}) \tag{2.2.10c}$$

As implied in Eq. (2.2.10), the method will be efficient only if the marginal and conditional CDFs can be inverted analytically. Consequently, when the random variables being considered are correlated, Monte Carlo simulation is not always completely applicable.

In practice, a major difficulty arises; it is that the demand on computer time is often unacceptably high, particularly where low probabilities of failure are sought. To overcome the problem, variance reduction techniques which can reduce variance (or error) without increasing the sample size, may be used (4-6). Frequently used approaches are Antithetic Variates, Correlated Sampling and Control Variates variance reduction techniques. However, even these techniques are not always helpful in reducing the computer time significantly.

2.2.2 Advanced First-Order Second-Moment Method

The advanced First-Order Second-Moment method (F.O.S.M.) is an approximate technique for calculating p_f. In the method, a reduced coordinate system, in which all random variables transform to equivalent standard normal variables, is used. Though it is a question how to obtain the equivalent variables, the system makes the n-dimensional axes of probability space identical so that the same probability density can be obtained at any point whose distance from the origin is the same. For the case of two random variables, corresponding to Fig. 2.2.1, the formulation based on reduced coordinates is shown in Fig. 2.2.4. The approximated failure surface is assumed to be a tangent plane to the actual failure surface at a point which is on the actual failure surface with minimum distance to the origin of the reduced coordinates. In the case of uncorrelated variables, X, the required minimum distance β may be determined as follows (1).

Introduce the reduced variables $\mathbf{X}'(X_1', X_2', \ldots, X_m')$:

$$X_i' = \frac{X_i - \mu_{X_i}^N}{\sigma_{X_i}^N} \qquad (2.2.11)$$

where: $\mu_{X_i}^N$ = mean of equivalent normal distribution for X_i (if X_i is a normal variable, $\mu_{X_i}^N$ is the mean of the original normal distribution)

$\sigma_{X_i}^N$ = standard deviation of equivalent normal

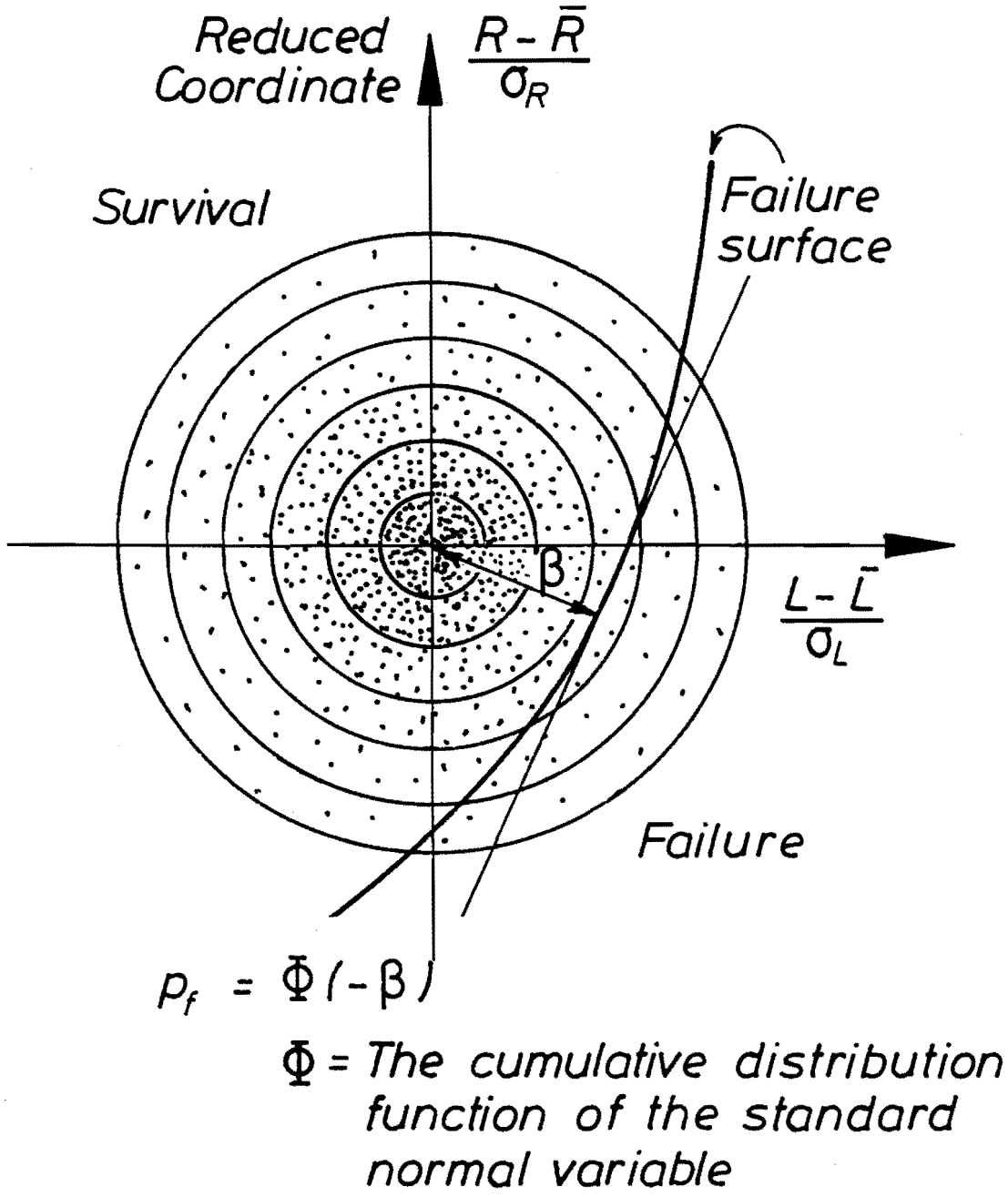

Fig. 2.2.4 Formulation of reliability analysis in reduced coordinates

distribution for X_i (if X_i is a normal variable, $\sigma^N_{X_i}$ is the standard deviation of the original normal distribution)

A possible way of obtaining $\mu^N_{X_i}$ and $\sigma^N_{X_i}$ will be given later. The distance from a point $\mathbf{X}'$ on the failure surface $g(\mathbf{X}) = 0$ to the origin of $\mathbf{X}'$ is:

$$D = (\mathbf{X}'^t \mathbf{X}')^{\frac{1}{2}} \tag{2.2.12}$$

In order to minimise the function D, subject to the constraint $g(\mathbf{X}) = 0$, the Lagrange multiplier method may be used. Accordingly let:

$$L = D + \lambda\, g\,(\mathbf{X})$$

$$= (\mathbf{X}'^t \mathbf{X}')^{\frac{1}{2}} + \lambda\, g\,(\mathbf{X}) \tag{2.2.13}$$

in which:

$$X_i = \mu^N_{X_i} + \sigma^N_{X_i} \cdot X_i'$$

Minimising L, we obtain the following set of n+1 equations with n+1 unknowns:

$$\frac{\partial L}{\partial X_i'} = \frac{X_i'}{\sqrt{X_1'^2 + X_2'^2 + \ldots + X_n'^2}} + \lambda \frac{\partial g}{\partial X_i'} = 0 \qquad (i=1,2,\ldots,n) \tag{2.2.14}$$

and:

$$\frac{\partial L}{\partial \lambda} = g(\mathbf{X}) = 0 \tag{2.2.15}$$

The above set of equations, Eq. (2.2.14), can be written in matrix notation as:

$$\frac{\mathbf{X}'}{(\mathbf{X}'^{t}\,\mathbf{X}')^{\frac{1}{2}}} + \lambda\,\mathbf{G} = 0 \qquad (2.2.16)$$

where:

$$\mathbf{G} = \left(\frac{\partial g}{\partial X_1'}, \frac{\partial g}{\partial X_2'}, \ldots, \frac{\partial g}{\partial X_n'}\right)$$

$$\frac{\partial g}{\partial X_i'} = \sigma^{N}_{X_i} \cdot \frac{\partial g}{\partial X_i}$$

So:

$$\mathbf{X}' = -\lambda\,\mathbf{D}\,\mathbf{G} \qquad (2.2.17)$$

Therefore:

$$D = [(\lambda D\mathbf{G}^{t})(\lambda D\mathbf{G})]^{\frac{1}{2}} = \lambda D(\mathbf{G}^{t}\mathbf{G})^{\frac{1}{2}} \qquad (2.2.18)$$

and thus:

$$\lambda = (\mathbf{G}^{t}\mathbf{G})^{-\frac{1}{2}} \qquad (2.2.19)$$

From Eqs (2.2.17) and (2.2.19):

$$\mathbf{X}' = \frac{-\mathbf{G}\,D}{(\mathbf{G}^{t}\mathbf{G})^{\frac{1}{2}}} \qquad (2.2.20)$$

Conversely:

$$D = \frac{-\mathbf{G}^{t}\mathbf{X}'}{(\mathbf{G}^{t}\mathbf{G})^{\frac{1}{2}}} \qquad (2.2.21)$$

By assuming that $\mathbf{X}'^{*}$ is the nearest point on the failure surface to the origin, the required minimum distance β, which is often called the safety or reliability index, is:

$$\beta = \frac{-G^{*t} X'^{*}}{(G^{*t} G^{*})^{\frac{1}{2}}} \tag{2.2.22}$$

In scalar form:

$$\beta = \frac{-\Sigma X_i'^{*} (\partial g/\partial X_i')_{*}}{\sqrt{\Sigma (\partial g/\partial X_i')^2_{*}}} \tag{2.2.23}$$

Therefore in general, a convergent procedure is required. A new nearest point for the next step can be obtained from Eq. (2.2.20) by:

$$X'^{*}(new) = \frac{- G^{*} \beta}{(G^{*t} G^{*})^{\frac{1}{2}}} \tag{2.2.24}$$

In scalar form:

$$X_i'^{*}(new) = -\alpha_i^{*} \beta \tag{2.2.25}$$

Where α_i^{*} is the direction cosine from the origin to the failure point and is given by:

$$\alpha_i^{*} = \frac{(\partial g/\partial X_i')_{*}}{\sqrt{\Sigma (\partial g/\partial X_i')^2_{*}}} \tag{2.2.26}$$

When the convergence is obtained, p_f is calculated by:

$$p_f = \Phi(-\beta) \tag{2.2.27}$$

in which:

Φ = the CDF of the standard normal variable

The equivalent normal distribution for a non-normal variable may be obtained in each convergent step such that the cumulative probability as well as the probability density ordinate of the equivalent normal distribution are equal to those of the corresponding non-normal distribution at the nearest point $\mathbf{X}'^{*}$.

For linear problems (linear performance function $g(\mathbf{X})$), no iteration is necessary. A linear performance function may be represented as:

$$g(\mathbf{X}) = a_o + \sum_{i=1}^{n} a_i X_i \tag{2.2.28}$$

In terms of the reduced variates, Eq. (2.2.11), the performance function becomes:

$$g'(\mathbf{X}') = a_o + \sum_{i=1}^{n} (\mu_{X_i} + \sigma_{X_i} X_i') \tag{2.2.29}$$

The minimum distance from hyper-plane $g'(\mathbf{X}') = 0$ to the origin is:

$$\beta = \frac{a_o + \sum_{i=1}^{n} (a_i \mu_{X_i})}{\sqrt{\sum_{i=1}^{n} (a_i \sigma_{X_i})^2}} \tag{2.2.30}$$

The nearest point on the failure surface to the origin is:

$$X_i'^{*} = - \beta \cdot \alpha_i \tag{2.2.31}$$

or:

$$X_i^{*} = \mu_{X_i} - \sigma_{X_i} \cdot \beta \cdot \alpha_i \tag{2.2.32}$$

where:

$$\alpha_i^* = \frac{(a_i \sigma_{X_i})_*}{\sqrt{\sum_{i=1}^{n} (a_i \sigma_{X_i})_*^2}} \quad \text{(direction cosines)} \quad (2.2.33)$$

If the random variables $X_1, X_2, \ldots X_n$ are uncorrelated normal variates, the failure probability p_f can be calculated by Eq. (2.2.27).

For correlated random variables, the original variables may be transformed to a set of uncorrelated variables. The required transformation is necessarily dependent on the covariance matrix of the original variables, and may be obtained as follows (1). Suppose the covariance matrix of the original variables **X** is:

$$[C] = \begin{bmatrix} \sigma_{X_1}^2 & , C_{ov}(X_1,X_2) & , \ldots , & C_{ov}(X_1,X_n) \\ C_{ov}(X_2,X_1) & , \sigma_{X_2}^2 & , \ldots , & C_{ov}(X_2,X_n) \\ \vdots & \vdots & & \vdots \\ C_{ov}(X_n,X_1) & , C_{ov}(X_n,X_2) & , \ldots , & \sigma_{X_n}^2 \end{bmatrix} \quad (2.2.34)$$

where: $C_{ov}(X_i,X_j)$ = the covariance between the pair of variables X_i and X_j

The covariance between a pair of reduced variables, X_i' and X_j' is:

$$C_{ov}(X_i',X_j') = E[(X_i' - \mu_{X_i'})(X_j' - \mu_{X_j'})]$$

$$= E[X_i' X_j']$$

$$= \frac{E[(X_i - \mu_{X_i})(X_j - \mu_{X_j})]}{\sigma_{X_i} \sigma_{X_j}}$$

$$= \frac{Cov(X_i, X_j)}{\sigma_{X_i} \sigma_{X_j}}$$

$$= \rho_{X_i, X_j} \tag{2.2.35}$$

Therefore, the covariance matrix of the reduced variables **X'** is the corresponding correlation matrix of the original variables **X**; that is, the covariance matrix of **X'** is:

$$[C'] = \begin{pmatrix} 1 & , \rho_{X_1,X_2} & ,\ldots, & \rho_{X_1,X_n} \\ \rho_{X_2,X_1} & , 1 & ,\ldots, & \rho_{X_2,X_n} \\ \vdots & \vdots & & \vdots \\ \rho_{X_n,X_1} & , \rho_{X_n,X_2} & ,\ldots, & 1 \end{pmatrix} \tag{2.2.36}$$

The safety index β of Eq. (2.2.22) for correlated variables finally becomes:

$$\beta = - \frac{\mathbf{G}^{*t}\, \mathbf{X}'^{*}}{(\mathbf{G}^{*t}[C']\mathbf{G}^{*})^{\frac{1}{2}}} \tag{2.2.37}$$

The F.O.S.M. method has been widely used in reliability studies and is analytically elegant. However two important questions concerning its credibility arise (7). The first is typical for any optimisation problem; is the minimum which was found global or local? In some cases, where more than one minimum exists, the solution depends strongly on the initial point chosen to start the numerical algorithm. The second question concerns the error due to the approximation, which involves the replacement of actual random variables by normal ones and a linearisation of the

performance function. This is why the result obtained by the F.O.S.M. method is sometimes called notional rather than actual reliability.

Such comments assume that the performance function and its variables, which are assumptions used in the F.O.S.M. approach are known and correct, or appropriate. However, the problem often lies in the assumptions concerning the data and underlying structural model, which lead to error levels or uncertainty greater than the errors inherent in the F.O.S.M. method. Therefore, the use of F.O.S.M. method is usually justified.

The F.O.S.M. method can also be applied to redundant structures (see Chapter 4), which have multiple failure modes. In order to assess the failure probability of the redundant structures, it is necessary to estimate correlations between different failure modes. However, it is usually difficult so that approximations are almost always necessary. Such approximations will be discussed in the next section.

2.3 RELIABILITY ANALYSIS OF REDUNDANT STRUCTURES

The problems considered in the previous section involve a single failure mode, defined by a single limit state. However, engineering problems usually contain multiple failure modes. In this section, the reliability of redundant structures with multiple failure modes is discussed.

Recently, research in this field has increased (8-22). The structures considered can be divided into elastic-plastic systems consisting of elastic plastic components (see Fig. 2.3.1 in which c = 1.0, M_y = yield moment of a section, ϕ = curvature, F_y = yield force of a member and δ = displacement) and elastic-residual systems consisting of elastic residual components (c = 1.0) and elastic plastic components.

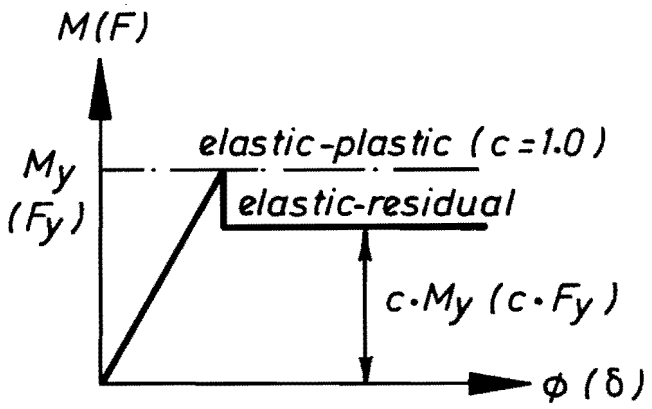

Fig. 2.3.1 Component behaviour

Major differences exist between the two systems. These are:

1. If a system is elastic-plastic, the failure modes of the system are independent of the failure sequences of the components. Such failures are exactly the same as the well-known plastic mechanism modes of failure. However, if elastic-residual components in an elastic-residual system yield, the failure modes of the system are sequence dependent.

2. In the case of an elastic-plastic system, conservative probabilities would be obtained if the components are assumed to be statistically independent. In contrast to this, conservative results would be obtained for an elastic-residual system if the components are assumed to be perfectly correlated.

Because of the sequence dependence, the reliability analysis of elastic-residual systems is more complicated than that of elastic-plastic systems.

Most research work in this area has certain common elements. Firstly, an inelastic static analysis with so called beam elements or truss elements is used, assuming the intensity and distribution of external loads. Secondly, the general criterion for collapse is that of loss of stability; i.e. that the stiffness matrix of the structure becomes singular. Thirdly, two latent problems in the work seem to be involved, as follows:

1. Systematic selection of dominant modes out of potentially possible failure modes

2. Calculation of bounds on the overall p_f using p_f for each mode with or without considering the correlation between failure modes (bounding operations)

Practical solutions for the two fundamental problems are

examined in the following two sections.

2.3.1 Selecting Dominant Failure Modes

In an analysis of redundant structural systems, all modes of failure are potentially of significance in the calculation of structural reliability. In practice, however, many modes do not contribute significantly. One of the issues is to identify those modes which are stochastically dominant. The selection of dominant failure modes is discussed in this subsection mainly based on the work of Melchers (8) and Hurotsu (10,11).

The probability p_{f_k} of the kth failure mode being developed is given by:

$$p_{f_K} = P[E_1 \cap E_2 \cap \ldots \cap E_n] \qquad (2.3.1)$$

where E_i denotes the event in which the ith resistance is subject to a demand reaching its capacity; for example the bending moment of the member ends i reaches its plastic moment capacity. In general, this event will be dependent on prior events. The failure probability for the structure as a whole is given by the union of all modal failures

$$p_f = P[F_1 \cup F_2 \cup \ldots \cup F_m] \qquad (2.3.2)$$

where: F_k denotes the event of failure in kth mode

The events E_i defined in Eq. (2.3.1) must be formulated.

When using for example beam elements in the inelastic static analysis, the bending moments generated at the member ends are calculated by using a matrix method and written in the form:

$$M_i = \sum_{j=1}^{N} b_{ij} L_j$$

$$(i=1,2,\ldots 2X(\text{number of members})) \qquad (2.3.3)$$

where L_j is the applied load and b_{ij} the deterministic load effect coefficients. The resistances of the member ends are represented by their plastic flexural strength R_i. The event E_i can then be expressed by:

$$E_i = [R_i - M_i = 0] \qquad (2.3.4)$$

When a member end is turned into a plastic hinge, it is treated in the following manner. The original stiffness matrix $[K_i]$ of the member is replaced by a reduced matrix to account for the plastic hinge, and artificial residual forces and moments are applied to the member ends. The total structural stiffness matrix [K] as well as the load vector have to be adjusted accordingly.

When any one member end yields, the internal forces are redistributed to elastic (non-yielding) member ends, then the next member to yield is determined. Progressing with this process structural failure is established when plastified member ends attain a specified number $E_1, E_2, \ldots, E_n$.

While evaluating the ith failure mode, it must be checked whether a search for another member to become plastic is worthwhile in order to select dominant modes. When the contribution of the failure probability p_{f_k} of the kth mode to the failure probability of the whole structure p_f turns out to be small, the calculation of the ith mode can be abandoned and this mode, being non-critical, can be eliminated. To achieve a solution two issues need to be clarified:

1. How to obtain an approximation of p_f for truncation at an early stage of the calculation; and

2. How to define the truncation criterion.

For the first problem, considering only the first q yields ($q < n$ in Eq. (2.3.1)) for the kth mode, p_f can be approximated by:

$$p_f \doteq \max_k \left(P[E_1 \cap E_2 \cap \ldots \cap E_q] \text{for kth mode}\right) \tag{2.3.5}$$

which is the so-called q-dimensional branching. For only the first yield in the sequence (q=1):

$$p_f \doteq \max_k \left(P[E_1] \text{for kth mode}\right) \tag{2.3.6}$$

The approximation for Eqs (2.3.2) and (2.3.1) seems quite rough regardless of the choice of a number for q. But it is nevertheless acceptable for the use in the truncation criterion.

For the second problem, a possible truncation criterion by which the ith failure mode could be ignored might be:

$$p_{f_i}/p_f \leq \eta \qquad (2.3.7)$$

where η is a (small) constant expressing the degree of accuracy desired in the value for p_f.

2.3.2 Bounding Operations

The existence of correlation among failure modes has made the exact solution of structural system reliability extremely complicated. As stated by Vanmarcke (20), "One of the most difficult problems in structural (system) reliability analysis is the way to deal with the statistical dependence between mode failure events". Accordingly approximations such as lower and upper bounds of the corresponding probability (1,19,21) are almost always necessary.

Correlation among failure modes is generally present as a result of the following facts (18):

1. Members are usually constructed by the same contractor from materials from the same supplier (built-in dependence).

2. Individual forces acting on different cross-sections of a structure are dependent when they result from

the same loading source (environmental dependence).

3. Common plastic hinges and loads are generally present in different failure modes (computational dependence).

The simplest bounds are:

$$\max_k(p_{f_k}) \leq p_f \leq 1 - \prod_{k=1}^{m}(1-p_{f_k}) \doteq \sum_{i=1}^{m} p_{f_k} \qquad (2.3.8)$$

assuming that failure modes are positively correlated. Such bounds are called uni-modal bounds. The separation between the lower and upper bounds will depend on the number of potential failure modes and on the relative magnitudes of the individual mode probabilities. For example, if there is a dominant mode the probability of failure will be dominated by this mode and indeed may be represented by the probability of occurrence of this single dominant mode. In such cases, the bounds will be narrow. In general, however, the bounds may be widely separated, especially if the number of potential failure modes is large.

The bounds can be improved by taking into account the correlation between pairs of potential failure modes; the resulting improved bounds will necessarily require the probabilities of joint events, such as E_iE_j ($E_iE_j = E_i \cap E_j$). They may thus be called bi-modal bounds.

Ditlevsen's bi-modal bounds (15) are:

$$p_{f_1} + \max\left[\sum_{i=2}^{m}\left(p_{f_i} - \sum_{j=1}^{i-1} P(E_iE_j)\right);\ 0\right] \leq p_f$$

$$\leq \sum_{i=1}^{m} p_{f_i} - \sum_{i=2}^{m} \max_{j<i} P(E_iE_j) \qquad (2.3.9)$$

The calculation of the joint probabilities $P(E_iE_j)$ in Eq. (2.3.9) remains difficult. Ditlevsen and Frangopol (18) proposed the approximation assuming that all basic variables are normal and that all joint probability functions are bi-variate normal, respectively. In general, the range of the bi-modal bounds of Eq. (2.3.9) will decrease as the single-mode failure probabilities decrease.

Ang and Ma (13,14) proposed a theoretically elegant upper bound, which is:

$$p_f \leq 1 - \prod_{\text{all}} (1 - p_{f,\text{group}}) \qquad (2.3.10)$$

where $p_{f,\text{group}}$ is the probability of the "representative" event of a group of failure modes with high correlation. The probabilistic network evaluation technique (PNET) avoids calculating probabilities resulting from conditions leading to failure via pairs of failure modes. This method is based on the notion of a demarcating correlation coefficient ρ_o, assuming those failure modes with high correlation ($\rho_{ij} \geq \rho_o$) to be perfectly correlated, and those with low correlation ($\rho_{ij} < \rho_o$) to be statistically independent. The failure modes must be arranged in decreasing order of their failure probabilities, and in each group the mode with the highest probability of occurrence is chosen as the

"representative" event of the group. Since the different groups are considered statistically independent, the overall probability of failure is approximated by the right hand side of Eq. (2.3.10).

According to recent sensitivity studies (18,19,22) which include correlation effects, a careful characterisation of strength and load correlations will generally allow much more precision in global safety calculations than increasing the accuracy in the methods for system reliability evaluation using bounding operations.

2.4 PROBABILISTIC RISK ASSESSMENT OF NUCLEAR POWER PLANTS

Probabilistic risk assessment has been used for nuclear power plants for the last 10 years (24-28). This is because the failure of such a plant may represent extraordinary consequences for the public. Risk assessment involves many uncertainties and requires numerous decisions by experts. However it is the most systematic approach at present available. Unfortunately the risk assessment techniques do not appear to be readily applicable to ordinary buildings, since they require an exorbitant amount of work and the procedure is site-dependent. In this section, the risk assessment of nuclear power plants is briefly reviewed to illustrate the underlying ideas and the difficulty of its application to ordinary buildings.

Risk assessment is composed of five steps, as follows:

1. Seismic Hazard Analysis - the intensity of ground acceleration at the site and its probability of occurrence are evaluated, considering the seismicity of the region.

2. Structure and Component Response Analysis - seismic responses of the structure and its components are stochastically evaluated, also considering uncertainties due to soil properties and methods of analysis.

3. Fragility Analysis - the probability of malfunction of the system and its components are stochastically evaluated.

4. Plant System / Accident Sequence Analysis - the probability of a radioactive substance leakage is evaluated using event tree and fault tree analyses.

5. Consequence Analysis - risk to human life and economic loss due to failure are stochastically evaluated.

Items 1 to 3 are closely related to the present study. They are examined in more detail in the next subsection.

2.4.1 Seismic Hazard Analysis

Seismic Hazard Analysis consists of 4 steps. Ultimately a

seismic hazard curve is obtained for the particular site concerned (see Fig. 2.4.1).

1. Earthquake Source Study and Modelling - Earthquake sources which are considered to affect the site, considering past earthquakes, geological and topographical surveys are established and modelled. The earthquake sources can be divided into active faults and seismotectonic provinces. Their location and size are determined from expert opinions.

2. Evaluation of the Intensity of an Earthquake and its Probability of Occurrence - When the location and size of each earthquake source has been determined, a design earthquake intensity due to the earthquake sources and its probability of occurrence can be evaluated, usually using Gutenberg and Richter's empirical equation (29) which relates magnitude to number of occurrences.

3. Evaluation of Attenuation - In order to obtain the expected maximum accelerations of ground motion at the site, an evaluation of the attenuation due to the distances from earthquake sources to the site is necessary. Because attenuation depends on the region in which the site is located, a number of different equations for different regions have been proposed, involving distances and earthquake magnitudes. Observed ground accelerations are known to be scattered around the expected value predicted

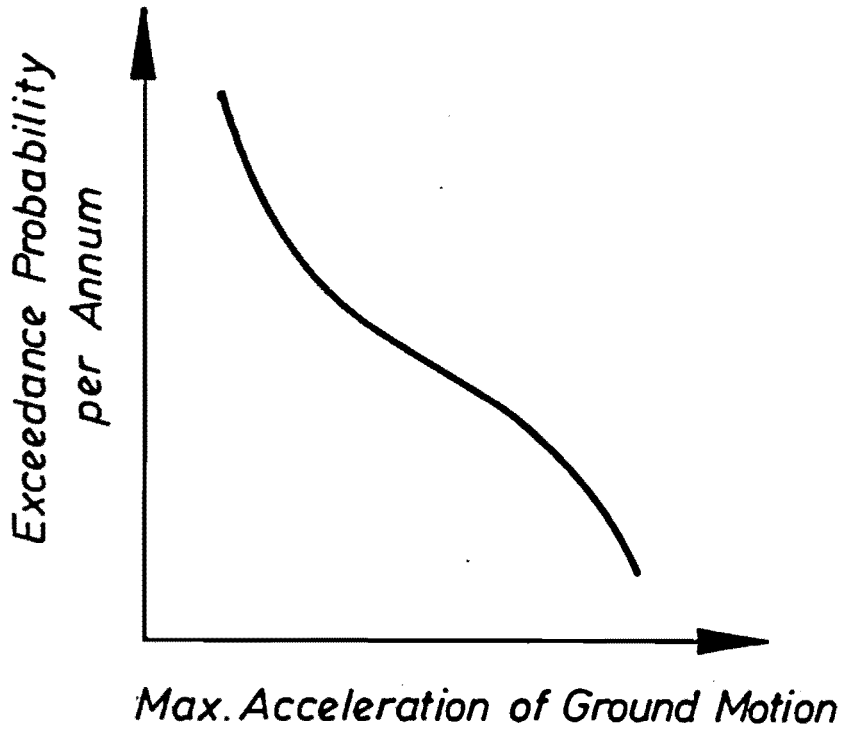

Fig. 2.4.1 Seismic hazard curve

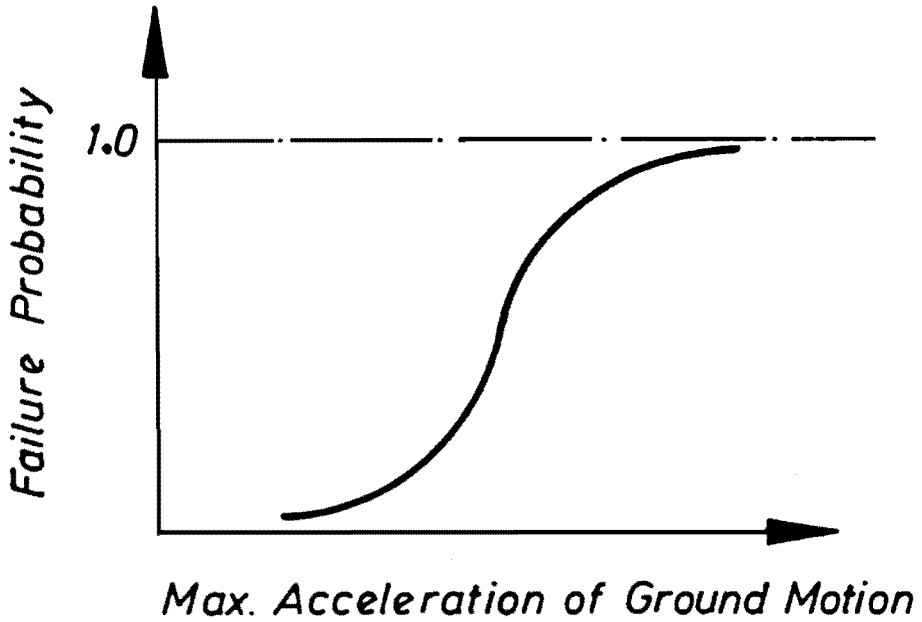

Fig. 2.4.2 Fragility curve

by an attenuation equation. This variability is taken into account in the prediction.

4. Seismic Hazard Curve - Finally, based on the data from 1 to 3, a seismic hazard curve is obtained to sum up the probable effects of each earthquake source, as illustrated in Fig. 2.4.1.

2.4.2 Seismic Response Analysis

The seismic response of structures is stochastically evaluated for different levels of ground acceleration. The analysis has two steps. Each contains several items contributing to uncertainties as follows.

1. Soil-Structure Interaction Analysis considers the following aspects:
   a. the type of wave motion and its angle of incidence;
   b. characteristics of soil and geologic formation;
   c. inelastic behaviour of soil;
   d. three dimensional effects;
   e. interaction with adjacent buildings.

2. Seismic Response Analysis considers the following aspects:
   a. material properties of a structure;
   b. damping of a structure;
   c. structural modelling;

d. composition of each modal response;

e. summation of structural responses due to three components of an earthquake;

f. variation of observed response spectrum.

These variations are taken into account, and a probabilistic distribution of responses for each part of the structure is obtained. However, in practice, the evaluation of a response distribution is so complicated that it is often dealt with deterministically (25) or by Monte Carlo simulation (27). The only one practical way to estimate the seismic response stochastically is the so-called safety factor method (26).

2.4.3 Fragility Analysis

Fragility analysis results in a fragility curve, such as shown in Fig. 2.4.2. The definition of failure must be formulated. Subsequently dominant failure modes are chosen from potential failure modes. Again expert opinions may be required. The resistance of the structure and its variability are evaluated by experimental tests, empirical equations and other suitable analyses. Once the resistance capacity and response distribution are known, a fragility curve can be obtained.

2.4.4 Contrast to the Present Study

In order to predict the reliability of a structure subjected to earthquake, seismic hazard and structural response and

damage need to be probabilistically estimated. The probabilistic risk assessment procedure applied to nuclear power plants is the only known thorough and systematic approach at present. It contains all procedures considered to be necessary. A very large amount of work is required to predict reliability of a particular nuclear plant plant. However, because a nuclear power plant is a special structure, the failure of which might have very serious consequences, such a computational effort is justified.

However, there is still a certain level of uncertainty due to limitations in the present state of the art. As mentioned in the previous subsection, some crude assumptions must be accepted. Other decisions rely on "expert" opinion, rather than cogent reasons based on theory. Therefore, the level of uncertainty is considerable.

What is desired to be achieved for code development is different from the requirements for nuclear power plants. Risk assessment is applied to each nuclear facility independently. For building codes we have to generalise and establish rules applicable to different structures and structural types at different locations. Thus in the course of development of a rational and balanced code a very large number of structures of all types must be analysed (the reason for this is explained in more detail in Chapter 5). Consequently a more general and yet less sophisticated analysis procedure to estimate reliability is desirable. Such simplification would lead to larger errors. However, because the uncertainty due to the lack of knowledge of the

basic data is considerable, errors resulting from simplification are not likely to influence strongly the total uncertainty. Thus, a simple approach can be justified.

It must be concluded that although the current probabilistic risk assessment of nuclear power plants is the most systematic way to estimate structural seismic risk, for the purpose of code development, it is not directly applicable to ordinary buildings.

2.5 CODE CALIBRATION PROCEDURE

Recent developments in probabilistic analysis have led to new concepts and tools for the assessment of the safety and reliability of structures which would be of interest to the structural engineer. Using those concepts and tools (33), some structural codes have been calibrated (30-32). Code calibration has been used to adjust code factors so that the resulting safety levels are the same as those obtained for successfully surviving structures designed to earlier codes. The purpose of this section is to outline details of the code calibration exercise undertaken in NBS577 (National Bureau of Standards Special Publication 577) (30), which influenced research in this field. In NBS577 the values of the resistance and load factors for a strength design code were selected such that the spread of code implied-safety levels among structures is minimised, while maintaining the existing or target safety level.

First, in order to understand the code calibration by NBS577, basic techniques and assumptions should be explained. The fundamental procedure uses the advanced First-Order Second-Moment (F.O.S.M.) method to estimate existing code-implied safety levels and conversely to obtain the resistance and load factors to be used in strength design codes for a given safety level. The application of the F.O.S.M. method is discussed in the next subsection. In the application, bias factors must be assumed which are the ratio of the mean resistance or load intensity value to the respective specified nominal value. In order to expose the difficulties involved in the earthquake load case, details of the assumptions on the bias factor for this are described in section 2.5.2. Subsequently, a code calibration procedure taken by NBS577 is discussed as well as the critical view of the work.

2.5.1 Application of Advanced First-Order Second-Moment Method to Code Calibration

The F.O.S.M. method is particularly useful for code calibration. In calibrating a structural code, there are two important aims; one is to establish existing safety levels, and the other is to determine code factors giving a target safety level. The procedure is briefly explained (1,30) using some simple examples.

Most code calibraton exercises, including NBS577, have evaluated the safety of a structural element on the basis of a linear performance function; that is:

$$g = R - \left(\sum_{i=1}^{m} Q_i \right) \tag{2.5.1}$$

where: R = the resistance of the element (e.g. flexural strength)

Q_i = ith load effect on the element

m = number of applied loads

In strength design codes, the most general format uses multiple resistance and load factors, in the following general form:

$$\phi R_n \geq \sum_{i=1}^{m} \gamma_i Q_{n_i} \tag{2.5.2}$$

where: ϕ = the resistance factor

γ_i = load factor to be applied to load Q_i

The subscript n denotes the "nominal" design values of resistance and loads, which are based on specified ways of obtaining them in a structural code. The nominal values are generally different from the corresponding mean values $\overline{R}$ and $\overline{Q}_i$. Thus, in order to estimate existing code implied safety level for a member using the F.O.S.M. method with Eq. (2.5.1) for the performance function, the ratios of the mean values to the respective specified nominal values must be evaluated, that is:

$$\nu_R = \frac{\overline{R}}{R_n} \tag{2.5.3}$$

$$\nu_{Q_i} = \frac{\overline{Q}_i}{Q_{n_i}} \quad (i=1,2,\ldots,n) \tag{2.5.4}$$

The ratios ν_R and ν_{Q_i} can be called the bias factors. In addition, the coefficients of variation (C.O.V.) for the bias factors must be assessed for the implied safety level. However, in general, it is not easy to estimate the values of the bias factors. The particular difficulties for earthquake loads are discussed in the next subsection.

Based on the assumptions for the bias factors, existing code-implied safety level can be calculated for specified load ratios Q_{n_j}/Q_{n_1} (j=2,3...,n).

For example

$$g(\mathbf{X}) = R - D - L \qquad (2.5.5)$$

where $D(=Q_1)$ = the dead load effect

$L(=Q_2)$ = the lifetime maximum live load effect

Suppose the requirement in a structural code is:

$$0.9\ R_n \geq 1.4\ D_n + 1.7\ L_n \qquad (2.5.6)$$

That is:

$$\phi = 0.9$$

$$\gamma_D(=\gamma_1) = 1.4$$

$$\gamma_L(=\gamma_2) = 1.7$$

Consider a nominal live load to dead load ratio of

$L_n/D_n(=Q_2/Q_1) = 0.68.$

Assume, also:

$$\nu_R = 1.05 \qquad \nu_D(=\nu_{Q_1}) = 1.05 \qquad \nu_L(=\nu_{Q_2}) = 1.15$$

and: C.O.V. $\nu_R = 0.11$ C.O.V. $\nu_D = 0.10$ C.O.V. $\nu_L = 0.25$

The ratio of the mean live load to dead load may be:

$$\frac{\overline{L}}{\overline{D}} = \frac{1.15L_n}{1.05D_n} = \frac{1.15}{1.05} \times 0.68 = 0.745$$

or: $\overline{L} = 0.745\ \overline{D}$

The requirement in Eq. (2.5.6) becomes:

$$0.9\ \frac{\overline{R}}{1.05} = 1.4\ \frac{\overline{D}}{1.05} + 1.7\ \frac{\overline{L}}{1.15}$$

from which the required mean resistance is:

$$\overline{R} = 2.831\ \overline{D}$$

Therefore, according to Eq. (2.2.30), the safety index is:

$$\beta = \frac{\overline{R} - \overline{D} - \overline{L}}{\sqrt{\sigma_R^2 + \sigma_D^2 + \sigma_L^2}}$$

$$= \frac{2.831\overline{D} - \overline{D} - 0.745\overline{D}}{\sqrt{(0.11 \times 2.831\overline{D})^2 + (0.10\overline{D})^2 + (0.25 \times 0.745\overline{D})^2}}$$

$$= 2.885$$

If the variables can be assumed to be normal, the underlying probability of failure would be:

$$p_f = \Phi(-2.885) = 1.96 \times 10^{-3}$$

Conversely, when a required (or target) safety level is known in addition to the values of the bias factors, a new set of resistance and load factors can be obtained by the F.O.S.M. method. A code format for the design of structural components is, for instance:

$$\phi R_n \geq \gamma_D D_n + \gamma_L L_n \qquad (2.5.7)$$

Let us determine the appropriate factors, ϕ, γ_D and γ_L, to achieve designs with a reliability of $\beta = 2.50$, using the same assumptions as the above example. The reliability index is:

$$\beta = \frac{\overline{R} - \overline{D} - \overline{L}}{\sqrt{\sigma_R^2 + \sigma_D^2 + \sigma_L^2}}$$

$$= \frac{\overline{R} - \overline{D} - 0.745\ \overline{D}}{\sqrt{(0.11\overline{R})^2 + (0.1\overline{D})^2 + (0.25 \times 0.745\overline{D})^2}}$$

$$= 2.5$$

resulting in the following quadratic equation:

$$\bar{R}^2 - 3.775\ \bar{D}\ \bar{R} + 2.992\ \bar{D}^2 = 0$$

The solution for $\bar{R}$ is:

$$\bar{R} = 2.643\ \bar{D}$$

and: $\sigma_R = 0.11\ \bar{R} = 0.291\ \bar{D}$

The direction cosines are (see Eq. (2.2.33)):

$$\alpha_R^* = \frac{\sigma_R}{\sqrt{\sigma_R^2+\sigma_D^2+\sigma_L^2}} = \frac{0.291\bar{D}}{\sqrt{(0.291\bar{D})^2+(0.1\bar{D})^2+(0.1863\bar{D})^2}}$$
$$= 0.809$$

$$\alpha_D^* = \frac{-\sigma_D}{\sqrt{\sigma_R^2+\sigma_D^2+\sigma_L^2}} = \frac{-0.1\bar{D}}{0.3597\ \bar{D}} = -0.278$$

$$\alpha_L^* = \frac{-\sigma_L}{\sqrt{\sigma_R^2+\sigma_D^2+\sigma_L^2}} = \frac{-0.1863\bar{D}}{0.3597\bar{D}} = -0.518$$

Hence, according to Eq. (2.2.32), the most probable points on the failure surface are:

$$R^* = \bar{R}(1 - 0.11 \times 2.5 \times 0.809) = 0.778$$

$$D^* = \bar{D}(1 + 0.10 \times 2.5 \times 0.278) = 1.07$$

$$L^* = \bar{L}(1 + 0.25 \times 2.5 \times 0.518) = 1.32$$

Hence, the appropriate mean resistance and load factors are:

$$\overline{\phi} = R^*/\overline{R} = 0.778$$

$$\overline{\gamma}_D = D^*/\overline{D} = 1.07$$

$$\overline{\gamma}_L = L^*/\overline{L} = 1.32$$

These mean factors should be used with the corresponding mean resistance and mean loads; that is, the code safety requirement would be:

$$0.78\ \overline{R} \geq 1.07\ \overline{D} + 1.32\ \overline{L}$$

Therefore, in terms of the nominal values, the above safety requirement becomes:

$$0.78(1.05R_n) \geq 1.07(1.05D_n) + 1.32(1.15L_n)$$

or: $$0.82\ R_n \geq 1.12\ D_n + 1.52\ L_n$$

It should be noted that code calibration discussed here is based on the safety of a member being considered, not on that of the entire structure.

2.5.2 The Estimation of Bias Factor for Earthquake Load

As explained in the previous subsection, to estimate existing code-implied safety or conversely to select a new set of code factors to correspond with a given target safety in code calibration (30), assumptions with respect to bias factors need to be made. The purpose of this subsection is to illustrate the difficulty in assessing the distribution of bias factors Q/Q_n for earthquake load. This is a matter of prime concern in the present project. The following four steps were used in NBS577 to obtain the distribution (30):

1. Determination of the mean value $\overline{Q}$ of load effect due to earthquake: Load effects for conventional buildings, representing the effects of seismic ground shaking, are normally determined by methods based on static analysis. Loads, which are proportional to base shear, are explicitly calculated from equations of the form:

$$Q = B \cdot A \cdot S_{V_0} \cdot S \cdot 1/\mu \cdot W \qquad (2.5.8)$$

where: A = peak ground acceleration

S_{VO} = spectral amplification factor (a function of structural period and damping)

S = soil factor (assumed equal to 1 for calibration purposes)

W = weight of structure

μ = system factor (ductility factor). This only

applies to some (older) codes. More modern codes incorporate μ into the inelastic response spectrum. Therefore load is not inversely proportional to μ.

B = a random factor with mean of unity, introduced to account for load modelling and other uncertainties

Assuming values of R=5, $S_{V_0} = 1.2/(T)^{2/3} = 2.7$ (for period T=0.3), then the mean value $\overline{Q}$ of load effect due to earthquake is:

$$\overline{Q} = 0.54\ \overline{A} \cdot \overline{W} \qquad (2.5.9)$$

where: $\overline{A}$ = the mean value of peak ground acceleration

$\overline{W}$ = the mean value of weight of structure

Statistical mutual independence between items in the equation is implicitly assumed.

2. Determination of nominal earthquake load Q_n: To relate nominal values to the mean $\overline{Q}$, a procedure from the 1976 Uniform Building Code (34) is used in which:

$$Q_n = Z \cdot K \cdot C \cdot I \cdot S \cdot W \qquad (2.5.10)$$

where: Z = zone factor

K = building factor (1 for ordinary frames)

C = base shear coefficient (0.12 for $T \leq 0.3$)

I = importance factor (1 for calibration

purposes)

S = soil factor (again 1 for calibration purposes)

W = equivalent weight of building

Therefore:

$$Q_n = 0.12 \cdot Z \cdot W \qquad (2.5.11)$$

3. Assumption of distribution of peak ground acceleration A: Following the Algermissen-Perkins study (35), the probability distribution of the 50-year maximum ground acceleration, in which the hazard is considered, is a Type II extreme value distribution, viz:

$$F_A(a) = \exp\left[-\left(\frac{0.38a_{10}}{a}\right)^{2.3}\right] \qquad (2.5.12)$$

where: a_{10} = the peak acceleration with a 10% probability of being exceeded

Evaluation of Eq. (2.5.12) gives:

$$\overline{A} = 0.60\ a_{10} \quad \text{(mean)} \qquad (2.5.13)$$

and:

$$V_A = 1.38 \quad \text{(coefficient of variation)} \qquad (2.5.14)$$

4. Determination of distribution of the bias factor Q/Q_n: Because the coefficient of variation of peak ground acceleration V_A is large compared to values of other factors, the earthquake load Q is taken to have a Type II

extreme value distribution with $V_Q = 1.38$. The mean value of Q is given from Eq. (2.5.9) and (2.5.11):

$$\overline{Q} = \frac{0.32\ a_{10}}{0.12\ Z} \cdot Q_n \qquad (2.5.15)$$

Using the mean and coefficient variation of earthquake load Q, its distribution is denoted by:

$$F_Q(q) = \exp\left[-\left(\frac{0.20\ a_{10}/0.12Z \cdot Q_n}{q}\right)^{2.3}\right] \qquad (2.5.16)$$

Thus, the distribution of the bias factor Q/Q_n is simply expressed by:

$$F_{Q/Q_n}(q/q_n) = \frac{1}{q_n} \exp\left[-\left(\frac{0.20a_{10}/0.12Z}{q/q_n}\right)^{2.3}\right] \qquad (2.5.17)$$

where: A_{10} = the Algermissen-Perkins mapped acceleration

Z = the corresponding 1976 UBC zone factor for any particular city

It is obvious that the assumptions for the bias factor Q/Q_n are very crude. The authors of NBS577 noted difficulties in making more reasonable assumptions for earthquake load. They remarked that these difficulties would encourage the earthquake engineering profession to attempt to express problems in the future in terms more compatible with other loads.

2.5.3 Code Calibration Procedure - A Critical View

The basic assumption made in NBS577 is that present code formats and existing safety levels for different load combinations are adequate. With this assumption, the values of resistance and load factors are selected so that the variability of code-implied safety levels among structures is minimised, while maintaining existing average safety levels. The code calibration procedure undertaken in NBS577 consists of the following four steps making use of the F.O.S.M. method described in 2.5.1:

1. Assume bias factors for different loads and resistances.

2. Obtain safety levels for the existing code over ranges of different load ratios. The safety levels are obtained for different load combinations, materials, and structural types. Based on the study, a target safety value for each load combination is determined so that it is a representative average value for the whole range of other parameters.

3. Select one set of load factors for each load combination that minimises the extent of deviation of safety from the target among different structures, when considered over all likely combinations of load.

4. Select resistance factors so that new minimum safety levels are adjusted to corresponding target safety values.

In NBS577, load factors for each load combination were estimated. For resistance factors, information relevant to relationships between safety levels and resistance factors was simply furnished to any code specification writing group.

Three questions arise with regard to the method of code calibration.

Firstly, a code is a set of laws or rules which must not be violated. A structural code must thus be considered to specify the minimum required quality or safety level for structures, not the average. This means, even a structure possessing the lowest safety level must be safe enough. Therefore, a minimum safety level must be the criterion for structural codes. The target values proposed in NBS577 are set at existing average safety levels. They are therefore inadequate from this viewpoint.

Secondly, the minimisation of variability of safety levels among structures is based on the assumption that present code formats are adequate. However, present code formats have not been examined as to the format which can produce minimum safety variability. Thus, to obtain the "global" minimum variability, code formats should be reconsidered as well as the values of code factors.

Thirdly, this method of code calibration, based on the safety of individual members, must be considered as being inadequate due to its emphasis on individual member behaviour. This is especially true for the earthquake provisions. The assessment of structural safety must necessarily be concerned with behaviour of the total structure and not with the reliability of individual elements only. Such a limitation is particularly serious in regions, such as New Zealand, where earthquake loading tends to dominate the controlling resistance of structures.

CHAPTER 3

CONSIDERATIONS OF FAILURE PROBABILITIES IN CODE DEVELOPMENT

3.1 INTRODUCTION

The prime matter of interest in the present study is structural safety. The intention in using probabilistic analyses in the structural safety is to make sure that a structure possesses at least the required minimum safety. The intention is attractive and simple, but its realisation runs into difficulties. One of the difficulties is conceptual, another is technical. Even when solutions to difficulties are beyond the engineer's capabilities, he is expected to design reasonably safe structures. This means that in site of the facts that conceptual agreement has not yet been attained and the necessary data and techniques are not fully available, it is necessary to arrive at solutions. The gap in concepts, data and techniques represents a significant hurdle in developing a reasonable code.

In a probabilistic analysis errors, uncertainties and correlations between parameters are considered. In contrast a deterministic analysis only takes account of a representative value, usually the mean, for each parameter. Therefore a probabilistic analysis requires additional data

relevant to uncertainty and correlation. Uncertainty and correlation must be considered in an analysis because they do exist in real situations and often affect markedly engineering decisions. Nevertheless doubts exist with respect to probabilistic analyses. The main cause of doubts stems from the questionable quality of data and techniques in the analysis. It is not easy to obtain the required additional data. Moreover, because the processing of additional data makes the analysis more complicated, approximations are usually required to enable results to be obtained. The use of incomplete data and of approximations in techniques leads to certain limitations in the application of probabilistic analyses.

The final aim of which the present study is a part is to develop a rational structural code in which all appropriate applications of probabilistic concepts are used. As discussed previously in Chapter 1, such a code may be called a "balanced code". The central purpose of the present chapter is to discuss the concept of a balanced code. In developing a balanced code, two important and interrelated aspects need to be considered. The first issue relates to code implied safety levels. The major purpose of a structural code is to ensure minimum safety levels for different structures subjected to different loads. The required safety levels may depend on the expected consequential losses. Hence, the required safety levels are necessarily different for different structures and different types of loading. Interestingly it has not been questioned for example how much safer a 10-storey office building

should be than a 2-storey apartment house or how much higher should safety levels be in earthquake provisions than those catering for gravity loads only. Conceptual difficulties are involved in assessing the required minimum safety level with which the lowest value of code implied safeties among structures must coincide.

The second issue relates to a desirable format of the code. The format should enable a classification of types of structures, materials, load combinations and other parameters to be made. Safety levels for classified structures should correspond to the required values. As the number of categories becomes smaller the code becomes simpler. However, at the same time the variation of code-implied safety from the required value becomes larger. A Large variation means that the implied safety levels of many structures differ from the target minimum value leading to a large number of overly conservative and hence uneconomic structures. This poses a dilemma for the code writer; a small number of classifications is desirable because a general structural code should be simple, while a large number leads to more economical structures. In developing a balanced code a compromise solution to the dilemma must be found.

Therefore difficulties exist both in technical and conceptual matters in developing a balanced code. The difficulties must lead to a necessity for crude assumptions to be introduced in code development. However, because it is even more difficult to justify the existing minimum

safety levels and appropriateness of format in present codes, to develop a balanced code must be a valuable exercise despite the limitations.

A major purpose of this chapter is to outline the means whereby a balanced code, using probabilistic techniques, may be formulated. Firstly, the appropriate applications of probabilistic analysis are described. Subsequently the scope of the present study is described, which is a significant step in the process leading to the development of a balanced code.

3.2 APPLICATIONS OF PROBABILISTIC ANALYSIS

Errors and uncertainties present in structural reliability analysis can be classified into three categories (36):

1. Random errors; these are inherent uncertainties associated with statistical variations.

2. Systematic errors; they are related to real physical phenomena and include errors introduced by inadequate data, inadequate modelling of probability distributions, approximations and simplifications made for expediency of calculation.

3. Human errors; these include blunders arising from human fallibility, errors in calculations, gross error in engineering judgements, etc.

In probabilistic analyses the relevance of such errors and uncertainties can be theoretically considered. However, in practice, not all the information can be taken into account in an analysis, because some may not be able to be handled numerically while others remain completely unknown. Surprisingly, this mismatch between theory and practice is not well known. Misunderstandings may arise from the notion that results takes into account all types of error . Accordingly a different classification is required whereby information is divided into two groups, i.e.:

1. Tractable information, which can be considered in a probabilistic analysis with appropriate reliability parameters; and

2. Intractable information, which cannot be directly quantified in an analysis.

It is therefore of considerable interest to establish how intractable information affects the results of probabilistic analyses, and how tractable information should enter such analyses.

3.2.1 Intractable Information and Probabilistic Analysis

Intractable information can be defined as data which is potentially related to the probability problem being considered, but which for some reason cannot be properly

quantified and assessed, and hence processed by the analysis. In many cases adequate information on factors which affect results is not available because of limitations of the present state of the art. In other cases information cannot be numerically quantified since its effect is too involved or insufficiently understood.

Human error is generally considered to belong to this group. The effects of human errors have been studied by considering the history of past accidents (37-39). According to Pugsley (39), possible sources of the occurrence of human errors are:

1. The use of new or unusual materials;
2. The introduction of new or unusual methods of construction;
3. The design of new or unusual types of structure;
4. Lack of experience in organisation, design and construction;
5. Unfavourable industrial climate;
6. Financial climate; and
7. Political climate.

Some researchers have attempted to bring human error into reliability studies (37,40) but they have encountered difficulties.

In spite of the presence of intractable information such as human error, structural safety levels have been assessed based only on tractable information, as described in Chapter

2. It is thus important to consider how the failure probabilities calculated without using intractable information should be understood. Using the classification of tractable and intractable information, failure probability P[F] can be expressed by (40):

$$P[F] = P[F|\bar{E}]\cdot P[\bar{E}] + P[F|E]\cdot P[E] \qquad (3.2.1)$$

where: $P[F|E]$ = conditional probability of failure given E, i.e. likelihood of failure when event E occurs

$P[F|\bar{E}]$ = conditional probability of failure given $\bar{E}$

E = the fundamental cause is due to matters involving intractable information (such as human error)

$\bar{E}$ = the fundamental cause is due to matters involving tractable information (such as low steel yield strength)

The probability P[F] corresponds to so called "observed" failure probability, and the term $P[F|\bar{E}]$ is the classical failure probability treated in reliability analyses only using tractable information which may be referred to as "calculated" failure probability.

According to Ellingwood (40), the majority of structural failures are due chiefly to errors in design and construction, rather than to stochastic variability in

structural strengths and loads. Only about 10% - 20% of failures are traceable to stochastic variability. Thus, the remaining 80% - 90% are found to be due to other causes associated with intractable information. That is, the conditional probability of the occurrence of failure events associated with intractable information given that a failure is found, $P[E|F]$, is between 0.8 and 0.9. Elms (41) also suggested that stochastically traceable failure probability can be 1% - 10% of the actual failure probability, i.e. $P[E|F] = 0.9\text{-}0.99$. This indicates that calculated values of failure probability using tractable information grossly underestimate the values of actual risks. Consequently, because of the presence and preponderence of intractable information, absolute values of calculated failure probability based only on tractable information should be considered meaningless.

Let us consider whether calculated failure probabilities based only on tractable information are useful for the derivation of relative risk levels. Equation (3.2.1) can be transformed into:

$$P[F] = P[F|\bar{E}] \cdot \frac{P[F]}{P[F|\bar{E}]}$$

$$= P[F|\bar{E}] \cdot M_I \qquad (3.2.2)$$

where:

$$M_I = \{1 - P[E|F]\}^{-1} \cdot P[\bar{E}] \qquad (3.2.3)$$

The term M_I may be thought of as an intractable information

multiplier of the classical failure probability $P[F|\bar{E}]$. If the multipliers for different structures were much the same, a calculated failure probability $P[F|\bar{E}]$ would be used as a relative risk level in place of P[F]. Thus, it is necessary to know the variation of M_I among different structures and structural types. Unfortunately a reasonable solution does not seem to be available. Figure 3.2.1 shows the relationship between P[E|F] and the first term $(1-P[E|F])^{-1}$ in M_I, together with the likely region of importance of P[E|F] after Ellingwood (40) and Elms (41).

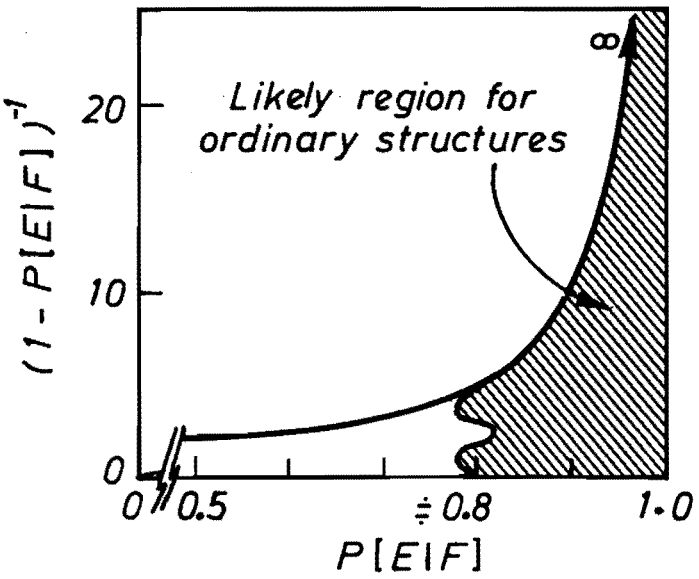

Fig. 3.2.1 Values of the first term in the intractable information multiplier (see Eq. 3.2.3)

Intuitively some structures may be considered to have larger values of P[E|F] than others. For instance, a carefully designed and at least relatively well quantified structure like a nuclear power plant, may have a larger P[E|F] value

than, say, a crudely designed soil structure. In other words, when a failure occurs in a nuclear power plant, human error is more likely to be involved than when a soil structure fails. Thus, the term $(1-P[E|F])^{-1}$ may vary from structure to structure. Similarly, the second term $P[\bar{E}]$ (or $1-P[E]$) in M_I may also depend on the structure, considering the possible sources for human error as stated earlier. However, it is likely that when we compare similar structural systems consisting of similar types of structures, materials, comparable loads, etc., the intractable information multipliers will also be similar. Therefore the reliability of the *comparison* of calculated failure probabilities will be reasonably high.

In conclusion, two important points need be emphasised in using a probability analysis (23).

(a) All probabilistic analyses are comparative in some way and hence should be thought of as such.

(b) The more alike are the situations compared, the more reliable the results will be.

Therefore, the results of calculations for failure probability should not be viewed in any sense as predictions of actual failure probability, but rather as matching criteria for a structure to be safe when considering some modes of failure (44).

The problem is related not only to probabilistic analyses.

It arises also in all engineering works, as intractable information is always involved. For example, a time history structural analysis would not be justified as a predicting tool, but it could have considerable use in enabling the analyst to understand the overall behaviour of complex structures.

3.2.2 Tractable Information and Probabilistic Analysis

In solving a safety problem, a wealth of information relevant to modelling and data is generally available. Such information which can be used in an analysis may be called tractable information. However, the accuracy (or degree of quality) of different data will vary; some are very accurate, while some are crude. Likewise, the accuracy and complexity of modelling may also be variable. Usually the more complicated the model, the more accurate the results that can be expected. Sensitivity of results to data and modelling will also be variable. A subtle change in data can strongly affect results. This means that some results are sensitive to the quality of data, while some others are hardly affected.

A question which arises is; what data out of the available tractable information should actually be used to obtain acceptable results while only consuming a reasonable effort. Accuracy, complexity and sensitivity are aspects to be considered in selecting usable information for solving a problem. For example, in dynamic structural analysis,

response results are very sensitive to the parameters defining the input earthquake motions. However, the quality of such input information is poor as explained in Section 5.2 and 7.2. Thus the quality of the result cannot be better than the quality of the definition of earthquake motions, even if complex analyses and accurate structural data are used. This means, that sophistication of analysis and accuracy of the structural data used are of no particular advantage. Similarly, in developing a reasonable system for probabilistic analysis it is often justifiable to avoid unnecessary complexity.

Probabilistic analyses demand more data than deterministic analyses. Not only is the mean value for each variable required, but also its variance is needed to determine the associated probability distribution. Such variables are called random variables. Generally correlation between random variables is also taken into account. The additional data makes probabilistic analyses so complicated that approximations are often needed to obtain a result. Therefore it is frequently necessary to reduce the number of random variables. Moreover, the quality of the additional data is often very variable. It may well be that the quality of only a few variables controls the quality of the result. In such cases the number of random variables can be reduced.

A useful concept for avoiding unnecessary complexity is the "Principle of Consistent Crudeness" (44) which postulates that for any system the sensitivity-modified quality of any

item of input information should not be made significantly better than that of the input item with the lowest quality.

The practical application of the principle involves some difficulties. In many situations, judgements about quality and sensitivity can be expressed only qualitatively rather than quantitatively. Typically qualifying phrases such as "very poor" or "somewhat sensitive" are used. Therefore in practice, subjective engineering judgement must often be used when applying the above principle.

Concluding statement (b) of 3.2.1 is valid also for the relationship between tractable information and probability analyses. The emphasis in the remark is that the nearer the compared situations are to each other, the smaller will be the effects of errors, uncertainties in modelling assumptions, etc. For instance, if failure probabilities for two different buildings subjected to earthquakes on the same site are compared, uncertainties of earthquake parameters cannot affect comparative results significantly. However, if the buildings are located on different sites, the effects of the uncertainties become greater and hence the result of the analysis will be less reliable than for the previous case.

In Section 3.2, three important issues have been examined, which are relevant to the application of probabilistic analyses to engineering problems; they are statements (a) and (b) of 3.2.1, and the principle of consistent crudeness. These issues will be carefully taken into account in

developing a procedure for assessing failure probabilities of structures subjected to earthquake, which is the major aim of the present study.

3.3 A BALANCED CODE

In applying various techniques of probabilistic analyses to an engineering system, new concepts with regard to the system most suitable for the applied techniques are usually required to be established. Such conceptual problems often puzzle engineers.

Techniques of probability analysis are not new. They have been applied to many engineering problems. Such analyses have also been employed in code development (see Section 2.5). However, the make up of a fully rational structural code, fully incorporating probabilistic concepts has not been established as yet despite the advances made in the development of limit-state codes. A structural code, among other matters, is expected to define the minimum allowable safety of structures. This aim faces a great deal of uncertainty. Two of the many questions which arise are; at what level should the minimum safety be? Should the minimum safety levels of structures subjected to different loading types be the same? Although these considerations are fundamental, they are not often considered by engineers. In this section, conceptual as well as technical difficulties relevant to the development of a rational code based on probabilistic concepts are discussed. Despite the difficulties, because of the limitations of present codes,

engineers must still try to develop a more rational code. This thesis aims to contribute to the development of such a rational code which, for reasons discussed below, will be called a "balanced code".

The idea of a balanced code is based on the concept of balanced risk. Therefore an application of the balanced risk concept to structural risks is described in the next subsection. It will be seen that estimates of the consequences of structural failure are subject to wide variations. Taking into account the uncertainty of consequences and the limitations of probability calculation, proposals for a reasonable balanced code relevant to structures in the same category of importance will be considered in Section 3.3.2.

3.3.1 Concept of Balanced Risk and Structural Risk

The concept of balanced risk was postulated by Wiggins (45). It implies that, for example, the risk of traffic accidents should be related to that of earthquakes. Starr (46) suggested a very similar concept. Risk can be expressed by:

$$(\text{Risk}) = \left[\begin{matrix}\text{Probability of} \\ \text{Occurrence}\end{matrix}\right] \times (\text{Consequences}) \qquad (3.3.1)$$

Therefore, the larger the expected consequences for the same risk, the smaller should be the probability of occurrence. Figure 3.3.1 quantifies and illustrates the application of the balanced risk concept in structural engineering. Based on statistical data of general accidents in a society,

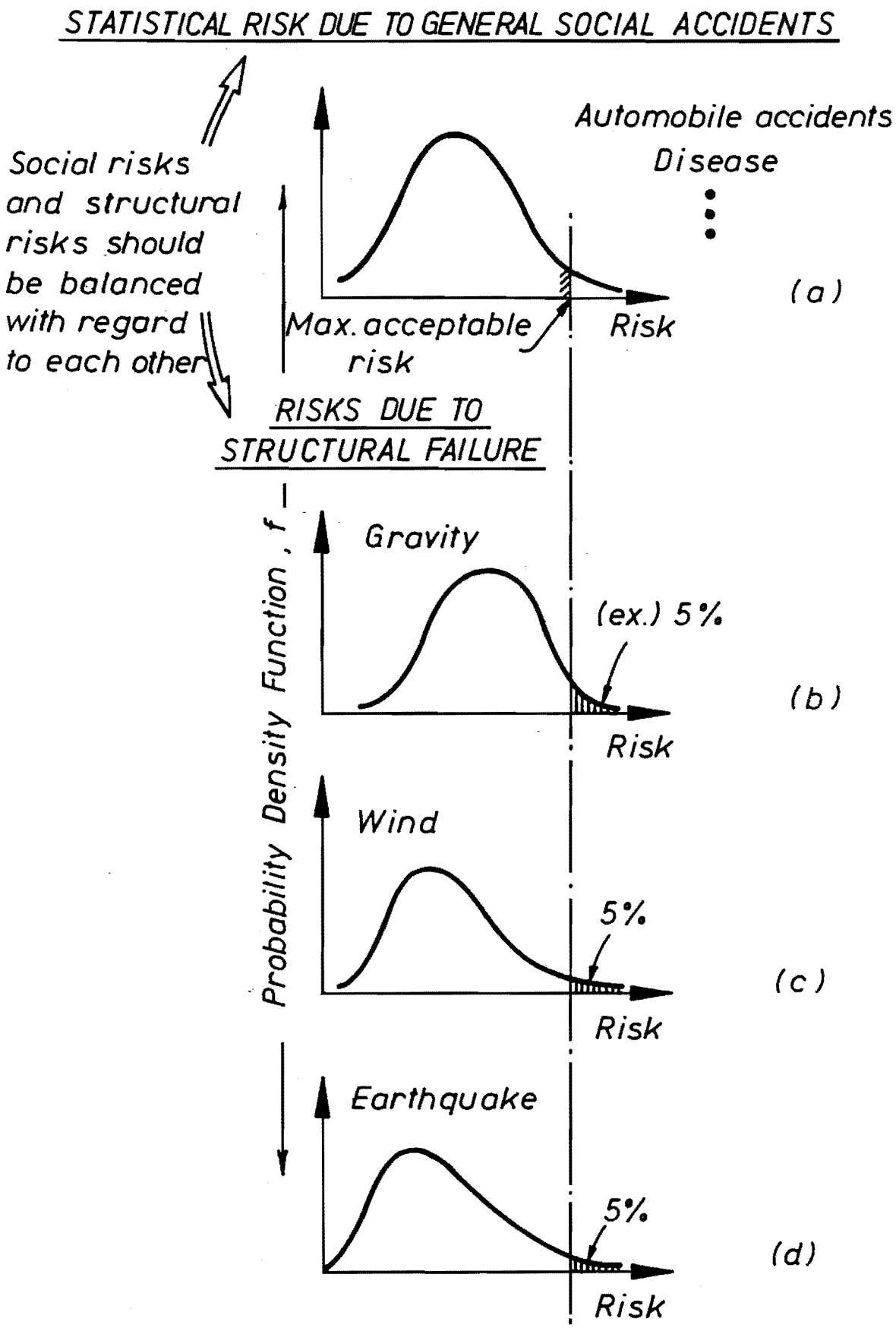

Fig. 3.3.1 Relationship between risks due to general social accidents and due to structural failure

associated for example with motor vehicles, work, disease, etc., a maximum acceptable risk ("social risk") can be determined. Figure 3.3.1(a) illustrates such an evaluation. The expected risks consequent on structural failure due to different causes, such as excessive gravity load, extreme wind or earthquake effects could then be related to the social risk as illustrated in Fig. 3.3.1(b). The task is then to establish a reasonable balance between the social and the structural-failure risks.

A fundamental difficulty in the application of this approach lies in obtaining the expectation of structural risks consistent with those of social accidents, because of the following reasons:

(1) Since the return periods of structural disasters are generally much longer than those of ordinary accidents in the community, not enough data has been amassed to predict the probability of occurrence and consequences of structural disasters; and

(2) The consequences of structural failure are expected to be more complex and involve more items, compared with those of ordinary social accidents which can be measured by loss of life.

Even if we had quite a few data of consequences of structural disasters, it would not be very easy to utilise the data for the application of the balanced risk concept.

Firstly, these data are based on observed structural failures which are dominated by effects of intractable information such as human error. In estimating adequate safety levels, tractable-information failures, not intractable, are needed. However, in general such information is seldom available. Secondly, design standards change with time. The basic concepts for designing a structure as well as the implied safety levels in recent structural codes are very different from those of, say, twenty years ago. Thus, statistics using observed data on damage of structures designed to old codes cannot be directly utilised for predicting the damage of structures designed according to a recent code. Moreover, the number of different types and causes of failure observed would be enormous, such as ductile and brittle member failures, total mechanisms of structures and excessive external loads and blunders. Thus, the observed data themselves are so involved that application of damage data to the balanced risk concept is not straightforward.

Interesting further questions which arise from item (2) above are; how to estimate different consequences of structural failure, and what measure is appropriate to express a total consequence. Some of the possible consequences of structural failure can be for example monetary loss, time loss, injury, loss of life, loss of prestige, displeasure and social aversion. To assess a total consequence, monetary value or utility value criteria can be used. These are widely used in decision analysis (1). A common difficulty in both the methods is that values

for criteria are highly dependent on decision makers (47). Suppose that a few structures collapsed during a small earthquake and that a few people died. A member of a structural committee may put greater emphasis on loss of prestige of the code, while an owner of a structure may only consider the monetary loss. Of paramount significance may be the loss of lives. Who should be the decision makers in such an event to determine the total value of the consequences? How can consensus be obtained? The difficulties are conceptual rather than technical. Indeed, it has been said that in these matters the philosophical difficulties are greater than the technical ones (48).

To bypass these difficulties, it could be assumed that loss of life is the only significant consequence in considering total structural risk. Based on this assumption, Wiggins (45) and Starr (46) made suggestions relevant to the relationship between social and structural risks. Wiggins proposed that engineers should design all buildings in a city so that the probability of getting killed in any particular building during an earthquake is equal to or less than that in getting killed in a car accident, or while working.

Similar suggestions of Starr conclude that the statistical risk of death from disease appears to be a psychological yardstick for establishing the level of acceptability of other risks.

However, the number of fatalities per accident and social

acceptance are not proportional. This means that a single accident with 120 fatalities per 10 years due to a structural collapse seems much more significant than accidents with one fatality each month for 10 years. Of course, it is not an easy task to predict the number of lives which may be lost as a consequence of a structural failure. Thus the simplified concept of risk balancing cannot be considered realistic enough to be used for the purposes of a balanced code.

Consequently, instead of estimating the consequences for each failure of a structure, classifications based on broad judgement with respect to expected consequences can be used. Such a classification is implied by a code with the use of risk and/or importance factors.+ The concern of the present study is limited to structures in the same classification. This is because it is difficult to quantify differences in consequences between classes. For example, it is difficult to quantify the consequences associated with the collapse of a hospital or a 30-storey building in comparison with those attached to an ordinary building. Moreover, if consequences were to be estimated, it would not be easy to achieve the relative differences in required safety levels to obtain the same risk using calculated failure probability $P[F|\overline{E}]$ because of the effect of intractable information on observed failure probability $P[F]$. As explained earlier, a

---

+ A risk factor assesses situations in which a single instance of structural failure could lead to significant loss of life. The importance factor on the other hand is intended to quantify the social and economic importance attached to the survival and functionality of a building.

calculated failure probability $P[F|\bar{E}]$ can be used instead of $P[F]$ when comparing relative safety levels for similar structures. However in general it is difficult to justify the use of $P[F|\bar{E}]$ for structures in different classes in terms of expected consequences of failure. This implies that the values of risk and importance factors used in a code are difficult to determine because of inevitable reliance on intractable information.

The consequences of failure of a structure due to different causes cannot be the same. Failure due to gravity load for example could be the failure of a single beam or slab. On the other hand an entire structure may be affected by a failure due to earthquake. As discussed earlier, the uncertainty relevant to these issues is overwhelming. To attempt to distinguish between quantified consequences of a particular model of failure appears at present to be meaningless exercise. Therefore for the purpose this study the consequences of failure of a structure subjected to different loads will be assumed to be the same.

Thus in the following subsection, structures in the same category in terms of expected consequences of failure will be considered. A balanced code for this type of structure will be discussed. Because of the assumed identity of consequences of failure, safety balancing or conversely balancing of failure probability can be substituted for the risk balancing expressed by Eq. (3.3.1).

3.3.2 A Balanced Code and Structural Safety

A balanced code must be based on the concept of balanced risk. As stated, because of simplifying assumptions "risk" can be replaced by "failure probability" (or safety). The contribution of structural safety to a balanced code is examined in this subsection.

To begin with, let us consider a procedure for developing an ideal code for structures in the same category in terms of failure consequences subjected to different loadings. Because of the limitation of the present state of the art, it seems impossible to develop an ideal code completely. But clarifying the nature of an ideal code helps us to understand what we can do towards the development. A procedure for an ideal structural code could be as follows.

(1) Set a minimum required safety level such that social risk and structural risk are balanced. The required safety should be identical for the different structures and loading types being considered, as explained in the previous subsection.

(2) Assess existing safety levels of structures for different loadings.

(3) Adjust the lowest existing safety level of structures in each class and for each load case to the minimum required safety level in order to

make sure that all structures possess at least the acceptable minimum safety.

(4) Minimise the spread of safety levels between structures in each category, keeping the lowest existing safety level unchanged. This will result in structures designed to the code being economical, for otherwise a large variability would mean a large number of structures would have safety levels well above the minimum required safety and their designs would be too conservative.

However, in practice, an appropriate minimum required safety cannot be well defined because the failure consequences of structures cannot be satisfactorily estimated. Moreover, it is difficult to adjust the lowest existing safety to the required safety. The existing safety could be estimated by using calculated failure probabilities $P[F|\bar{E}]$. However, the minimum required safety is based on observed failure probabilities $P[F]$. Thus it would be necessary to obtain the value of the intractable-information multiplier M_I in Equation (3.2.3), but this is generally unknown. The existing safety level could also be evaluated from observed structural damage. However, we would have to wait for uncontrollable experiments to occur to obtain enough information for the lowest existing safety; an impractical alternative.

Because of these limitations, the ideal procedure for developing a balanced code cannot be followed. A practical

procedure will involve some compromise. We proceed by stating two criteria for practical code development:

(1) Minimum safety levels for different loadings should be the same.

(2) The spread of reliability between structures should be minimised.

The criteria can be achieved by comparison between relative calculated failure probabilities. However, significant uncertainty exists with respect to these criteria, which must be relied on to ensure that the failure risks of structures designed with the aid of the balanced code are equal to the acceptable social risks.

In addition considerable uncertainty is also expected in predicting earthquake characteristics, as explained in Section 5.2 and 7.3. Thus, an important question arises, which is, whether the proposed approach for developing a balanced code is worthwhile in the light of the underlying difficulties and data uncertainty. Can the proposed procedure lead to a better code than existing codes; that is, would it lead to more consistent and economic designs? The answer is, almost certainly, yes. Existing codes have the disadvantage that the balance of relative severity between loading cases is unknown, primarily because of the difficulty of predicting safety levels due to earthquake loading.

Finally, it should be noted that in accordance with the principle of consistent crudeness (see 3.2.2), the uncertainty involved does not justify the use of sophisticated techniques for safety evaluation.

3.3.3 Developments for a Balanced Code

The code to be considered is based on strength using a load factor method. This has been adopted in many countries using such names as limit states or L.R.F.D. codes. The sequence of design of such a code is shown in Fig. 3.3.2. A typical code of this type classifies structures in terms of structural types, locations, occupancies, etc. (Fig. 3.3.2(a)). The required strength of an element in a structure can be determined using the required format of load combinations (Fig. 3.3.2(b)) and appropriate values of the factors given in Fig. 3.3.2(c). These are related to assumptions made in strength analysis and loads (Fig. 3.3.2(d)). Finally, details of all components and connections are determined. Although the applied load and strength demands resulting from it represent a complex phenomenon, codes must necessarily treat situations in a relatively simple manner, both for practical reasons and because the uncertainty of present knowledge does not justify a more complex approach. There is thus an inherent mismatch in complexity between physical behaviour and code idealisation (47).

Of the items in the sequence, the usual structural modelling techniques and the format of load effect derivation (Fig.

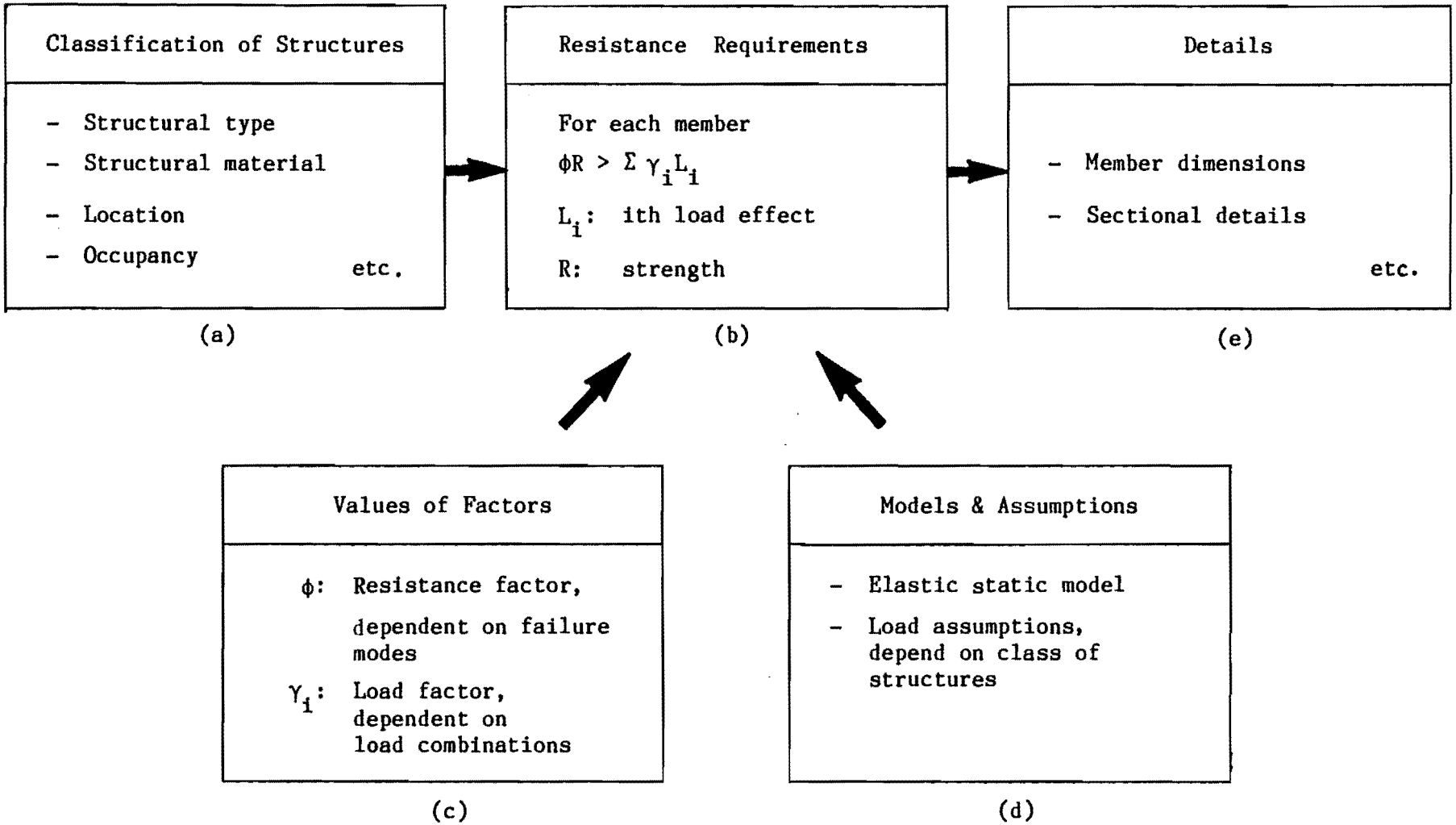

Fig. 3.3.2 The design flow implicit in a strength design code

3.3.2(b) and (d)) need not be changed for achieving a balanced code. An elastic static analysis with an assumed intensity and distribution of loads is used to obtain the required resistance capacity for each member. Moment redistributions are allowed in beams, taking account of resistance capacity based on plastic analysis for an assumed ultimate state. Thus, the analysis is elastic, but the effect of inelastic behaviour is indirectly considered in the design. Moreover, as a substitute for static analysis, the use of a dynamic analysis would be unjustifiably complex because of the uncertainty involved in loading assumptions etc. For the same reason, the simple summation of different load effects with weight factors γ_i can also be considered acceptable.

Therefore the items in Fig. 3.3.2(a) and (c) can be utilised in developing the code. As discussed in 2.5.3, the value of resistance and load factors, ϕ and γ_i, can be selected so that the variance of safety levels among structures is minimised, while maintaining an overall minimum safety. This technique can also be used for the balanced code.

Another item which relates to the minimising of the variability of safety levels is the classification of structures. The effects of code classification on reducing the variance are illustrated in Fig. 3.3.3. Fig. 3.3.3(a) shows an example of how the total distribution can be divided into three groups each of which represents one class of structures and whose variance is smaller than that of the total distribution. By suitably shifting each group

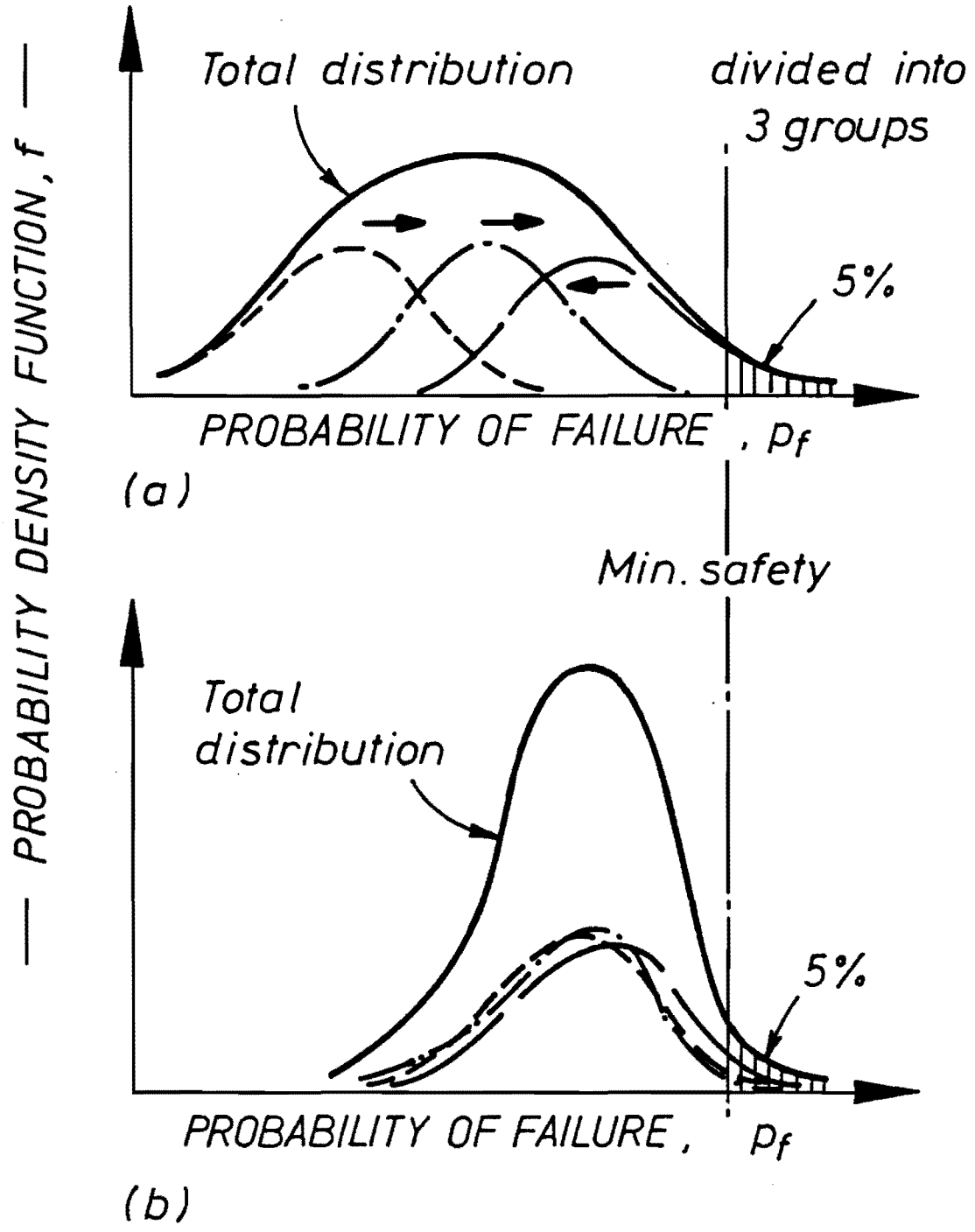

Fig. 3.3.3 Effect of classification to reduce variance

distribution, a new distribution can be achieved such that the minimum safety level is still the same as that required (Fig. 3.3.3(b)) but whose variance is smaller.

In an extreme case, by classifying each structure into a separate group, the safety of each structure can be identical with the minimum safety level. Hence, the variance becomes zero. However, since the corresponding structural code must deal with individual structural conditions, such a code would be far too complicated.

In the earthquake provisions of the New Zealand Code (49), there are three seismic categories, at least seven structural classes and factors for five different structural materials. Different structures belonging to these categories are to be designed for different specified loads. It is questionable, however, whether the total number of categories are sufficient and whether the categories for different items are well balanced. The first question is related to the acceptable level of complexity of a code. For the second question, the total variation of safety for each item is involved; the larger the total variance, the larger the number of categories required for the item. Further details for developing a balanced code will not be taken up here.

By revising resistance and load factors and the classification of structures, a balanced code which reflects the two criteria in the previous subsection can be developed.

3.4 THE SCOPE OF THIS STUDY

The present study should be of assistance in establishing an appropriate procedure for assessing structural failure probabilities, which has an important role in developing a balanced code. This section gives the scope of the study.

Firstly, earthquake loads are primarily considered. The selection of an appropriate model for seismic attack is considerably more difficult than for other load cases. One of the main reasons is that an earthquake inflicts damage to structures by forces generated by ground motions, while other loads such as wind, snow and gravity are all real loads. In the case of real loads, reasonable distributions of intensity can be assumed by some means and the magnitude of the specified load may be the only parameter to express its intensity. Moreover, using a static analysis to derive load effects is acceptable. In the case of an earthquake, however, not only its intensity but also spectral characteristics and the intensity envelope in the time domain will affect the behaviour of a structure. The characteristics of an earthquake depend also on fault mechanisms and on local foundation conditions. Moreover, the behaviour of a structure subjected to earthquake is not static but dynamic. Thus to estimate structural damage, time-dependent cyclic behaviour should be taken into account. Another consideration stems from the fact that the entire structural system is likely to be subjected to critical earthquake effects, while only some components in

the vicinity of a high live or snow load may be critically affected. Because of these difficult variables, an adequate structural model applied to seismic probabilistic analyses has not yet been established. Therefore, the failure probability of structures subjected to earthquake is the main issue of this report.

Secondly, failure due to an earthquake must be defined. From the viewpoint of strength design principles applied to earthquake loading, there might be three limit states as shown below. The violation of any of these is considered to constitute failure

(a) No damage during small and frequent earthquakes. This is essentially a stiffness criterion.

(b) No inelastic structural deformation during moderate earthquakes. This may be considered as a strength criterion for elastically responding structures.

(c) No collapse during the largest expected earthquake in the locality. This may be called a ductility criterion.

Each failure model involves corresponding consequences. However for the following reasons, collapse will be considered as the most appropriate limit state for the definition of failure.

(1) The collapse criterion (c) generally dominates a

design in areas of high seismic risk. That is, the criteria (a) and (b) are believed to be automatically satisfied if criterion (c) is met.

(2) Collapse is closely related to loss of life, which is the best single measure of consequences for social accidents.

Thirdly, the failure modes considered in the present study leading to the development of a collapse mechanism will be limited. For example for reinforced concrete structures, shear failures, beam column joint failures and other brittle failure models are not admitted. It is emphasised in many structural codes that such failure modes must not be allowed to occur. Therefore, structural codes usually specify prefered ductility failure mechanisms or energy dissipating regions. This indicates that in developing codes efforts have been made to ensure that:

(1) The probability of occurrence of unfavourable brittle mechanisms can be considered to be negligibly small; and

(2) The probability of occurrence of failure with a prefered mechanism can be satisfied with minimum safety levels.

This does not mean that the occurrence of unfavourable mechanisms is automatically negligible. An aim of probabilistic methods is to ensure that the probability of

such an occurrence is very small. Figure 3.4.1 shows failure hierarchies, explicitly or implicitly specified in the New Zealand Code (50), and illustrates how to achieve them. For example, in order to make the occurrence of a shear failure negligibly small, the shear strength of members should be greater than their flexural strength, taking into account variances. This is shown in Fig. 3.4.1(a). Similarly, to avoid beam column joint failures (Fig. 3.4.1(b)) greater strength of a joint compared with that of adjacent beams and columns is necessary. In comparison with the complexity of probabilistic analysis, a relatively simple probabilistic procedure has been developed to establish desirable failure hierarchies.

The problems associated with damage relations between storeys as shown in Fig. 3.4.1(c) and of failure probabilities with prefered mechanisms are much more difficult. Not only the strengths of the members, but also earthquake induced damage distributions among storeys need to be evaluated. Therefore the resistance mechanism of the entire structure mobilised during earthquake excitations must be estimated. Moreover, earthquake characteristics which may affect damage distribution should also be predicted. A probabilistic procedure applicable for such problems has not yet been established. A contribution toward the development of such a procedure is the aim of the present study. In this, it is assumed that the relationship between shear, beam-column joint and other brittle failures and the flexural strength of a member has been established with existing probabilistic analyses and that the

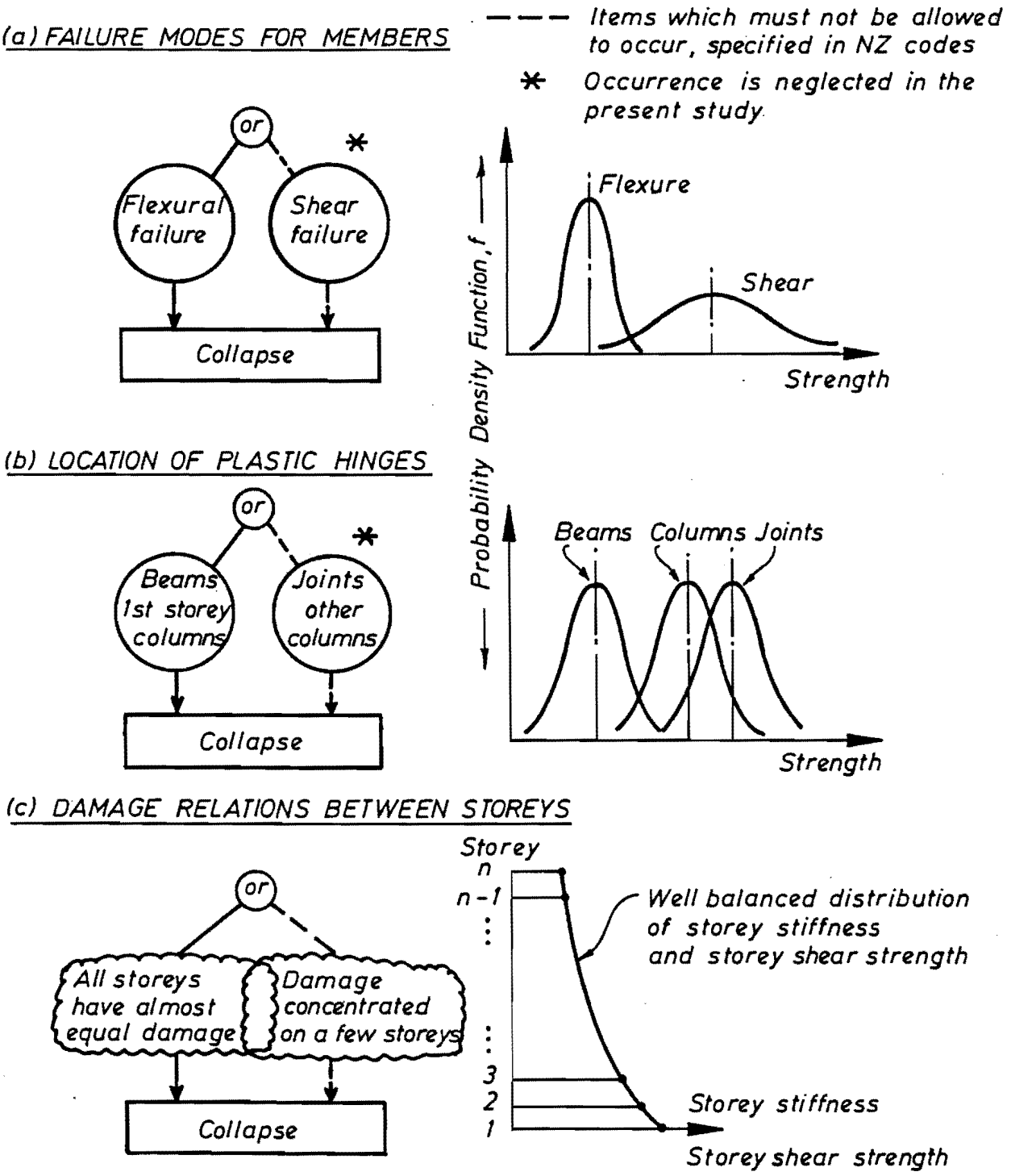

Fig. 3.4.1 Paths until collapse and code requirements

probability of occurrence of such brittle failures can be considered to be negligible.

It is particularly important to develop a balanced code for New Zealand where earthquake effects tend to dominate structural design. The existing method in New Zealand is called "Capacity Design". Its philosophy is as follows (51,52).

In the capacity design of earthquake resistant structures, energy dissipating elements or mechanisms are chosen and suitably detailed and other structural elements are provided with sufficient reserve strength capacity to ensure that the chosen energy-dissipating mechanisms are maintained at near full strength throughout the deformations that may occur.

Therefore, to develop a probabilistic method, which would enable failure probabilities occurring with the chosen mechanisms to be predicted would be of great value.

CHAPTER 4

PROBABILISTIC ANALYSIS OF A REINFORCED CONCRETE PORTAL FRAME

4.1 INTRODUCTION

This chapter discusses some of the difficulties in the realistic application of probabilistic analyses, and introduces a pilot exercise relevant to the developing of a balanced code (53). Probabilistic analysis is applied to a very simple structure subjected to dead, live and wind loads as well as earthquake forces in order to examine its limitations and to show the need for many unavoidable simplifying assumptions. The exercise indicates the technical difficulties involved in assessing a failure probability even for a simplest possible structure.

A fundamental problem in the development of any structural code is the matter of achieving consistency between its various provisions. This is particularly true with regard to the safety implications of a code. It is important to ensure, for instance, that the wind load provisions of a code are not much more severe than, say, the gravity or earthquake provisions. This is the basic concept of a balanced code. A reasonable probabilistic procedure to calculate total structural safety plays an important role in achieving such a code.

Past attempts at assessing the relative safety implications of a code have generally used an advanced First-Order Second-Moment approach, leading to the determination of reliability indices. The approach may be the only one suitable for practical usage. However, important questions concerning its credibility arise as explained in 2.2.2. A major limitation is that the reliability indices have been computed only for individual sections, and no attempt has been made to assess the probability of failure of the structure as a whole (8-14,30). Such a limitation is particularly serious in New Zealand where earthquake loadings tend to dominate structural design. Where earthquake effects are preponderant it is necessary to consider the behaviour of the structure as a whole. A piecemeal approach based on individual sections is totally inadequate, as an assessment of structural safety where earthquake loads are concerned, must necessarily be concerned with total structure behaviour and not with the reliability of individual elements.

As an approach to the development of a simple methodology for calculating total structural safety, it was decided to attempt to assess the safety of the simplest of structures first. Accordingly, a single span portal frame was chosen. This was designed in concrete (the most usual New Zealand material) using the relevant New Zealand codes (49,50). A preliminary discussion of the frame and of problems involved in its analysis is given in Reference (54). This chapter deals with the problem is considerably more depth.

Details of the frame are given in Fig. 4.1.1. Consideration of the design moment envelope, derived from elastic analysis and given in the diagram, shows that for the most part the gravity load provisions of the code predominate, with wind provisions governing for some slight reverse moment conditions.

4.2 ASSUMPTIONS AND PARAMETERS

Assumptions for calculating failure probabilities of the portal frame are discussed, which are associated with loadings, resistance, failure modes and failure criteria. Even for the simple structure, a large number of random variables are involved and many simplifying assumptions have to be made. The assumptions for earthquake loading used in Chapter 4 are rather conventional. More reasonable model for realistic structures for this load case will be discussed in the following three chapters.

4.2.1 Loading Assumptions

Four loads were taken into account such as dead (D), live (L), wind (W) and earthquake (E). It was assumed that all loads were uniformly distributed along the appropriate members except for earthquake loading which was assumed to be concentrated at beam level and also assumed to be a quasi-static force. Complete correlation of wind loads was assumed for all the members to which they were applied. Following Turkstra's rule (55), the load combinations used

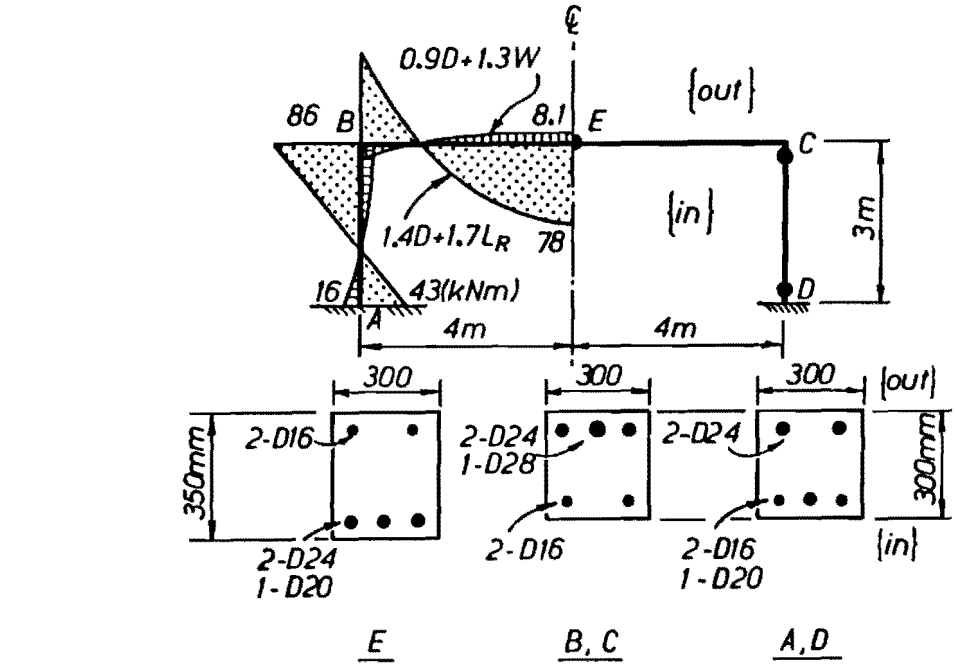

Fig. 4.1.1 Details of example portal frame

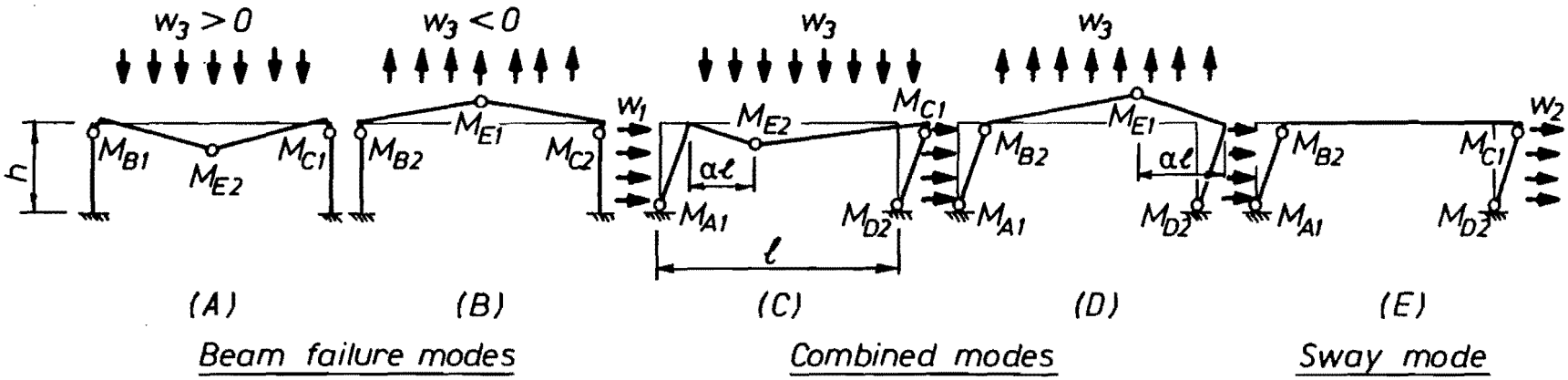

Fig. 4.2.1 Failure modes

were:

$$\begin{aligned} S_1 &= D + L_{50} \\ S_2 &= D + L_{50} + W_{APT} \\ S_3 &= D + L_{APT} + W_{50} \\ S_4 &= D + L_{APT} + E_{50} \end{aligned} \tag{4.2.1}$$

where the subscripts refer to an arbitrary point in time (APT) or to a 50 year maximum (50). This is an approximation applied to the integration in Eq. (2.2.3) or (2.2.4). That is, assuming that all loads and resistances (R) are statistically independent, from Eq. (2.2.4) the failure probability p_f can be given by:

$$p_f = \int\int\int\int\int_{g(D,L,W,E,R)<0} f_D(d)\cdot f_L(1)\cdot f_W(w)\cdot f_E(e)\cdot f_R(r)\,dd\,dl\,dw\,de\,dr \tag{4.2.2}$$

in which $f_D(d)$, $f_L(1)$, $f_W(w)$, $f_R(r)$ = probability density functions of dead, live, wind and earthquake loads, and resistance respectively; g = performance function.

Using Eq. (4.2.1), p_f can be approximated by:

$$p_f \doteq \sum_{i=1}^{4} \int\int_{g(S_i,R)<0} f_{S_i}(s_i)\cdot f_R(r)\,dS_i\,dr \tag{4.2.3}$$

Load combinations are assumed to be statistically independent. The basic random variable for wind loading was the peak gust velocity V_{APT} or V_{50}. On the windward column the uniformly distributed wind load was 0.001224 V^2 kN/m,on

the leeward column the uniformly distributed suction was $0.002456\ V^2$ kN/m, and on the beam the wind caused an uplift force of $0.003186\ V^2$ kN/m. The horizontal concentrated earthquake load at beam level was taken as:

$$E_{50} = 2.0(D + L_{APT})\alpha_{50} \qquad (4.2.4)$$

where α_{50} is the 50 year peak earthquake acceleration coefficient. The distribution types and parameters used for the basic loading variables are given in Table 4.2.1. These variables are all mutually independent, and they are also independent of the resistance effects.

4.2.2 Resistance Assumptions

The resisting moments M_u were calculated using the basic variables given in Table 4.2.2. The variable T is required as the concrete strength f_c' varies with time (56). As the variables f_c' and f_y were relevant to the static loading, their values were scaled to $1.2\ f_c'$ and $1.05\ f_y$ when wind and earthquake effects are considered (30). Because of the time wise correlation of f_c' and the assumed correlation of f_y, all the moment capacities were correlated to some degree. The correlation coefficients ranged from 0.45 to 0.85. In order to compare the results with similar results calculated on the basis of zero correlation between moment capacities, moment capacities calculated using Monte Carlo simulation, were assumed to have a lognormal distribution.

Table 4.2.1 Load basic variables

Items		Symbol	Distribution type	Mean	C.O.V.
1	Dead	D	normal	4.78 kN/m	0.100
2	Live	L_{50}	type 1	8.3	0.250
3		L_{APT}	gamma	2.35	0.700
4	Wind velocity	V_{50}	type 1	41.0 m/s	0.230
5		V_{APT}	type 1	7.82	0.590
6	Acceleration	α_{50}	type 2	0.622g	0.343

Notes: (1) A subscript "50" indicates a 50-year maximum and "APT" stands for an arbitrary point in time.

(2) The all assumptions were made by S. Gallot of DSIR (Department of Scientific and Industrial Research).

Table 4.2.2 18 basic variables for M_u calculation

			Distribution type	Mean	C.O.V.
1	$f'_{c\ 28\text{-day}}$	column	normal	19 MPa	0.180
2		beam			
3	T	time	uniform	25 year	0.577
4	f_y	all reinforcement	normal	312 Mpa	0.116
5	d	M_{A1}	normal	242.5 mm	0.06
6		M_{B1}		240.5 mm	
7		M_{B2}		246.5 mm	
8		M_{C1}		240.5 mm	
9		M_{C2}		246.5 mm	
10		M_{D2}		244.5 mm	
11		M_{E1}		296.0 mm	
12		M_{E2}		293.0 mm	
13	B	M_{A1}	normal	302.0 mm	0.03
14		M_{B1}, M_{B2}			
15		M_{C1}, M_{B2}			
16		M_{D2}			
17		M_{E1}, M_{E2}		302.4 mm	
18	$\frac{M_{exp}}{M_{cal}}$	all M	normal	1.05	0.120

Notes: All 18 variables are mutually independent

$f'_{c\ 28\text{-day}}$ = uniaxial compressive strength of concrete in 28 days

T = time when a failure occurs ($0 < T \leq 50$ years)

f'_c = concrete strength when a failure occurs (MPa)

= $f'_{c\ 28\text{-day}}$ x (time effect)

f_y = yield strength of longitudinal reinforcement

d = distance from extreme compression fibre to centroid of tension reinforcement (mm)

B = width of section (mm)

M_{exp} = ultimate moment obtained by an experiment

M_{cal} = ultimate moment obtained by a calculation

A subscript "1" and "2" indicate that the tension side of a member is on the outside or inside of the frame respectively.

4.2.3 Failure Modes

The failure modes (mechanisms) taken into account are shown in Fig. 4.2.1. Note that for the combined modes the beam hinge is assumed to occur at the point of maximum moment. Generally, this will not be in the centre of the beam. For a more complex and representative structure, it would have been necessary to take into account also other cuases of failure such as due to shear, the failure of joints. In this case failure modes associated with flexure only were considered.

4.2.4 Failure Criteria and Failure Surfaces

The criterion for failure in any mode is in general the intersection of a set of inequalities. These inequalities are expressed in terms of the basic random variables defined in the previous subsections. Thus the failure criteria will have to take into account 18 resistance variables and either two or three load variables. The inequalities, for example with load S_3 in Eq. (4.2.1) are as follows. For failure to take place in mode A, which is a beam failure mode (Fig. 4.2.1) they are:

Mode A

$$w_3 = D + L_{APT} - 0.003186\, V_{50}^2 \geq 0 \qquad (4.2.5)$$

$$g_A = M_{B1} + M_{C1} + 2M_{E2} - \tfrac{1}{4} l^2 w_3 \leq 0 \qquad (4.2.6)$$

Mode B is also a beam failure mode. It differs from mode A

only in that uplift on the beam governs its strength. Failure criteria for mode B are:

Mode B

$$w_3 \leqq 0 \tag{4.2.7}$$

$$g_B = M_{B2} + M_{C2} + 2M_{E1} + \tfrac{1}{4}1^2 w_3 \leqq 0 \tag{4.2.8}$$

Likewise, for mode C and D which are combined modes, the failure criteria are:

Mode C

$$w_3 \geqq 0 \tag{4.2.9}$$

$$g_c = 4F + 8M_{C1} + 8M_{E2} - w_3 1^2 - 4F^2/(w_3 . 1^2) \leqq 0 \tag{4.2.10}$$

$$\alpha = F/(w_3 1^2) + \tfrac{1}{2} \geqq 0 \tag{4.2.11}$$

$$\alpha \leqq 1 \tag{4.2.12}$$

where: $F = M_{A1} + M_{D2} - \tfrac{1}{2}h^2(w_1 + w_2)$

$w_1 = 0.001224\ V_{50}^2$

$w_2 = 0.002456\ V_{50}^2$

Mode D

$$w_3 \leqq 0 \tag{4.2.13}$$

$$g_D = 4F + 8M_{B2} + 8M_{E1} + w_3 l^2 + 4F^2/(w_3 l^2) \leq 0 \quad (4.2.14)$$

$$\alpha = -F/(w_3 l^2) + \tfrac{1}{2} \geq 0 \quad (4.2.15)$$

$$\alpha \leq 1 \quad (4.2.16)$$

Finally for mode E, a sway mode, the inequality is:

Mode E

$$g_E = 2(M_{A1} + M_{B2} + M_{C1} + M_{D2}) - h^2(w_1 + w_2) \leq 0 \quad (4.2.17)$$

Note that the equation of g for each mode is the more normally accepted limit state or failure inequality. Other inequalities are criteria for the existence of the mode. The probability of failure occurring in each mode due to a particular load combination is given by the integral of the joint probability density function (Eq. (4.2.3)) for all the random variables concerned over the multi-dimensional space defined by corresponding inequalities. A failure of a load combination is represented by a space bounded by the envelope of the existence of various failure modes. Hence, the results for different modes cannot be combined directly because the modes are not mutually exclusive.

Calculation of probabilities of failure is difficult for this problem for two reasons. Firstly, the large number of random variables involved makes the problem complex.

Complexity itself is not necessarily a barrier with modern computing equipment. However, complexity also means that the problem becomes opaque, and difficult to comprehend in detail. The second problem is the non-linearity and discontinuity of the surfaces bounding the failure regions. The situation is multi-dimensional and it is impossible to illustrates visually such multi-dimensional failure surfaces. Therefore a two-dimensional slice of it is drawn in Fig. 4.2.2 such that all variables, other than L_{APT} and V_{50}, have been given their mean values. Even that, the failure surfaces are pretty complex. The figure shows the kinematically admissable regions (that is, the failure regions) for modes C and D. It can be seen that the two kinematically admissable regions are not contiguous to one another. There are thus various combinations of live load and wind which cannot fail the structure in a combined mode no matter how large the loads become. This is not to say, of course, that the structure will not fail at all. It will fail in one of the other modes. Failure surfaces for modes A, B and E are also shown on the diagram. A further point to note is that wind velocity can, of course, be negative so that strictly speaking, Fig. 4.2.2 represents only half the region of interest. Mirror image failure surfaces should be drawn on the left hand side of the load axis.

4.3 METHODS OF ANALYSIS

It is theoretically possible to calculate the probability failure by direct numerical integration of the joint probability distribution over the failure region. Such an

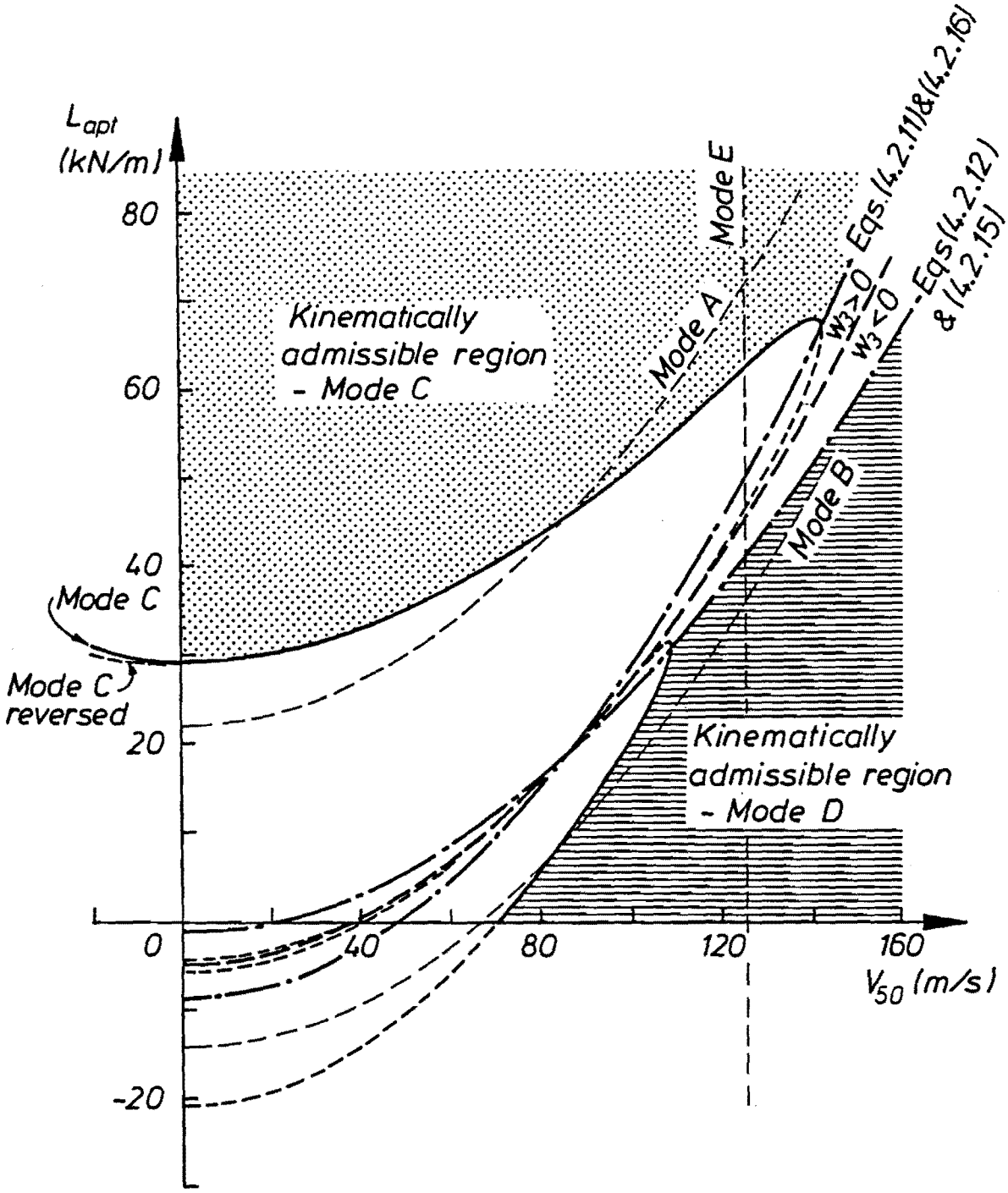

Fig. 4.2.2 Failure surfaces ($D + L_{APT} + V_{50}$)

approach is infeasible in practice, however. Not only is there a difficulty because of the non-linearities of the failure surface, but also there are severe numerical problems associated with integration over an unbounded space, particularly where the dimensions of the space are large. Direct integration was therefore not attempted as a means of solving the problem.

An advanced First-Order Second-Moment method and Monte Carlo simulation were used to calculate the failure probabilities. A purpose of using the latter simulation is to check the accuracy of results obtained by the former method. The advanced First-Order Second-Moment approach may not produce good approximations to the probability of failure, because even if Fig. 4.2.2 is transformed into standardised normal space (i.e. reduced coordinates) it is still highly non-linear, as shown in Fig. 4.3.1. The failure region indicated by linear approximation of the method is totally different from the real failure region for the combined mode. (The transformation into a reduced coordinate system and the linear approximation in the advanced First-Order Second-Moment method was explained in 2.2.2. See Fig. 2.2.4.) A further difficulty is that highly non-linear failure surfaces and other reasons can lead to numerical instability of the algorithm. Nevertheless, in many cases the First-Order Second-Moment method will lead to good approximations.

Another technique that can be used is the Monte Carlo simulation, which may be thought of either as a series of

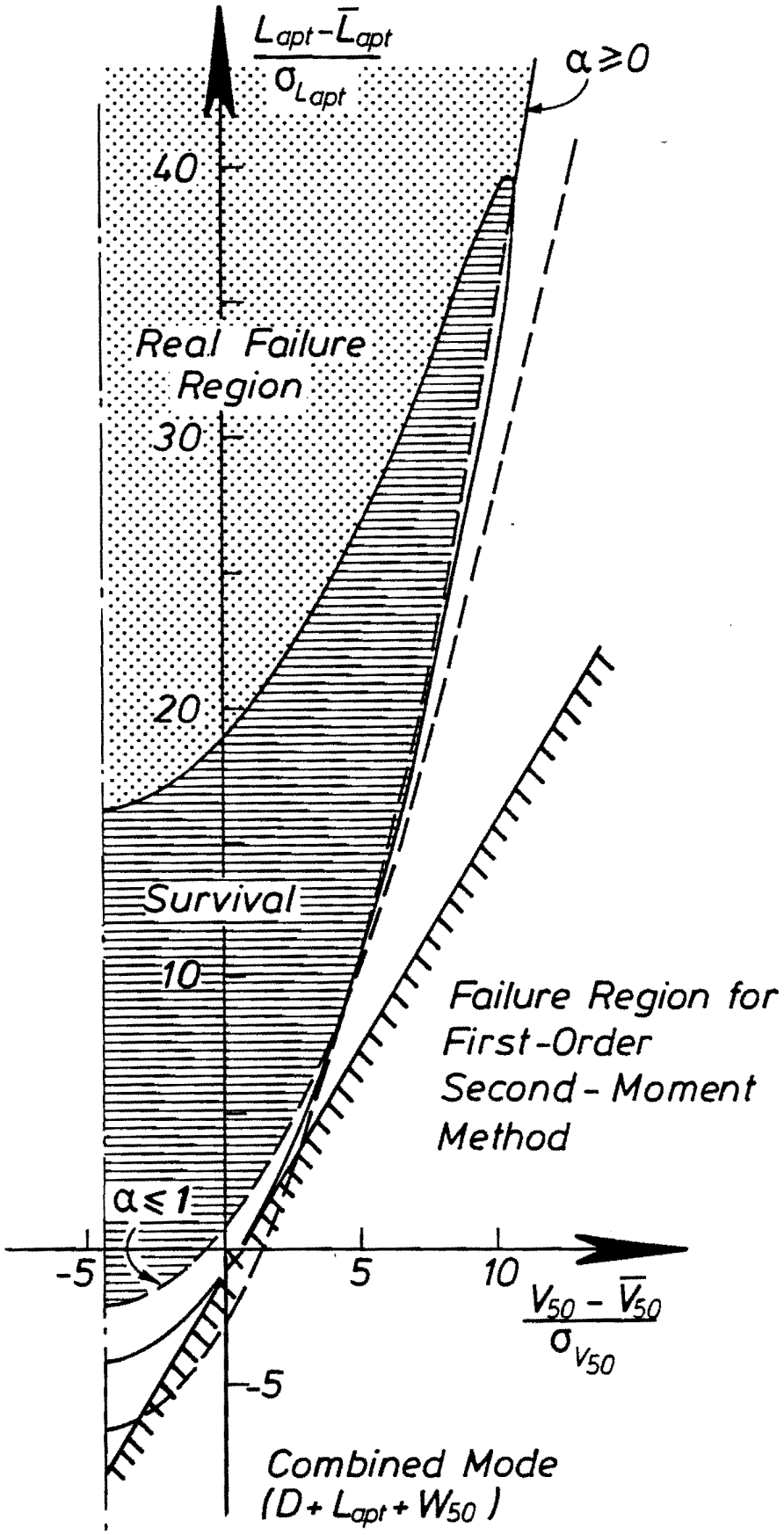

Fig. 4.3.1 Comparison of failure region by First-Order Second-Moment method with real failure region

deterministic experiments whose results can be investigated statistically, or as a means of numerical integration in a random rather than a systematic fashion. Monte Carlo simulation is extremely demanding on computer time, particularly where low probabilities of failure are sought. It is therefore necessary to look for methods of reducing the sample size necessary for a given accuracy of result. As with any approach requiring repeated experiments, the Monte Carlo method is subject to sampling error. The magnitude of the error can be described in terms of the variance of the result. If purely random sampling is used, the variance is purely a function of the sample size; the larger the sample, the less the error, and the lower the variance. However, in some cases strategies of non-random sampling can be used as variance reduction techniques (VRTs) to reduce the variance for a given sample size (3). Two such approaches were used here; the method of antithetic variates, and the condition expectation VRT.

The method of antithetic variates is relatively well known (3,4). If two sets of experiments are carried out each with the same number of random samples, and if the results are Z' and Z'' respectively, the combined result Z is the average of the two, and its variance is:

$$\mathrm{Var}[Z = \tfrac{1}{2}(Z' + Z'')] = \tfrac{1}{4}[\mathrm{Var}(Z') + \mathrm{Var}(Z'')] \qquad (4.3.1)$$

if Z' and Z'' are independent. If, however, Z' and Z'' are negatively correlated, then the combined variance will be

less than the value given in Eq. (4.3.1). Negative correlation can be achieved by choosing two sets of random numbers, the second being the negative complement of the first. The idea is that a large sample value will tend to be counteracted by a small, so reducing the variance. The reduction in variance achieved depends on the problem considered.

The conditional expectation variance reduction technique (3,57) has been used for structural reliability calculations by Ayyub and Haldar (5). Let X be a random variable for which an estimate q = E[X] is required. If there is another random variable Y for any value of which the conditional expectation E[X|Y = y] can be calculated, then:

$$q = E[E[X|Y]] \tag{4.3.2}$$

and:

$$\begin{aligned} Var[E[X|Y]] &= Var[X] - E[Var[X|Y]] \\ &\leq Var[X] \end{aligned} \tag{4.3.3}$$

In the present case the quantity with the highest variance is chosen for a particular mode and limit state equation. Random values are chosen for the other variates and an estimate of probability of failure is obtained from the known distribution of the chosen variate. This process continues until a sufficient number of samples have been taken.

4.4 CALCULATION RESULTS

The results of the various calculations are summarised in Table 4.4.1. The first three rows of figures show the main results, obtained by Monte Carlo simulation with a sample size of 300,000 and including correlations between the ultimate moments at the various sections. The total overall probability of failure and the total probability of failure for each load combination are calculated using the antithetic variates technique alone ([A] in the Table). Where the conditional expectation variance reduction technique is used as well ([A] + [C] in the Table), estimates or probability of failure for individual modes are given, together with sample coefficients of variation. However, because any specific combination of basic variables might be in the kinematically admissable zone of more than one mode, the modes are not in general mutually exclusive and a total probability of failure cannot be obtained from individual modal probabilities. Further down the table, the equivalent results are shown for the much smaller sample size of 10,000, followed by figures obtained by using the advanced First-Order Second-Moment technique. Despite using various initial values in some instances the calculations could not be made to converge ([NC] in the Table). The method has not been applied to combined modes because it is obvious that the approximation leads to entirely wrong results, as alluded to in the previous section. The last four rows of Table 4.4.1 show the same results repeated but with the assumption that the beam and column resisting moments are uncorrelated.

Table 4.4.1 Comparison of results

Number				1	2	3	4	5	6	7	8	9	10
Load combination				$D + L_{50}$	$D + L_{50} + W_{APT}$		$D + L_{APT} + W_{50}$					$D + L_{APT} + E_{50}$	
Failure modes				beam	combined	beam	combined		beam		sway	combined	sway
				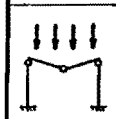	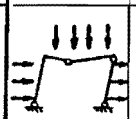	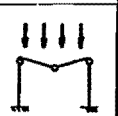	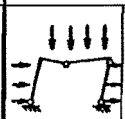	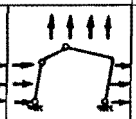	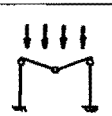	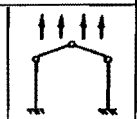	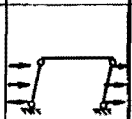		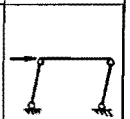
correlated M's	Monte Carlo Simulation Sample Size 300 000	[A]	P_f (Σ = .00936)	.00213	.00182		.00531					.000010	
		[A] + [C]	$\bar{P}_{fi}$	.00250	$.988 \times 10^{-4}$	.00219	$.630 \times 10^{-8}$	.00365	$.149 \times 10^{-6}$	.00531	$.354 \times 10^{-5}$	$.813 \times 10^{-5}$	$.103 \times 10^{-4}$
			COV	.0096	.0246	.0099	.0728	.0276	.0372	.0223	.0050	.1853	.0049
	Monte Carlo Simulation Sample Size 10 000	[A]	P_f (Σ = .00880)	.00280	.00230		.00370					0	
		[A] + [C]	$\bar{P}_{fi}$	.00250	$.938 \times 10^{-4}$	.00219	$.490 \times 10^{-8}$	.00290	$.123 \times 10^{-6}$	.00438	$.362 \times 10^{-5}$	$.708 \times 10^{-5}$	$.104 \times 10^{-4}$
			COV	.0462	.0821	.0469	.1740	.1716	.1129	.1328	.0263	.1638	.0259
	First-order (Σ = .00814) second-moment method			.00253		.00236			$.156 \times 10^{-6}$	.00325	[NC]		[NC]
uncorrelated M's	Monte Carlo Sample Size 300 000	[A]	P_f (Σ = .00573)	.000770	.000673		.00428					.000010	
		[A] + [C]	$\bar{P}_{fi}$	.000785	$.122 \times 10^{-4}$	.000680	$.117 \times 10^{-9}$	.00256	$.134 \times 10^{-7}$	.00418	$.198 \times 10^{-5}$	$.215 \times 10^{-5}$	$.961 \times 10^{-5}$
			COV	.0044	.0063	.0043	.0216	.0330	.0158	.0250	.0018	.1874	.0056
	First-order (Σ = .00484) second-moment method			.000865		.00080			$.200 \times 10^{-7}$	.00317	[NC]		[NC]

[A] = Antithetic Variates VRT [C] = Conditional Expectation VRT [NC] = no convergence

A number of conclusions may be made from a study of Table 4.4.1. The major points are as follows.

1. The results of the First-Order Second-Moment method were similar to those obtained by Monte Carlo simulation. However, this observation must be treated with caution as in each of the three cases considered, the dominant mode, and hence the mode to which the calculations were applied, was a beam mode. Almost certainly, far more difficulty would be found if a combined mode were dominant, because of the complexity of the failure surface as shown in Figs 4.2.2 and 4.3.1.

2. The effect of ultimate moment correlation varies between modes. It is particularly marked for the first and second load combinations. The assumption of uncorrelated moments always leads to a lower estimate of failure probability for this frame. It must be concluded that in general, correlation effects should be taken into account. This agrees with conclusions of other researchers (13,18).

3. The combination of the two variance reduction techniques seemed to be efficient, since the results obtained from the relatively small sample size of 10,000 were in reasonable agreement with those from a sample size of 300,000. The coefficients of variation are of course larger for the smaller sample.

4. Gravity loads dominated the design of the frame, with wind producing only small negative moments in the beam. However, Table 4.4.1 shows that the highest probability of failure occurs with the wind load combination. Indeed, the wind load failure probability would have been higher still if the frame had not been designed with 2.5-4.0 times as much reinforcement to resist negative moments as that required by the design envelope. The increased steel content was due to the practical requirements of construction. It would thus appear that for this type of building, designed in reinforced concrete, the code wind load provisions are too low compared with the gravity load provisions. This is in part due to the very high variance of load effects due to load components in opposition to one another. For balancing the failure probabilities between the load cases, the wind load should be increased by a factor of about 1.7 (i.e. the combination 0.9 D + 1.3 W should be changed to 0.9 D + 2.2 W) for this particular type of structure.

4.5 CONCLUSIONS

It appears that the problem of computing the probability of failure of a total structure is extremely complex, even for the simplest of structures. The advanced First-Order Second-Moment method cannot always lead a reasonable answer

because of the complexity of a failure surface even after making any simplifying assumptions with regard to load and resistance variables. As a pilot exercise working towards code calibration, the exercise has been successful in various different ways as follows:

1. It shows the extreme difficulties involved in any estimation of probability of failure.

2. It shows that the advanced First-Order Second-Moment approach, while giving reasonable results for simple failure modes, is basically impractical when applied in an unsophisticated way to situations with complex failure modes.

3. It shows that the Monte Carlo simulation is good with the use of powerful variance reduction techniques, but that it can consume too much computer power to make it a universally practical tool.

4. It shows that in this specified case, it would seem that the wind load provisions of the code are unconservative, and that for a balanced code they should be increased by a factor of 1.7 for this particular type of structure.

CHAPTER 5

BASIC REQUIREMENTS AND ASSUMPTIONS FOR CALCULATING FAILURE PROBABILITIES

5.1 INTRODUCTION

The aim of developing a procedure for calculating failure probabilities of multi-storey buildings subjected to earthquake has been stated. In the present chapter, a specific proposal for the development of such a procedure is presented.

It has been emphasised in previous chapters that the assessment of safety levels of structures is indispensible in establishing a balanced code. A balanced code enables minimum levels of structural safety for different loadings to be consistent for all structural types. The minimum safety for earthquake, for example, should be equal to that for wind load. Therefore, probabilistic safety assessments for different loadings are required to be developed. However in the case of earthquakes, safety assessment is considerably more difficult than for other load cases.

An earthquake is a ground motion and not a clearly defined load applied to a structure. Thus, not only its intensity, but other characteristics such as spectral characteristics

and the time-domain intensity envelope may affect structural behaviour. Moreover, ground motion induces time dependent cyclic demands. Hence, the inelastic behaviour of structures and prediction of failure are more difficult to quantify. It is generally the entire system of a structure that will react to and resist an earthquake, whereas for say live loading adequate resistance could be provided locally by only one beam. Because of these and other difficulties, an appropriate procedure for assessing earthquake failure probability has not yet been established. This in outline is the incentive for the development of a suitable procedure.

Two major questions must be addressed in developing an assessment procedure. They are (see Fig. 5.1.1):

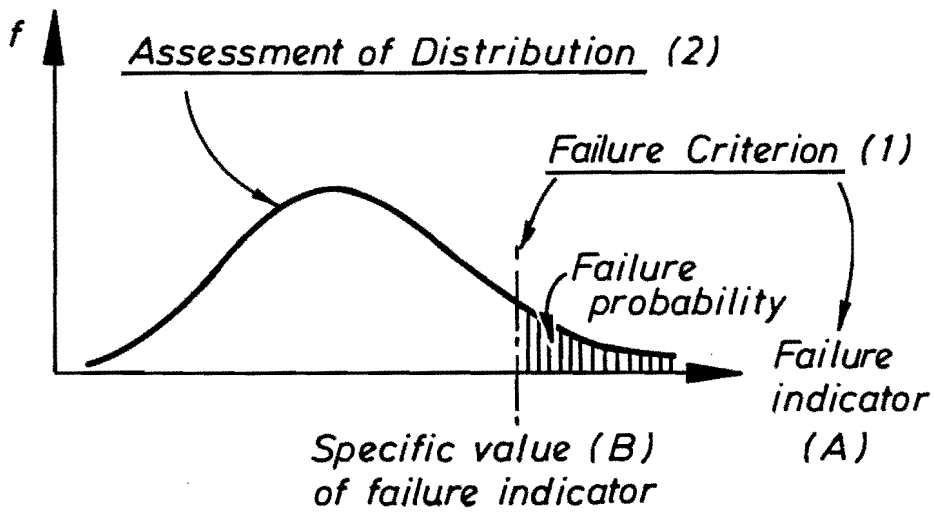

Fig. 5.1.1 Items necessary to assess failure probabilities

1. Failure criterion - what numerical measure (A) and what specific value (B) of the measure are appropriate for expressing the failure of structures subjected to earthquake?

2. Assessment of probability distribution - what method is appropriate for estimating the probability distribution of a seismic response in terms of the measure used in the definition of the failure criterion?

To answer these questions is the main aim in the remainder of the present study.

In dealing with the above questions, much attention should be paid to the inherent uncertainty and errors involved. Uncertainty in data and modelling and errors inherent in solution procedures relate to accuracy of results. Generally, the smaller the uncertainty and errors, the more precise the results. On the other hand, engineers must usually make a greater effort if uncertainty and errors are to be reduced. In making appropriate assumptions, it is important to consider the relationship between accuracy of results and engineers' effort. A result by a more complicated method could be more accurate, but it would take a longer time to get the answer. An appropriate choice of method also depends on the uncertainty of the data used in the analysis. When the data uncertainty is big, use of a complicated method may not be reasonable because the

accuracy of the result using a simpler method is not much different. Thus, by using too complicated a method, engineers might be required to exert fruitless effort. To avoid unnecessary complexity, the inherent uncertainty of the problem should first be evaluated and considered. The principle of consistent crudeness (44) can contribute to making suitable assumptions, as explained in 3.2.2. However, because the uncertainty can usually be expressed only qualitatively rather than quantitatively, it is not easy to apply the principle to real problems. In practice, engineering judgement must generally be used bearing the principle in mind.

In the present chapter, a failure criterion and the necessary preparations for developing a new procedure for safety assessment are discussed. Firstly, the inherent uncertainty involved in the process for achieving a balanced code is described as well as basic requirements for the new procedure. Secondly, a failure criterion is defined taking into account the inherent uncertainty. Because collapse has been chosen as a definition of failure, failure criteria are examined by considering collapse mechanisms. Thirdly, once the general requirements and failure criterion have been set up, suitable analytical models for calculating failure probability are selected. It is found that the advanced First-Order Second-Moment method is the only practical approach. However, an appropriate performance function has to be established. Hence finally, as a preparation for developing the performance function a new measure of earthquake damage is introduced. A performance function

using the new damage measure will be proposed in Chapter 6.

5.2 INHERENT UNCERTAINTY IN ACHIEVING A BALANCED CODE AND BASIC REQUIREMENTS FOR ASSESSING FAILURE PROBABILITIES

Two important matters arise in the development of a procedure for achieving a balanced code and in making the necessary assumptions. They are the magnitude of the inherent uncertainty involved in the procedure itself, and fundamental requirements for its development. As explained earlier in 3.2.2 and 5.1, the inherent uncertainty can be used as a yardstick by which too-complicated assumptions and models may be eliminated. Fundamental requirements determine the right choice for development and must be satisfied by the selected procedure. Therefore,it is essential to determine both the inherent uncertainty and the basic requirements before embarking on the development.

The main points which are relevant to this development as discussed in the previous two chapters are as follows:

1. The final aim of which the present study is a part is to establish a balanced code. Computing failure probabilities is a necessary part of achieving it (see 3.2.2).

2. There is currently no appropriate method for assessing the safety of a structure subjected to earthquake loading, yet this is generally the most

important load case for structural engineering in New Zealand (see 3.4).

3. A balanced code must originally be based on the balanced risk concept. However, practical proposals for achieving such a code include a large amount of uncertainty (see 3.3).

4. In evaluating total structural safety, even for the simplest possible structure, a large number of random variables are involved and many simplifying assumptions must necessarily be made (see Chapter 4).

5. The advanced First-Order Second-Moment method is the only practical way to estimate failure probability. The method is, however, basically impractical when applied to situations with complex failure modes unless considerable simplifications are made (see Chapter 4).

A particular matter which must be appreciated with regard to uncertainty is the difficulty of predicting earthquake characteristics. The prediction of earthquake characteristics is indispensable for the safety assessment of structures subjected to earthquake. Three measures are needed to characterise an earthquake. They are:

1. maximum ground intensity;
2. spectral characteristics; and

3. time-domain intensity envelope.

However, of the three, one can at present only manage to predict earthquake intensity probabilistically (see section 7.2). Intensity is a measure designed to describe the effects of earthquakes on man, structures and their surroundings. Thus, earthquake intensity is a function not only of maximum ground intensity but also of duration of motion and spectral characteristics. Intensity is the best single parameter for measuring damage. Smith (58) has estimated the likelihood of earthquake shaking throughout New Zealand using Modified Mercalli intensity, which is one of three major intensity scales (59).

However,it is known that the intensity scales involve a great deal of uncertainty for predicting earthquake characteristics. The correlation of earthquake intensity scales with recorded peak horizontal ground acceleration has been investigated by many researchers (59,60). The maximum difference between their results was about one order of magnitude in terms of acceleration. The difference is surprisingly large. Thus, in predicting maximum ground acceleration from an intensity value, considerable uncertainty is involved. Moreover, it is impossible to estimate spectral characteristics and an intensity envelope from an intensity value. There appears to be no possibility to bypass a high level of uncertainty when predicting earthquake characteristics. Earthquake characteristics affect structural responses markedly. This suggests that the use of complicated assumptions and method for assessing

the failure probability of structures is not justified, following the principle of consistent crudeness (see 3.2.2).

With respect to the necessary requirements for assessing failure probabilities, two matters must be considered. Firstly, a probabilistic approach is required. As explained in 2.2 and Chapter 4, Monte Carlo simulation and the advanced First-Order Second-Moment (F.O.S.M.) method are the most commonly used methods in probabilistic analyses, but neither of them are completely suitable for practical use. The former method is a simulation which is usually used as a last resort method when a problem is too complicated to be dealt with by a systematic application of technical concepts and knowledge. In engineering problems a systematic way to assess the essence of the matter is generally considered to be preferable to obtaining results by a simulation. In addition, a Monte Carlo simulation consumes too much computer power to make it a universally practical tool. It appears that the F.O.S.M. approach is the only practical available method. In the use of the F.O.S.M. method, a performance function is required, in terms of which a failure criterion can be written. Accordingly, establishing a performance function regarding the failure of structures subjected to earthquake is one of the basic requirements for obtaining probabilities of failure. However, the F.O.S.M. method is basically impractical when applied to situations with complex failure modes, whereas the seismic behaviour of structures and the corresponding failure modes are generally complicated. To resolve the conflict, a simple performance function is desirable, but its achievement is far from easy.

Secondly, a procedure for assessing failure probabilities should not be complicated but should be relatively simple if it is to be of practical use. In achieving a balanced code, the safety levels of various kinds of structure need to be examined. For this purpose, structures could be grouped by:

1. Location (different seismicity);
2. Structural system (frame, structural walls, etc);
3. Material (reinforced concrete, steel, etc.);
4. Occupancy (office, storehouse, etc.);
5. Scale (3-storey, 10-storey, etc);

and so on. If only three buildings for each category are chosen, the total number of buildings to be analysed will be $3^5 = 243$. Thus any procedure for calculating failure probability must be applied to many structures so that too complicated a method is impractical. It is therefore imperative to develop a simple and straightforward technique for assessing earthquake failure probability.

5.3 A FAILURE CRITERION

One of the major problems in developing a procedure for assessing failure probability is to define a suitable failure criterion. Since collapse has been chosen as a basis for defining failure (see Section 3.4), it should be determined what numerical measure and what value of the measure are appropriate for an indicator of structural collapse. In trying to solve these problems, it should be

noted that the definition of the failure criterion need not be complicated. This is because of the large inherent uncertainty, mentioned in the previous section. Despite the complexity of the collapse phenomenon in practice, this section takes advantage of the presence of inherent uncertainty to define a simplified failure criterion.

A particular difficulty in determining a quantitative measure and its appropriate value arises from the fact that the meaning of collapse of an entire structure is fuzzy. A failure of one member can be defined as loss of its strength. When a column gets damaged and cannot resist the sustaining loads, the column fails. The failure of a column causes subsequent failure of the adjacent beams and slabs. Moreover, other columns must sustain the loads carried by the failed column. This may cause other column failures or the failure of a whole storey. On the other hand, beam failure is generally a local event. Even if a beam lost its strength and failed, the storey would not need to be in danger. Thus, collapse of a whole structure can be defined in terms of the number of column failures. When all columns of a structure fail, it must be collapse. However, when one storey or only few storeys of a structure fail, can this be defined as leading to collapse? How many columns need to fail to be considered as a whole storey collapse? Indeed, there can be considerable variations in the nature and consequences of a collapse due to earthquake. Figure 5.3.1 shows some examples:

(a) collapse of one column and part of the floor;

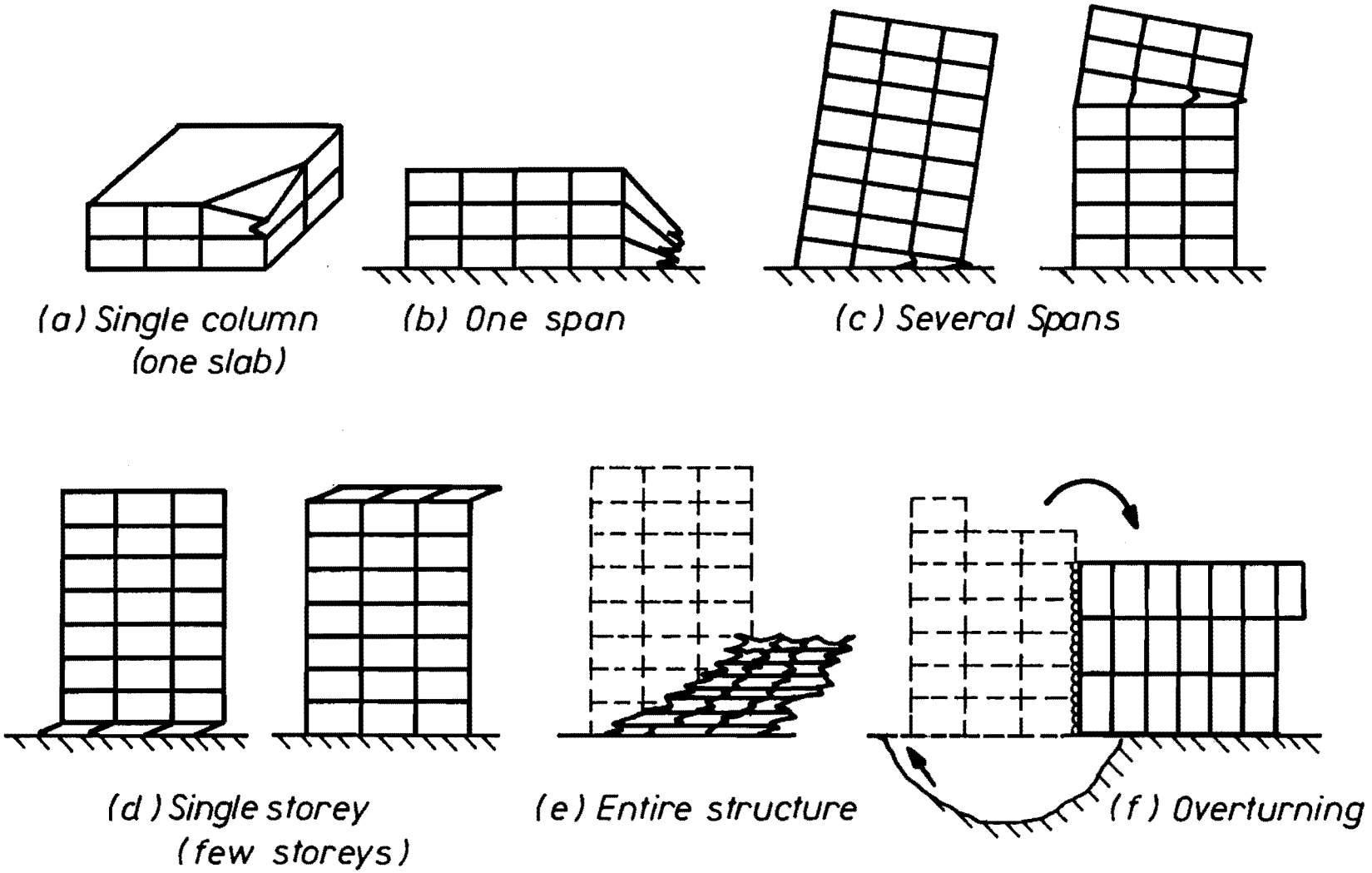

Fig. 5.3.1 Variations of collapse

(b) collapse of one bay resulting from the failure of one column;

(c) partial collapse of one storey;

(d) total collapse of one storey;

(e) total collapse of the entire structure; and

(f) overturning.

The last case (f) is relevant to soil failure and is not considered in this study.

Generally a failure of a (soft) storey will be or should be assumed to be followed by collapse of the whole building. There are of course cases when the upper parts, consisting of several storeys, come down by one storey without very serious damage. However, the people in the soft storey will be in danger. Moreover, it is questionable whether differences of fatalities due to different types of collapse (Fig. 5.3.1) are distinct enough in the light of the inherent uncertainty discussed in Section 5.2. The prediction of earthquake characteristics probably involves the greatest degree of uncertainty. When attempting to predict the mode of collapse, the differences between, say, the three cases (c), (d) and (e) in Fig. 5.3.1, might not be very obvious. Hence, for simplicity, collapse of a single storey is assumed to constitute the failure criterion. Although the consequences of collapse of the first storey are different from those of top storey collapse, again this aspect will be assumed to be negligible.

The next task is to choose a quantitative measure, the value

of which will express collapse of a storey. In order to develop such a measure, collapse mechanisms are examined. For simplicity, a single storey model is used initially.

Because of its relevance, it is useful to discuss first the difference between static and dynamic conditions of instability. Equilibrium for the two conditions can be expressed by:

$$k \cdot \Delta\delta = \Delta F \qquad \text{(static loads)} \qquad (5.3.1)$$

for static loads and:

$$m\ddot{\delta}(t) + C(t)\dot{\delta}(t) + k(t)\delta(t) = F(t) \qquad \text{(dynamics)} \qquad (5.3.2)$$

for the dynamic condition, in which:

k = stiffness

δ = relative displacement from the ground

F = external horizontal force

m = mass

c = damping coefficient

t = time

Δ = increment

In the load incremental method for static analysis, when the stiffness k is equal to zero or becomes negative, the system achieves instability as shown in Fig. 5.3.2. Instability generally indicates a situation in which a unique load-displacement relationship cannot be determined. For

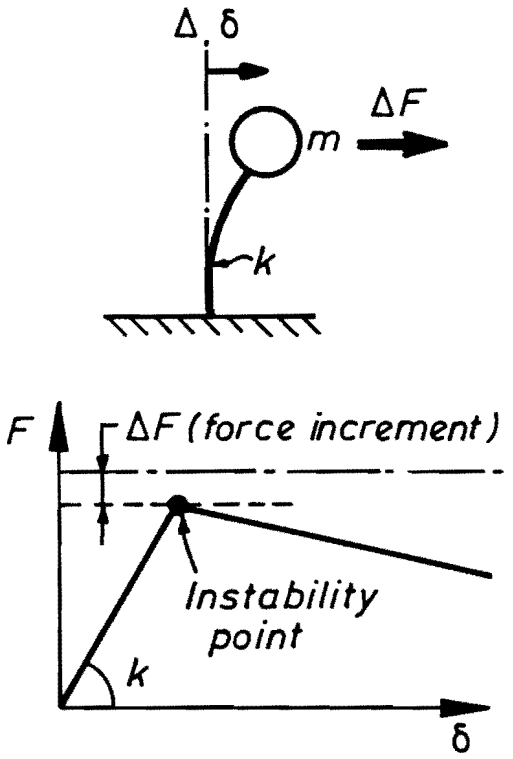

Fig. 5.3.2 Instability point in a load incremental method for a static analysis

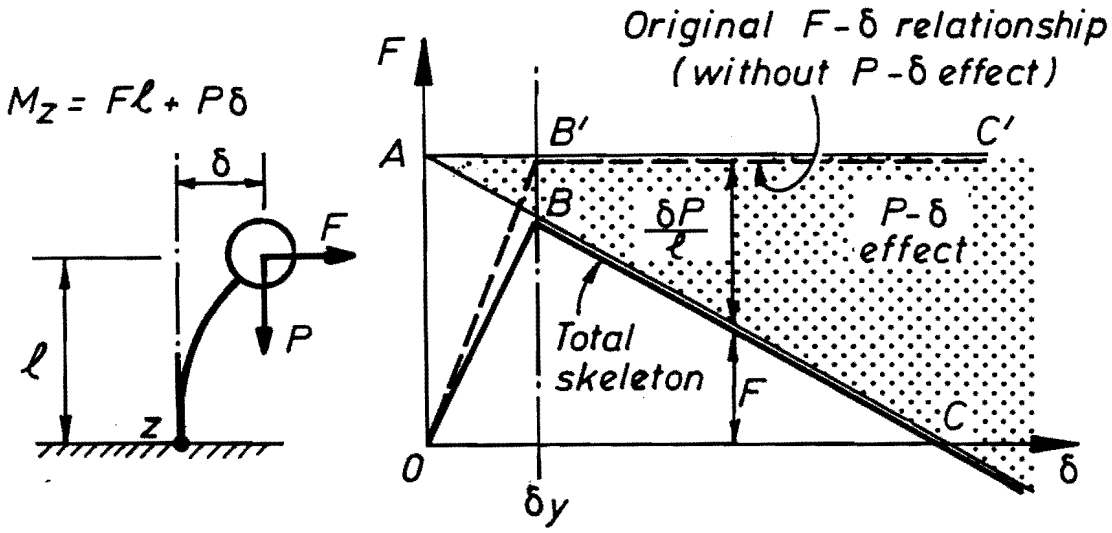

Fig. 5.3.3 Illustration of P-δ effect

the static case, once the system becomes unstable, it cannot resist the applied force any more and collapses. On the other hand, in a dynamic analysis such a condition for collapse following instability does not generally exist. Based on the linear acceleration method (61) where input and response accelerations are assumed to be linear during a time increment Δt, an effective dynamic stiffness $k_e(t)$ can be defined as:

$$k_e(t) = k(t) + \frac{6}{\Delta t^2} m + \frac{3}{\Delta t} C(t) \tag{5.3.3}$$

$$k_e(t) \cdot \Delta\delta(t) = \Delta F_e \tag{5.3.4}$$

where: $\Delta\delta$ = displacement increment

ΔF_e = effective force increment (given)

Even when $k(t)$ is negative or zero, $k_e(t)$ is generally positive and instability does not occur. Therefore, a load incremental model as used for static analysis is inadequate in considering instability during earthquake excitation. Note that static instability based on a load incremental model must be considered for a structure subjected to gravity load when earthquake oscillation ceases. A displacement incremental model is more appropriate in examining dynamic instability.

From this point of view, the failure criterion for the earthquake load case of a portal frame, assumed in Chapter 4, is not adequate. In that analysis, earthquake effects

were represented by a static lateral load and the failure criterion assumed that collapse occurs when the applied force is equal to the resisting force and the stiffness becomes zero in a load incremental method for a static analysis. Such a criterion is not realistic for earthquake failure because the seismic behaviour of structures is a dynamic rather than a static phenomenon.

Important factors in studying mechanisms of collapse are:

(1) the so called P-δ effect; and
(2) deterioration of strength due to large deformations and a cyclic loading effect.

Contribution of these factors to a collapse mechanism is discussed in defining a failure criterion.

The P-δ effect is an effect of geometric non-linearity. A horizontal displacement δ, illustrated in Fig. 5.3.3, leads to additional overturning moment because a gravity load P is also displaced. Therefore, under static loading, in addition to the overturning moment produced by lateral load (F) the secondary moment Pδ must also be resisted. This moment increment in turn will produce additional drift. Hence δ will increase further. An important result of the P-δ effect is the deterioration of strength against lateral load. The original F-δ relation without the P-δ effect is assumed here to be a bi-linear elasto-plastic. The additional moment Pδ due to the P-δ effect increases linearly with δ. Because the additional moment reduces the

original strength against lateral load, the effect may be described by the negative slope AC in Fig. 5.3.3. As Fig. 5.3.3 shows, up till reaching yield displacement δy, since additional drift is produced by the additional moment, the stiffness reduces (OB'-OB). During displacement beyond δy, the original strength is assumed to remain constant (B'C'). However, the additional moment due to the P-δ effect increases. Thus, the total effect on the F-δ relations becomes negative (BC). That is, the strength with respect to lateral load F is reduced. When the drift reaches the value at point C, no resistance to F remains in the spring system.

In statics, the point C in Fig. 5.3.3 is an instability point. At this stage collapse must occur. The situation is similar to that illustrated in Fig. 5.3.4, when the weight (m) becomes equal to the load carrying capacity of the spring with a constant spring constant Fy.

As explained earlier, in dynamics such a situation does not always lead to collapse. A dynamic model simulating a similar situation is shown in Fig. 5.3.5. Unless the weight of the mass is far larger than the capacity Fy damping and inertia systems may contribute to resisting it. This indicates that defining a collapse criterion in dynamic situations is difficult.

Thus, the P-δ effect may lead to a collapse mechanism in static situations, when oscillation of the structure stops, or when the earthquake response acceleration and velocity

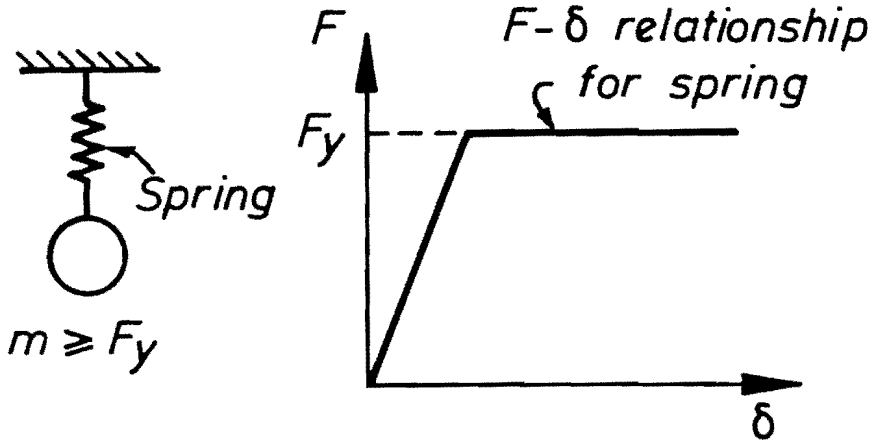

Fig. 5.3.4 A static model and instability

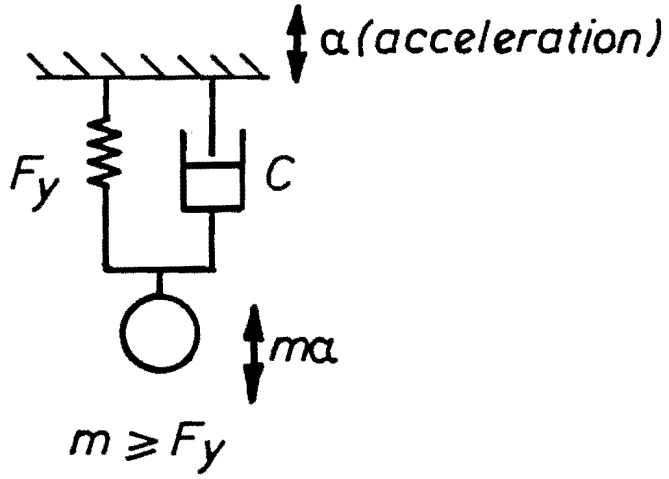

Fig. 5.3.5 A dynamic model

are negligibly small during earthquake excitation. The latter condition that the response acceleration and velocity become negligible during the excitation occurs only for a very short time and is not universal. Therefore, the structure does not collapse but a residual displacement induced during previous oscillations is left. This influences the collapse mechanism due to the P-δ effect.

It is useful to observe the P-δ effect quantitatively. Using the simple model, shown in Fig. 5.3.6, the required moment capacity $M_{cap.}$ is calculated from:

$$M_{cap.} = C_d \cdot w_t \cdot 1 \qquad (5.3.5)$$

where: C_d = base shear coefficient

w_t = m.g

1 = height

The additional moment $M_{P\delta}$ due to the P-δ effect is given by:

$$M_{P\delta} = w_t \cdot \delta = w_t \cdot 1 \cdot \gamma \qquad (5.3.6)$$

in which:

γ = deflection angle ($=\delta/1$)

Thus, the deterioration ratio for lateral load resistance $M_{P\delta}/M_{cap.}$ is expressed by:

$$M_{P\delta}/M_{cap.} = \gamma/C_d \qquad (5.3.7)$$

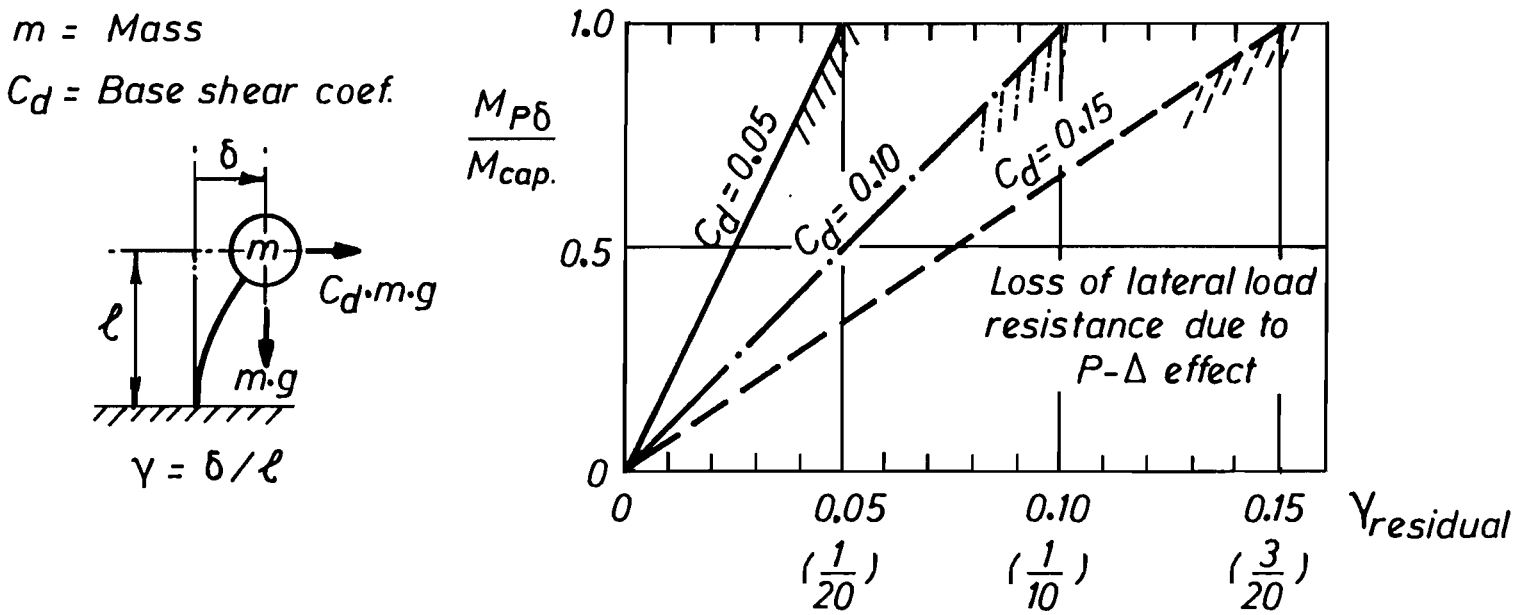

Fig. 5.3.6 Loss of lateral load resistance due to P-δ effect

The relationships between the deterioration ratio and the residual value of γ for C_d values of 0.05, 0.10 and 0.15 are shown in Fig. 5.3.6. It is generally true that taller buildings have a smaller design value of C_d. Moreover, when C_d can be considered as the ratio of the shear strength of a storey to the weight of the structure it sustains, the lower parts of storeys usually have smaller values of C_d. Therefore, the taller the building and the lower the storey being considered, the greater the deterioration of resistance due to the P-δ effect.

The other factor which influences the mechanism of collapse is the possible deterioration of strength due to large imposed deformations and cyclic loading. The bi-linear envelope on the relationship between lateral force F and drift δ, shown in Fig. 5.3.7 is idealised. It assumes no deterioration of strength. However, in reality, quite apart from the P-δ effect, deterioration occurs.

One cause of the strength deterioration is large deformation. This can be seen in monotonic loading tests in a laboratory. When the deformation becomes large, the resistance against lateral load may gradually decrease and finally become negligible at the point C in Fig. 5.3.7. The other major factor is the effect of cyclic loading. A low cycle fatigue type of failure is an extreme example of the effect. In an earthquake, the number of imposed cycles is not as large as encountered in usual fatigue problems. However, cyclic demands impose larger inelastic

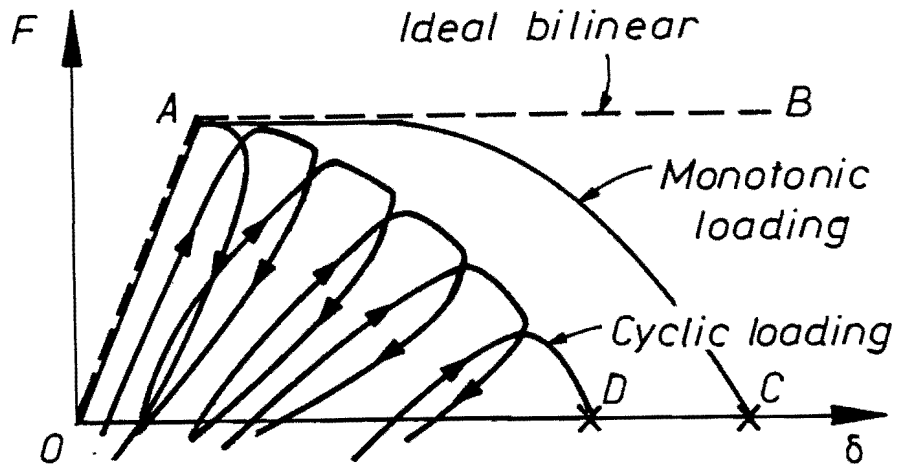

Fig. 5.3.7 Deterioration of strength due to large deformation and cyclic loading effect

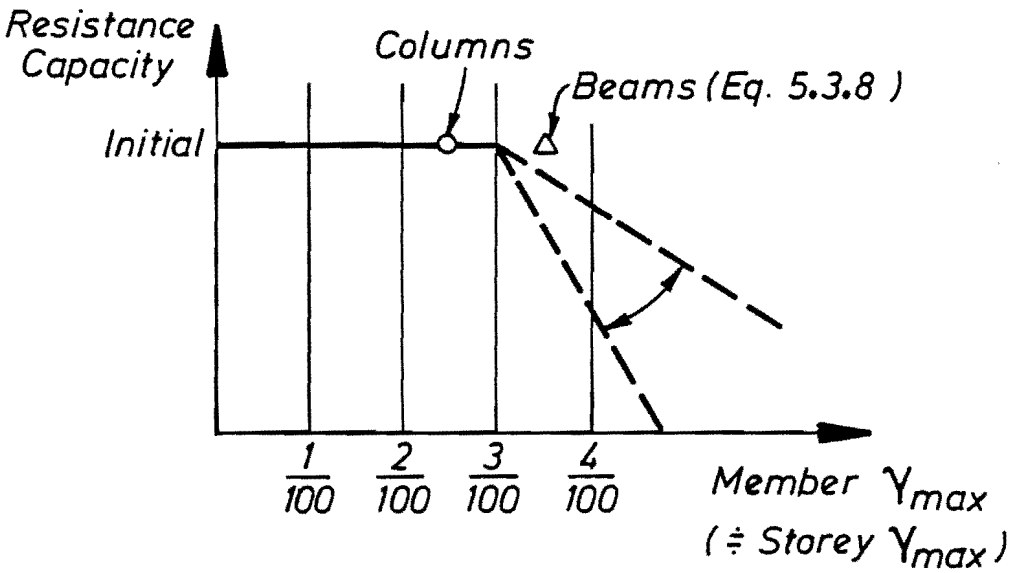

Fig. 5.3.8 Simple assumption for deterioration of strength due to large deformation and cyclic loading effect

deformations. A typical F-δ curve is shown as (O-A-D) in Fig. 5.3.7, which illustrates deterioration due to both large deformation and cyclic loading effect.

The qualitative trend of deterioration has been described. However, it is difficult to predict it quantitatively, because of the following reasons:

1. The number of cycles for different deformation levels depends on the earthquake.

2. The amount of deterioration due to the number of cycles for different deformation levels varies for structural members, the nature of detailing and the materials used.

A simple assumption is introduced to evade the difficulties. Based on a knowledge of static structural tests in a laboratory, ultimate deflection angles for carefully detailed columns and beams in reinforced concrete frames are assumed as follows (62).

$$\gamma_u = 25 \times 10^{-3} \text{ (rad)} \doteqdot 1/40 \text{ (columns)}$$

$$\gamma_u = 35 \times 10^{-3} \text{ (rad)} \doteqdot 1/30 \text{ (beams)} \qquad (5.3.8)$$

It has been suggested that reinforced concrete members designed to New Zealand standards would not be expected to suffer serious deterioration due to a reasonably expected number of loading cycles until the corresponding deflection

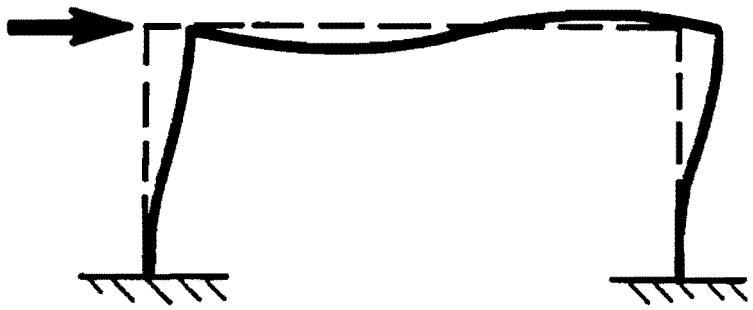

Elastic

+

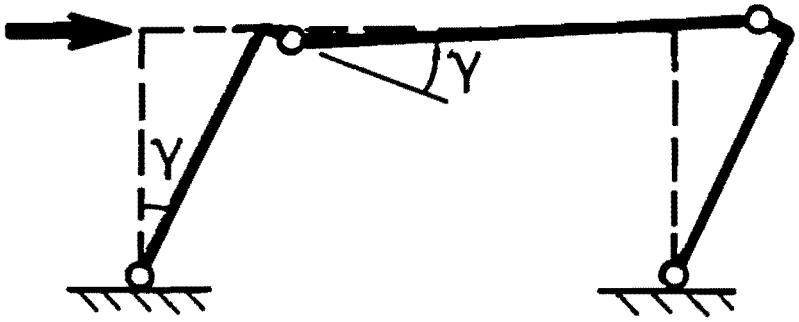

Plastic (dominant)

$$\{\text{Member } \gamma_{max}\} \doteq \{\text{Storey } \gamma_{max}\}$$

Fig. 5.3.9 Relationship between storey and member deflection angles

angles are reached. It can then be more simply assumed that when the maximum deflection angle γ_{max} of a member during earthquake excitation exceeds γ_u = 3/100 (rad), the strength decreases rapidly as shown in Fig. 5.3.8.

Since failure is concerned with collapse of a whole storey, the relationship between storey and member deflection angles must be determined. The total deformation is made up of elastic and plastic deformations as sketched in Fig. 5.3.9. Plastic hinge formation is based on the assumption that the effect of gravity load is very small compared with that of earthquake. In collapse situations, the total deformation will be very large. Thus, plastic deformation can be assumed to dominate. For plastic deformation, it can be assumed that the storey deflection angle is equal to that of the members. Accordingly, the maximum deflection angle γ_{max} of individual members in Fig. 5.3.8 can be replaced with that of the storey.

In assessing the strength of the total collapse mechanism with respect to lateral load, the P-δ effect and the deterioration of strength due to large deformation and cyclic loading must be combined. Collapse is assumed to occur only in a static situation when oscillation of the structure ceases. The criterion of collapse for a single storey frame is given as follows:

$$C - D_{\gamma_{max}} - D_{\gamma_{residual}} = 0$$

or:

$$D_{\gamma_{max}}/C + D_{\gamma_{residual}}/C = 1 \qquad (5.3.9)$$

where: C = initial strength of a single storey model

$D_{\gamma_{max}}$ = deterioration of strength due to large deformation and cyclic loading which is assumed to be a function of maximum storey deflection angle γ_{max} during excitation

$D_{\gamma_{residual}}$ = deterioration of strength due to P-δ effect, which is assumed to be a function of residual storey deflection angle $\gamma_{residual}$

$D_{\gamma_{max}}/C$, $D_{\gamma_{residual}}/C$ = deterioration ratios corresponding to $D_{\gamma_{max}}$ and $D_{\gamma_{residual}}$ respectively.

The deterioration ratios in the criterion are shown in Figs. 5.3.6 and 5.3.8. However, in view of the errors and uncertainty related to the criterion and the inherent uncertainty discussed in 5.2, the criterion seems unnecessarily complicated. Thus, a further simplification is justified.

To make the criterion simpler, in addition to the assumptions implied in Fig. 5.3.8, a relationship between γ_{max} and $\gamma_{residual}$ is assumed. The probability of occurrence that $\gamma_{residual}$ is large when γ_{max} is also large, is considerable. That is, when γ_{max} exceeds 3/100 (rad), $D_{\gamma_{residual}}$ will also be significant. Therefore, the collapse criterion can be simplified to:

$$\gamma_{max} \geq \gamma_u = \frac{3}{100} \tag{5.3.10}$$

where: γ_{max} = maximum storey deflection angle

γ_u = ultimate storey deflection angle

Note that γ_{max} and γ_u in Eq. (5.3.10) are based on real phenomena which includes the P-δ effect and strength deterioration.

The failure criterion has been examined using a single storey model. For multi-storey buildings, the situation is not as simple. The P-δ effect will depend on the drift of different storeys. The relationship between storey and member deflection angles will be more complicated. Generally, during an earthquake, hinges form gradually throughout the structure. Thus especially for multi-storey buildings, the total seismic behaviour is usually somewhere in between elastic behaviour and the behaviour when a mechanism forms. However, it is justifiable to apply the simple criterion in Eq. (5.3.10) to each storey of a multi-storey building, because considerable uncertainty already exists.

Consequently, collapse is assumed to occur when the maximum storey deflection angle of any storey reaches 3/100 (rad) during an earthquake excitation. This particular value is appropriate for ductile reinforced concrete frames which are common in many countries. This structural type will be used as an example in the rest of the present study when developing a procedure for assessing failure probability. However, this does not mean that the general idea of the procedure is restricted to reinforced concrete frame

structures.

Since the failure criterion has been established a major remaining problem is to predict the maximum storey deflection angle probabilistically as shown in Fig. 5.1.1. For such a prediction a simplified structural model must be used. The criterion of collapse in Eq. (5.3.10) which is based on a consideration of real phenomena, must therefore be transformed into another criterion appropriate for the simplified model. An appropriate analytical approach to the prediction of deflection angles and the formulation of a failure criterion for the simplified model are discussed in the next section.

5.4 REQUIREMENTS FOR A PERFORMANCE FUNCTION

5.4.1 Need for a New Performance Measure, and Its Desiderata

In the previous section, the failure criterion was defined in terms of maximum storey deflection angle γ_{max}. Thus according to Fig. 5.1.1 the task remaining for obtaining failure probabilities is to assess the probability distribution of γ_{max} for each storey of a multi-storey building subjected to earthquake. Probability of failure can be calculated based on the area of the probability distribution (probability density function) exceeding the ultimate storey deflection angle γ_u. Such a distribution can be computed by Monte Carlo simulation (see Section 2.2.1) using an inelastic dynamic analysis on the assumption

of the distributions of the basic demand (seismic) and structural variables. However, as explained earlier, this approach is not practical. The only feasible approach is to use the advanced First-Order Second-Moment (F.O.S.M.) method (see Section 2.2.2) which requires a performance function. The performance function to represent structural failure for earthquake must include the basic demand and structural variables in explicit form and must be of a suitable form for expressing the failure criterion. To seek the appropriate performance function is the central problem. The performance function g in terms of the performance measure γ_{max} is, from Eq. (5.3.10):

$$g = \gamma_u - \gamma_{max} \tag{5.4.1}$$

When g is negative, failure occurs. Hence, the significant problem in applying Eq. (5.4.1) to the performance function is whether the performance measure, γ_{max} or maximum inelastic storey drift δ_{max} ($\delta_{max} = \gamma_{max} \times 1$ where 1 = storey height), can be expressed in terms of the basic variables for an earthquake and structure.

Unfortunately for inelastic behaviour of multi-storey buildings, there is no explicit relationship between γ_{max} and the characteristics of earthquake and structure. A formidable barrier to its formulation is the complexity of seismic behaviour of structures. The complexity results chiefly from two factors. Firstly, a large number of variables concerning both earthquake and structure are involved in characterising structural behaviour. For

instance, earthquake variables include spectral characteristics and time domain intensity envelope, while the mass, initial stiffness, yield strength and post yield stiffness of each member are structural variables. The portal frame study presented in Chapter 4 illustrates the large number of variables required for the assessment of the failure probability of even a simple structure. Secondly, the variables are related to the inelastic dynamic behaviour of structures in a complex manner. Although elastic response is relatively easily obtained and a number of analytical techniques exist such as mode superposition and frequency domain analysis (61), the only method of solution for inelastic dynamic problems involves step-by-step integration in the time domain, recalculating the response at each time step.

Attempts have been made to propose an approximation for inelastic behaviour, in order to understand the behaviour in a simpler manner. One of the most commonly used methods is based on the approximation that the effects of yielding can be accounted for by linear elastic analysis of the building using the design spectrum for inelastic systems, determined from the elastic design spectrum and an allowable ductility factor (61,63,64). The approximation is founded on the established relationship between elastic and inelastic dynamic response, shown in Fig. 5.4.1. The shape of the design spectrum is assumed based on past recorded earthquakes (Fig. 5.4.1(a)). Suppose the fundamental period of a single degree of freedom (S.D.O.F.) system is in the small region S of the period. When the system yields, the

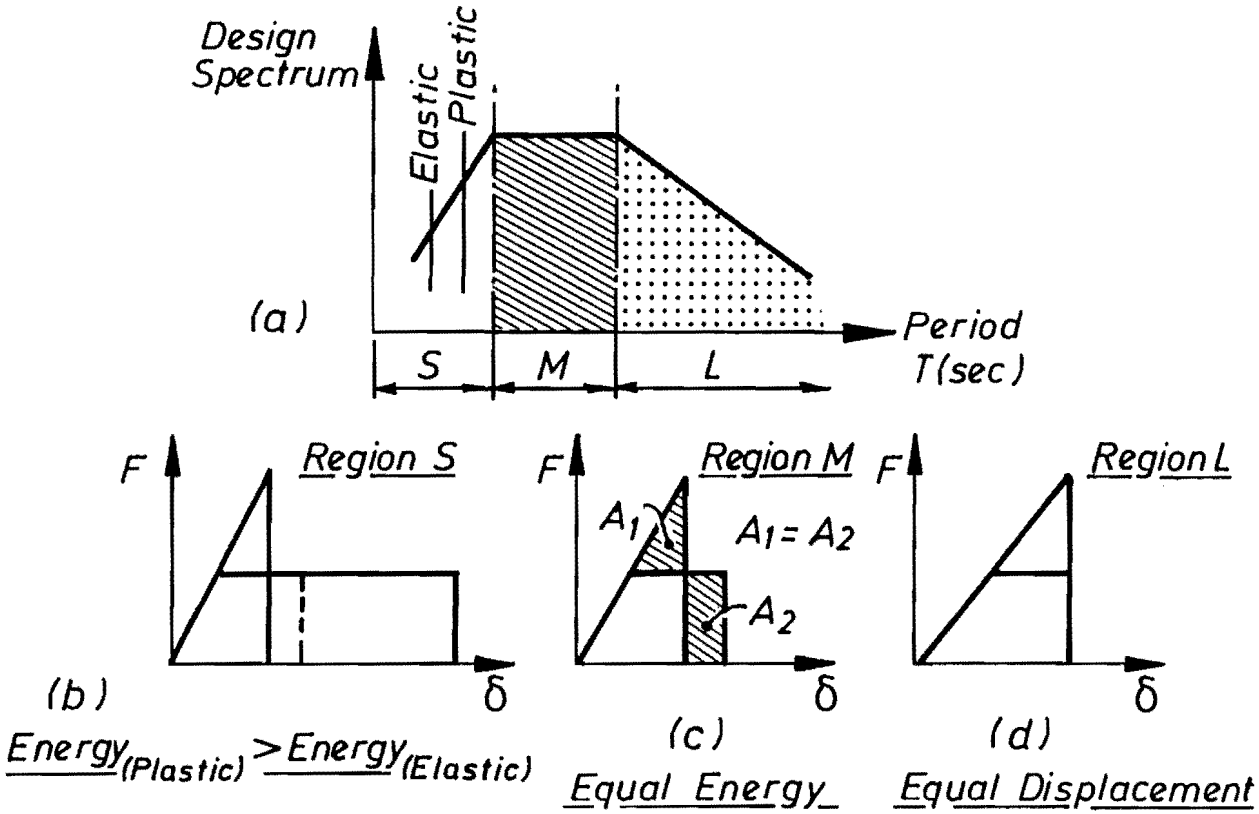

Fig. 5.4.1 Simplification made for elastic and inelastic dynamic analyses

resonant period becomes larger than the elastic one. By the shift of the resonant period, earthquake effects increase (see Fig. 5.4.1(a)). Thus, the absorbed energy for the inelastic behaviour is larger than that for the corresponding elastic behaviour (same initial stiffness and mass, but no yielding is considered) (see Fig. 5.4.1(b)). In the middle region of the period, M, the design spectrum is constant. This means that irrespective of whether behaviour is elastic or plastic, the input energy does not change. Thus for S.D.O.F. systems in this period range, the equal energy concept can be applied (Fig. 5.4.1(c)). However, in the region of long periods, L, the elastic and inelastic response displacements are found to be almost equal because the input energy decreases due to the shift of resonant period (Fig. 5.4.1(d)). Thus, broad tendencies can be obtained for the relationship between the elastic and inelastic response in all three regions. However, the effect of higher modes is not taken into account, and the method is only applicable to a S.D.O.F. system, like a bridge. Moreover, even when the method is assumed to be applicable to multi-storey buildings, it is awkward that the structures need to be divided into groups (in this case three) based on questionable assumptions for the design spectrum. In another commonly used simple method, use is made of an equivalent linear system (65) with an equivalent natural period and damping. However, this method has been developed only for a S.D.O.F. system, too.

Therefore we cannot use Eq. (5.4.1) as a performance function. The whole idea of a relationship between the

input basic variables and the output γ_{max} (or δ_{max}) demands that there be a definable invariant or overall single parameter which describes inelastic dynamic behaviour. This could bypass the complexity of inelastic structural behaviour resulting from the two factors explained earlier. The invariant would be employed as another performance measure which could be used either for direct formulation of a failure criterion, or as an intermediate variable related directly to the original performance measure γ_{max}, and which would be expressed in terms of the basic demand and structural variables. For instance, suppose we were to find an appropriate performance measure, which could represent inelastic dynamic behaviour and be expressed in terms of the basic variables. A new failure criterion in terms of the new measure could be established related to the criterion in terms of γ_{max}. As we would have a new criterion and a new performance measure, a new performance function could then be obtained. Hence, the new measure would be employed for establishing a new failure criterion and performance function. However, at the same time, γ_{max} could be predicted by an equation based on the new measure. It would enable Eq. (5.4.1) to be used as a practical performance function. Thus, the new measure could also be considered as an intermediate variable enabling the use of Eq. (5.4.1) as a performance function.

Therefore, such a new performance measure must have the following three requirements:

1. It must be able to be used in a performance

function which can be used in a failure criterion.

2. It must be expressed in terms of the basic demand and structural variables. This is not easy for the inelastic dynamic behaviour of a complex structure as a whole.

3. It must be a function of only a relatively few basic demand and structural variables, otherwise the F.O.S.M. approach becomes impractical.

A new performance measure which meets the above requirements will be introduced in Section 5.5.

5.4.2 Analytic Model for Determining a Performance Function

An essential step in the development of a performance function is to choose an appropriate analytic model. In developing a performance function, explicit relationships between a performance measure and basic variables must be obtained. For their development an analytic model is required. Because the nature of seismic behaviour is dynamic and maximum inelastic storey drift δ_{max} is chosen as a definition of failure, an appropriate analytical model for an inelastic dynamic analysis to assess δ_{max} must be determined.

A number of different models for the dynamic analysis of multi-storey buildings could be used for calculating maximum

inelastic storey drifts during earthquake excitations. Figure 5.4.2 shows three widely used examples. Model (a) consists of column and beam elements, while models (b) and (c) are composed of one stiffness element and a lumped mass for each storey. The element in model (b) is the so-called beam element with 4 degrees of freedom. In model (c), a shear spring element with a single degree of freedom is used. Though the model (a) is an accurate modelling for a structure, it is too complicated for developing a performance function. In choosing an adequate model from models (b) and (c) one should consider deformation types the models can represent. Figure 5.4.3 shows two typical deformation types. Both types are related to flexural deformation of columns, but in type (a) no column extension and shortening occurs. Thus the interstorey drift of each storey is dependent only on the shear force applied to the storey. This type of deformation may be called a shear type of deformation. On the other hand, the interstorey drifts in type (b) are coupled because the rotation of a floor due to column extension and shortening affects storey drift. This type of deformation may be referred to as a bending type. Model (b) in Fig. 5.4.2 can express both shear and bending types of deformation, while model (c) is applicable only to the shear type. The dominant type of deformation depends on the arrangement of columns and walls, plastic hinge formation, etc. In a broad way for a frame structure, when H/B shown in Fig. 5.4.3 becomes big, the bending type of deformation is not negligibly small. For existing buildings especially in high seismicity regions, such slender buildings may be considered to be rare. Thus, it can be

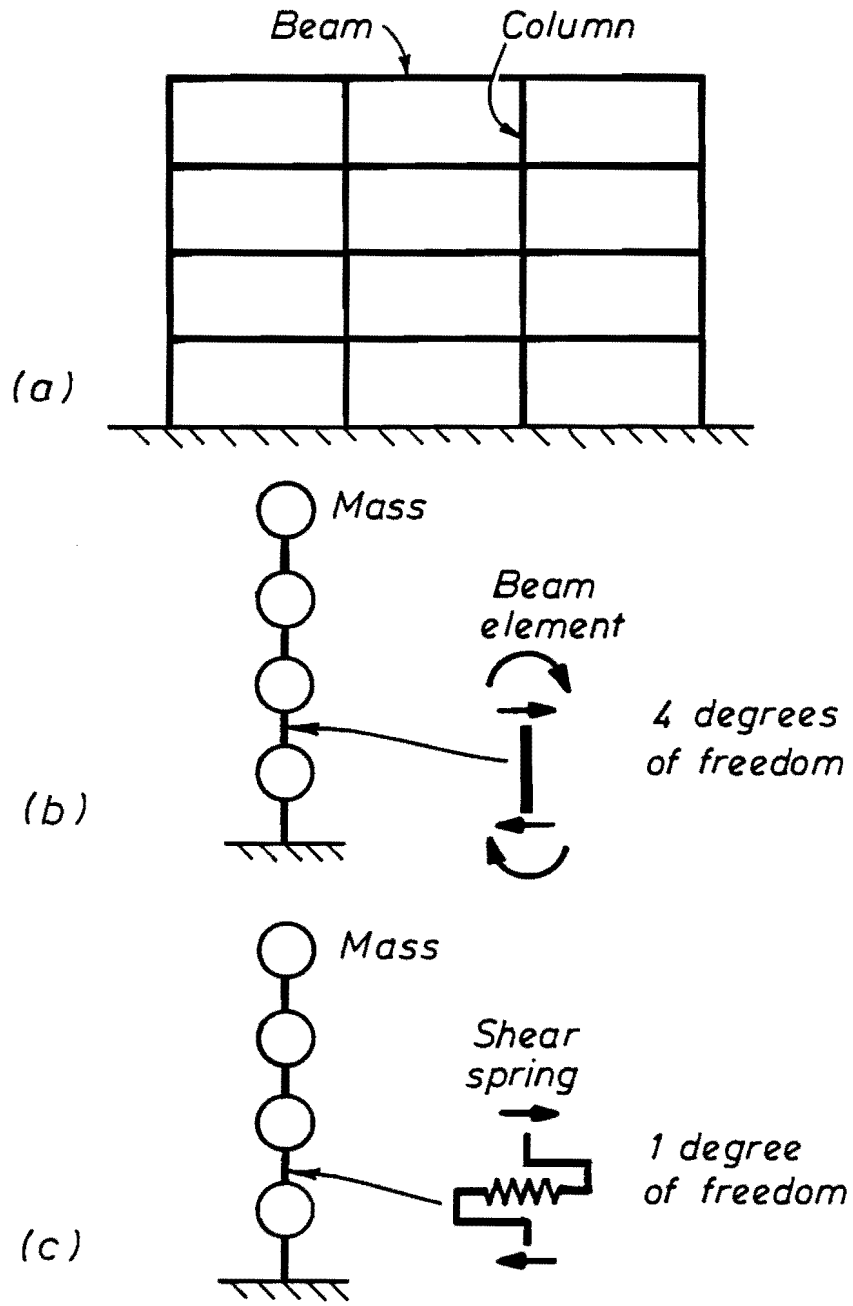

Fig. 5.4.2 Structural models for a non-linear dynamic anlaysis

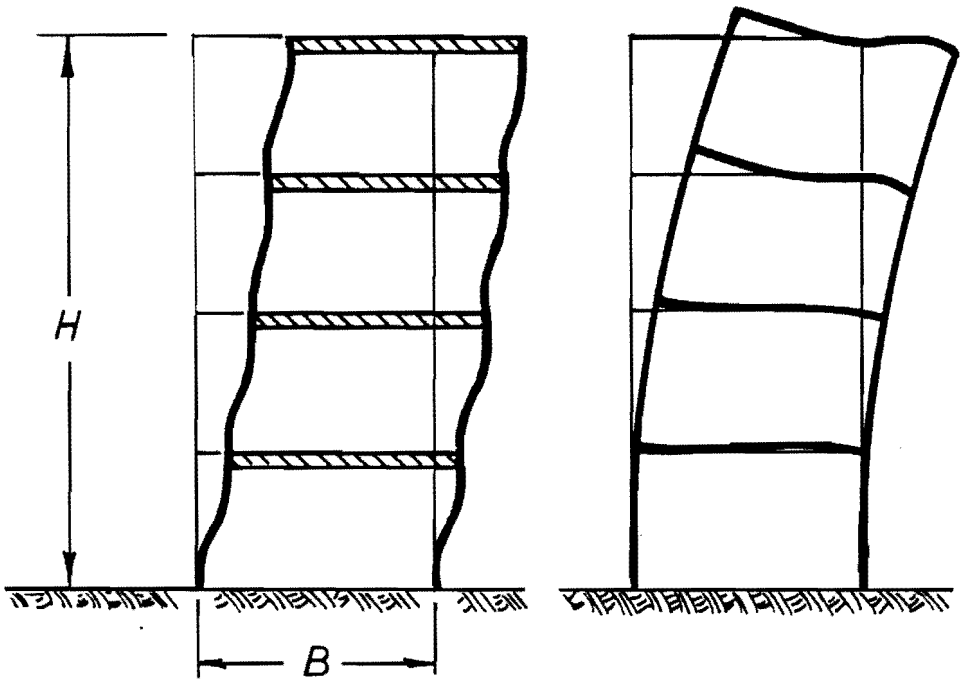

Fig. 5.4.3 Types of deformation

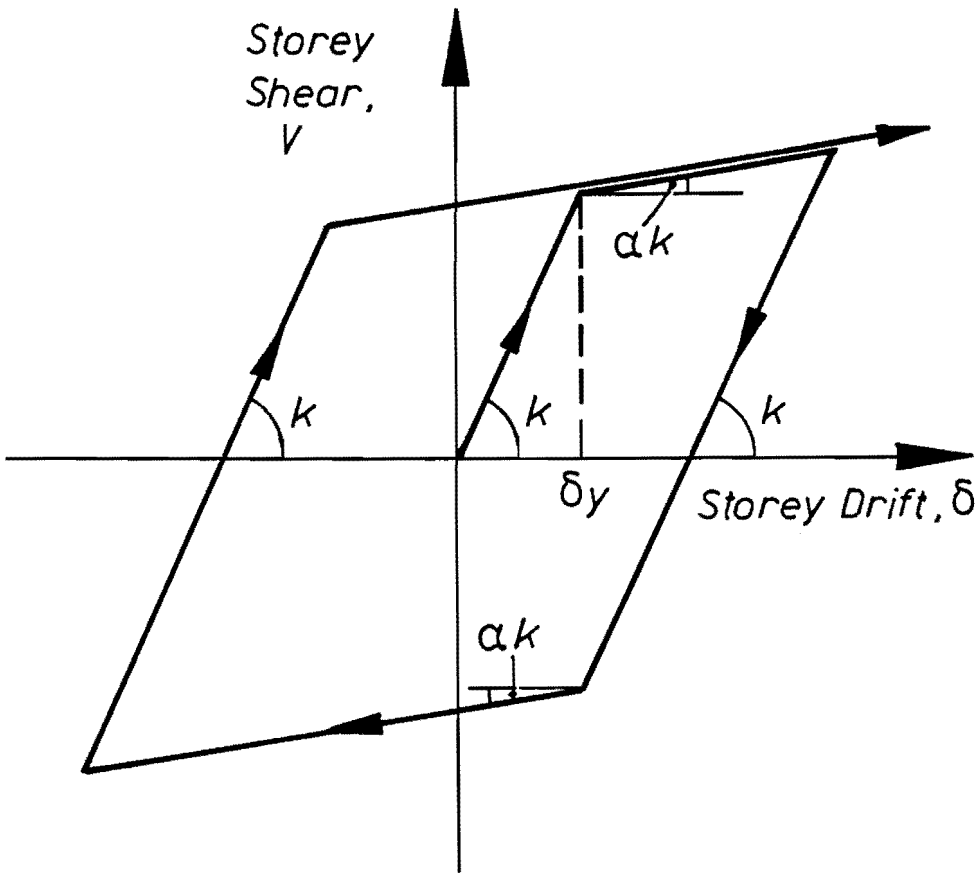

Fig. 5.4.4 Bi-linear hysteresis rule

assumed that the shear type of deformation is dominant for ordinary multi-storey buildings. Therefore, model (c) which is the simplest model for dealing with δ_{max} is good enough. For this reason and because any model has a high degree of inherent uncertainty, as discussed in 5.2, model (c) will be chosen as the appropriate model for the present study. It will be called the spring-mass model.

An appropriate means of dealing with non-linearity must also be determined. Two types of non-linearity occur in structural problems; (1) material non-linearity and (2) geometric non-linearity (66). The first type is due to the non-linearity of the structural material and can be expressed in the spring-mass model by a non-linear spring constant with hysteresis. Again, in the light of considerable inherent uncertainty, the simple bi-linear hysteresis rule, shown in Fig. 5.4.4, is considered to be adequate. The second type of non-linearity occurs when deflections are large enough to cause significant changes in geometry, so that the equations of equilibrium must be reformulated for the deformed configuration. Because we are concerned with collapse, large deflections must be considered. However, such an analysis is very complex and is impractical in the present context. Therefore, geometric non-linearity cannot be dealt with by an approach involving reformulation of the equations of equilibrium.

Using bi-linear hysteresis and neglecting geometric non-linearity in the analysis mean that deterioration of strength due to large deflection, cyclic loading and the P-δ

effect is not directly considered. The deterioration effects can be taken into account by the simple assumption that the actual deflection angle will increase by 50% when the storey deflection angle calculated by the dynamic analysis without considering strength deterioration reaches a value of, say, 2/100 (62). Thus to take the effect of the deterioration into account indirectly, the basic failure criterion of Eq. (5.3.10) is modified to:

$$\gamma_{max} \geq \gamma_u = 1/50 \qquad (5.4.2)$$

where γ_{max} is obtained by the dynamic analysis without considering the deterioration of strength due to large deflection, cyclic loading and the P-δ effect.

Thus a spring mass model with a bi-linear hysteresis rule is chosen as an appropriate analytic model for the project, with the failure criterion given in Equation (5.4.2).

5.5 AN INVARIANT MEASURE OF EARTHQUAKE DAMAGE

As previously stated the advanced First-Order Second-Moment (F.O.S.M.) approach is the only practical method to assess failure probabilities. The approach requires a performance function relating the basic variables and a failure criterion.

As explained in the previous section, in order to establish an appropriate performance function, it is desirable to find an invariant which describes the overall inelastic dynamic behaviour of a structure. It must take into account complete structural behaviour - the complete time history of a structure - as well as the behaviour of all relevant parts of a structure. The invariant can be used as an intermediate performance measure in the performance function in terms of γ_{max}. Three requirements for the new performance measure were described in the previous section.

In this section, a new performance measure to satisfy the three requirements is introduced. Though the performance measure is related to a failure criterion, it is in general concerned with damage. Before discussing the appropriate measure, an outline of previous work on measures for earthquake damage is given in the next section.

5.5.1 Review of Previous Work on Measures of Earthquake Damage

Previous work attempting to define measures of earthquake damage is relatively sparse. Table 5.5.1 summarises several approaches (67-71). In the table, all approaches except that of Akiyama used damage indicators based on single member behaviour. Akiyama, on the other hand, developed an indicator based on the behaviour of an entire storey.

Banon et al. (67,68) developed a probabilistic model of

Table 5.5.1 Summary of previous work on measures of earthquake damage

Reference	Damage indicator for each member	Damage criterion for each member	Damage prediction for an entire structure
Banon et al. [67] [68]	(1) FDR (Flexural Damage Ratio) = {post cracking flexural stiffness} / {minimum reduced secant stiffness} (2) En (Normalized Dissipated Energy) = {energy dissipated by rotation at one end of a member} / {the maximum elastic energy stored in a member}	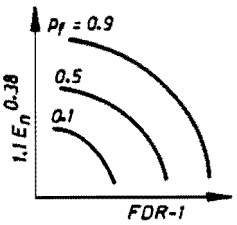	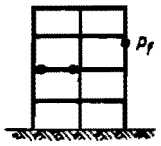 Used in a dynamic frame analysis
Meyer et al. [69]	(1) DR (Damage Ratio) = {initial stiffness} / {minimum reduced secant stiffness} (2) CW (Crack Width) = {widths of all the cracks in the end region of a beam}	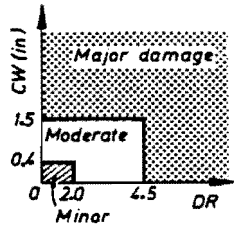	(No explanation)
Czarnecki and Biggs [70]	$D = \frac{A_x}{A_T}$ A_T = {total inelastic energy absorption capacity} A_x = {amount of inelastic energy absorbed to develop a strain ε_x} 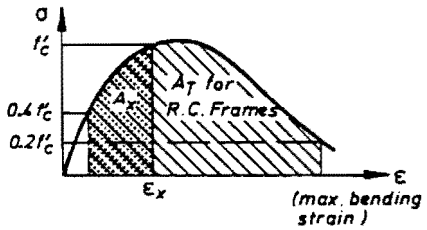 Confined Concrete	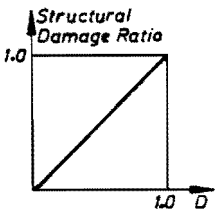 Columns only	$\overline{D} = \frac{1}{k} \sum_{\text{all columns}} \frac{A_x}{A_T}$ k: number of columns {average structural damage ratio} = $\frac{1}{n} \sum_{\text{all storeys}} \overline{D}$ n: number of storeys
Reference	Damage indicator for a storey	Criterion of collapse for a structure	
Akiyama [71]	η = cumulative plastic ductility ratio = $\sum_i \mu_i$ (over the entire duration of an earthquake) 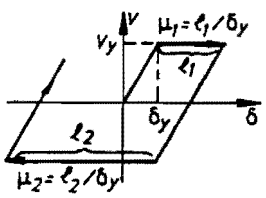	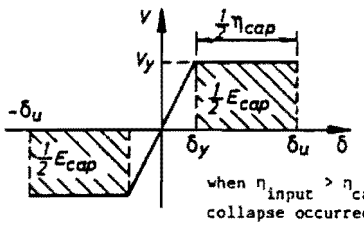 when $\eta_{input} > \eta_{cap}$ collapse occurred	

member failure. Five damage indicators were compared with 29 experimental results obtained from full-size members or large scale frame subassemblages in order to select appropriate indicators. However, none attained stable values. Based on the accuracy of the results and on physical principles, flexural damage ratio (FDR) and normalised dissipated energy (E_n) were chosen as suitable damage indicators for a probabilistic model of member resistance. FDR is defined for a structural member as:

$$FDR = k_f / k_r \tag{5.5.1}$$

where: K_f = $24\ EI/L^3$

EI = stiffness of cracked member

L = member length

K_r = reduced secant stiffness at maximum displacement

The dissipated energy E_n is given by:

$$E_n = \int_0^t M(\tau)\theta(d\tau) \Big/ \frac{My^2 \cdot L}{12\ EI} \tag{5.5.2}$$

in which:

t = time elapsed since the beginning of loading

$M(\tau)$ = moment at one end of the member at time, τ

$\theta(d\tau)$ = rotation increment at one end of the member during the time interval τ to $\tau + d\tau$

M_y = yield moment

FDR and E_n represent damage due to large deformations and cumulative fatigue-type damage respectively. Introducing a so-called hazard function, the path-independent failure probability in the (FDR-1, 1.1 $E_n^{0.38}$) plane was determined, as shown in Table 5.5.1. The complicated coordinates, FDR-1 and 1.1 $E_n^{0.38}$, were derived from simplifications of the integral assessing the cumulative distribution function. The results were used in a non-linear dynamic analysis to predict failure probabilities of members.

Meyer, Arzoumanidis and Shinozuka (69) developed an analysis procedure which permits the safety assessment of existing buildings, especially putting emphasis on buildings which may have been damaged in previous earthquakes. Two damage indicators, damage ratio (DR) and crack width (CW), were chosen on a member level. The damage ratio is expressed by:

$$DR = K_0 / K_r \tag{5.5.3}$$

where: K_o = initial stiffness

K_r = as defined in Equation (5.5.1)

The procedure reflects the stiffness as well as the strength degradation of a member and therefore is considered to be a good indicator of structural damage. CW is assumed to

combine the widths of all the cracks in the end region of a beam, which can be estimated by field inspection after an earthquake. If CW is large, the beam would be expected to indicate a corresponding severity of concrete failure. DR and CW are highly correlated and the relationship was evaluated by using Monte Carlo simulation for a single member structure (CW was computed using an approximation). A definition of damage states was given in the plane of DR and CW, as shown in Table 5.5.1. It can establish the damage classification of a structure relevant to previous earthquakes, in a manner consistent with the degree of accuracy achieved when the degree of structural damage is estimated by means of field inspection.

Czarnecki and Biggs (70) developed a method for the estimation of earthquake damage to tall buildings based on the building's response. Damage to typical building components is estimated by comparing the amount of energy absorbed by a particular component to the maximum energy absorption capacity of that component. For example, for columns of reinforced concrete frames the damage ratio D can be given by:

$$D = A_X / A_T \qquad (5.5.4)$$

where: A_T = total inelastic energy absorption capacity, which is the area A_T in the figure given in Table 5.5.1 using the assumed stress-strain curve

A_X = amount of inelastic energy absorbed to

develop the maximum bending strain ε_x, which is the area A_X in Table 5.5.1

Only damage to columns is assumed to be important. The average damage ratio $\overline{D}$ for each storey is given by:

$$\overline{D} = \frac{1}{k} \sum_{\substack{\text{all columns} \\ \text{in storey}}} A_X / A_T \qquad (5.5.5)$$

in which:

k = number of columns in the storey

The average structural damage ratio for the whole building is then:

$$\left(\begin{matrix}\text{Average Structural} \\ \text{Damage Ratio}\end{matrix}\right) = \frac{1}{n} \sum_{\text{all storeys}} \overline{D} \qquad (5.5.6)$$

in which:

n = number of storeys

The method was applied to some the buildings which were damaged during the 1971 San Fernando earthquake. It was concluded that the method for the estimation of damage could predict general trends of damage but might be considerable error in any specific case.

Akiyama (71) proposed a new seismic design approach based on energy considerations. The total amount of energy

introduced by an earthquake to a building was found to be a very stable quantity. The effect of ground motions on the building was expressed in terms of total energy input. The corresponding resistance of the building was quantified in terms of the energy absorption capacity of the frame. In developing a seismic design method, applicable to any type of multi storey structure, the issues were summarised by Akiyama as follows:

1. In what manner can the energy input due to earthquakes be related to the mechanical properties of structures?

2. How is the total energy input distributed over every part of a structure?

3. What functional relation may be found between the energy absorption capacity of a structural frame, its material properties and the geometry of the frame?

As a contribution to the first two issues, elasto-plastic response analyses of a large number of vibrational models were carried out. By the abstraction of individual results of numerical analyses and the development of concepts with respect to the "giving and receiving" of energy, the third issue was worked out. Hence the design method for earthquake resistance was developed. Akiyama's research is closely related to the present study, so further details are given in 6.2.

In Akiyama's work, the cumulative plastic ductility ratio η was chosen as a damage indicator for a storey. The term plastic ductility factor μ was used to measure the plastic strain energy dissipated. It is related to the conventional ductility factor μ_Δ by the simple relationship $\mu = \mu_\Delta - 1$. The cumulative plastic ductility ratio is defined as the sum of the plastic ductility factors derived from displacements in every half-cycle summed over the entire duration of an earthquake (see Table 5.5.1). Figure 5.5.1 shows the general hysteresis rule chosen, based on the assumption that a curve obtained by connecting sequential load-displacement relations in one loading direction, positive or negative, agrees with that under monotonic loading, drawn by dashed lines. The energy absorption capacity $E_{cap.}$ was defined as the absorption capacity of plastic strain energy for the assumed monotonic envelope until the storey shear strength became zero. The absorption capacity $E_{cap.}$ was used in calculating the ductility ratio capacity $\eta_{cap.}$ for the corresponding elasto-fully-plastic hysteresis (see Fig. 5.5.1), i.e.:

$$\eta_{cap.} = E_{cap.} / V_y \cdot \delta_y \qquad (5.5.7)$$

where: V_y = yield shear strength

δ_y = yield storey drift

On the other hand, the required energy related to damage, $E_{req.}$ demanded by an earthquake was estimated by the required energy input for an entire structure and the damage

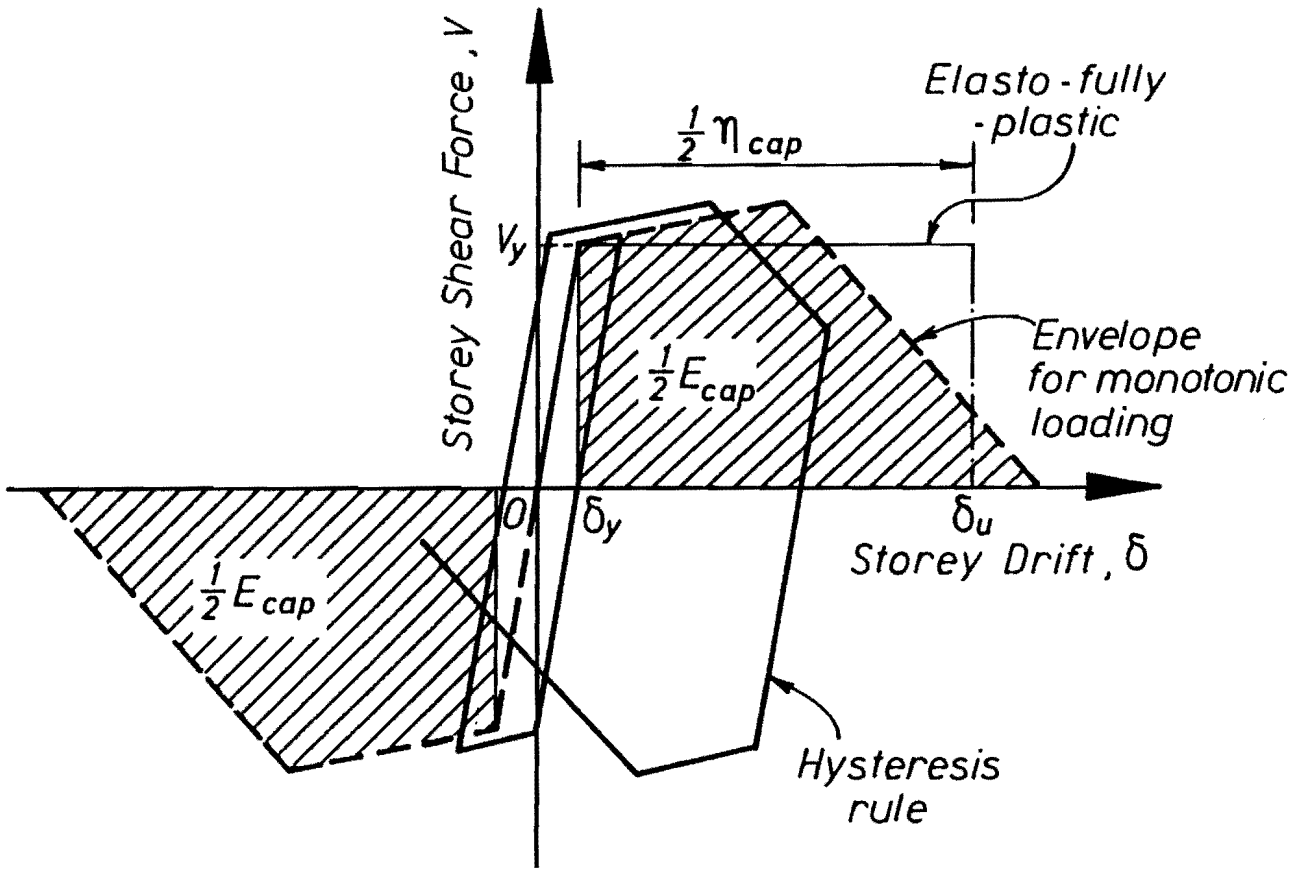

Fig. 5.5.1 Hysteresis rule and energy absorption capacity assumed by Akiyama

contribution of the storey. Likewise, the required ductility ratio $\eta_{req.}$, could be calculated by E_{req}. The criterion of collapse was then given by:

$$\eta_{cap.} - \eta_{req.} < 0 \qquad (5.5.8)$$

5.5.2 An Invariant Measure of Earthquake Damage

An appropriate performance measure which meets the three specified requirements is introduced in this subsection. It will be demonstrated in Chapters 6 and 7 that the three criteria are fulfilled. As explained earlier, a new performance measure must be an invariant which describes inelastic dynamic behaviour and is related to the maximum storey deflection angle γ_{max}. Though γ_{max} is used in a failure criterion, it is basically concerned with structural damage due to earthquake. It is thus important to consider what item in a dynamic equilibrium expressed in terms of energy is most suitable for expressing structural damage. The reason for considering equilibrium is to be able to choose a new measure easily understood in physical terms. Furthermore, since energy is a scalar and cumulative, energy is a single quantity which could express the total damage occurring during the bi-directional cyclic excitation of an earthquake.

Dynamic equilibrium for a single-degree-of-freedom-system is expressed by Eq. (5.3.2). Multiplying by $\dot{\delta}(t)dt$ and integrating over the entire duration S of an earthquake, Eq. (5.3.2) may be transformed into an equation in terms of

energy (71,72), as follows:

$$m\int_0^S \ddot{\delta}(t)\dot{\delta}(t)dt + \int_0^S C(t)\dot{\delta}(t)^2 dt + \int_0^S V(t)\dot{\delta}(t)dt = \int_0^S F(t)\dot{\delta}(t)dt \qquad (5.5.9)$$

where: $V(t)$ = shear force of the spring system at time t

The right-hand side of the above equation expresses the total amount of energy E_T input to the structure in an earthquake. The left-hand side expresses the contribution of responses in terms of energy corresponding to the total energy input. Clearly, damage of the structure is not directly related to the right hand side term. The first term on the left hand side of the equation can be reduced using partial integration to:

$$m\int_0^S \ddot{\delta}(t)\dot{\delta}(t)dt = \tfrac{1}{2} m \dot{\delta}(s)^2 \qquad (5.5.10)$$

This gives the kinematic energy E_K at the point when the earthquake motion vanishes. The second term of the left-hand side expresses the energy consumed by the damping mechanism (E_D). The energies, E_K and E_D, are not directly related to structural damage.

The third term of Eq. (5.5.9) denotes the strain energy absorbed in the spring system, which consists of cumulative elastic strain energy E_E stored and cumulative plastic strain energy dissipated when the earthquake motion ceases. Using the bi-linear hysteresis rule, which is adopted in the

present study as explained in 5.4, it may now be examined whether or not these energies are related to earthquake damage. The bi-linear hysteresis shown in Fig. 5.4.4 consists of two types of line distinguished by their slopes. One line is characterised by an initial stiffness k, and the other by a reduced stiffness αk ($0 \leq \alpha < 1$). The two lines are marked (1) and (2) respectively in Fig. 5.5.2(1). Regardless of whether the structure is represented by line (1) or line (2), the amount of strain energy due to the deformation from A to B in Fig. 5.5.2(2) is equal to the shaded trapezoidal area. When the response is defined by line (1), either for loading or unloading, the structure behaves elastically. This implies that no damage accumulates in the structure. Elastic strain energy is being stored when a deformation occurs along a line (1). Elastic strain energy is not related to earthquake damage. As shown in Fig. 5.5.2(3), elastic strain energy is taken as positive when loading and negative when unloading. For the elasto-fully-plastic hysteresis (α=0), the maximum elastic strain energy is $1/2 \cdot V_y \cdot \delta_y$, where V_y = yield storey shear strength and δ_y = yield storey drift (see Fig. 5.5.2(4)). The cumulative elastic strain energy E_E and kinematic energy E_k together constitute the elastic vibrational energy when an earthquake motion ceases.

On the other hand, a deformation along line (2) in Fig. 5.5.2(1) is considered to be plastic deformation. This results in damage for the structure. Plastic strain energy is the strain energy to plastic deformation. Therefore, plastic strain energy must be closely related to structural

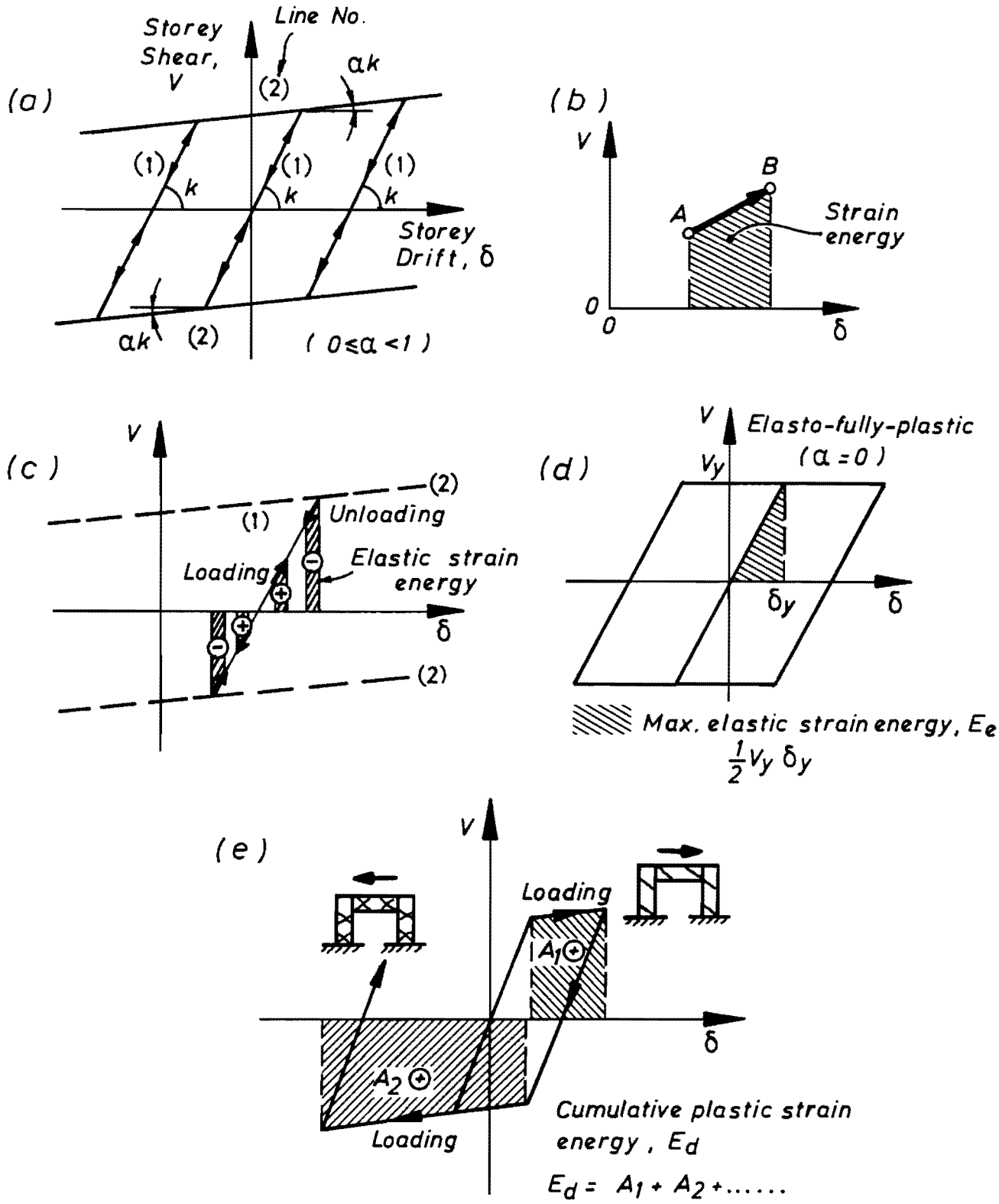

Fig. 5.5.2 Elastic and plastic strain energies for the bi-linear hysteresis rule

damage. Because plastic deformation occurs only during loading, not unloading, the energy dissipated is always taken as positive irrespective of the direction of the loading, as shown in Fig. 5.5.2(5). Thus, during the reversed cyclic excitation of an earthquake, when plastic deformation occurs regardless of direction and time, damage due to deformation can accumulate in the structure as cumulative plastic strain energy. Thus, cumulative plastic strain energy is the most promising item for expressing earthquake damage. It will be referred to as E_d, where subscript d denotes damage. It is chosen as the new performance measure. This indicator of earthquake damage itself is virtually the same as that of Akiyama (Table 5.5.1).

Equation (5.5.9) can be transformed into:

$$E_k + E_D + E_E + E_d = E_T \qquad (5.5.11)$$

in which:

E_k = the kinetic energy when the earthquake motion vanishes

E_D = the cumulative energy dissipated by the damping mechanism

E_E = the cumulative elastic strain energy

E_d = the cumulative plastic strain energy, which is related to earthquake damage

E_T = the total energy input by an earthquake

Since the new performance measure, cumulative plastic strain energy E_d, must be related to the maximum storey deflection angle γ_{max} or maximum inelastic storey drift δ_{max}, it is an important question whether there is a straightforward relationship between δ_{max} and E_d. Conceptually, the relation could have different patterns as shown in Fig. 5.5.3. Some earthquakes may induce a number of displacement cycles with a small amplitude which would eventually reach a specific value of E_d. Others might reach the same values of E_d with only a few cycles at a large displacement. Obviously, the maximum inelastic storey drift in the latter case would be bigger than that for the former. When the magnitudes of deformation in the two directions are not identical, asymmetric "walking" may occur (see Fig. 5.5.3(3)). The maximum drift could be bigger again. The inconsistency may result in the calculation of E_d from the simple summation of plastic strain energy. For example, the effect of cyclic loading on structural damage is not constant between cycles, as shown in Fig. 5.5.4(1); the first cycle is likely to cause more damage than the 2nd or 3rd, even tracing the same path. Another example of concern in the evaluation of damage is the effect of deformation magnitude, illustrated in Fig. 5.5.4(2). Even when the plastic strain energies for the two cases are the same, the plastic deformation of (2) would lead to greater damage than that of (1). This might indicate that a weighting factor is required in summing up the plastic strain energy for each type in order to get an universal relationship for maximum inelastic storey drift. However in practice, such a weighting factor would be difficult to determine. Moreover,

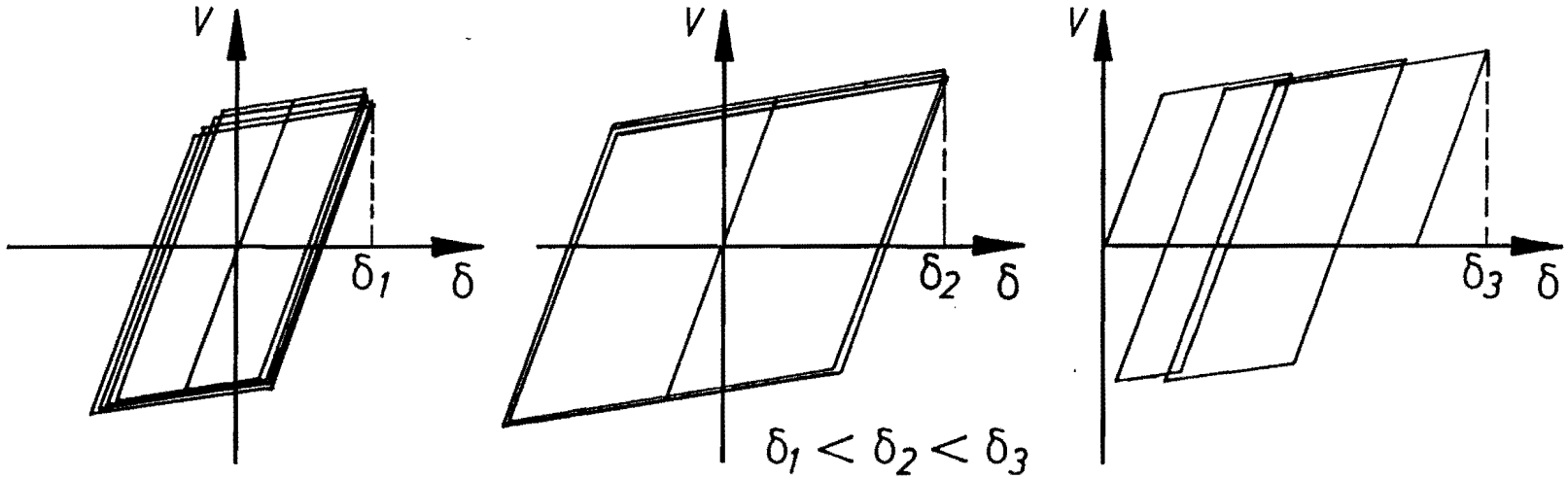

(a) A number of cycles in a constant small displacement level

(b) A few cycles in a constant large displacement level

(c) A few cycles in asymmetric walking

Fig. 5.5.3 Comparison of maximum inelastic storey drifts for different inelastic paths absorbing the same total plastic strain energy

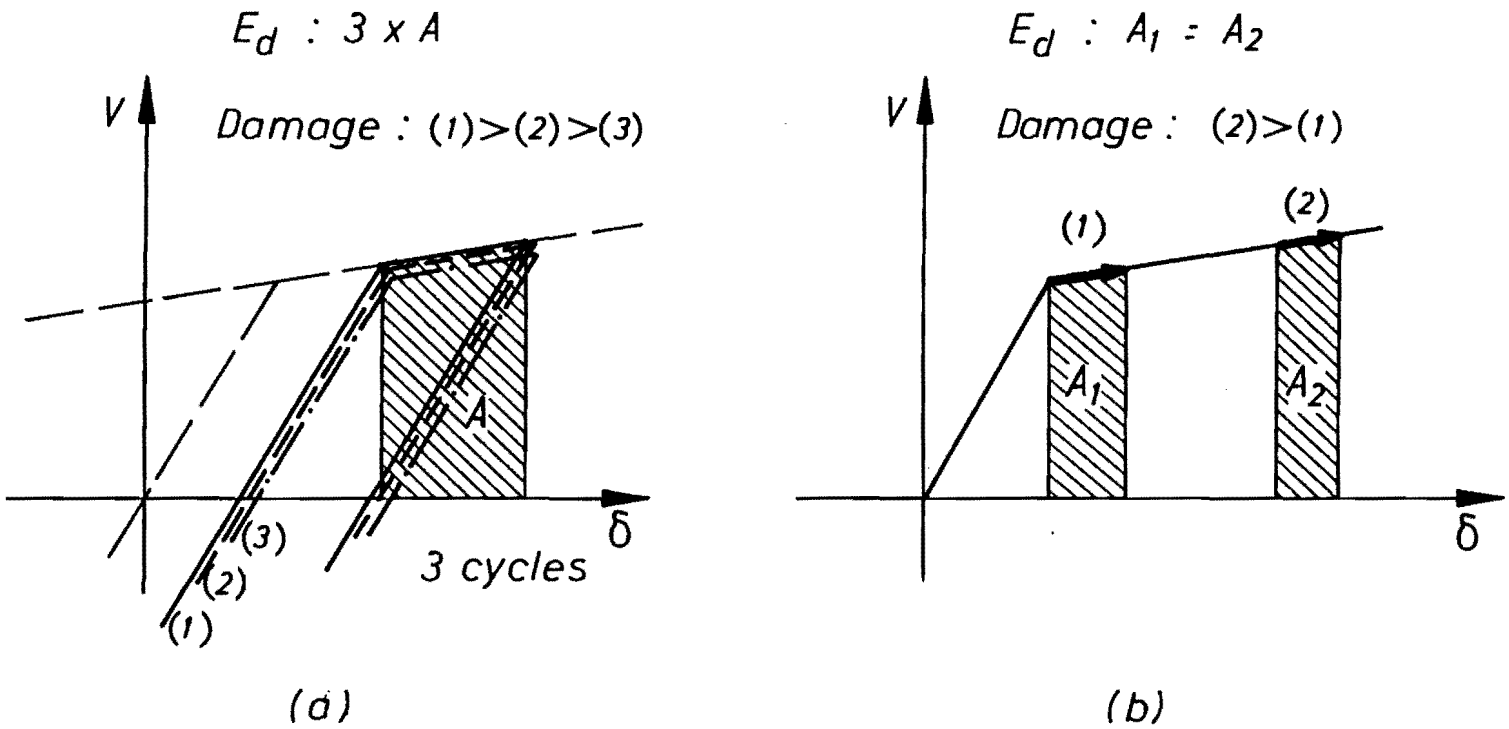

Fig. 5.5.4 Relationship between cumulative plastic strain energy and expected damage

in the light of the inherent uncertainty, this requirement does not appear to be justified.

In the next chapter, a performance function in terms of cumulative plastic strain energy E_d is established by estimating the relationship between maximum inelastic storey drift δ_{max} and E_d, and by formulating the function in terms of the basic seismic and structural variables. Thus, the first two requirements for the new performance measure, discussed in 5.4.1, are fulfilled; i.e. the new performance measure must be used in a proposed performance function and be expressed in terms of the basic variables. Chapter 7 shows that the F.O.S.M. approach using the performance function is practical. This meets the last requirement.

CHAPTER 6

SIMPLE PREDICTION OF MAXIMUM INELASTIC STOREY DRIFTS FOR MULTI-STOREY FRAME BUILDINGS BY MEANS OF CUMULATIVE PLASTIC STRAIN ENERGY

6.1 INTRODUCTION

In establishing a balanced code, failure probabilities for a large number of structures are required to be assessed. By using the results, one can examine whether the lowest safety level of any structural type meets the failure criterion, and whether the variability of safety levels is reasonably small. These are the criteria for a balanced code. In calculating failure probabilities, a performance function needs to be established for use in the advanced First-Order Second-Moment method. A performance function consists of a relationship between the basic variables and a failure criterion. A failure criterion in terms of maximum storey deflection angle γ_{max} was introduced in section 5.3. It is possible to form a performance function with the performance measure γ_{max}. However, γ_{max} cannot be expressed in terms of the basic demand and structural variables because of the complexity of the seismic behaviour of structures. Thus, a performance function in these terms is not feasible. For developing an appropriate performance function, a new performance measure, cumulative plastic strain energy, was introduced.

This chapter shows that using cumulative plastic strain energy, maximum inelastic storey drift δ_{max} ($\delta_{max} = \gamma_{max} \times 1$, where 1 = storey height) can be expressed in terms of the basic variables. In order words, a simple equation is proposed for predicting δ_{max} for multi-storey buildings. Hence the original performance function in terms of γ_{max} can then be usable. Furthermore, a new failure criterion in terms of cumulative plastic strain energy can be defined and calibrated against the original failure criterion in terms of γ_{max}. It enables us to obtain a new performance function in terms of cumulative plastic strain energy. Therefore, the performance function proposed in this chapter can be considered either as a workable form of the original performance function or as a new performance function.

In making a proposal for a prediction method for interstorey drifts it is necessary to evaluate the relationship between the absorbed cumulative plastic strain energy in a storey and the corresponding maximum inelastic storey drift. Hence, the following three major problems must be resolved.

1. Estimation of the total cumulative plastic strain energy absorbed by an entire structure

2. Estimation of the proportion of the total energy in each storey

3. Estimation of the maximum inelastic storey drift for each storey induced by the energy absorbed by that storey

To solve the three problems and propose a prediction method are the main aims of this chapter. They are dealt with in section 6.3 and 6.4. The accuracy of the proposed prediction method is then checked by comparison with the results of a more complex dynamic analysis in section 6.5.

Appendix A gives details of the sample structures used in this chapter and Chapter 7. These are 3, 7 and 30-storey reinforced concrete frame buildings, designed to New Zealand codes (49,50) which represent the most popular structural type in this country. Thus, strictly the prediction method proposed in this chapter is limited only to reinforced concrete frame buildings. However, it can be applicable to other building types using the fundamental concept in the method with some minor alterations.

The approach to the prediction method is based on energy concepts. It is not new to interpret earthquake effects in terms of energy. A summary of its development is given in the following section.

6.2 SURVEY OF LITERATURE ON INPUT ENERGY INDUCED BY EARTHQUAKES

The history of the development of energy approaches to the characterisation of earthquake intensity started about 30 years ago. Not many workers have considered earthquake effects on an energy basis. Nevertheless, three notable contributions have been made by Tanabashi, Housner and Akiyama. Tanabashi (73) conducted elasto-plastic analyses

of buildings exposed to pulse like artificial ground motions and concluded that the square of the maximum velocity of ground motions could be used as an indication of the earthquakes destructive force.

Housner (74) made a quantitative evaluation of the total amount of energy input contributing to a building's response using velocity response spectra for the elastic system. The total energy E_T was expressed by:

$$E_T = \frac{1}{2} M_T S_V^2 \qquad (6.2.1)$$

where: M_T = total mass of a structure

S_V = velocity response spectral value

He assumed that the following equation holds for elasto-plastic vibrational systems:

$$W_p + W_e \leq E_T \qquad (6.2.2)$$

where: W_p = cumulative plastic strain energy
(= E_d in Equation (5.5.11))

W_e = elastic vibrational energy, which consists of the kinetic and elastic strain energy remaining when the earthquake motion vanishes (= $E_E + E_K$ in Equation (5.5.11))

The sum of the two energies $W_p + W_e$ can be considered as the energy input leading to damage. The total energy E_T, therefore is the upper bound for the energy input

contributing to damage. Based on this assumption, Housner developed a straight forward prediction of damage (72).

Akiyama (71) corroborated the usefulness of Housner's assumption through numerical analysis and constructed a framework for the a seismic limit design of buildings in the basis of the concept of energy input. The outline of his work was explained in Section 5.5.1. In his book he made some comments which relate to this chapter as follows:

1. It may be advisable to consider the sum of the energy inputs resulting from bi-directional horizontal ground motion as the basis of earthquake resistant design.

2. The total energy input depends on the fundamental natural period, the total mass and the minimum value of the yield shear coefficient α_{min}. ($\alpha_{min} = \min(\alpha_i)$, where $\alpha_i = V_{y_i} / \sum_{j=i}^{n} m_j \cdot g$, V_{y_i} = yield shear strength of the ith storey, m_i = mass of the ith storey and n = total number of storeys). As a result, the total energy input in the simplest one-mass vibrational system can apply to the general multi-storey case. Also, the total energy input, which is only slightly affected by α_{min}, can be assumed to be independent of α_{min}.

3. The damage distribution between storeys in shear-type multi-storey frames is considered as the extent of deviation from the optimum yield shear coefficient distribution . The optimum distribution was obtained by a trial and error procedure of numerical analysis as

follows:

$$\overline{\alpha_i} = \overline{(\alpha_i/\alpha_1)} = f\left(\frac{i-1}{n}\right) \qquad (6.2.3)$$

where: for $x > 0.2$

$$f(x) = 1 + 1.593x - 11.852x^2 + 42.583x^3 - 59.483x^4 + 30.159x^5$$

for $x \leq 0.2$

$$f(x) = 1 + 0.5\,x$$

and where:

n = total number of storeys

The damage fraction for each storey for the case of $\alpha_i/\alpha_1 = \overline{\alpha_i}$ is given by:

$$\frac{W_{pi}}{W_p} = \frac{S_i}{\sum_{j=1}^{n} S_j} \qquad (6.2.4)$$

in which:

W_{p_i} = cumulative plastic strain energy consumed by ith storey

$$W_p = \sum_{j=1}^{n} W_{p_j}$$

$$S_i = \left(\sum_{j=i}^{n} \frac{m_j}{M}\right)^2 \cdot \overline{\alpha_i}^2 \cdot \left(\frac{k_1}{k_i}\right)$$

k_i = initial stiffness of the ith storey

M = total mass

The extent of deviation of α_i / α_1 from the optimum value $\overline{\alpha_i}$ can be expressed by:

$$P_i = \frac{\alpha_i}{\alpha_1 \cdot \overline{\alpha_i}} \qquad (6.2.5)$$

Using the deviation P_i, the general damage distribution was obtained by a large number of numerical analyses and is given by:

$$\frac{W_{pi}}{W_p} = \frac{S_i \; P_i^{-12}}{\sum_{j=1}^{n} S_j \; P_j^{-12}} \qquad (6.2.6)$$

The final equation is a rather complex based on an opaque model. It is not easily understood in physical terms.

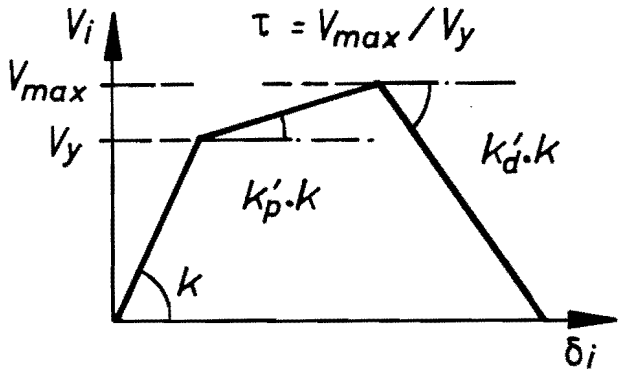

Fig. 6.2.1: Assumed load-deflection relation by Akiyama.

4. When the load deflection relation for one storey of a shear-type multi-storey frame under unidirectional shear

is approximated by three line segments as shown in Fig. 6.2.1, the capacity of cumulative plastic ductility ratio, $\eta_{cap.}$, converted to the value of the elasto-perfectly plastic system, can be expressed by the following equation:

$$\eta_{cap.} = 2\left[\frac{\tau^2-1}{2}\left(\frac{1}{k_p'} + \frac{1}{|k_d'|}\right) + \frac{g_i}{|k_d'|}\right] \qquad (6.2.7)$$

where: τ = the strength increasing ratio (see Fig. 6.2.1)

k_p' = the ratio of the slope in the inelastic range to the elastic slope

k_d' = the ratio of the slope in the degrading range to the elastic slope

g_i = the limit degradation ratio of the ith storey, i.e.

$$g_i = \frac{4 + \sum_{\forall j \neq i} \frac{S_j P_j^{-12}}{S_i P_i^{-12}}}{14\left(1 + \sum_{\forall j \neq i} \frac{S_j P_j^{-12}}{S_i P_i^{-12}}\right)}$$

The capacity $\eta_{cap.}$ is equal to that given in Table 5.5.1.

A lot of work has been done by Akiyama to establish a design procedure using cumulative plastic strain energy. However, as pointed out earlier, some of the main point are quite complicated and not easily physically understood. In the next two sections, different assumptions corresponding to the above four comments by Akiyama will be introduced for the prediction of inelastic storey drift in terms of cumulative plastic strain energy.

6.3 CUMULATIVE PLASTIC STRAIN ENERGY INPUT FROM AN EARTHQUAKE

6.3.1 Introduction

The effect of the ground motion is to feed different types of energy into a structure, such as kinetic energy, strain energy and energy consumed by the damping mechanism, as explained in Section 5.5.2. Cumulative plastic strain energy was chosen as the energy type most closely related to damage. Thus, the cumulative plastic strain energy can be simply called damage energy.

In calculating the damage energy absorbed by a structure, two important questions arise, as follows:

1. How to calculate total damage energy absorbed by an entire structure.

2. How to obtain the distribution of damage energy between storeys.

The techniques for satisfying these questions are required to be relatively simple, avoiding the complexity of using a non-linear dynamic analysis with a multi-degree of freedom system. Hence, the main purpose of this section is to propose appropriate approaches to satisfy this aim.

To reply to the first question, the relationship on the damage energy between single-degree-of-freedom and

multi-degree-of-freedom systems must be established. The total damage energy for a multi-degree-of-freedom system can be obtained by a non-linear dynamic analysis using a series of single-degree-of-freedom systems and by an elastic modal analysis of the multi-degree-of-freedom system. It is discussed in Section 6.3.3. In resolving the second question, an assumption is made that the ratio of damage energy in one storey to that for the whole structure is the same as the energy ratio calculated by elastic analysis. The assumption is introduced and justified using numerical analyses in Section 6.3.4.

First, fundamental equations of calculating damage energy for a multi-degree-of-freedom system must be developed. This is done in the next subsection.

6.3.2 Fundamental Equations in Terms of Energy

The basic dynamic equation for a spring mass model of a multi-degree-of-freedom (M.D.O.F.) system (Fig. 6.3.1) may be written:

$$[M]\{\ddot{x}\} + [C]\{\dot{x}\} + [K]\{x\} = -\ddot{y}[M]\{1\} \qquad (6.3.1)$$

where:

$$[M] = \begin{bmatrix} m_n & & 0 \\ & \ddots & \\ 0 & & m_1 \end{bmatrix} \quad \text{(diagonal terms only)}$$

$[C]$ = damping matrix

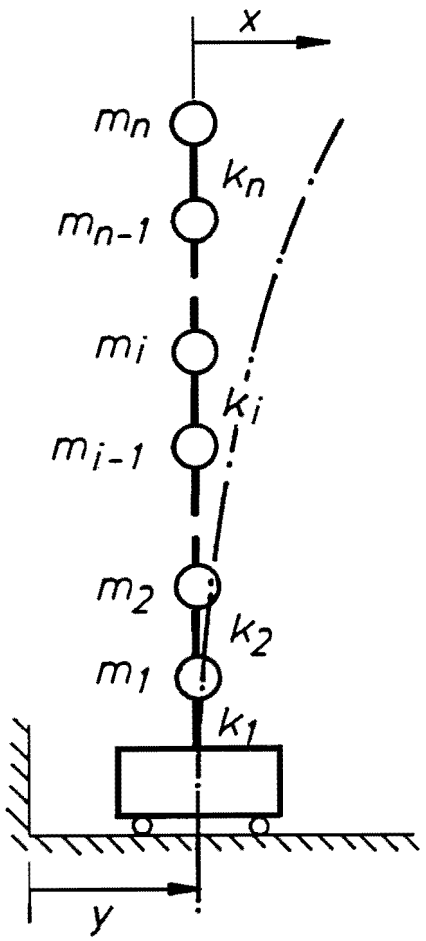

n : Number of storeys (number of degrees of freedom)

m_i : Mass of ith floor

k_i : Stiffness of ith storey

x : Displacement of the mass relative to the ground

y : Horizontal ground motion

Fig. 6.3.1 A spring-mass model

$$[K] = \begin{bmatrix} k_n, & -k_n & & & & 0 \\ -k_n, & k_n+k_{n-1}, & -k_{n-1} & & & \\ & \ddots & \ddots & \ddots & & \\ & & \ddots & \ddots & \ddots & \\ & & & -k_3, & k_3+k_2, & -k_2 \\ 0 & & & & -k_2, & k_1+k_2 \end{bmatrix}$$

$\{x\}$ = vector of displacements

As explained in Section 5.5.2 for a single-degree-of-freedom (S.D.O.F.) system, multiplying by $\{\dot{x}\}^T dt$ and integrating over the entire duration of an earthquake, S, Eq. (6.3.1) may be transformed into an equation in terms of energy as follows:

$$\int_0^S \{\dot{x}\}^T [M]\{\ddot{x}\}dt + \int_0^S \{\dot{x}\}^T [C]\{\dot{x}\}dt + \int_0^S \{\dot{x}\}^T [K]\{x\}dt$$

$$= -\int_0^S \{\dot{x}\}^T [M]\{1\}\ddot{y}\, dt \qquad (6.3.2)$$

The four terms in Eq. (6.3.2) have the same meaning of those for a S.D.O.F. system. Equation (6.3.2) is based on absolute deformations. The third term can be rewritten in terms of storey relative displacements.+

+ $$\{\dot{x}\}^T [K]\{x\} = \begin{Bmatrix} \vdots \\ \dot{x}_i \\ \dot{x}_{i-1} \\ \vdots \end{Bmatrix} \begin{bmatrix} & & (i) & (i-1) & \\ \cdots & -k_{i+1}, & k_{i+1}+k_i, & -k_i & \cdots \\ & \cdots & -k_i, & k_i+k_{i-1}, & -k_{i-1} \cdots \end{bmatrix} \begin{Bmatrix} \vdots \\ x_i \\ x_{i-1} \\ \vdots \end{Bmatrix}$$

Terms related to k_i in the third term of Eq. (6.3.2) can be transformed to: (terms related to k_i) $\dot{x}_i k_i (x_i - x_{i-1}) - \dot{x}_{i-1} k_i (x_i - x_{i-1}) = (\dot{x}_i - \dot{x}_{i-1})(x_i - x_{i-1}) k_i = \dot{\delta}_i \delta_i k_i$

$$\int_0^S \{\dot{x}\}^T [K]\{x\}dt = \int_0^S \{\dot{\delta}\}^T [\delta]\{K\}dt$$

$$= \int_0^S \{\dot{\delta}\}^T \{V\}dt \qquad (6.3.3)$$

where:

$$\{\dot{\delta}\} = \begin{Bmatrix} \dot{\delta}_n \\ \vdots \\ \dot{\delta}_1 \end{Bmatrix} ; \quad \delta_i = \text{interstorey drift of ith storey}$$

$$i \neq 1 \quad \delta_i = x_i - x_{i-1}$$

$$i = 1 \quad \delta_1 = x_1$$

$$[\delta] = \begin{bmatrix} \delta_n & & & 0 \\ & \ddots & & \\ & & \ddots & \\ 0 & & & \delta_1 \end{bmatrix}$$

$$\{K\} = \begin{Bmatrix} k_n \\ \vdots \\ k_1 \end{Bmatrix}$$

$$\{V\} = \begin{Bmatrix} V_n \\ \vdots \\ V_1 \end{Bmatrix} ; \quad V_i = \text{shear force of ith storey}$$

The term denotes the strain energy, which consists of cumulative elastic strain energy E_E and cumulative plastic strain energy E_d. From Eq. (6.3.3), the total strain energy, $(E_E + E_d)_T$, can be calculated by the summation of the strain energy for each storey, i.e.:

$$(E_E+E_d)_T = \sum_{i=1}^{n} \left(\int_0^S \dot{\delta}_i(t)\ V_i(t)dt \right) \tag{6.3.4}$$

Elastic strain energy is taken as the strain energy when a deformation occurs along line (1) in Fig. 5.5.2(a), whereas plastic strain energy corresponds to deformation along line (2). Hence, the cumulative elastic and plastic strain energy E_{E_i} and E_{d_i} for the ith storey can be denoted by:

$$E_{E_i} = \sum_{j=0}^{N-1} \left[\int_0^{\Delta t} \dot{\delta}_i(t+j\cdot\Delta t)\cdot V(t+j\cdot\Delta t)dt \times \{1 - H_i(j\cdot\Delta t)\} \right] \tag{6.3.5}$$

$$E_{d_i} = \sum_{j=0}^{N-1} \left[\int_0^{\Delta t} \dot{\delta}_i(t+j\cdot\Delta t)\cdot V(t+j\cdot\Delta t)dt \times H_i(j\cdot\Delta t) \right] \tag{6.3.6}$$

in which:

Δt = time increment

N = $S/\Delta t$ (total number of time steps)

$H_i(t)$ = step function for ith storey such that

$H_i(t)$ = 0 when $V_i - \delta_i$ at time t is on the line (1) in Fig. 5.5.2(a)

$H_i(t)$ = 1 when $V_i - \delta_i$ at time t is on the line (2) in Fig. 5.5.2(a).

Thus, the total strain energy can be given by:

$$(E_E + E_d)_T = \sum_{i=1}^{n} (E_{E_i} + E_{d_i}) \tag{6.3.7}$$

The total cumulative plastic strain energy E_{d_T} absorbed by the entire structure is:

$$E_{d_T} = \sum_{i=1}^{n} E_{d_i} \qquad (6.3.8)$$

Damage energy, which is cumulative plastic strain energy, is calculated by Eqs (6.3.6) and (6.3.8). For numerical integration of Eq. (6.3.6), the linear acceleration method (61,75) is used in which linearity of acceleration for each time increment is assumed (see Fig. 6.3.2).

6.3.3 Cumulative Plastic Strain Energy Absorbed by an Entire Structure

A model for the total damage energy E_{d_T} absorbed by a whole structure is proposed in this subsection, for a given structure and earthquake.

First, though, there is the question of the appropriate components of ground motion to be taken into account. A structural model in the present study is based on one frame of a structure, and the question arises as to which earthquake components should be considered in estimating the damage of the structural model. The ground motion is comprised of three translational and three rotational components in an orthogonal coordinate system. Of these, only the translational components are considered significant for buildings. Moreover, as Akiyama (71) has pointed out, the influence of the vertical ground component is at most 12% of the total input energy and can be regarded as negligible. In fact the vertical component and the three rotational earthquake components are not known to have ever

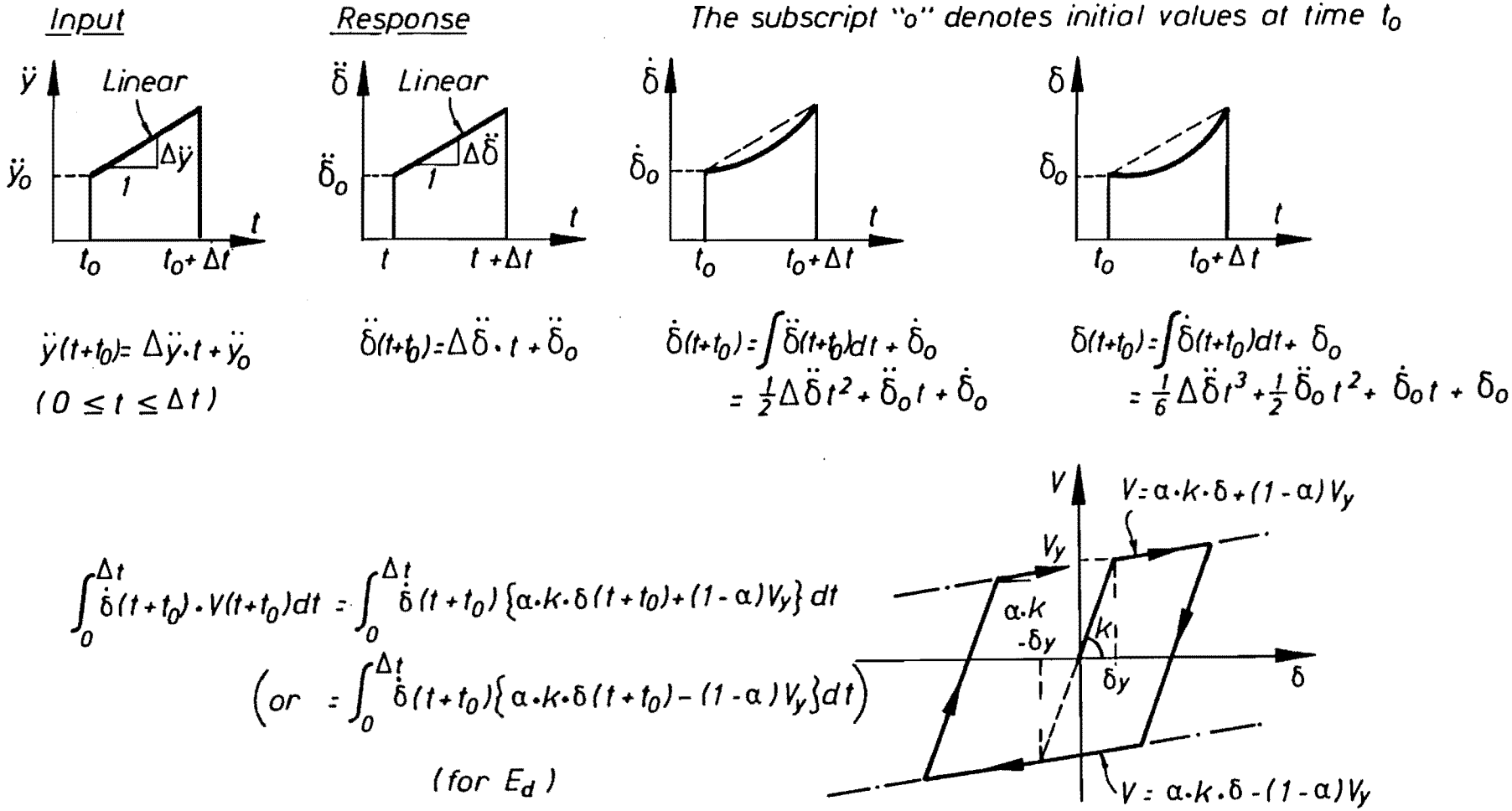

Fig. 6.3.2 Integration using linear acceleration method

been considered in the design of ordinary buildings.

Therefore, two horizontal components of earthquake motions remain for consideration. As sketched in Fig. 6.3.3, beams perpendicular to a load direction are not expected to get damaged and only columns are affected by the two dimensional effect. According to the "strong column weak beam" concept used in New Zealand for multi-storey frames, almost all plastic strain energy is supposed to be absorbed by beam hinges rather than columns, as shown in Fig. 6.3.4. Consequently, the damage energy E_{d_T} for a structural model is assumed to be induced by only one horizontal component of ground motion, aligned with the same direction of the model. Once again the simplicity of this assumption is justified for failure probability calculations, because the resulting error is much lower than the considerable uncertainty involved in the prediction of earthquake parameters.

Now, let us consider the relationship of total energy input E_T (see Equation (5.5.11)) in elastic problems between a S.D.O.F. and M.D.O.F. system. From mode superposition, the vector of M.D.O.F. displacements can be written as (76):

$$\{x\} = \sum_{j=1}^{n} \{U_j\}\, q_j$$

$$= \sum_{j=1}^{n} \{U_j\}\, \beta_j\, {}_s q_j \qquad (6.3.9)$$

where: $\{U_j\}$ = mode shape of jth mode

q_j = time function of jth mode

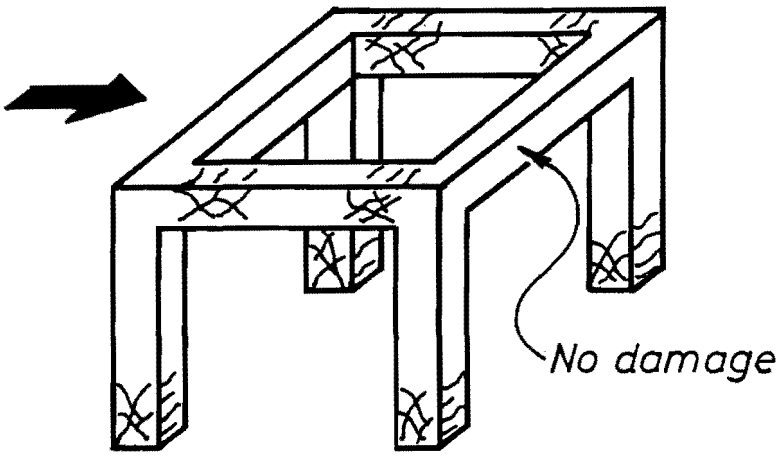

Columns are affected by two dimensional effect of ground motion

Fig. 6.3.3 Two dimensional earthquake effect on space frames

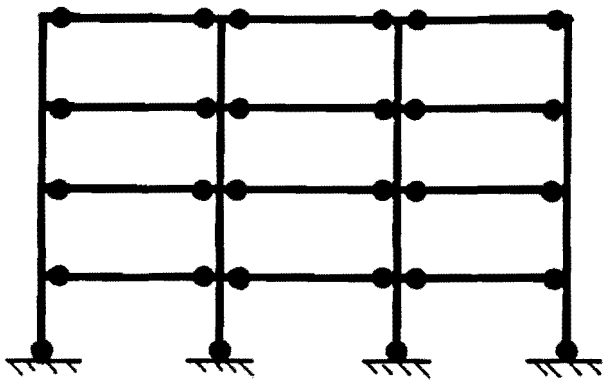

Fig. 6.3.4 Favourable failure mode in New Zealand code

$$\beta_j = \frac{\{U_j\}^T [M] \{1\}}{\{U_j\}^T [M]\{U_j\}}$$

(modal participation factor)

${}_s q_j$ = displacement response of a S.D.O.F. system with the same resonant period and critical damping ratio as the jth mode, using the same earthquake wave.

The total energy input E_T for the M.D.O.F. system is given from Eqs (6.3.2) and (6.3.9) by:

$$E_T = -\int_0^S \{\dot{x}\}^T [M]\{1\}\ddot{y}\, dt$$

$$= -\sum_{j=1}^{n} \int_0^S \{U_j\}^T [M]\{1\}\beta_j\, {}_s\dot{q}_j\, \ddot{y}\, dt \qquad (6.3.10)$$

Now, the total energy for the jth mode E_{T_j} is introduced. Since the vector {1} can be rewritten:

$$\{1\} = \sum_{j=1}^{n} \{U_j\}\beta_j \qquad (6.3.11)$$

Equation (6.3.1) may be expressed by the sum of each modal participant, as follows:

$$\sum_{j=1}^{n} [M]\{U_j\}\ddot{q}_j + \sum_{j=1}^{n} [C]\{U_j\}\dot{q}_j + \sum_{j=1}^{n} [K]\{U_j\}q_j$$

$$= \sum_{j=1}^{n} - \ddot{y}[M]\{U_j\}\beta_j \qquad (6.3.12)$$

Thus, the equation of motion for the jth mode can be expressed by:

$$[M]\{U_j\}\ddot{q}_j + [C]\{U_j\}\dot{q}_j + [K]\{U_j\}q_j = -\ddot{y}[M]\{U_j\}\beta_j \qquad (6.3.13)$$

which on premultiplying by $\{U_j\}^T$ becomes:

$$\{U_j\}^T[M]\{U_j\}\ddot{q}_j + \{U_j\}^T[C]\{U_j\}\dot{q}_j + \{U_j\}^T[K]\{U_j\}q_j = -\ddot{y}\{U_j\}^T[M]\{1\} \qquad (6.3.14)$$

where: $\{U_j\}^T [M] \{U_j\}$ = generalised mass for jth mode

$\{U_j\}^T [C] \{U_j\}$ = generalised damping for jth mode

$\{U_j\}^T [K] \{U_j\}$ = generalised stiffness for jth mode

$-\ddot{y} \{U_j\}[M] \{1\}$ = generalised load for jth mode

By analogy with Eq. (6.3.2), the total energy for the jth mode E_{T_j} is given by:

$$E_{T_j} = -\int_0^S \{U_j\}^T [M] \{1\} \dot{q}_j \ddot{y} \, dt$$

$$= -\int_0^S \{U_j\}^T [M] \{1\}\beta_j \, {}_s\dot{q}_j \ddot{y} \, dt \qquad (6.3.15)$$

Hence, from Eqs (6.3.10) and (6.3.15):

$$E_T = \sum_{j=1}^{n} E_{T_j} \qquad (6.3.16)$$

which means the total energy input for a M.D.O.F. system in elastic problems can be obtained from the sum of the total energy for each mode. This can be readily understood because mode superposition holds in elastic problems.

For a S.D.O.F. system with unit mass and with frequency and damping corresponding to the jth mode of the M.D.O.F. system:

$$ {}_s\ddot{q}_j + 2h\,\omega_j\,{}_s\dot{q}_j + \omega_j^2\,{}_sq_j = -\ddot{y} \qquad (6.3.17) $$

where: h = critical damping ratio

ω_j = circular frequency of the S.D.O.F. system

Thus, following Eq. (6.3.2) the total energy ${}_sE_{Tj}$ for the S.D.O.F. system may be expressed by:

$$ {}_sE_{Tj} = -\int_0^S {}_s\dot{q}_j\,\ddot{y}\,dy \qquad (6.3.18) $$

Accordingly, from Eqs (6.3.15) and (6.3.18):

$$ E_{Tj} = {}_sE_{Tj} \times {}_{ef.}M_j \qquad (6.3.19) $$

in which ${}_{ef.}M_j$ is the effective mass of the jth mode given by:

$$ {}_{ef.}M_j = \frac{(\{U_j\}^T\,[M]\{1\})^2}{\{U_j\}^T\,[M]\,\{U_j\}} \qquad (6.3.20) $$

Consequently, the total energy input E_T of the M.D.O.F. system can be expressed in terms of the total energy input of the S.D.O.F. system with unit mass, ${}_sE_{T_j}$, from eqs (6.3.16) and (6.3.19) as:

$$E_T = \sum_{j=1}^{n} ({}_sE_{T_j} \times {}_{ef.}M_j) \tag{6.3.21}$$

This is correct for the total energy input E_T in elastic problems. However, whether the relation can be applied to cumulative plastic strain energy E_d must now be examined. Since E_d is obtained by an inelastic dynamic analysis, when Eq. (6.3.21) is applied to E_d, it is not an elastic problem anymore. Moreover, E_d is a component of E_T as given in Eq. (5.5.11). In applying the relation of Eq. (6.3.21) to E_d, therefore, the following assumptions need to be made:

1. The relationship of Eq. (6.3.21) holds for the total energy input of inelastic problems.

2. The total energy input for inelastic problems is dominated by cumulative plastic strain energy.

These assumptions will be justified later by comparison with full time-history analysis. Adopting them, however, the cumulative plastic strain energy E_{d_T} absorbed into a M.D.O.F. system is given by:

$$E_{d_T} = \sum_{j=1}^{n} ({}_sE_{d_j} \times {}_{ef.}M_j) \tag{6.3.22}$$

where: ${}_sE_{d_j}$ = the cumulative plastic strain energy

input into a S.D.O.F. system with unit mass, corresponding to the jth mode of the M.D.O.F. system

It is probably implied from Eq. (6.2.1) that energy input is proportional to the total mass of a system. Therefore it would be meaningful to standardise energy with regard to mass. In addition, as explained in Section 7.4.2, standardising energy in this way will also be convenient when considering the energy input from an earthquake. Thus Eq. (6.3.22) may be rewritten as:

$$\frac{E_{d_T}}{w_t} = \sum_{j=1}^{n} \left(\frac{{}_sE_{d_j}}{g} \times \frac{ef.{}^{M_j}}{M_T} \right) \qquad (6.3.23)$$

where: M_T = total mass of the M.D.O.F. system

$$M_T = \sum_{j=1}^{n} ef.{}^{M_j}$$

g = acceleration of gravity

w_t = $M_T \cdot g$ (total weight of the M.D.O.F. system)

$\frac{ef.{}^{M_j}}{M_T}$ = effective mass ratio for mode j

The ratio E_{d_T}/w_t may be called the standard damage energy.

The reason why E_{d_T} is divided by w_t in Eq. (6.3.23) rather than M_T is the units used in the present study, as shown in Table 6.3.1, which follow the S.I. unit system. When storey

Table 6.3.1 Units used in the present study

Items	Symbols	Unit	Items	Symbols	Unit
Weight	w_t	kN	Damage energy	E_{d_T}	kN•mm
Stiffness	k	kN/mm	Standard damage energy	E_{d_T}/w_t	mm
Yield shear strength	V_y	kN		$_sE_{d_j}/_g$	"
Storey drift	δ	mm	Non-dimensional damage energy	$E_{d_T}/w_t \cdot \ell$	-
Storey deflection angle	γ	-			

(ℓ: Storey height (mm))

heights of a structural model considered are known, non-dimensional energy is used, obtained by dividing the standard energy by the storey height. However,if unknown, a unit of displacement, mm, is chosen as the unit of energy, like the standard damage energy. Energy expressed non-dimensionally and energy in units with dimensions of displacement correspond in terms of units to storey deflection angle and storey drift, respectively. These are related to the criterion of collapse, discussed in section 5.3.

In order to confirm the validity of the relation in Eq. (6.3.23), numerical analyses were carried out to compare the standard damage energy from Eq. (6.3.23) with that obtained by a time-history elasto-fully-plastic analysis. The structural models used in the analyses were the 3, 7 and 30-storey frames described in Appendix A. The stiffness and yield shear strength of each storey were obtained by a static analysis assuming an inverted triangular distribution of the applied load. Another simpler way to calculate storey characteristics obtained is discussed in Appendix A. But,the characteristics by the static analysis will be mainly used in Chapter 6 and 7. Response results for models with different storey characteristics are compared in Section 6.5. For earthquake input, the 5 recorded earthquakes in Appendix B were used. The procedure used for checking the validity of Eq. (6.3.23) is as follows:

1. In the preliminary calculation, damage energy values $_{s}E_{d}$ for the S.D.O.F. system were

calculated for every 0.1(sec) interval of period T by a time-history elasto-fully-plastic ($\alpha=0$) analysis for each earthquake record. The S.D.O.F. systems with a critical damping ratio of 5% have the same base shear coefficient C_d as the minimum of C_{d_i} ($C_{d_i} = V_{y_i} / \sum_{j=i}^{n} m_j \cdot g$ and $C_d = C_{d_1}$) for the 3, 7 and 30-storey frames (continuous lines in Figs 6.3.5-6.3.7).

2. Modal analyses were carried out using 3, 7 and 30 degree of freedom systems to obtain the resonant periods and corresponding effective mass ratios.

3. Using the results of the above two terms, the standard damage energies, E_{d_T}/w_t for the 15 cases (3 frames x 5 earthquakes) were calculated by Eq. (6.3.23). In estimating ${}_sE_{d_j}$ corresponding to the jth mode in the equation, the damage energy ${}_sE_d$ for every 0.1 (sec) interval was interpolated.

4. To compare values of E_{d_T}/w_t obtained from Eq. (6.3.23), time-history elasto-fully-plastic analyses with 3, 7 and 30-degree of freedom systems were carried out. The critical damping ratio for each mode was assumed to be 5% (61). The results obtained with and without a secondary slope α are also shown in Figs 6.3.5-6.3.7.

Figures 6.3.5 to 6.3.7 show the results for 3, 7 and

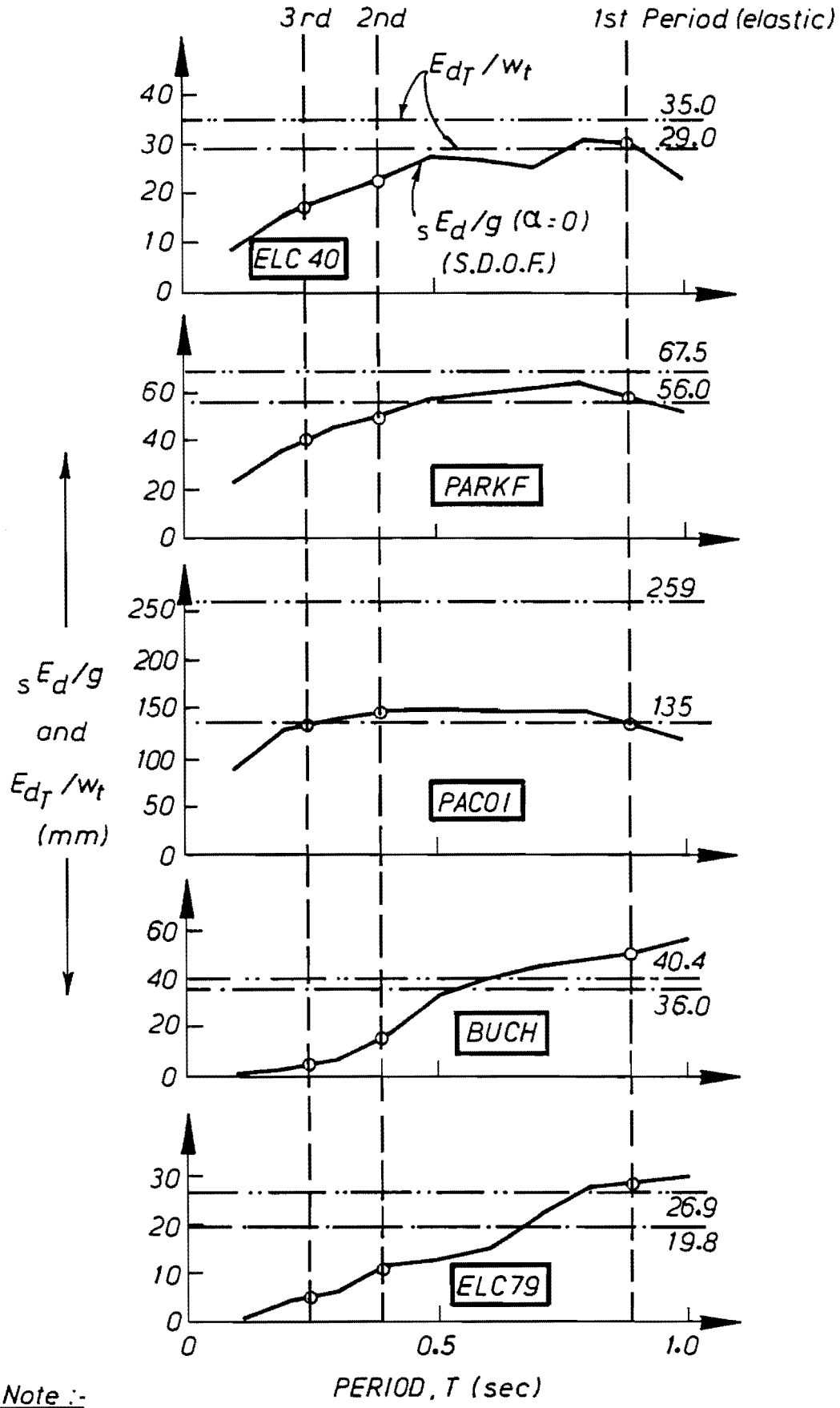

Note :-

3-Storey model (3 degrees of freedom)

h = 0.05 ; —··— α considered

C_d = 0.170 ; —·— α = 0

Fig. 6.3.5 Calculation results for total damage energy

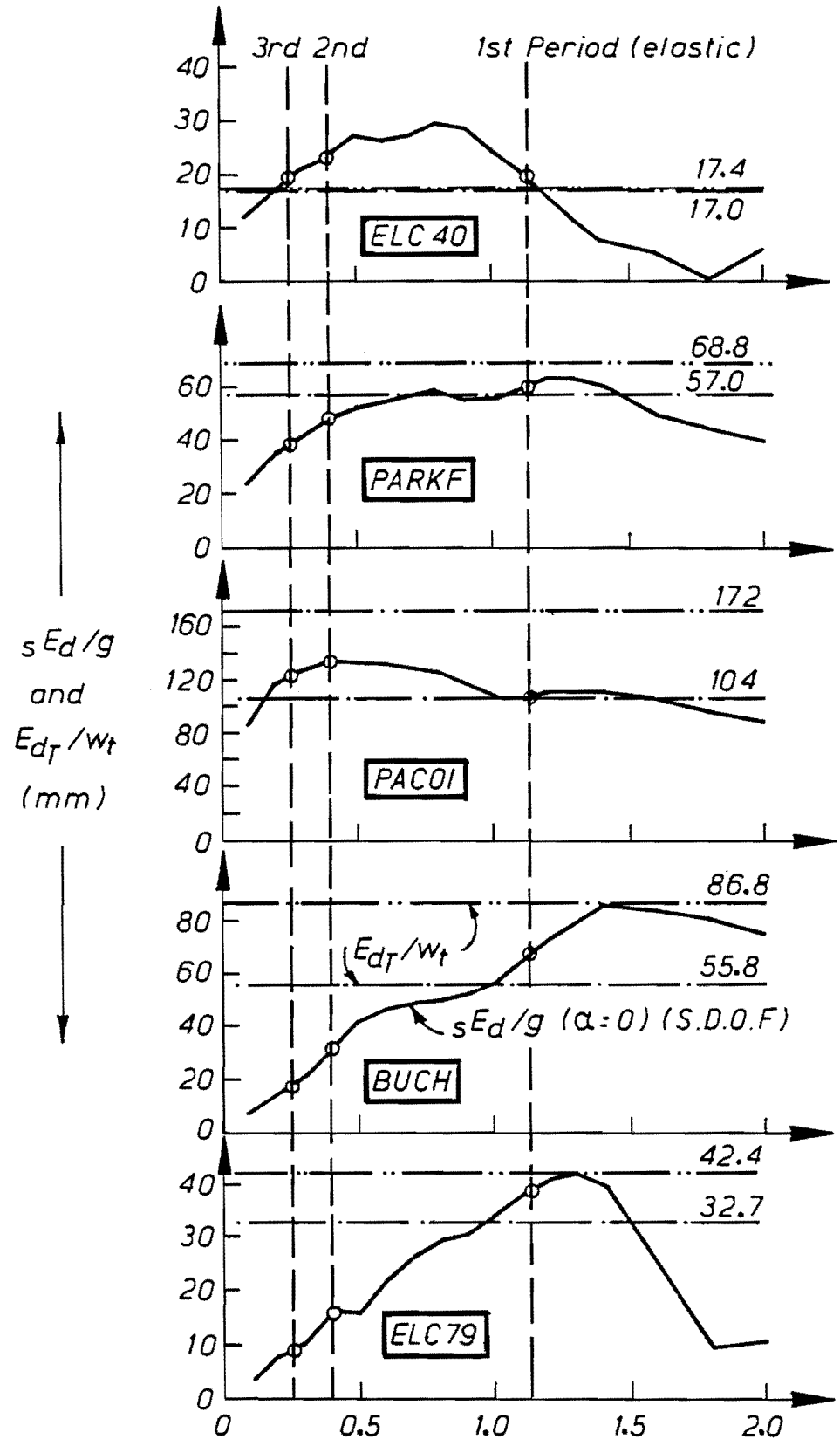

Note :

7-Storey model (7 degrees of freedom)

$h = 0.05$; ——··—— α considered

$C_d = 0.135$; ——·—— $\alpha = 0$

Fig. 6.3.6 Calculation results for total damage energy

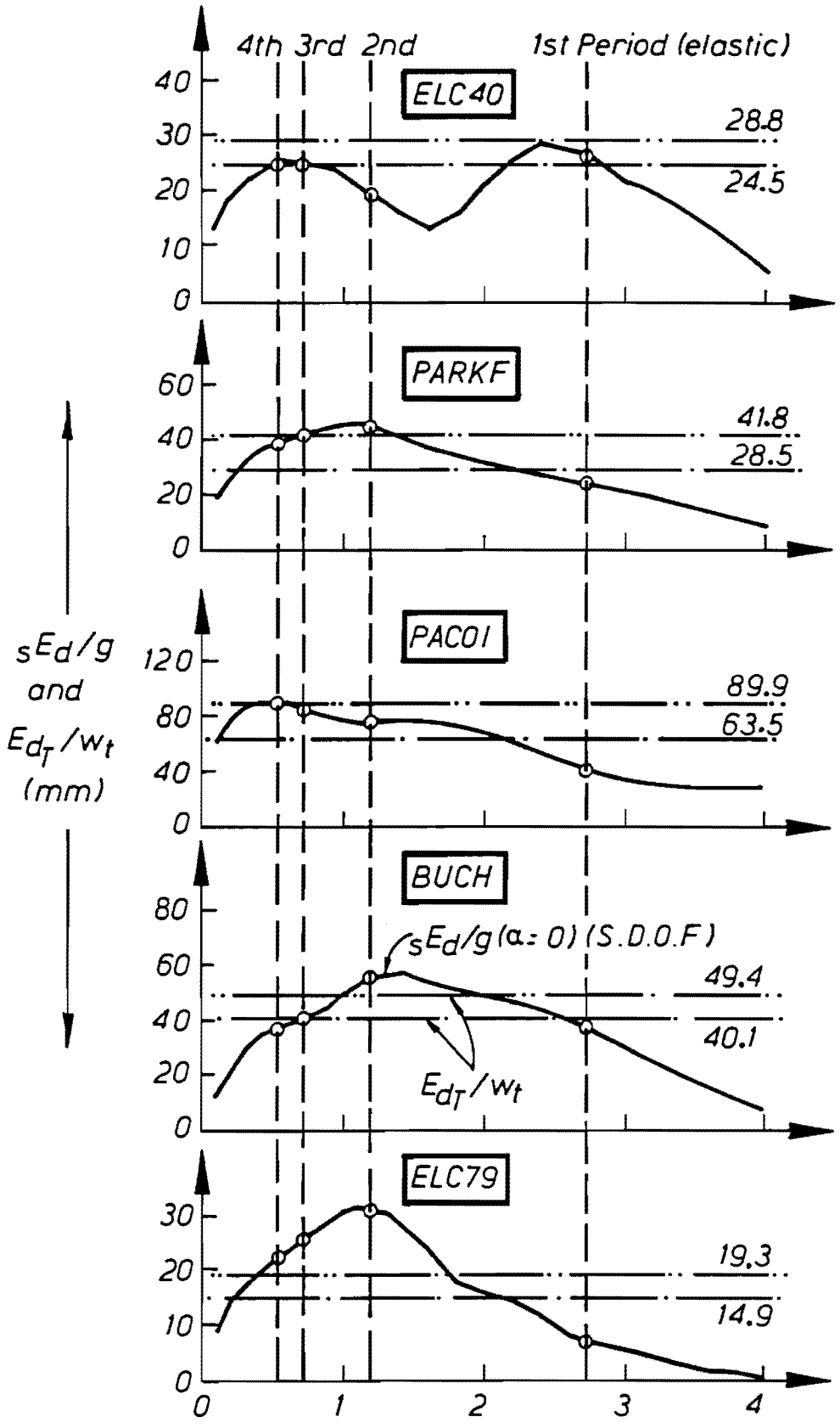

Note :-

30 -Storey model (30 degrees of freedom)

h = 0.05 ; —··— α considered

Cd = 0.070 ; —·— α = 0

Fig. 6.3.7 Calculation results for total damage energy

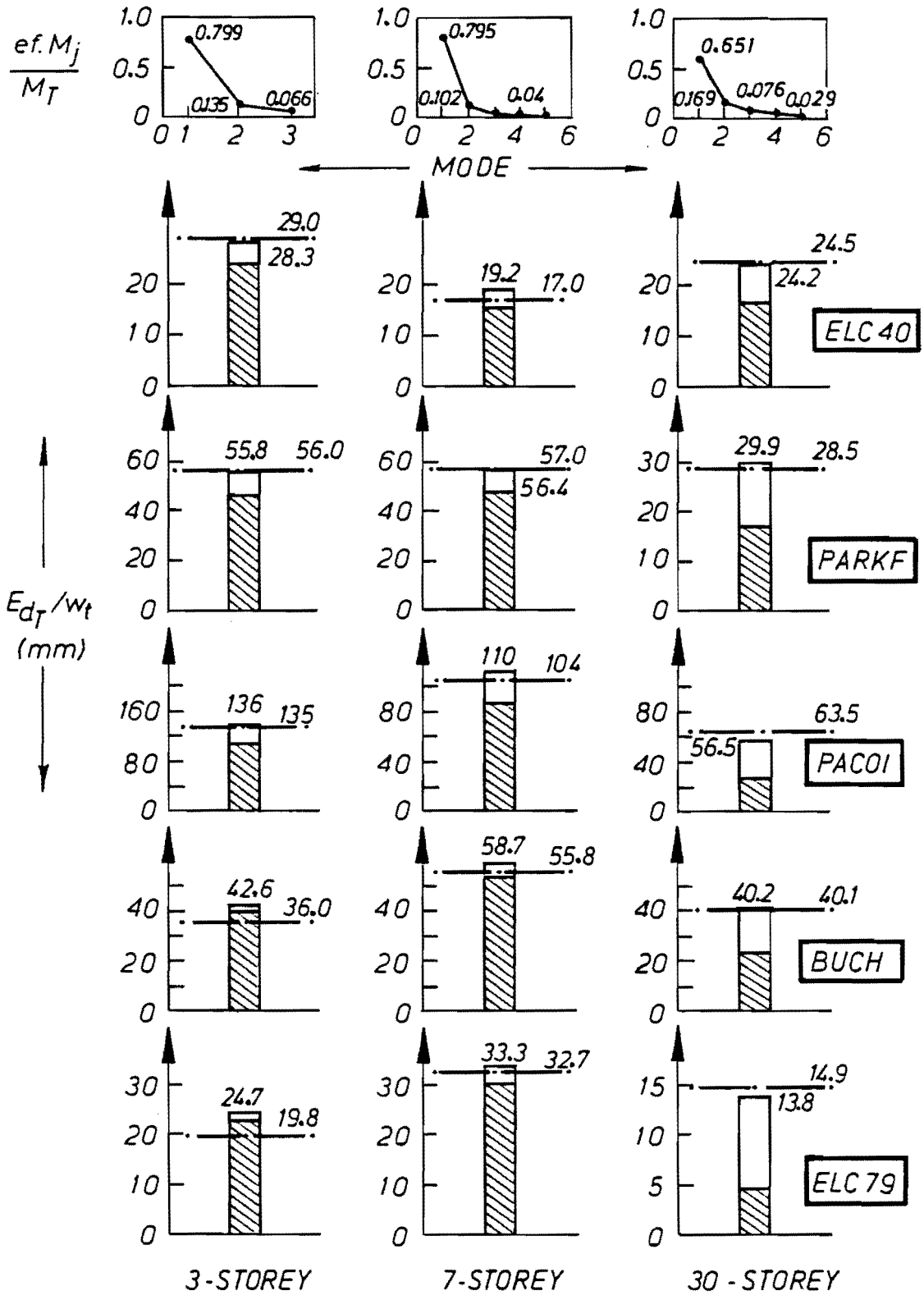

Fig. 6.3.8 Comparison of total damage energy

30-storey frames respectively obtained from steps 1, 2 and 4. Each figure contains the relationships between ${}_sE_d/g$ and T, and E_{d_t}/w_t by time-history analyses for the five earthquakes. The abbreviations of the names of earthquakes used in the figures are shown in Appendix B. The first few resonant periods for the frames are also shown. They were used to obtain the values of ${}_sE_{d_j}$ corresponding to the jth period (step 3). At the top of Fig. 6.3.8, the effective mass ratios for the frames are shown which were calculated by the modal analyses (step 2). The two values of E_{d_T}/w_t obtained from Eq. (6.3.23) and by a time-history analysis are compared in the figure for the 15 cases (3 frames x 5 earthquakes).

Considering the comparison of values of E_{d_T}/w_t, the correspondence is close in most cases (Fig. 6.3.8). Therefore, the two assumptions used in applying Eq. (6.3.21) to damage energy are considered acceptable, though they cannot be mathematically justified.

Consequently, the damage energy input E_{d_T} for a M.D.O.F. system can be obtained firstly by inelastic dynamic analysis using a series of unit mass S.D.O.F. systems whose elastic periods are the same as those of the first few M.D.O.F. modes and which have the same base shear coefficient, and secondly by elastic modal analysis of the M.D.O.F. system. Though an inelastic dynamic analysis is usually complicated, the inelastic analysis used here is relatively simple, because of the use of S.D.O.F. systems and the bi-linear hysteresis rule. The modal analysis of a M.D.O.F. spring

mass model is an elastic analysis and is therefore also relatively simple. Thus, the damage energy for a M.D.O.F. system may be calculated without the need for a complex analysis.

The conclusion reached here is somewhat different from Akiyama's. He implied that the energy related to damage is dependent only on the fundamental natural period of a structure. This is generally true for structures which do not have a high natural period. However, for high-rise buildings, the contribution of the energy input deriving from higher modes is greater and is by no means negligible. In order to further clarify this issue, the contribution of first modes alone to the standard damage energy E_{d_T}/w_t for the numerical analyses above was calculated by Eq. (6.3.23) and is shown in Fig. 6.3.8 by the cross hatched bars. The higher modes of the 30-storey frame contribute 30-70% of the total standard damage energy. This varies with the input earthquakes, but the contribution is found significant in all cases. Accordingly, in general it is not good enough to consider only the fundamental natural period of a structure in calculating the total standard damage energy.

To find the sensitivity of the standard damage energy E_{d_T}/w_t to the natural period T and shear coefficient ratio C_d, E_{d_T}/w_t was calculated for different values of T and C_d using S.D.O.F. systems subjected to the 5 different earthquake records. The original wave was magnified or reduced such that its maximum acceleration α_{max} becomes 0.35 g. The results are shown in Fig. 6.3.9. The differences in E_{d_T}/w_t

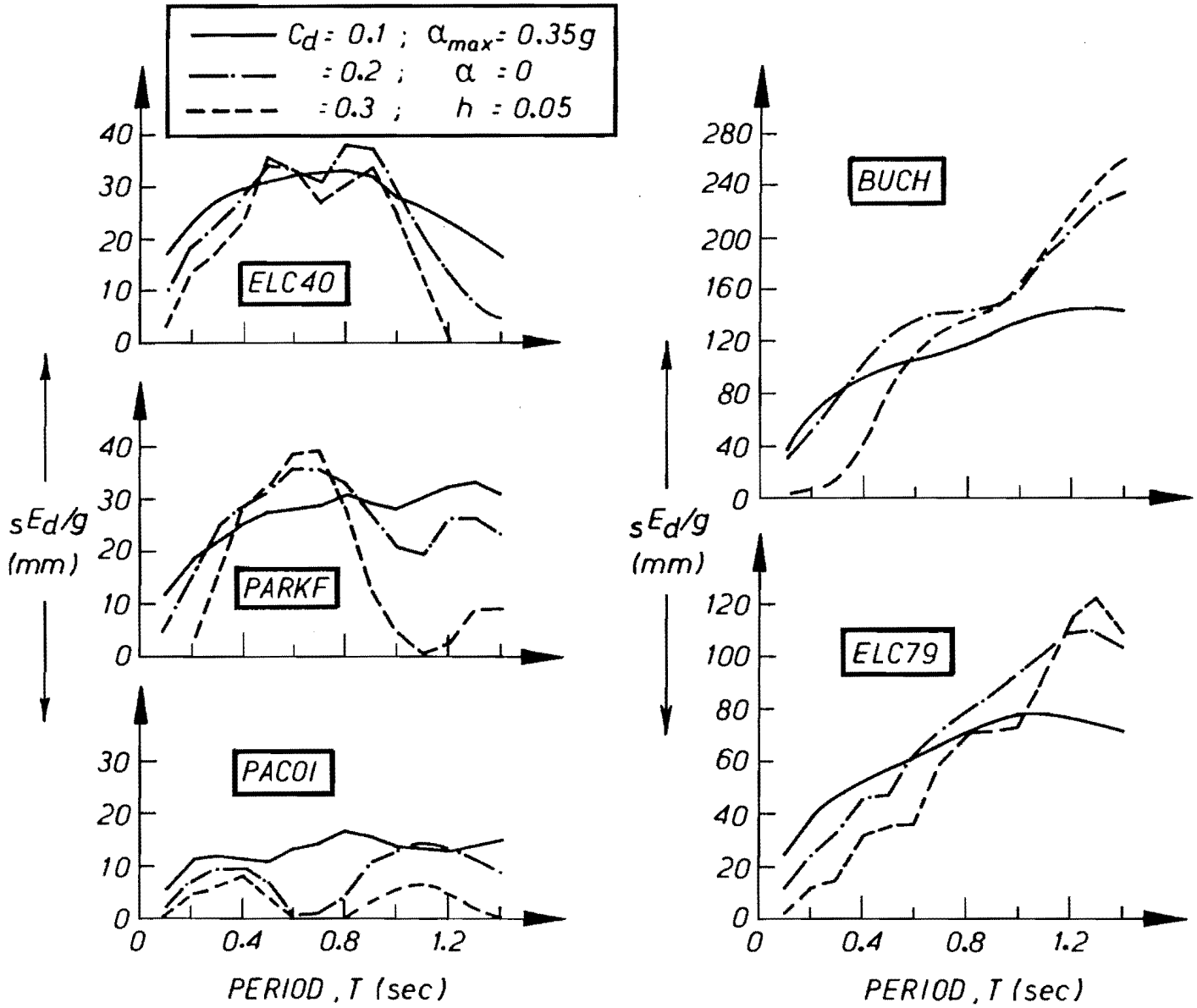

Fig. 6.3.9 Comparison on total damage energy between different earthquakes

due to the change of T and C_d are relatively smaller than those due to earthquake records, even though the latter were scaled to the same maximum acceleration. The difference due to earthquake records with the same value of α_{max} can be considered to be uncertainty inherent in the calculation procedure of failure probability, because as explained in section 5.2 and 7.2, the maximum ground acceleration is the only parameter that can be taken into account probabilistically, while the other characteristics of an earthquake must remain as unknown factors. Thus, the variation of E_{d_T}/w_t due to T and C_d is smaller than the inherent uncertainty arising from the earthquake models. Therefore, in calculating the standard damage energy the resonant periods and base shear coefficient for the S.D.O.F. models need not be calculated very accurately. They are functions, respectively, of initial stiffness and mass and of yield shear strength and mass. It is probably implied that the use of a simple elasto-fully plastic hysteresis relation is justified because the effect of using a second stiffness slope for a storey seems to be unimportant compared with the initial stiffness and yield shear strength, and even for these an accurate calculation is not required.

6.3.4 Proportion of Cumulative Plastic Strain Energy Absorbed by a Storey

As one can see in past major earthquakes, damage is often distributed throughout a building. In certain cases it concentrates on a weak storey. Such damage concentration

means the total input energy related to damage is absorbed mainly by the weakest storey. The estimation of the distribution of absorbed energy between storeys is essential in predicting collapse of buildings. In this section, a method is proposed for predicting the fraction of total input energy absorbed by each storey.

The basic assumption in resolving the problem is that the ratio of damage energy in one storey to that for the whole structure is the same as the energy ratio calculated by elastic analysis. The total input energies for elastic and inelastic analyses are not always the same, as illustrated in Fig. 5.4.1. Therefore, a simple inelastic analysis with S.D.O.F. systems is used to obtain the total damage energy, referred to in the previous section. In order to estimate the proportion of the total energy absorbed by a storey it is assumed that an elastic dynamic analysis can be used. The justification of the assumption is examined by numerical studies later in this section. The assumption is at least physically clearer than Eq. (6.2.6) as proposed by Akiyama.

A random vibration method for stationary Gaussian processes (61,77-80) is used for the prediction of the ratio of the damage energy E_{d_i} for the ith storey to that for an entire structure, E_{d_T}. The random vibration method is an elastic probabilistic dynamic analysis based on the frequency domain. It seeks to determine the distribution of the maximum response in a direct way.

To estimate the maximum response, say the maximum relative

displacement, due to ground motion, the response spectrum approach is the simplest and most common way. The response spectrum is utilised to produce the maximum modal displacement. These are read from the response spectrum at the appropriate frequency and for the correct critical damping ratio. The maximum displacement is then often predicted deterministically by the "root-sum-square" rule (81). Therefore, the response spectrum approach is an approximation and is not a direct way to estimate the maximum response.

In the random vibration method, certain moments of the response spectral-density function play an important role. Before explaining the application of the method to this project, the response spectral-density function (or power spectral-density function) $G_r(\omega)$ (r = response) which shows the contribution of average power of the response for each frequency ω, must be discussed, taking into account the relationship between time domain and frequency domain analyses. (The average power is $\sum_{i=1}^{N} x_i^2/N$, when there are N samples, x_1, x_2, ..., x_N, such as response data for every Δt second).

An outline of the relationship between time domain and frequency domain analyses in elastic problems is given in Fig. 6.3.10 (82). The left hand side figures show the relationship between an input wave, an impulse response function and the corresponding response in the time domain analysis. The response may be obtained by the convolution of the input wave and the impulse response function.

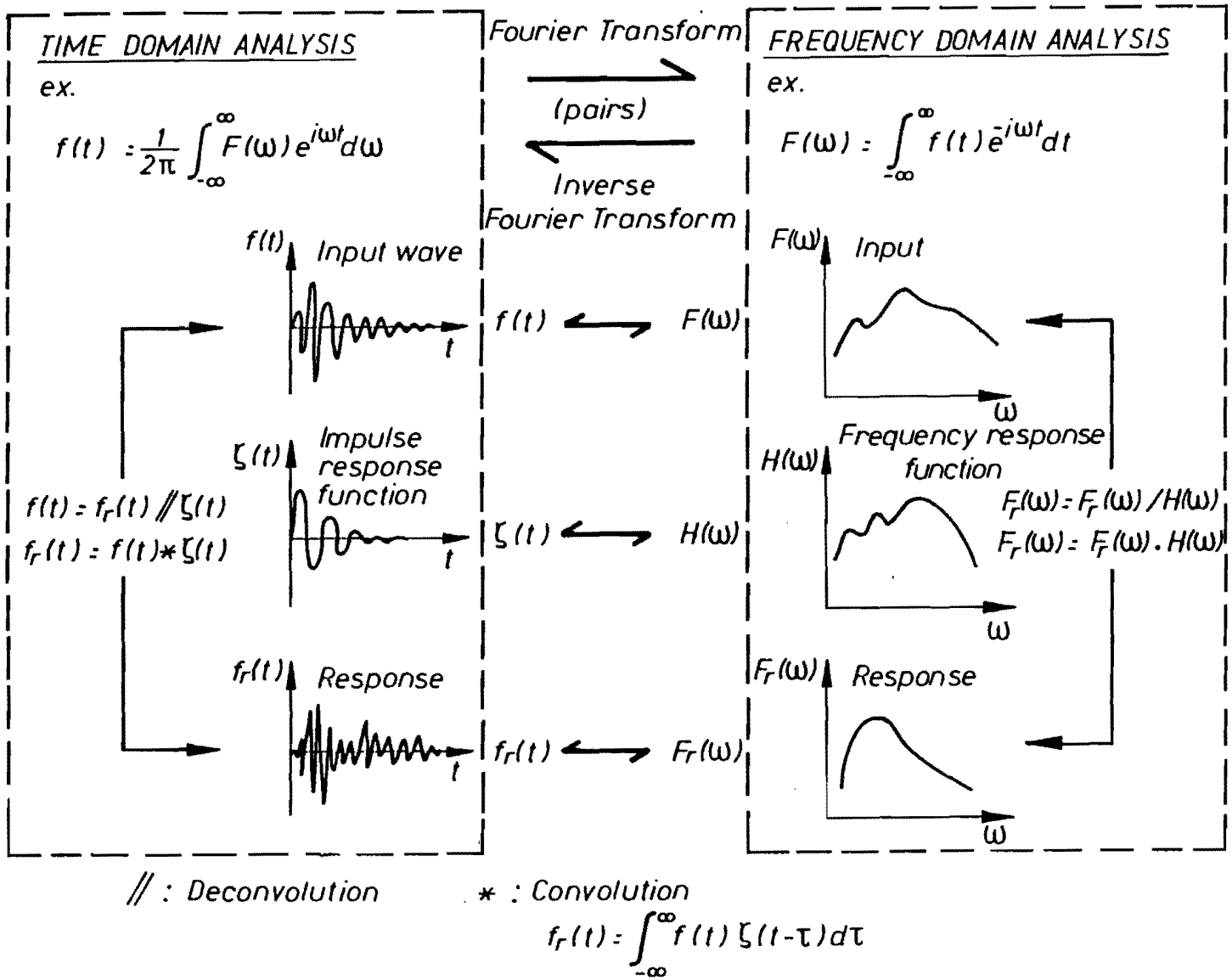

Fig. 6.3.10 Relationship between time and frequency domain analyses

Likewise, an input, frequency response function and response in a frequency domain analysis are illustrated in the right hand side figures. The response may be calculated by the product of the input and frequency response function. The three correspondances in time and frequency domain analyses are Fourier transform pairs.

There are two ways to obtain a response spectral density function $G_r(\omega)$. The first is to calculate a response result, such as a storey drift $\delta(t)$ in the time domain using a time domain analysis, and then to transform it into the frequency domain using a Fourier transform. Once a response result is found in the frequency domain, it is straightforward to obtain $G_r(\omega)$. The second approach is to transform a recorded earthquake wave in time into frequency. A frequency domain analysis is then used to get a response result and $G_r(\omega)$. Regardless of the way, the two results are the same. Assuming that a response result in the time domain has been computed, the means of calculating $G_r(\omega)$ must now be briefly explained. In addition, because we are primarily concerned with obtaining a response result for storey drift, the means of obtaining a result using a frequency domain analysis must also be discussed.

Suppose a response result is calculated in the time domain, as shown in Fig. 6.3.11(a). There are N discrete values x_m ($m=0,1,\ldots,N-1$; N is even number) separated by a uniform time interval Δt. Although an infinite number of continuous functions can be fitted to the N values, a trigonometric function may be used as an appropriate continuous

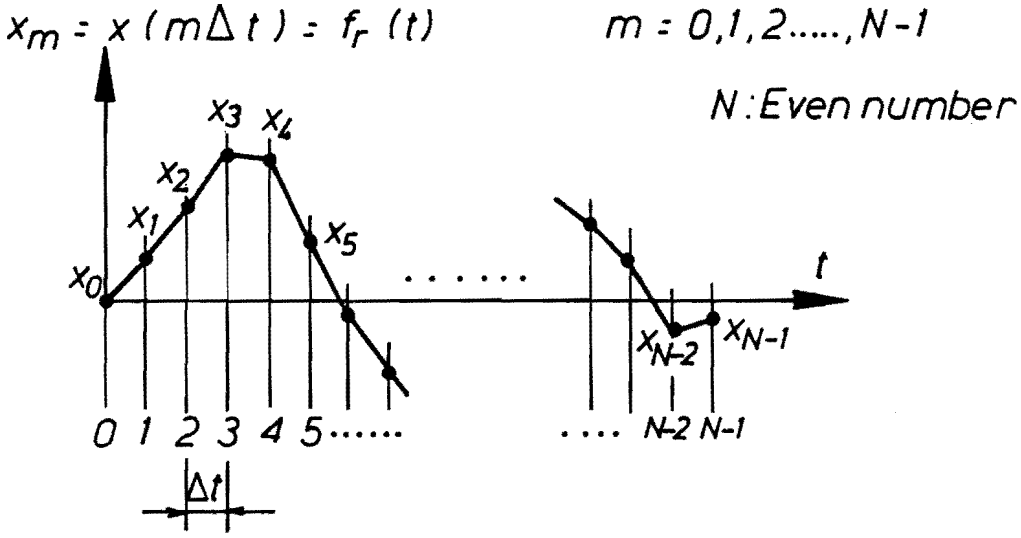

(a) Response result in the time domain

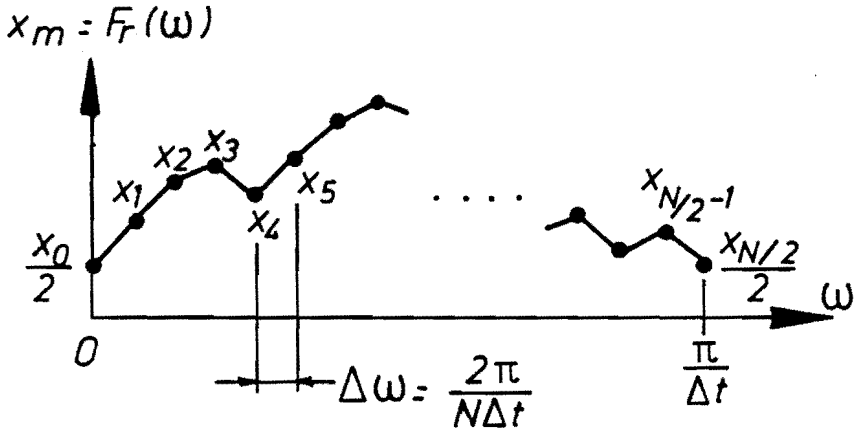

(b) Response amplitude spectrum in the frequency domain

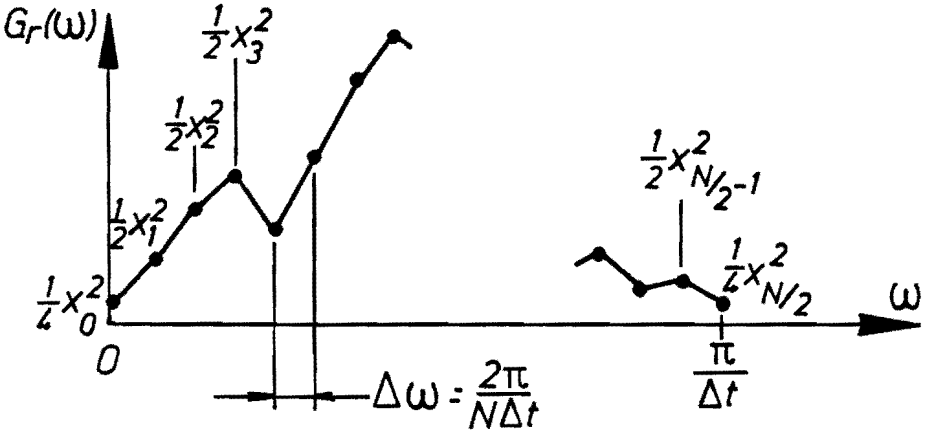

(c) Response spectral-density function

Fig. 6.3.11 Response results in the time and frequency domains

approximation. That means, it is approximated by a sum of sinusoidal waves. Introducing k to represent one of a series of sinusoidal waves, the function chosen is:

$$x(t) = \frac{A_0}{2} + \sum_{k=1}^{N/2-1} \left(A_k \cos \frac{2\pi kt}{N \cdot \Delta t} + B_k \sin \frac{2\pi kt}{N \cdot \Delta t} \right) + \frac{A_{N/2}}{2} \cos \frac{2\pi (N/2) t}{N \cdot \Delta t}$$

$$= \frac{X_0}{2} + \sum_{k=1}^{N/2-1} X_k \cos (\omega_k \cdot t + \phi_k) + \frac{X_{N/2}}{2} \cos \omega_{N/2}\, t \qquad (6.3.24)$$

in which:

$$X_k = \sqrt{A_k^2 + B_k^2}$$

$$\phi_k = \tan^{-1} (- B_k / A_k)$$

$$\omega_k = \frac{2\pi k}{N \cdot \Delta t} \qquad \text{(kth circular frequency)}$$

A_0, A_k, B_k and $A_{N/2}$ = constants

The term X_k expresses the amplitude of a vibration with circular frequency ω_k and ϕ_k is its phase angle. The transform from discrete time domain values to amplitudes and phase angles in the frequency domain is called a Fourier transform and the inverse transform an Inverse Fourier transform. Another Fourier series formula commonly used follows from the complex-valued relations:

$$C_k = \frac{1}{N} \sum_{m=0}^{N-1} x_m \, e^{-i(2\pi km/N)} \qquad (k=0, 1, 2, \ldots, N-1) \qquad (6.3.25)$$

(Fourier transform)

$$x_m = \sum_{k=0}^{N-1} C_k \, e^{i(2\pi km/N)} \qquad (m=0, 1, 2, \ldots, N-1) \qquad (6.3.26)$$

(Inverse Fourier transform)

where:

$$C_{N-j} = C_j^* \quad (j=1, 2, \ldots, N/2-1; \ * = \text{conjugation})$$

$$C_k = \tfrac{1}{2} (A_k - iB_k)$$

The amplitude of vibration at a given frequency is important. A graph of the relationship between ω and the amplitude X_m of the Fourier terms is called the response amplitude spectrum (Fig. 6.3.11(b)). The average power for all time increments is defined as:

$$\frac{1}{N} \sum_{m=0}^{N-1} x_m^2 = \frac{1}{2} \left[\frac{X_0^2}{2} + \sum_{k=1}^{N/2-1} x_k^2 + \frac{X_{N/2}^2}{2} \right]$$

$$= |C_0|^2 + 2 \sum_{k=1}^{N/2-1} |C_k|^2 + |C_{N/2}|^2 \qquad (6.3.27)$$

The amount of power between frequencies ω and $\omega + \delta\omega$ is $G_r(\omega)\,\delta\omega$ where $G_r(\omega)$ in Fig. 6.3.11(c) is the response spectral density function. Thus, the discrete spectral density function becomes:

$$G_r(0) = \frac{1}{\Delta\omega} |C_0|^2 \qquad (6.3.28)$$

$$G_r\left(\frac{2\pi j}{N\cdot\Delta t}\right) = \frac{2}{\Delta\omega} |C_j|^2 \qquad (6.3.29)$$

$$(j=1, 2, \ldots, N/2-1)$$

$$G_r\left(\frac{\pi}{\Delta t}\right) = \frac{1}{\Delta\omega} |C_{N/2}|^2 \qquad (6.3.30)$$

where:

$$\Delta\omega = \frac{2\pi}{N\cdot\Delta t} \quad \text{(frequency interval)}$$

When $\Delta t \to 0$, the discrete spectral density function $G_r(j\Delta\omega)$ becomes a continuous spectral density function $G_r(\omega)$.

As noted earlier, the response amplitude spectrum may also be calculated by a frequency domain analysis. As indicated in Fig. 6.3.10 the displacement response of a S.D.O.F. system with natural frequency ω is given by:

$$X(\Omega_k) = H(\Omega_k)\ \ddot{Y}(\Omega_k)$$

$$= \frac{-1}{\omega^2 - \Omega_k^2 + i\ 2h\ \omega\ \Omega_k}\ \ddot{Y}(\Omega_k) \qquad (6.3.31)$$

where:

Ω_k = $\Delta\omega$ k (k=0, 1, ..., N/2)
(a series of discrete circular frequencies)

$\ddot{Y}(\Omega_k)$ = Fourier amplitude of input earthquake acceleration

$H(\Omega_k)$ = frequency response function

h = critical damping ratio

Considering Eq. (6.3.9), the displacement response of the ith mass in the jth mode of a M.D.O.F. system (Fig. 6.3.1) is given by:

$$X_{j,i}(\Omega_k) = U_{j,i}\ \beta_j\ X_j(\Omega_k) \tag{6.3.32}$$

in which $U_{j,i}$ is the mode shape value of ith mass in jth mode and $X_j(\Omega_k)$ is calculated from Eq. (6.3.31) where ω is the resonant frequency of the jth mode. Therefore, the storey drift of the ith storey is given by:

$$\Delta_i(\Omega_k) = \sum_{j=1}^{n}(U_{j,i} - U_{j,i-1})\beta_j\ X_j\ (\Omega_k) \tag{6.3.33}$$

The response amplitude of each Ω_k is calculated from Equation (6.3.33) from which the response amplitude spectrum on storey drift is obtained.

The moments of the response spectral-density function are most important in the random vibration approach. If the response is stationary, the ith moment of the response spectral density function is given by (80):

$$\lambda_{i,r} = \int_0^{\infty} \omega^i \, G_r(\omega) \, d\omega \qquad (6.3.34)$$

In the random vibrational approach, the mean threshold-crossing rate may be calculated (79). A classical formula for the mean crossing rate of a level b by a stationary random process X(t) is (83):

$$\nu_b = \int_{-\infty}^{+\infty} |\dot{x}| \, f_{X,\dot{X}}(b,\dot{x}) \, d\dot{x} \qquad (6.3.35)$$

where $f_{X,\dot{X}}(x,\dot{x})$ is the joint probability density function of X(t) and its derivative $\dot{X}(t)$. Since X(t) is stationary, the random variables X(t) and $\dot{X}(t)$ are uncorrelated. If they are also independent, which is guaranteed in the case where X(t) is Gaussian, then:

$$\nu_b = f_X(b) \int_{-\infty}^{+\infty} |\dot{x}| \, f_{\dot{X}}(\dot{x}) d\dot{x} = f_X(b) E[|\dot{x}|] \qquad (6.3.36)$$

where $f_x(b)$ is the normal (or Gaussian) distribution, and $E[|\dot{x}|]$ is the mean of the absolute value of the slope of X(t). Every b-upcrossing (crossing of level b with positive slope) is followed by a b-downcrossing. Therefore the mean rates of up- and downcrossings, respectively ν_b^+ and ν_b^- are given by:

$$\nu_b^+ = \nu_b^- = \tfrac{1}{2} \nu_b = \tfrac{1}{2} f_x(b) \; E[|\dot{x}|] \qquad (6.3.37)$$

Differentiation being a linear operation, if X(t) is Gaussian, its derivative $\dot{X}$ will also be Gaussian with zero

mean. Hence:

$$E[|\dot{x}|] = 2\int_0^{\infty} \frac{\dot{x}}{\sqrt{2\pi}\,\sigma_{\dot{x}}} \exp\left(-\frac{\dot{x}^2}{2\sigma_{\dot{x}}^2}\right) d\dot{x} = \sqrt{2/\pi}\,\sigma_{\dot{x}} \tag{6.3.38}$$

Combining Eqs (6.3.37) and (6.3.38) yields, for Gaussian X(t), the familiar relationship:

$$\nu_b^+ = \frac{1}{2\pi}\frac{\sigma_{\dot{x}}}{\sigma_x}\exp\left(-\frac{b^2}{2\sigma_x^2}\right) = \frac{\Omega_x}{2\pi}\exp\left(-\frac{b^2}{2\sigma_x^2}\right) \tag{6.3.39}$$

in which:

$$\sigma_x^2 = \lambda_{0,x} \quad \text{(zero-order moment of } G_x(\omega)\text{)}$$

$$\Omega_x = \sqrt{\lambda_{2,x}/\lambda_{0,x}} = \sigma_{\dot{x}}/\sigma_x$$

Consequently, the total number of occurrences for which X(t) goes outside the range (b,-b) is:

$$N = 2\nu_b^+ S = \frac{\Omega_x \cdot S}{\pi}\exp\left(-\frac{b^2}{2\sigma_x^2}\right) \tag{6.3.40}$$

in which S is the strong motion duration. Figure 6.3.12 shows a random process X(t) and N (Eq. (6.3.40)) in relation to fixed thresholds b and -b.

As stated earlier, the aim of using a random vibration approach is to obtain the elastic energy $_eE_d$ which

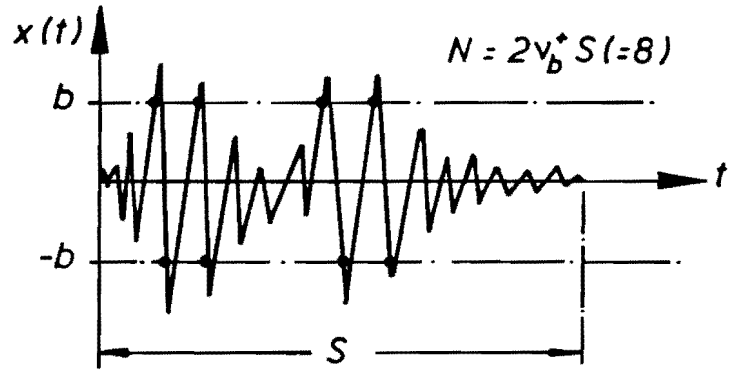

Fig. 6.3.12 Total number of occurrences for which x(t) goes outside the range (b,-b)

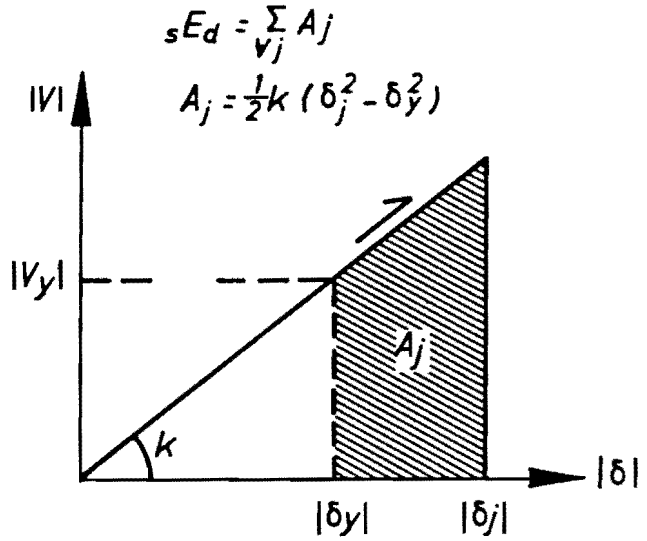

Fig. 6.3.13 Elastic energy corresponding to cumulative plastic strain energy

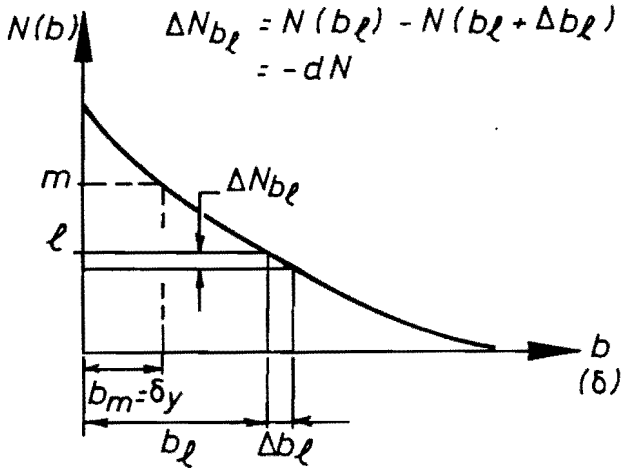

Fig. 6.3.14 Relationship between total number of occurrence N(b) and threshold b

corresponds to the cumulative plastic strain energy absorbed by a storey. This can be expressed as in Fig. 6.3.13 by:

$$
\begin{aligned}
{}_{e}E_{d} &= \sum_{j=1}^{m} \tfrac{1}{2}k\,(\delta_j^{\,2} - \delta_y^{\,2}) \\
&= \tfrac{1}{2}k \sum_{j=1}^{m} \delta_j^{\,2} - \tfrac{1}{2}m\,\frac{V_y^{\,2}}{k} \qquad (6.3.41) \\
&\quad (|\delta_j| > |\delta_y|)
\end{aligned}
$$

where: m = the number of the crossings of δ outside the range $(-\delta y, \delta y)$

δ_y = yield storey drift

k = initial storey stiffness

δ_j = maximum storey drift of the jth crossing in the time domain

From Eq. (6.3.40) m is given by:

$$
m = N_{b=\delta_y} = \frac{\Omega_\delta \cdot S}{\pi} \exp\left[-\frac{\delta_y^{\,2}}{2\sigma_\delta^{\,2}}\right] \qquad (6.3.42)
$$

where the subscript δ stands for the response drift of a storey. Further, the item $\sum_{j=1}^{m} \delta_j^{\,2}$ in Equation (6.3.41) may be written (see Fig. 6.3.14):

$$
\begin{aligned}
\sum_{j=1}^{m} \delta_j^{\,2} &= \sum_{1=m}^{0} \Delta N_{b_1} \cdot b_1^{\,2} \\
&= \int_{m}^{0} -dN \cdot b_1^{\,2}
\end{aligned}
$$

$$= \int_0^m b_1^2 \, dN \tag{6.3.43}$$

where: b_1 = storey drift b_1 such that $N(b_1) = 1$

ΔN_{b_1} = number of occurrence for which equals to b_1

From Eqs (6.3.40) to (6.3.43):

$$e^{E_d} = \frac{\Omega_\delta \cdot S \cdot k \cdot \sigma_\delta^2}{\pi} \exp\left(-\frac{\delta_y^2}{2\sigma_\delta^2}\right) \tag{6.3.44}$$

Using the result of the random vibration method, an approximation of the ratio of the damage energy absorbed by the ith storey to that for the entire structure is given by:

$$R_i = \frac{e^{E_{d_i}}}{e^{E_{d_T}}} \tag{6.3.45}$$

in which:

$$e^{E_{d_i}} = \Omega_{\delta_i} \cdot k_i \cdot \sigma_{\delta_i}^2 \cdot \exp\left[-\delta_{y_i}^2 / 2\sigma_{\delta_i}^2\right] \tag{6.3.46}$$

$$e^{E_{d_T}} = \sum_{i=1}^{n} e^{E_{d_i}} \tag{6.3.47}$$

Note that the strong motion time duration S and π are eliminated from Eq. (6.4.46) whereas they occur in Eq. (6.3.44). This is because they are common factors for all

storeys and need not be included in calculating Eq. (6.3.45) numerically. However, it is necessary to check the unit of ${}_eE_{d_i}$ after eliminating S. Following the units shown in Table 6.3.1, the unit of the displacement response spectral density function $G_\delta(\omega)$ is mm^2 sec. Thus, as the units of $\lambda_{0,\delta}$ and $\lambda_{2,\delta}$ are mm^2 and mm^2/sec^2, σ_δ has the unit of mm and Ω_δ 1/sec. Therefore, ${}_eE_{d_i}$ in Eq. (6.3.46) has the unit of kN·mm/sec, the physical meaning of which may be damage energy per second. This is consistent with the assumption of a stationary random process in which the spectral shape is assumed to be constant with regard to the duration time. Therefore, it can be justified to eliminate S from Eq. (6.3.46) not only for numerical but also for the physical reasons. Consequently, based on the random vibration approach, Eq. (6.3.45) is introduced for the approximation to the ratio of the damage energy absorbed by a storey to that for an entire structure.

In order to justify the approximation given by the ratio R_i, it is compared with values of E_{d_i}/E_{d_T} obtained from Eqs (6.3.6) and (6.3.8) by a non-linear time-history analysis. The 3 and 7 storey frames, detailed in Appendix A, were chosen as example structures. Both the storey mass m_i and yield shear strength V_{y_i} of the models were assumed to have a coefficient of variation of 0.1. Their mean values and other characteristics are shown in Table A.1. Two earthquake records were used (El Centro 1940 NS and Bucharest 1977 NS), the maximum acceleration values α_{max} for each being scaled to 0.20, 0.35 and 0.70 g. Thus in the 12 cases (2 frames x 2 earthquake records x 3 different values

of α_{max}), the distribution of ${}_eE_{d_i}/{}_eE_{d_T}$ by the random vibration approach was compared with that of the corresponding E_{d_i}/E_{d_T} by a non-linear time history analysis. The sample size (S.S.) was 100 for the 3-storey frame and 50 for the 7-storey frame. When no inelastic behaviour was observed, the trial was not counted in the sample. For the 7-storey building, the 2nd, 4th and the 6th storeys were chosen to be examined, while comparisons were made for all storeys for the 3-storey frame. The results are shown in Figs 6.3.15-6.3.18. The mean and standard deviation were calculated for each distribution. Moreover, the mean values of standard damage energy, $\overline{E_{d_T}/w_t}$ by the time history analyses are given in the figures for all 12 cases. According to the result, the accuracy of the approximation seems to depend on the structural models and earthquake records used. In the 3-storey frame for the El Centro record and the 7-storey frame for the Bucharest, the two distributions are quite close. However, the distributions for the 7-storey frame subjected to the El Centro record are quite different. Moreover, in general, when the damage energy input is small, the distributions of ${}_eE_{d_i}/{}_eE_{d_T}$ and E_{d_i}/E_{d_T} are different. It is therefore necessary to consider a reason for the discrepancy.

In a time history analysis, when the damage energy input is small, only a few storeys are expected to enter the plastic range. The storeys where inelastic behaviour is observed depend on characteristics of the structure and earthquake record. Thus, by changing the storey characteristics, m_i and V_{y_i}, the ratio E_{d_i}/E_{d_T} may vary markedly when the energy

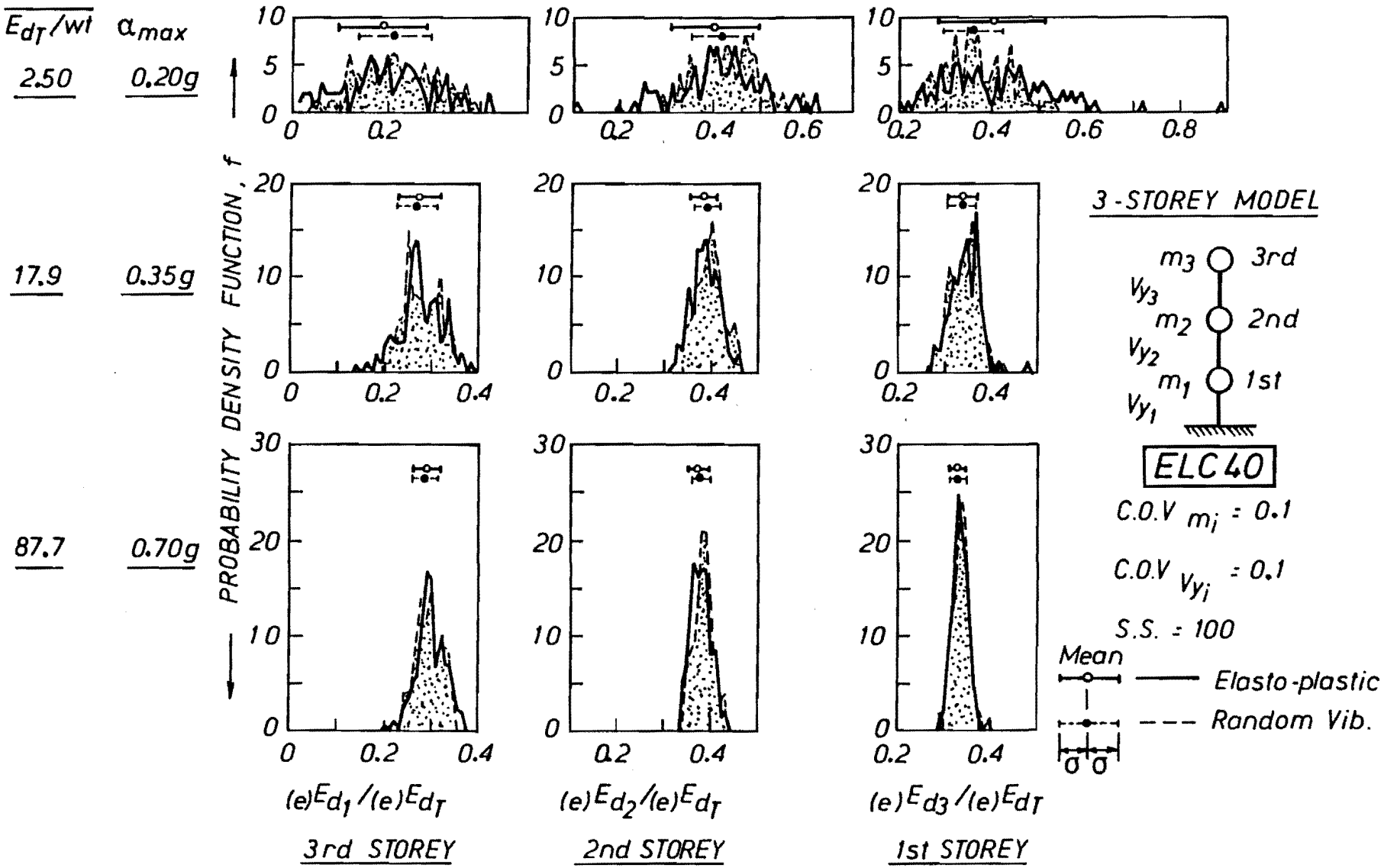

Fig. 6.3.15 Comparison of the proportion of damage energy absorbed by a storey

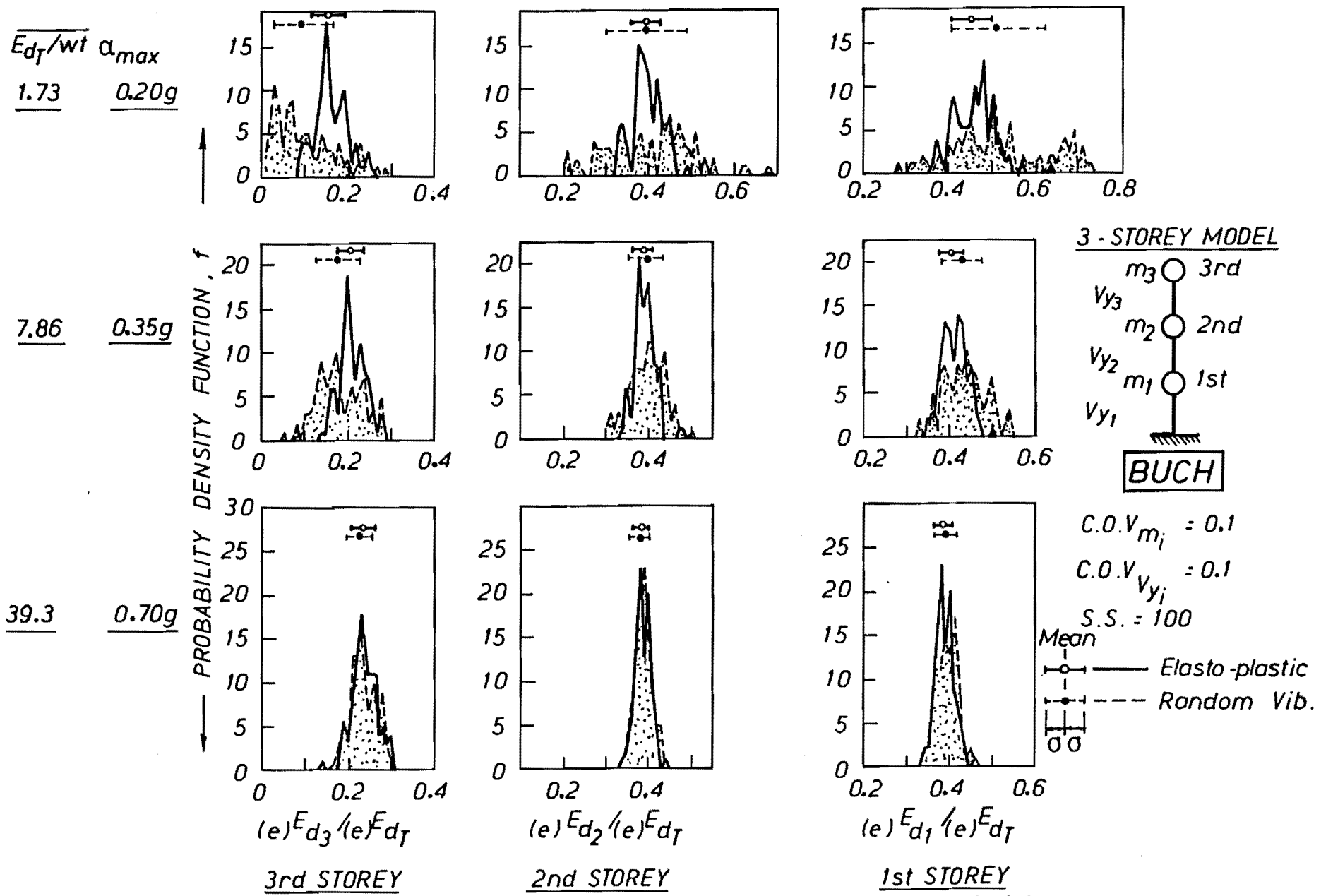

Fig. 6.3.16 Comparison of the proportion of damage energy absorbed by a storey

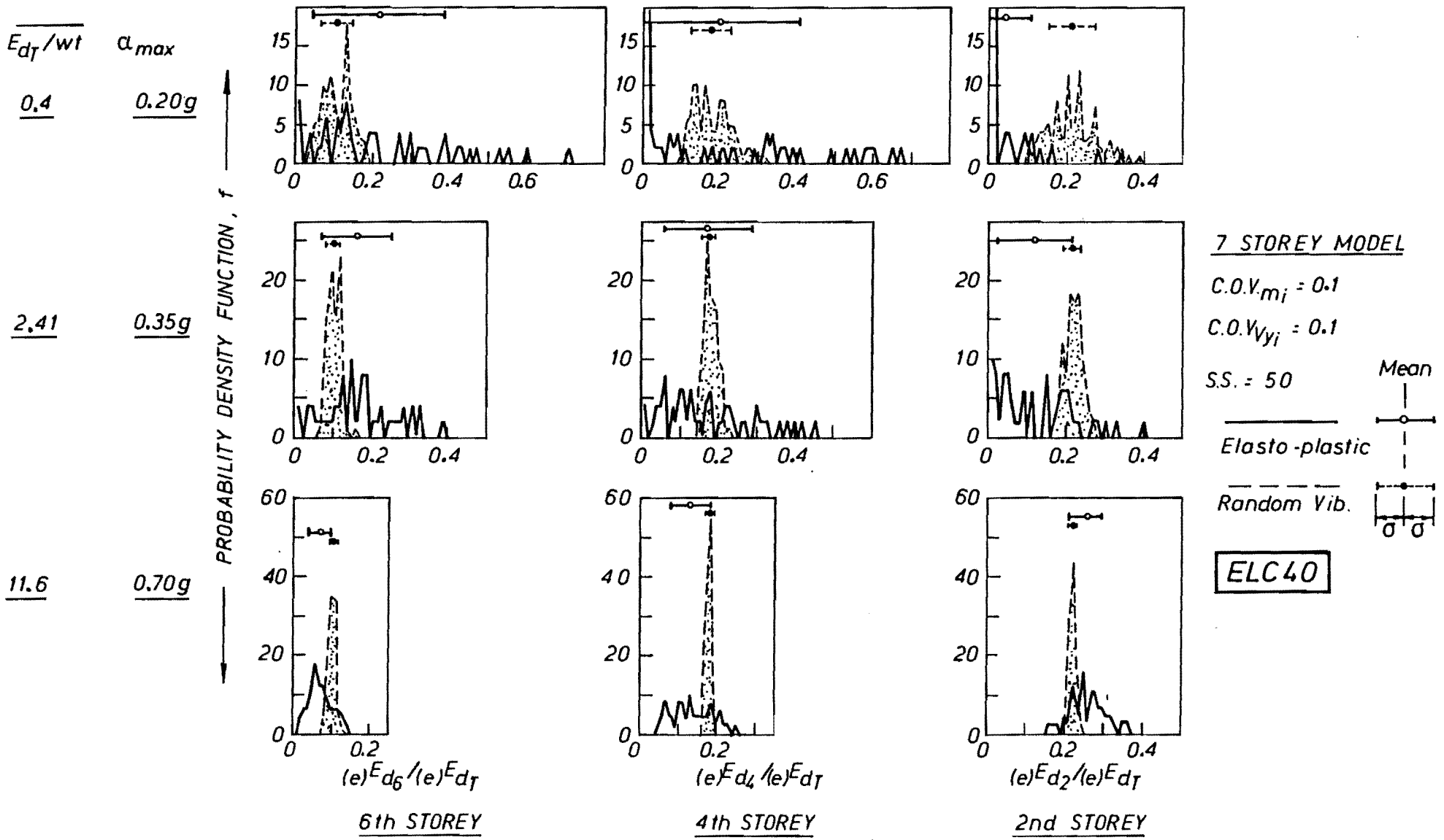

Fig. 6.3.17 Comparison of the proportion of damage energy absorbed by a storey

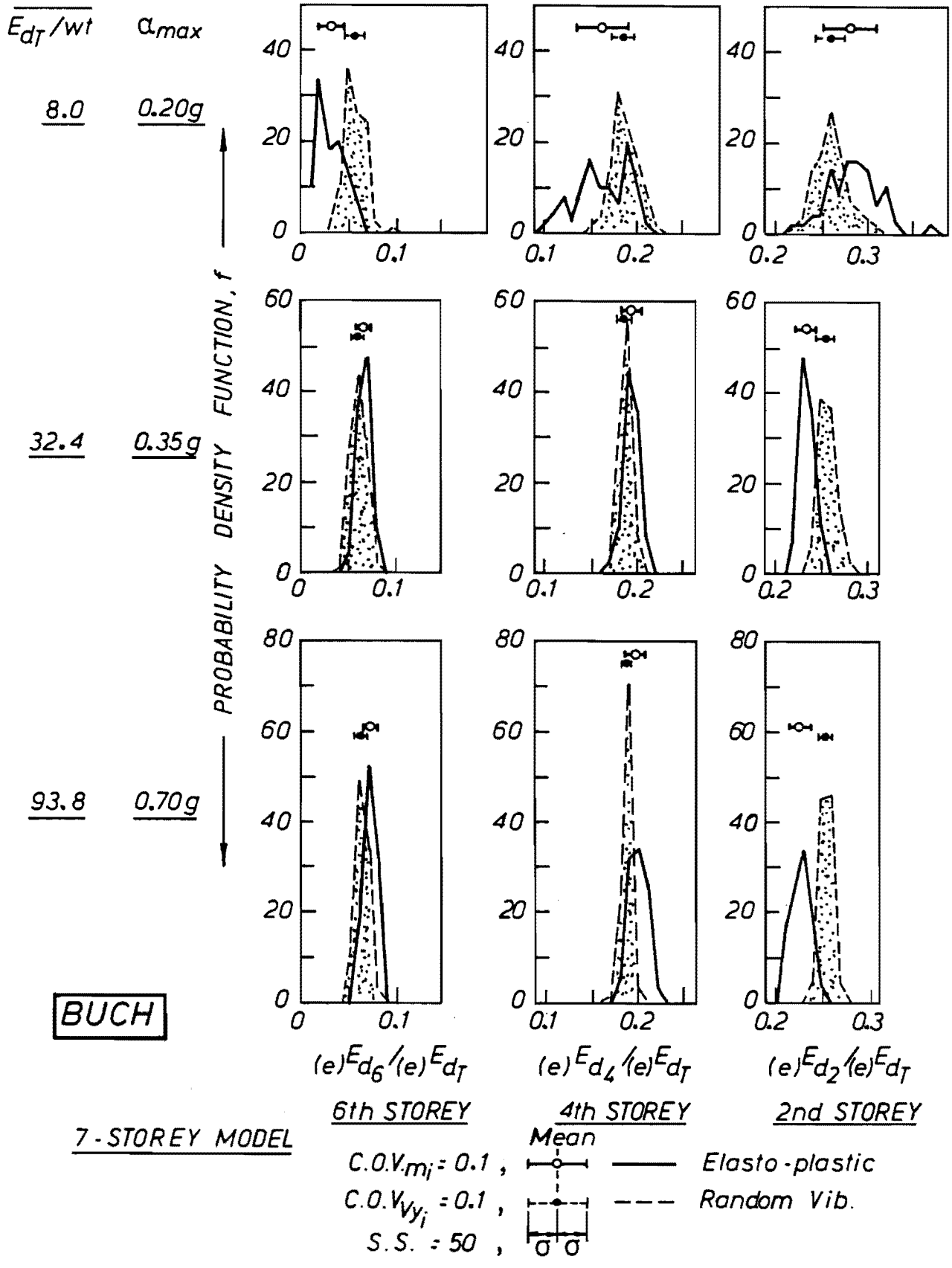

Fig. 6.3.18 Comparison of the proportion of damage energy absorbed by a storey

input is small. On the other hand, when an earthquake intensity is large, all storeys may become inelastic. The ratio E_{d_i}/E_{d_T} is still dependent on the characteristics of the structure and earthquake record, but the sensitivity to m_i and V_{y_i} is not as high as in the case of small earthquake intensity. The same argument can be applied to the approximation using the random vibration approach. The term which most strongly affects the ratio R_i is the exponential term in Eq. (6.3.46). Following Eqs (6.3.49) and (6.3.50), if the exponential term did not exist in the equation, the ratio R_i would be constant in relation to the scaling of an earthquake. Figure 6.3.19 shows the relationship between the value of the exponential term and $\delta y/\sigma_\delta$. When the damage energy input is large, the value of $\delta y/\sigma_\delta$ is small, say less than 0.5, because σ_δ becomes large. By changing the values of m_i and V_{y_i} the exponential term changes only by 10 to 20%. However, when the energy input becomes small and the value of $\delta y/\sigma_\delta$ is somewhere between 0.5 and 2.0, the exponential term can be easily changed in the range of 100-200%. Thus, it was found that the sensitivities of the ratios, both E_{d_i}/E_{d_T} and ${}_eE_{d_i}/{}_eE_{d_T}$, to structural characteristics are high when the damage energy input is small. High sensitivity does not directly mean that distributions of the ratios obtained by the time-history analysis and by the approximation are different. However, because one is based on an inelastic analysis and the other on an elastic analysis, the sensitivities to the characteristics may be different. This is a possible cause of the discrepancy between the distributions of E_{d_i}/E_{d_T} and ${}_eE_{d_i}/{}_eE_{d_T}$ when the damage energy input is small.

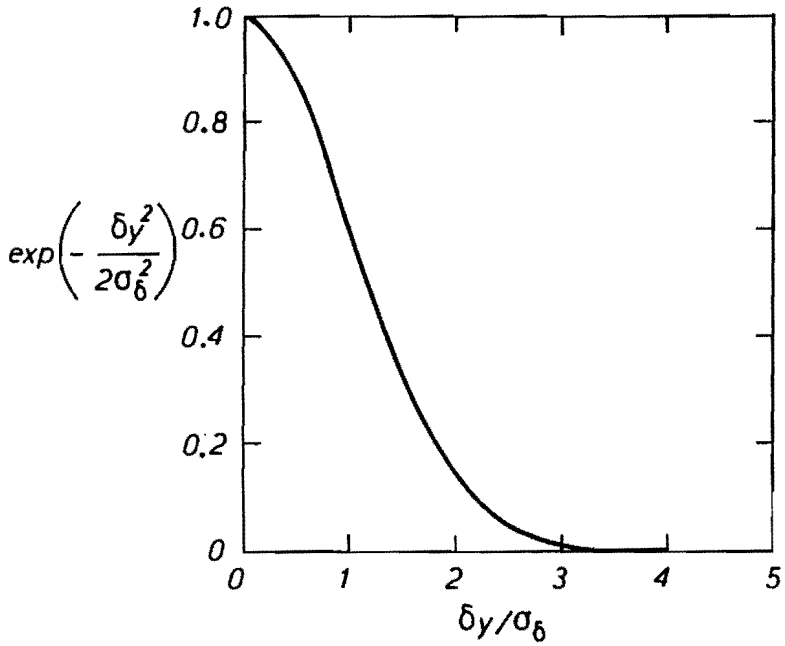

Fig. 6.3.19 $\exp(-\delta_y{}^2/2\sigma_\delta{}^2) - \delta_y/\sigma_\delta$ relationship

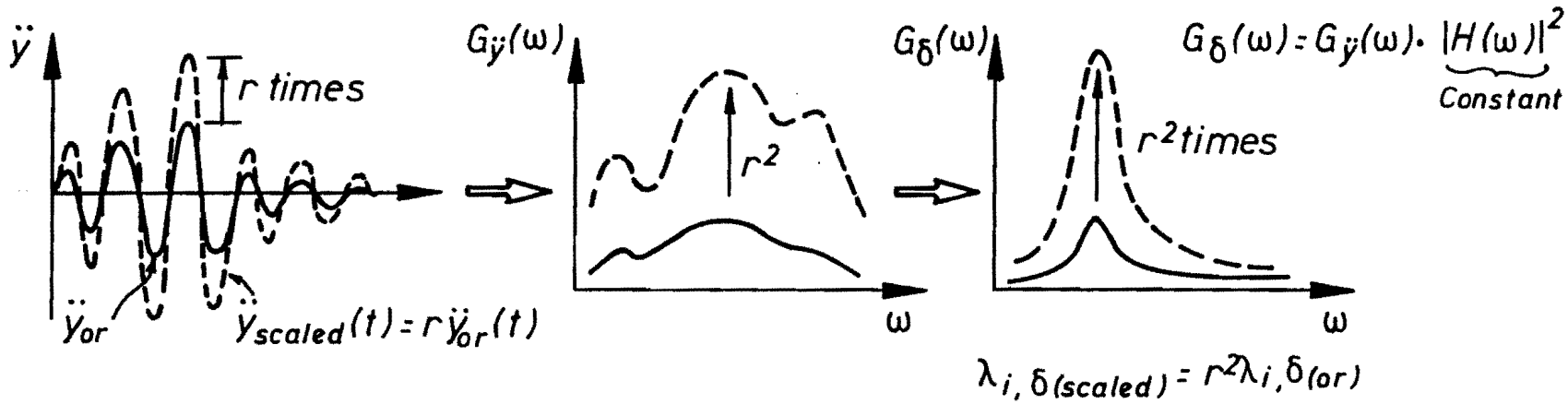

Fig. 6.3.20 Effects of scaling in ground accelerations

Though the discrepancies are found under some circumstances, the approximation using the random vibration approach is generally satisfactory for predicting the fraction of total damage energy absorbed by each storey. Consequently, Eq. (6.3.45) can be used as the approximation for estimating the fraction of total damage energy by a storey.

It is worthwhile to discuss the change of the ratio when an original earthquake acceleration record is scaled by a factor r (see Fig. 6.3.20), because the calculation of the ratio for different values of α_{max} is necessary in estimating the failure probabilities of a structure, as explained in Section 7.3, and the scaling of an original earthquake record may be expected. Since k_i and δ_{y_i} in Eq. (6.3.45) are constant for the scaling, σ_{δ_i} and Ω_{δ_i} should be estimated for the scaled earthquake record. However as the random vibration method is an elastic analysis, once the ratio of Eq. (6.3.45) is calculated for an original record, it is easy to obtain the ratio for the scaled record. From Eq. (6.3.27), the average power for the scaled acceleration is r^2 times as big as the original wave and so, therefore, is the response spectral-density function $G_\delta(\omega)$ as shown in Fig. 6.3.20. Thus, the ith moment of $G_\delta(\omega)$ is given by:

$$\lambda_{i,\delta(\text{scaled})} = r^2 \cdot \lambda_{i,\delta(\text{original})} \tag{6.3.48}$$

Therefore:

$$\sigma_{\delta_i(\text{scaled})} = r \cdot \sigma_{\delta_i(\text{original})} \tag{6.3.49}$$

$$\Omega_{\delta_i(\text{scaled})} = \Omega_{\delta_i(\text{original})} \tag{6.3.50}$$

Accordingly, where the original acceleration is magnified by r to change the maximum acceleration, only a simple calculation is required to get the ratio R_i for the scaled earthquake record.

In conclusion, the ratio of the damage energy absorbed by a storey to that for a whole structure can be assumed to be the same as the ratio obtain by an elastic probabilistic dynamic analysis, that is, a random vibration approach. Because linear elastic analysis is used, calculation of the ratio is straightforward. Hence, the damage energy absorbed by each storey may be obtained without any complicated analyses from the conclusions of sections 6.3.3 and 6.3.4.

6.4 BASIC EQUATION FOR PREDICTING MAXIMUM INELASTIC STOREY DRIFT

6.4.1 Introduction

As described in the previous section, the cumulative plastic strain energy absorbed into each storey can be easily calculated for a given structure and earthquake. The absorbed energy is believed to be closely related to the damage level experienced by the structure. Hence, if the amount of energy absorbed is small the structure probably suffers little damage, and if it is very large, the structure could collapse.

The question is therefore how much energy can be absorbed before the structure collapses. This can be called the energy absorbing capacity of the structure. It represents a failure criterion for a structure in terms of energy. Its precise formulation can be established.

The basic failure criterion assumed for this project was described in Section 5.3 in terms of maximum storey drift. Thus, for an energy failure criterion, the relationship between the absorbed damage energy for a storey and maximum storey drift must be clarified. However, in general, the relationship is not unique; for the fatigue types of failure experienced with long-duration earthquakes, the maximum storey drift for reaching an energy absorbing capacity is quite small, while for an earthquake whose motion has one predominant spike, the drift would be expected to be large to absorb the same amount of energy. This comparison is illustrated in Fig. 5.5.3. The behaviour of structures subjected to more normal earthquakes, however, may be somewhere in between, and a relationship between energy and drift may exist. In this section, the relationship between damage energy absorbed by a storey and the maximum storey drift is investigated to establish a basic equation in terms of the energy required to produce a maximum inelastic storey drift.

In section 6.4.2, a basic prediction equation is introduced. It is based on the assumption that the absorbing capacity of cumulative plastic strain energy in a dynamic analysis is related to the maximum plastic strain energy for monotonic

static loading. A coefficient is introduced to connect the former with the latter. From numerical results based on the relationship between cumulative plastic strain energy and maximum storey drift, the coefficient for predicting maximum storey drift is determined. In section 6.4.3, a failure criterion in terms of the energy is calibrated with regard to that in terms of maximum storey deflection angle, making use of the result of section 6.4.2.

6.4.2 Basic Prediction Equation for Maximum Inelastic Storey Drifts

To establish a basic prediction equation in terms of cumulative plastic strain energy for maximum inelastic storey drift, we need to know the relationship between absorbed cumulative plastic strain energy E_d and the maximum storey drift δ_{max}. That is, we require the δ_{max} induced by E_d. In the previous section, simple ways to estimate the total damage energy and the proportion of the total energy absorbed by a storey during an earthquake excitation were established. Thus, the damage energy input for a storey can now be obtained without using complicated analyses. Corresponding to the input damage energy, E_d, a resistant damage energy E_R must be defined. The amount of a resistant damage energy E_R must be equal to that of a damage energy input E_d. The resistant energy represents how the input energy is absorbed by a storey in terms of cumulative plastic strain energy. This is also equivalent to assuming a relationship between E_R and δ_{max}.

In order to relate E_R to δ_{max}, the static monotonic plastic strain energy $E_{R(static)}$ absorbed to develop a maximum storey drift δ_{max} is introduced, as shown in Fig. 6.4.1. The following equation is assumed for the relationship between E_R and $E_{R(static)}$.

$$E_R = C \cdot E_{R(static)}$$

$$= 2 \cdot C \cdot E_e \cdot (\mu-1)[1+\tfrac{1}{2}\alpha(\mu-1)] \qquad (6.4.1)$$

in which:

C = a constant

E_e = 1/2 V_y δ_y (maximum elastic strain energy)

μ = δ_{max}/δ_y (displacement ductility factor)

α = ratio of post yield stiffness to initial stiffness

The assumption will be justified later by examining whether the value of C is a certain constant number. Because E_R is defined and must be equal to the damage energy input E_d, the basic equation in terms of cumulative plastic strain energy for the ith storey must be:

$$E_{R_i} - E_{d_i} = 0 \qquad (6.4.2)$$

That is:

$$2 \cdot C \cdot E_{e_i} \cdot (\mu_i-1)[1+\tfrac{1}{2}\alpha_i(\mu_i-1)] - E_{d_T} \cdot \frac{e^{E_{d_i}}}{e^{E_{d_T}}} = 0 \qquad (6.4.3)$$

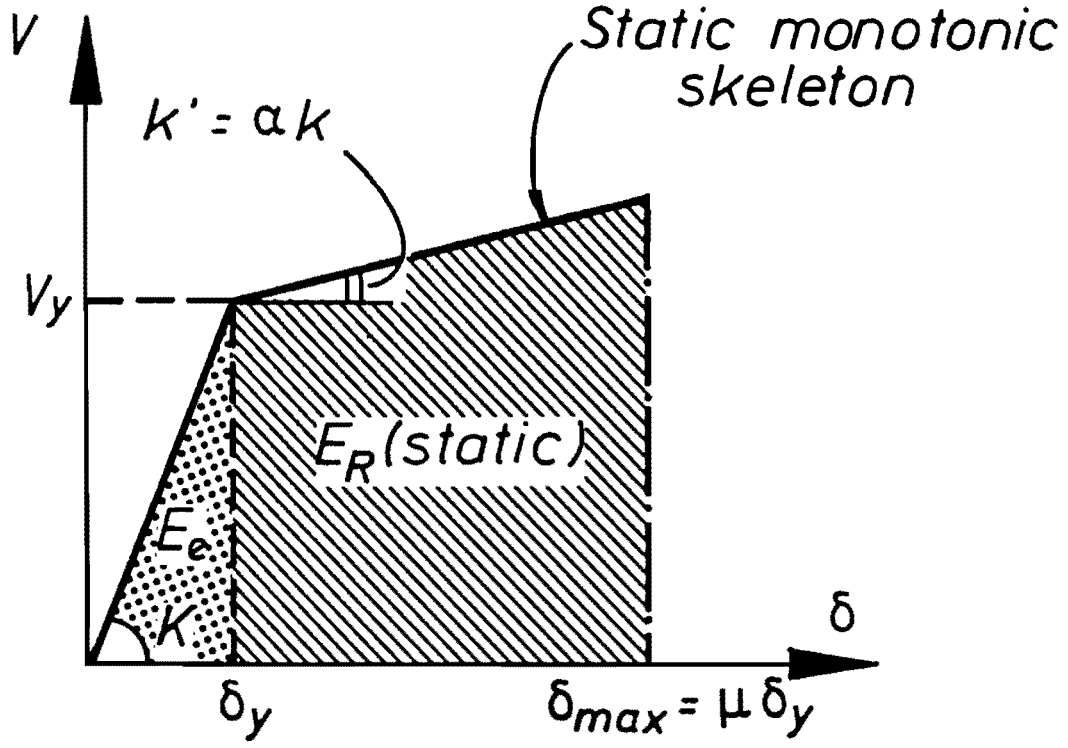

$$E_e = \frac{1}{2} V_y \delta_y$$

$$E_R(static) = 2E_e(\mu - 1)\left\{1 + \frac{1}{2}\alpha(\mu - 1)\right\}$$

$$E_R = C \cdot E_R(static)\ ;\ C:\ Coefficient$$

Fig. 6.4.1 Assumption of the relationship between a resistant damage energy and a static monotonic plastic strain energy

The meaning of the second term will be understood from the discussion in the previous section. Accordingly, from Eq. (6.4.3) the maximum storey drift of the ith storey δ_{max_i} is given by:

$$\delta_{max_i} = \mu_i \cdot \delta_{y_i} \tag{6.4.4}$$

where:

$$\mu_i = 1 - \frac{1}{\alpha_i} + \sqrt{\left(\frac{1}{\alpha_i}\right)^2 + \frac{E_{d_T}}{C \cdot E_{e_i} \cdot \alpha_i} \cdot \frac{e^{E_{d_i}}}{e^{E_{d_T}}}}$$

In the above equation, the constant C is the only unknown value. Once C is obtained, one can predict δ_{max_i} without using a time consuming and complex inelastic dynamic analysis for M.D.O.F. systems.

In order to examine the range of values for C, the relationship between the term $E_{d_i}/w_{t\ above_i}$ and δ_{max_i} was examined by numerical studies. The item $E_{d_i}/w_{t\ above_i}$ is the absorbed damage energy per sustained weight. The 3 and 7 storey models in Appendix A subjected to the El Centro 1940 NS and Parkfield 1966 N65E earthquake motions were used assuming a critical damping ratio of h = 0.05. Each storey mass and yield shear strength was assumed to have a coefficient of variation of 0.1. The maximum ground acceleration was changed such that the distribution of maximum acceleration had the type II asymptotic form, following the assumption in Chapter 4. Using an inelastic dynamic analysis for a 3 or 7-degree-of-freedom system, the relationships between $E_{d_i}/w_{t\ above_i}$ and γ_{max_i} were

obtained, as shown in Figs 6.4.2 and 6.4.3. The term E_{d_i} was calculated by Eq. (6.3.6). The results indicate that for a larger energy related to damage $E_{d_i}/w_{t\ above\ i}$ absorbed in a storey, a larger maximum storey drift δ_{max} is induced. The relation seems to be different for different storeys, but independent of earthquake motion.

To examine the matter in detail, a relation between $E_{d_i}/w_{t\ above_i}$ and δ_{max_i} may be formulated from Eqs (6.4.2) - (6.4.4) as follows:

$$E_{d_i} = C \cdot V_{y_i} \cdot \delta_{y_i} \cdot (\mu_i - 1)[1 + \tfrac{1}{2}\alpha_i(\mu_i - 1)]$$

$$E_{d_i}/w_{t\ above_i} = C \cdot C_{d_i} \cdot (\delta_{max_i} - \delta_{y_i})$$

$$[1 + \tfrac{1}{2}\alpha_i(\delta_{max_i}/\delta_{y_i} - 1)] \qquad (6.4.5)$$

where: $C_{d_i} = V_{y_i}/w_{t\ above\ i}$

For different values of the coefficient C, the results of the $E_{d_i}/w_{t\ above\ i}$ - $\gamma_{max\ i}$ relationship obtained by inelastic analysis were compared with those given by Eq. (6.4.5). The comparisons are shown in Figs 6.4.4 and 6.4.5. From the figures, the values of C for El Centro record were slightly higher than that for Parkfield. However, it can be seen that the value of C varies within a range of 2 to 4, regardless of structural models and storeys.

As the range of values of C has been obtained, δ_{max_i} is now inversely calculated by Eq. (6.4.4) to examine the sensitivity of δ_{max_i} to C and to determine the value of C.

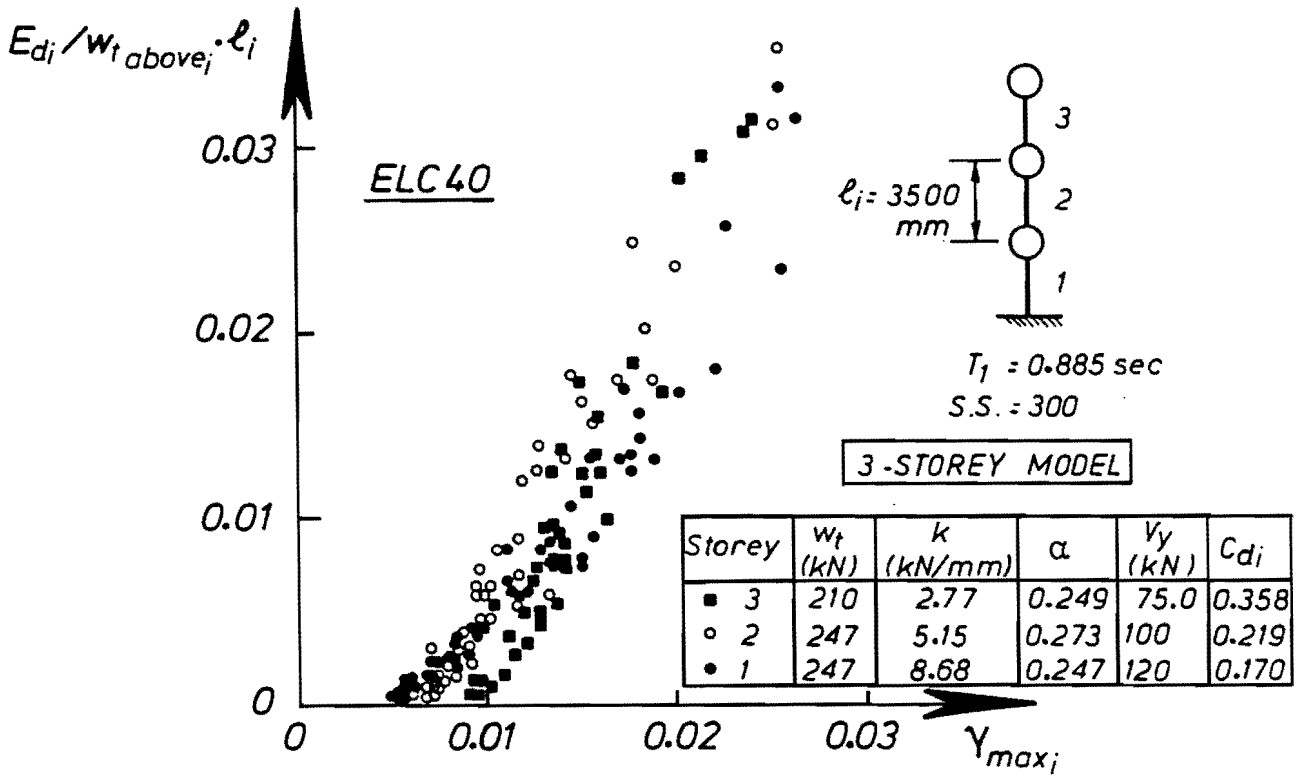

Storey	w_t (kN)	k (kN/mm)	α	V_y (kN)	C_{di}
■ 3	210	2.77	0.249	75.0	0.358
○ 2	247	5.15	0.273	100	0.219
● 1	247	8.68	0.247	120	0.170

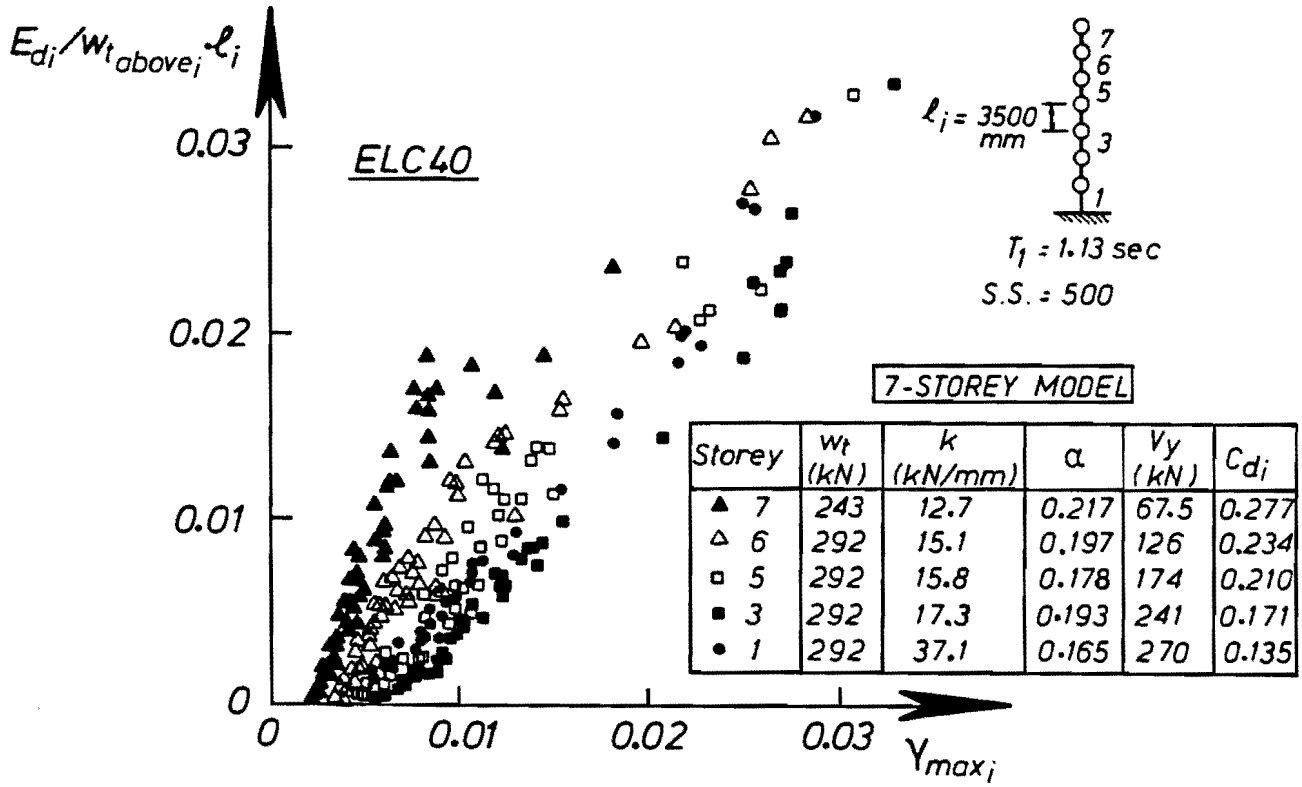

Storey	w_t (kN)	k (kN/mm)	α	V_y (kN)	C_{di}
▲ 7	243	12.7	0.217	67.5	0.277
△ 6	292	15.1	0.197	126	0.234
□ 5	292	15.8	0.178	174	0.210
■ 3	292	17.3	0.193	241	0.171
● 1	292	37.1	0.165	270	0.135

Fig. 6.4.2 Storey deflection angle induced by non-dimensional damage energy

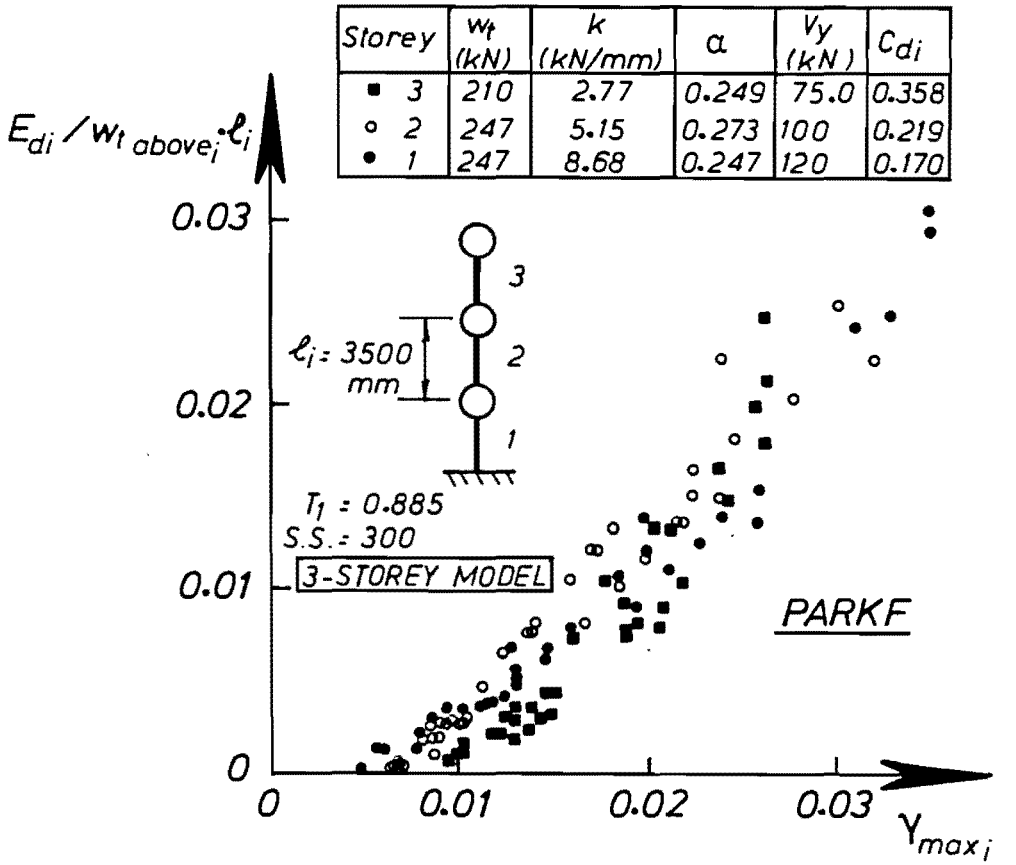

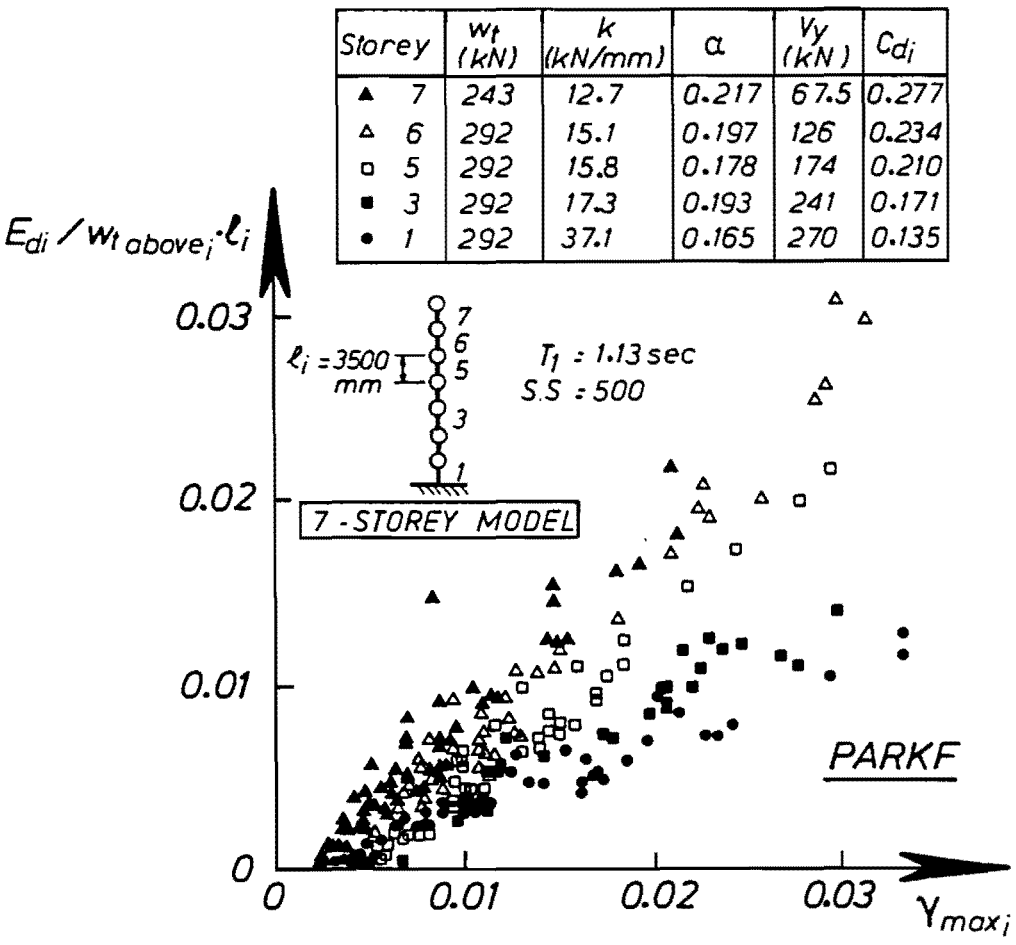

Fig. 6.4.3 Storey deflection angle induced by non-dimensional damage energy

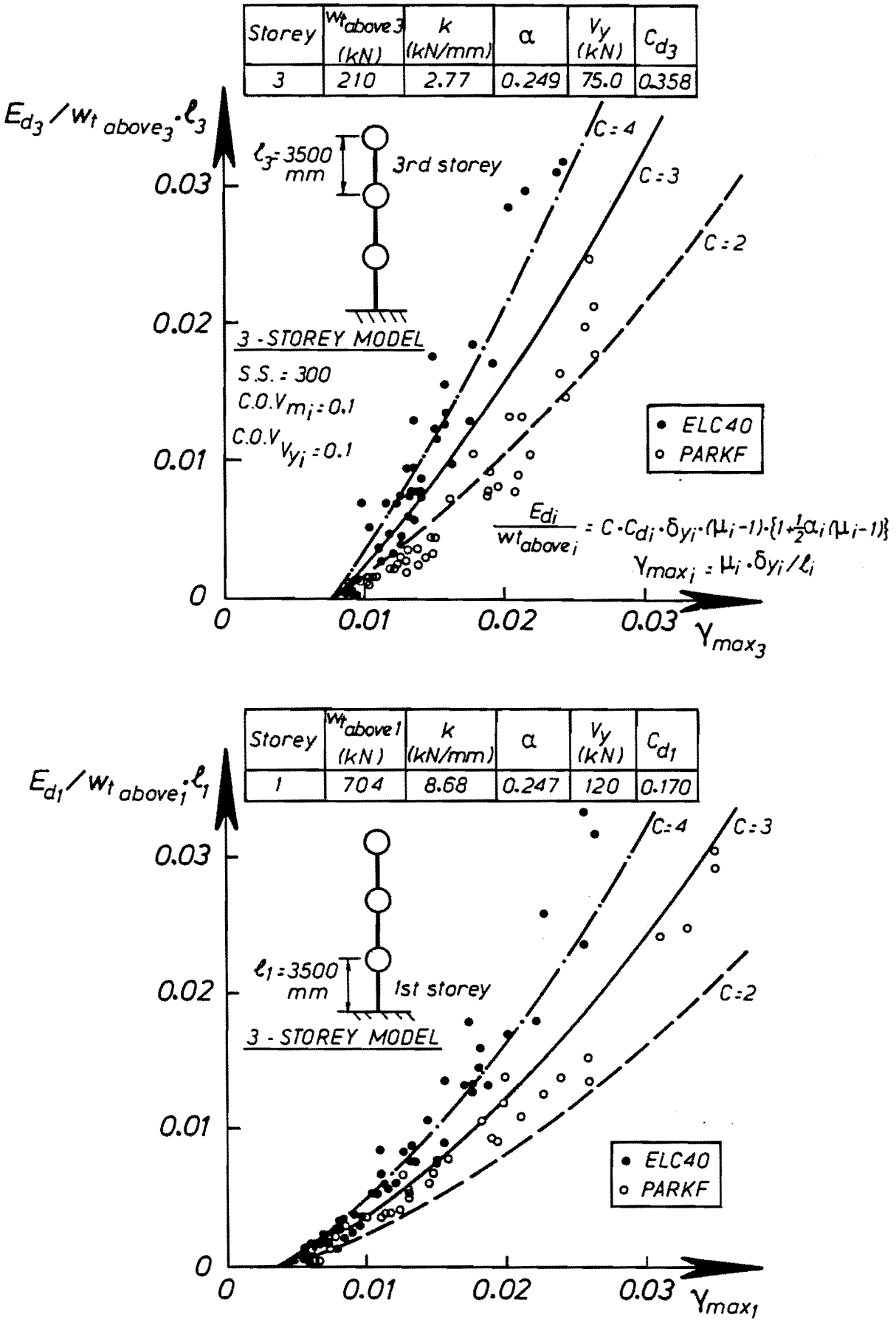

Fig. 6.4.4 Storey deflection angle induced by non-dimensional damage energy

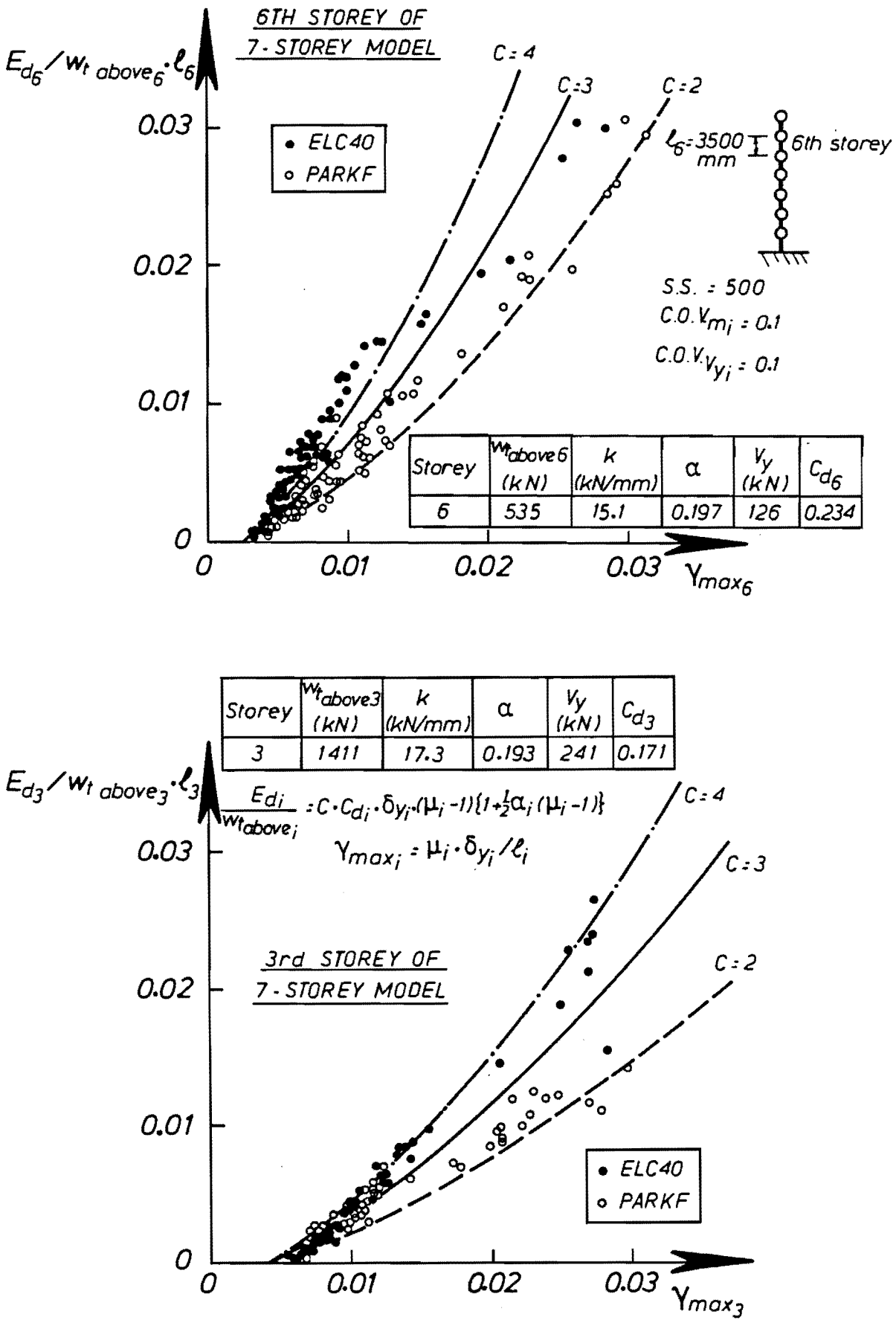

Fig. 6.4.5 Storey deflection angle induced by non-dimensional damage energy

In computing δ_{max_i}, E_{d_T} in Eq. (6.4.4) is obtained by a M.D.O.F. inelastic dynamic analysis (see "considered" in Figs 6.3.5-6.3.7) not by Eq. (6.3.22) based on a S.D.O.F. system. The simplifying assumptions that α is equal to zero and that E_{d_T} may be calculated by Eq. (6.3.22) (or Eq. (6.3.23)) will be discussed later; they are adopted in this project finally. The value of δ_{max_i} predicted by Eq. (6.4.4) is compared with that obtained by a M.D.O.F. inelastic dynamic analysis with the bi-linear hysteresis rule. The storey characteristics used in the analysis are shown in Table A.1, which were calculated by a static non-linear analysis. In a spring-mass model using the bi-linear hysteresis rule, this analysis seems most accurate because the storey characteristics including a post yield storey stiffness are carefully determined by using the static analysis. The results from the inelastic dynamic analysis need to be considered first as target results. The results are shown in Fig. 6.4.6 and include 30-storey models. The value of δ_{max_i} from Eq. (6.4.4) is not very sensitive to the value of C, so that C could be assumed to have a value of 3. Because it is found that the constant C has a certain number, the assumption of Eq. (6.4.1) can now be justified. Consequently, it turns out that the proposed method using cumulative plastic strain energy is a practical approach for calculating the maximum inelastic storey drift and hence the likelihood of collapse of multi-storey framed buildings.

Before suggesting further simplifications in the basic equation and its justification, the value of the critical

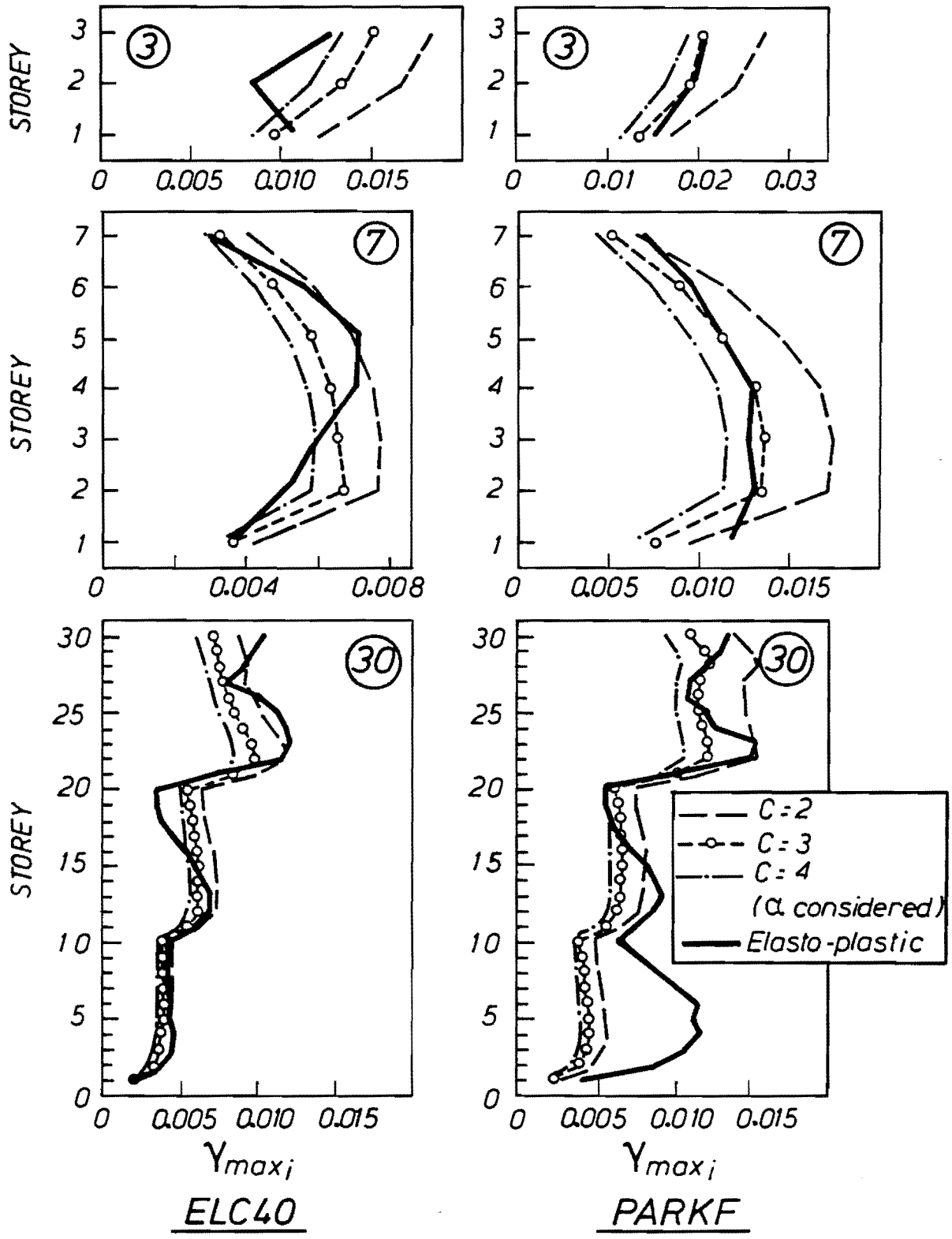

Fig. 6.4.6 Prediction of maximum storey deflection angle ($\alpha \neq 0$)

damping ratio h considered in this study must be described. Generally, in dynamic analysis, it is difficult to estimate appropriate values of h for structures. The damping matrix [C] in Eq. (6.3.1), which is determined by h, is often chosen primarily for convenience of calculation. For reinforced concrete structures, values of h from 0.02 to 0.1 are generally used for both elastic and inelastic ranges. In this report, h for each resonant mode is simply assigned a value of 0.05 and [C] is calculated such that the generalised damping matrix $[U]^T[C][U]$ becomes diagonal using the chosen values of h (61). This is done simply because h of 0.05 is the value most commonly used and also for reasons of convenience of calculation. Furthermore, the value of h does not affect the relationship between E_{d_i} and δ_{max_i} for inelastic behaviour. As shown in Fig. 6.4.7, when h becomes larger, both E_{d_i} and δ_{max_i} become smaller and the relationship between E_{d_i} and δ_{max_i} remains essentially unchanged. Accordingly, regardless of the value of h, C can be assumed to vary from 2 to 4. As can be seen, δ_{max_i} is not sensitive to h, compared with the effects of the uncertainty of maximum ground acceleration. Therefore, the use here of the commonly used value h = 0.05 is justified.

With a view to further simplification, let us consider whether the ratio of post yield stiffness to initial stiffness can be assumed to be zero for predicting δ_{max_i} by an inelastic dynamic analysis using bi-linear hysteresis. This assumption affects the following three items:

1. Total damage energy input E_{d_T};

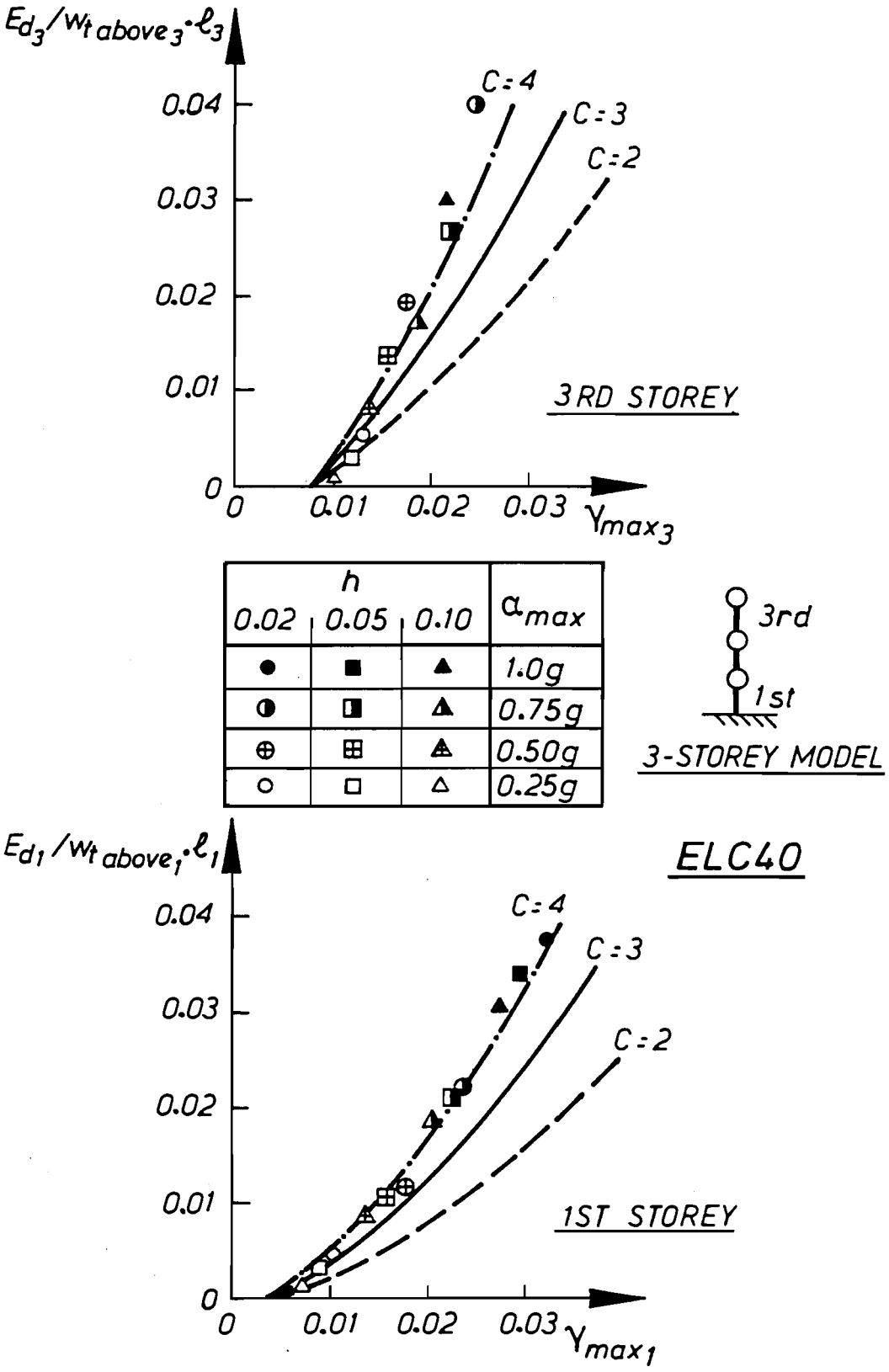

Fig. 6.4.7 Effect of critical damping ratio to the relationship between maximum deflection angle and non-dimensional damage energy

2. Resistant damage energy for the ith storey E_{R_i};

3. Constant C.

When the value of α_i is equal to zero for all storeys, the damage energy E_{d_T} is always smaller than that for positive values of α_i as shown in Figs 6.3.5-6.3.7. The energy E_{d_T} with $\alpha_i = 0$ can be easily calculated from Eq. (6.3.22) using a S.D.O.F. analysis with $\alpha = 0$. The calculation of E_{R_i} becomes simpler than that for a positive α_i and Eqs (6.4.3) and (6.4.4) can be converted into:

$$2 \cdot C \cdot E_{e_i} (\mu_i - 1) - E_{d_T} \cdot \frac{e^{E_{d_i}}}{e^{E_{d_T}}} = 0 \qquad (6.4.6)$$

$$\delta_{max_i} = \mu_i \cdot \delta_{y_i} \qquad (6.4.7)$$

where:

$$\mu_i = \frac{E_{d_T}}{2 \cdot C \cdot E_{e_i}} \cdot \frac{e^{E_{d_i}}}{e^{E_{d_T}}} + 1$$

It should be noted that, by assuming α is zero, the total damage energy E_{d_T} and resistant energy E_{R_i} decrease. This broad tendency implies that the appropriate value of C will not be changed very much, compared with its value for positive values of α. The comparison of δ_{max_i} obtained by Eq. (6.4.7) with that from an inelastic dynamic analysis assuming that α=0 is shown in Fig. 6.4.8, corresponding to Fig. 6.4.6. As expected, δ_{max_i} predicted by Eq. (6.4.7) is similar to that obtained from Eq. (6.4.4) in Fig. 6.4.6 and C can be also assumed to be 3 for this prediction. Therefore, in order to predict δ_{max_i} by an inelastic

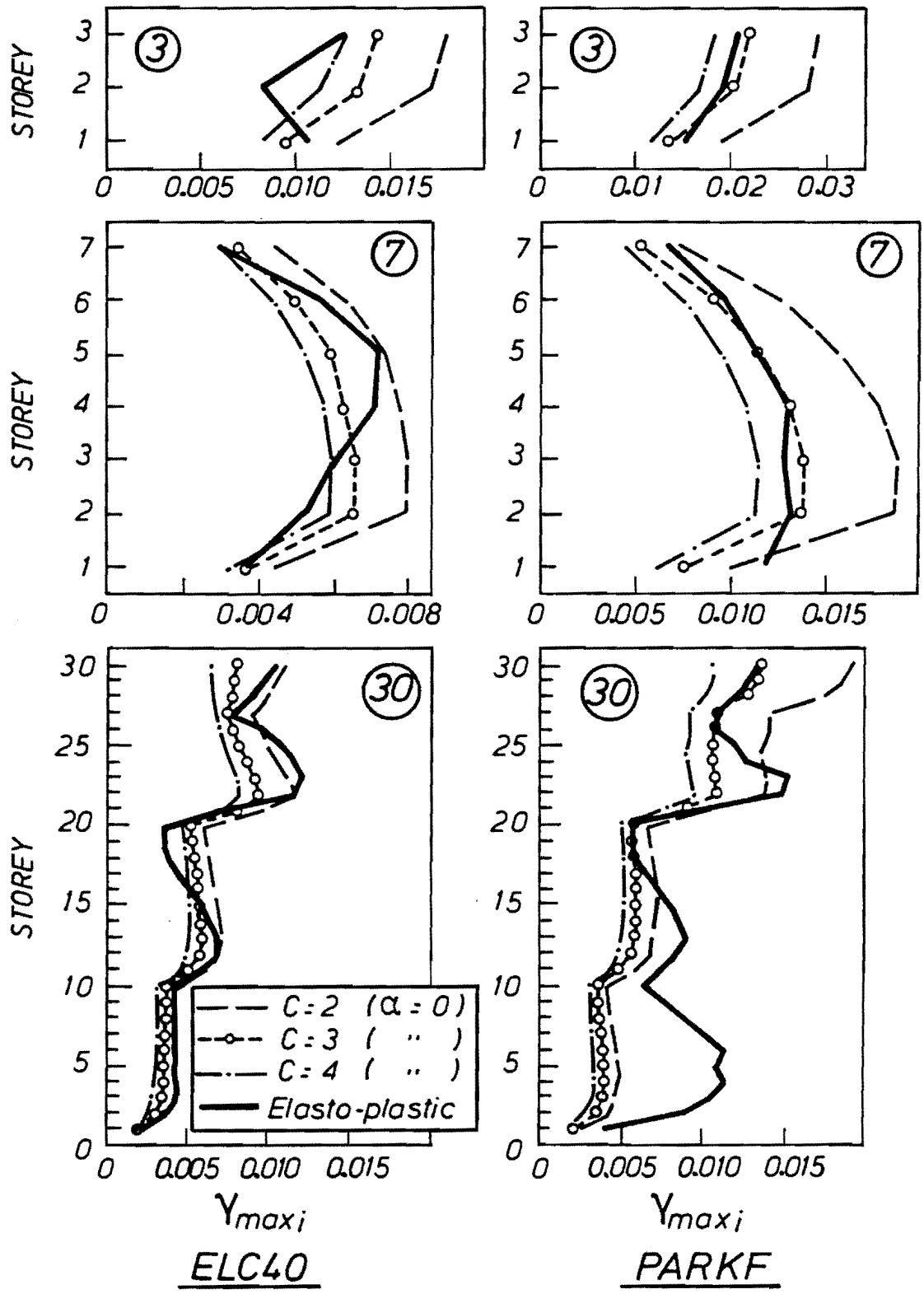

Fig. 6.4.8 Prediction of maximum storey deflection angle (α=0)

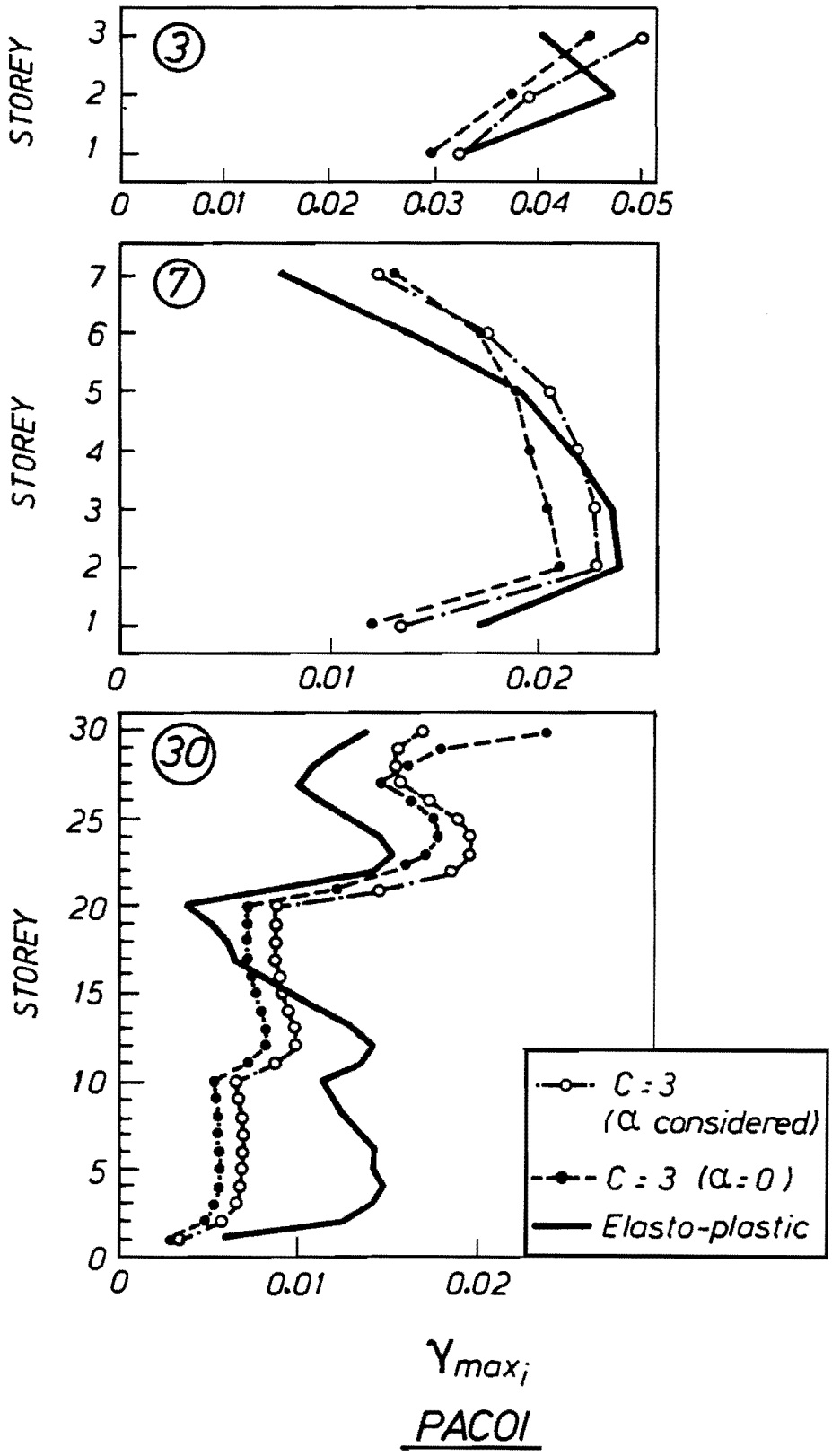

Fig. 6.4.9 Prediction of maximum storey deflection angle (α=0)

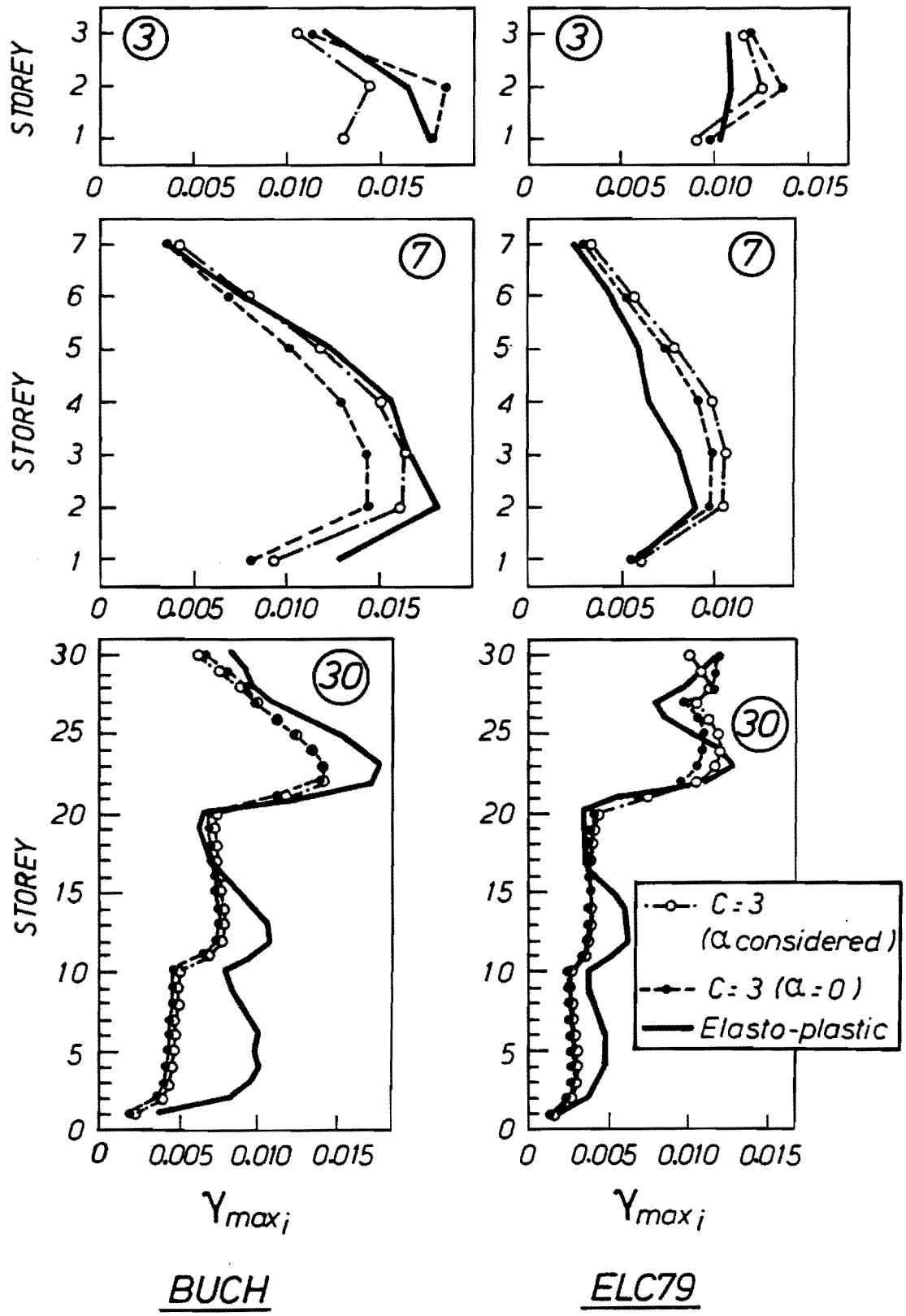

Fig. 6.4.10 Prediction of maximum storey deflection angle (α=0)

dynamic analysis for a M.D.O.F. system, Eq. (6.4.7) based on cumulative plastic strain energy and elasto-fully-plastic hysteresis can be used.

To confirm the applicability of Eq. (6.4.7) using other earthquake motions such as Pacoima Dam 1971 S14W, Bucharest 1977 NS and El Centro 1979 NS, values of γ_{max_i} for the 3, 7 and 30-storey frames were calculated to compare with their tangent values as well as those computed by Eq. (6.4.4). The results are shown in Figs. 6.4.9 and 6.4.10. In all numerical results, values of γ_{max_i} from Eq. (6.4.4) and Eq. (6.4.7) were quite similar. The results from the proposed prediction equations were not greatly different from the tangent results. Therefore, it can be said that Eq. (6.4.7) gives a good prediction of δ_{max_i} and considering the simplicity and uncertainty of earthquake prediction, the results obtained by Eq. (6.4.7) are satisfactory.

The frame models used here were designed according to current New Zealand codes and the storey stiffness and yield shear strength almost always reduces gradually from the 1st storey to the top (Table A.1). As an example of a case they do not reduces gradually, a base isolated frame was considered, and the proposed method of prediction for δ_{max_i} was applied. The base isolated frame is the 7 storey model given in Appendix A with base isolation. It is expected that energy will be concentrated into the base isolation devices, unlike the frames designed according to the codes. The prediction results of δ_{max_i} using two earthquake records are shown in Fig. 6.4.11, as well as δ_{max_i} by an

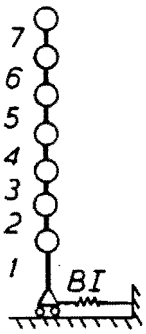

Storey	w_t (kN)	k (kN/mm)	α	V_y (kN)	C_{di}
7	243	12.7	0.217	67.5	0.277
6	292	15.1	0.197	126	0.234
5	"	15.8	0.178	174	0.210
4	"	16.1	0.179	212	0.189
3	"	17.3	0.193	241	0.171
2	"	19.4	0.197	260	0.152
1	"	37.1	0.165	270	0.135
B.I.	578	13.0	0.155	129	0.050

B.I.-Base Isolation

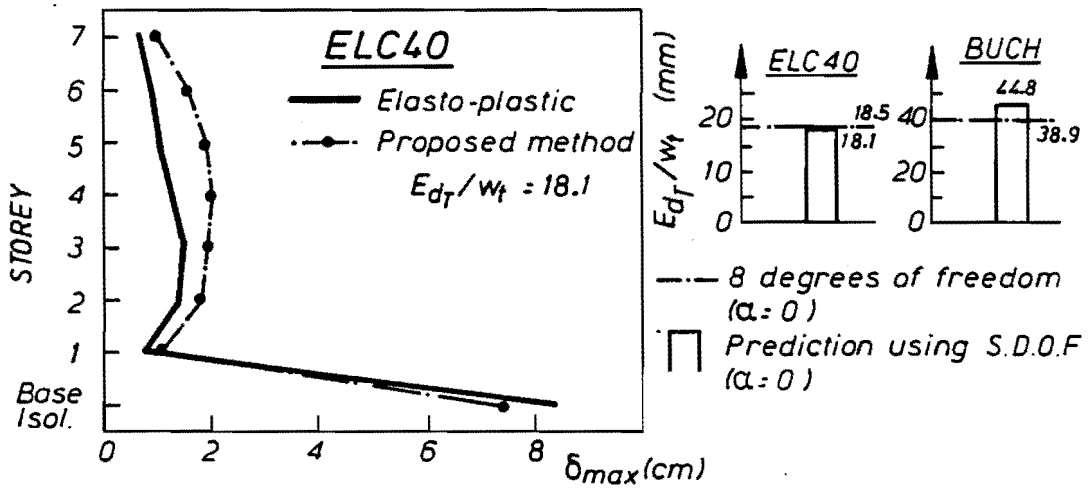

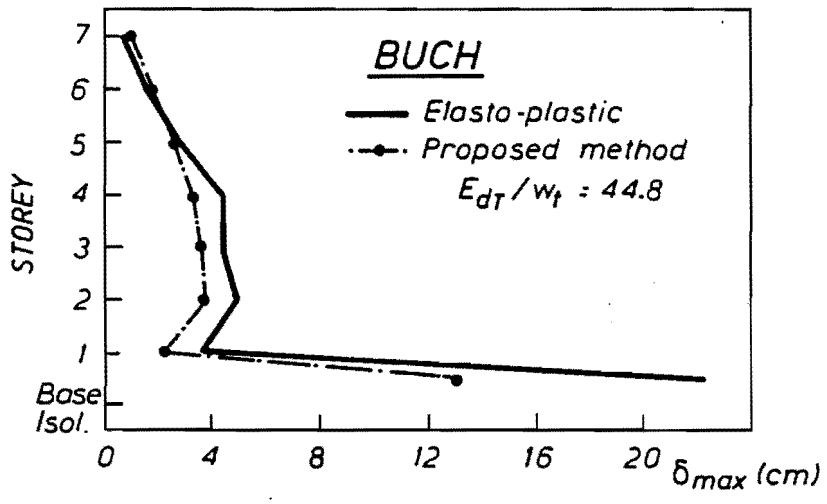

Fig. 6.4.11 Prediction of maximum inelastic storey drift (α=0)

inelastic dynamic analysis. The results using Eq. (6.4.7) were quite close to those computed by inelastic dynamic analysis. Therefore, the proposed prediction method can also be applied to energy concentrated frame types, provided that the spring mass model is an appropriate model for this type of structure (see 6.5).

A justification of the proposed approach for predicting δ_{max_i} will be discussed further in Section 6.5.

In conclusion, Eq. (6.4.7) based on cumulative plastic strain energy with C=3 is considered to be an acceptable approximation for predicting maximum inelastic storey drifts for M.D.O.F. systems.

6.4.3 Failure Criterion in Terms of Cumulative Plastic Strain Energy

The basic failure criterion in terms of maximum storey drift was defined in Section 5.3 and 5.4. The structure was deemed to have failed if the deflection angle (=maximum inter-storey drift divided by the storey height) in any storey exceeded 1/50. An equivalent failure criterion in terms of energy can be defined and calibrated against the basic failure criterion, making use of results in the previous subsection.

The resistant damage energy E_{R_i} for ith storey is given from Eq. (6.4.1) taking the post yield as zero and the value of the constant C as 3, by:

$$E_{R_i} = 6E_{e_i}(\mu_i - 1) \tag{6.4.8}$$

The ultimate ductility factor μ_{u_i} at which the storey deflection angle of the ith storey reaches 1/50 is expressed by:

$$\mu_{u_i} = \frac{l_i}{50 \cdot \delta_{y_i}} \tag{6.4.9}$$

where: l_i = height of the ith storey

Therefore from Eqs (6.4.2), (6.4.8) and (6.4.9), the failure criterion in terms of the damage energy becomes:

$$E_{d_i} > 6E_{e_i}\left(\frac{l_i}{50 \cdot \delta_{y_i}} - 1\right)$$

$$= \eta_{R_i} \cdot E_{e_i} \tag{6.4.10}$$

where: $\eta_{R_i} = 6\left(\frac{l_i}{50 \cdot \delta_{y_i}} - 1\right)$

The factor η_{R_i} which may be called dimensionless resistant energy capacity, is the ratio of the damage energy at collapse to maximum elastic strain energy (see Fig. 5.5.2(4)) for the ith storey. It can be called the dimensionless failure energy. From Eqs (6.4.6) and (6.4.10), a performance function used in predicting the failure probability of structures in Chapter 7 can be written as:

$$g_i = \eta_{R_i} - \eta_{I_i} \cdot \frac{e^{E_{d_i}}}{e^{E_{d_T}}} \qquad (6.4.11)$$

in which:

$$\eta_{I_i} = \frac{E_{d_T}}{E_{e_i}}$$

g_i = performance function of the ith storey ($g_i < 0$ means failure).

The term η_{I_i} which may be called dimensionless damage energy input, is a factor by which the maximum ith storey elastic strain energy E_{e_i} would have to be multiplied by to equal the total damage energy E_{d_T}.

6.4.4 Summary of the Proposed Method for Predicting Maximum Inelastic Storey Drifts

A simple prediction method for maximum inelastic storey drifts has been proposed in terms of cumulative plastic strain energy, which is now summarised.

A fundamental relation equating the resistant and input damage energy for the ith storey is expressed by:

$$E_{R_i} - E_{d_i} = 0 \qquad (6.4.2)$$

where:

$$E_{R_i} = 6E_{e_i}(\mu_i - 1) \qquad (6.4.12)$$

$$E_{e_i} = \tfrac{1}{2} V_{y_i} \cdot \delta_{y_i} \quad \text{(maximum elastic strain energy)}$$

$$\mu_i = \delta_{max_i} / \delta_{y_i} \qquad \text{(ductility factor)}$$

$$E_{d_i} = E_{d_T} \cdot R_i \tag{6.4.13}$$

E_{d_T} = total damage energy input

$R_i = \frac{e E_{d_i}}{e E_{d_T}}$ = ratio of damage energy absorbed by the ith storey to that for the entire structure

From the fundamental equation, the maximum inelastic storey drift δ_{max_i} is calculated by:

$$\delta_{max_i} = \mu_i \cdot \delta_{y_i} \tag{6.4.7}$$

where:

$$\mu_i = \frac{E_{d_T}}{6 E_{e_i}} \cdot R_i + 1 \tag{6.4.14}$$

In computing Eq. (6.4.14) calculation of the two items E_{d_T} and $e E_{d_i} / e E_{d_T}$ is required. They can be estimated as follows:

(i) E_{d_T} - the total damage energy (cumulative plastic strain energy) for the entire structure is given by:

$$\frac{E_{d_T}}{w_t} = \sum_{j=1}^{n_M} \left(\frac{s E_{d_j}}{g} \times \frac{ef. M_j}{M_T} \right) \tag{6.4.15}$$

where: n_M = number of modes considered

$_sE_{d_j}$ = cumulative plastic strain energy due to an earthquake for a single degree of freedom system with unit mass with stiffness corresponding to the jth mode and with the same base shear coefficient as the multi-degree of freedom system.

$_{ef.}M_j$ = effective mass for the jth mode, i.e.

$$_{ef.}M_j = \frac{(\{U_j\}^T[M]\{1\})^2}{\{U_j\}^T [M] \{U_j\}} \tag{6.3.20}$$

Thus in calculating E_{d_T}, an inelastic dynamic analysis of a single-degree-of-freedom system for each mode of the multi-degree-of-freedom systems considered is required, together with an elastic modal analysis of the multi-degree-of-freedom system.

(ii) R_i - the ratio R_i of damage energy absorbed by the ith storey to that by an entire structure is obtained by:

$$R_i = \frac{e^{E_{d_i}}}{e^{E_{d_T}}} \tag{6.3.42}$$

where:

$$e^{E_{d_i}} = \Omega_{\delta_i} \cdot k_i \cdot \sigma_{\delta_i}^2 \cdot \exp(-\delta_{y_i}^2/2\sigma_{\delta_i}^2) \tag{6.3.43}$$

$$e^{E_{d_T}} = \sum_{i=1}^{n} e^{E_{d_i}} \tag{6.3.44}$$

n = number of stages

$$\sigma_{\delta_i}^2 = \lambda_{0,\delta_i} \tag{6.4.16}$$

$$\Omega_{\delta_i} = \sqrt{\lambda_{2,\delta_i}/\lambda_{0,\delta_i}} \tag{6.4.17}$$

λ_{j,δ_i} = jth moment of the response spectral density function on the storey drift δ_i

$$\lambda_{j,\delta_i} = \int_0^\infty \omega^j \cdot G_{\delta_i}(\omega)\, d\omega \tag{6.3.31}$$

Therefore it is necessary to carry out a frequency domain (elastic) analysis with a multi-degree-of-freedom system to estimate the ratio R_i.

From Eqs (6.4.2), (6.4.12) and (6.4.13) as well as the definition of collapse discussed in sections 5.3 and 5.4, the performance function used in estimating failure probability of structures is written as:

$$g_i = \eta_{R_i} - \eta_{I_i} \cdot R_i \tag{6.4.11}$$

where:

$$\eta_{R_i} = 6\left(\frac{l_i}{50 \cdot \delta_{y_i}} - 1\right)$$

l_i = height of the ith storey

$$\eta_{I_i} = \frac{E_{d_T}}{E_{e_i}}$$

(g_i < 0 means failure)

6.5 MODEL CHECK

A new method for predicting the maximum inelastic storey drifts of M.D.O.F. systems has been developed in terms of cumulative plastic strain energy. In order to justify the proposed method, further numerical studies are carried out in this section. Major problems concerning the accuracy of the method are as follows:

1. The accuracy of results obtained by a dynamic analysis with a spring-mass model compared with those by a more sophisticated analysis.

2. The accuracy of the proposed method in calculating probabilities of failure of more realistic buildings.

Because five different earthquake records were used in the numerical analyses in the previous two chapters, an examination of the applicability to other earthquake motions is not considered necessary. In the present section, El Centro 1940 NS record alone is used as an input earthquake for the numerical studies.

The first problem is concerned with a spring mass model used in an inelastic dynamic analysis. An inherent problem in the use of a spring mass model is now discussed. The

spring-mass model consists of storey springs and masses. Because of its simplicity, the model is often used in practice in dynamic analyses. However, also because of its simplicity, the results are not always the same as those obtained by a more complex and perhaps more reliable dynamic analysis. The most serious disadvantage in the use of a spring-mass model is probably that the model cannot represent the so-called coupling effect between storeys. This effect is generally observed in structural behaviour where plastic hinges develop in beams rather than in columns (84). This means the model is believed to give good approximations for structures which are expected to be dominated by column hinges. Umemura (84) warned that one should be careful in estimating a result using a spring-mass model for a structure most of whose earthquake energy is absorbed in beams and for which one storey has a very low storey shear capacity compared with the others. Buildings designed according to New Zealand codes (49,50) are expected to develop beam hinges, but they would rarely have a single weak storey. A spring-mass model might be applied to buildings in New Zealand. However, because response coupling between storeys is likely to occur, the accuracy of the spring-mass model should be examined.

In practice the problem of the coupling effect arises in estimating storey characteristics. As explained in Appendix A, storey characteristics for a spring-mass model such as initial stiffness, yield shear strength and so on must be estimated by assuming a horizontal load distribution over the height when using a static inelastic frame analysis.

Without assuming such a load distribution, the characteristics for each storey cannot be obtained independently because they are coupled between storeys. The assumption of a load distribution affects a subsequent failure mode. Thus, it may also determine a failure mode. It is not rational that a failure mode should first be determined in order to get the structural characteristics required for an analysis. In the present study, the commonly used inverted triangular lateral force distribution was adopted. The assumption may lead to errors, which must therefore be examined compared with responses by a more complicated dynamic analysis.

The storey characteristics for spring-mass models used here so far were obtained by static inelastic frame analysis. However, it is not reasonable to use such a time consuming analysis for obtaining storey characteristics if they are to be employed in a simple method for predicting failure probability. Therefore it can be significant to find a simpler way to obtain the characteristics of structures of a spring-mass model. A straightforward way to obtain them for frame structures is explained in Appendix A. The appropriateness of a spring-mass model with the characteristics calculated by the simple way should also be examined.

For this purpose, maximum storey drifts computed by 3 different models will be compared in the present section. The models are:

1. a two-dimensional whole frame model;
2. a spring-mass model with characteristics obtained by a static inelastic analysis (spring mass model A); and
3. a spring mass model with characteristics obtained by the simple method (spring mass mode B).

The second problem is concerned with the accuracy of the proposed method for predicting interstorey drift and whether the technique is applicable to many different types of buildings. It is not very clear how many different buildings need to be analysed to conform the method. The 3, 7 and 30-storey models used in the previous two sections are simple and to some extent unreal buildings. It would seem sensible to apply the proposed method to a more realistic building. Thus, an existing building was used as a sample structure. The building chosen was "Clarendon Towers", a 19-storey reinforced concrete frame building designed to New Zealand codes.

Comparison of results between a whole frame model and spring-mass models for Clarendon Towers is made first. The exercise also demonstrates the approach to predicting maximum inelastic storey drift summarised in Section 6.4.4. Subsequently, results with those obtained for 3, 7 and 30-storey frames described in Appendix A are compared.

6.5.1 Analytic Models and Results for Clarendon Towers

Clarendon Towers is in central Christchurch. The building

is under construction at the time of writing with an estimated completion date of September 1988. Details of the building are shown in Appendix D. Typical plan dimensions are 37.0 m x 24.0 m and a typical floor to floor height is 3.4 m. It has a basic requirement to retain the facade of the old Clarendon Hotel over the lower 3 storeys of the building. The upper 3 storeys are set back to form a tower. The structural system is such that lateral loads are resisted by peripheral frames only, whereas gravity loads are also sustained by internal beams and columns. No structural walls exist even around the core. In order to avoid the difficult placing of cast in situ concrete in the congested beam-column joint core region, precast beams which include the joint region are used. Columns are cast in situ.

The frames of the building running parallel to the X direction shown in Fig. D.2 were chosen for analysis. Because of the axis symmetry for the lien F, frames A and D only are taken into account. Since irregularity exists in the 1st storey and above the 17th storey, only the frames between the 2nd and 16th storeys are taken into consideration. Such a simplification is acceptable given that the purpose of choosing a realistic frame is to check the proposed prediction approach for δ_{max_i}. Frames of the analytic models are shown in Figs D.4 and D.5. As in any frame, plastic hinges are expected to occur at the bottom of the 1st storey columns. Since the section details of the 1st and 2nd storey columns are identical, no changes to the details of the 2nd storey columns are made by not including

the 1st storey in the analytic model.

As a relatively complicated analytical method, the computer program "Ruaumoko" (85) was used. This is a two dimensional non-linear time-history analysis program for framed structures. Because of the two dimensional limitation of the program, 3 dimensional analysis could not be carried out directly. Hence as a pseudo-3-dimensional model, the two frames A and D are set in parallel, and the lateral displacements of all nodes at a same floor level are assumed to be equal. The assumption is equivalent to assuming that the transverse stiffness of each floor slab is infinitely large. The other modelling assumptions are as follows:

1. A beam element was used for each beam and column member.

2. The mass was assumed to be uniformly distributed in an element, and a consistent mass matrix was used.

3. Bi-linear hysteresis was chosen as a hysteresis rule for each element with post yield stiffness factors of 0.1 for columns and 0.08 for beams.

4. Dimensions and material properties were the same as the design values.

5. Rayleigh damping was applied for the 1st and 8th modes with a critical damping ratio of 5%.

6. For the time history analysis, an integration time step of 1/100 (sec) was used.

7. A length of rigid end block equal to one half of the depth of the adjacent members at both ends of each element was assumed.

The maximum storey deflection angles γ_{max_i} obtained by Ruaumoko are shown in Fig. 6.5.1(1). The maximum value of γ_{max_i} occurred in the 9th storey: the value was 3.83 x 10^{-3} (rad). Time histories of total lateral displacement at the top and 9th storey drift are shown in Fig. 6.5.2. The central processing unit (CPU) time for the computation was about 7 hours using the Burroughs B6900 mainframe computer at the University of Canterbury.

As discussed earlier, two spring-mass models were considered. The storey characteristics, k_i and V_{y_i}, of spring-mass models A and B corresponding to the frame A are shown in Table D.1 for Appendix D. The static analysis gave the characteristics for spring-mass model A, while they were formed by the straight forward method described in Appendix A for spring mass model B. Because a storey mass was determined such that lateral displacements of all frames at the same floor level are identical (the same assumption was used for Ruaumoko), it is sufficient to analyse only a single frame (frame A) for estimating δ_{max_i} for any one building direction. The details of evaluating the storey mass are given in Appendix D. Using spring-mass model A,

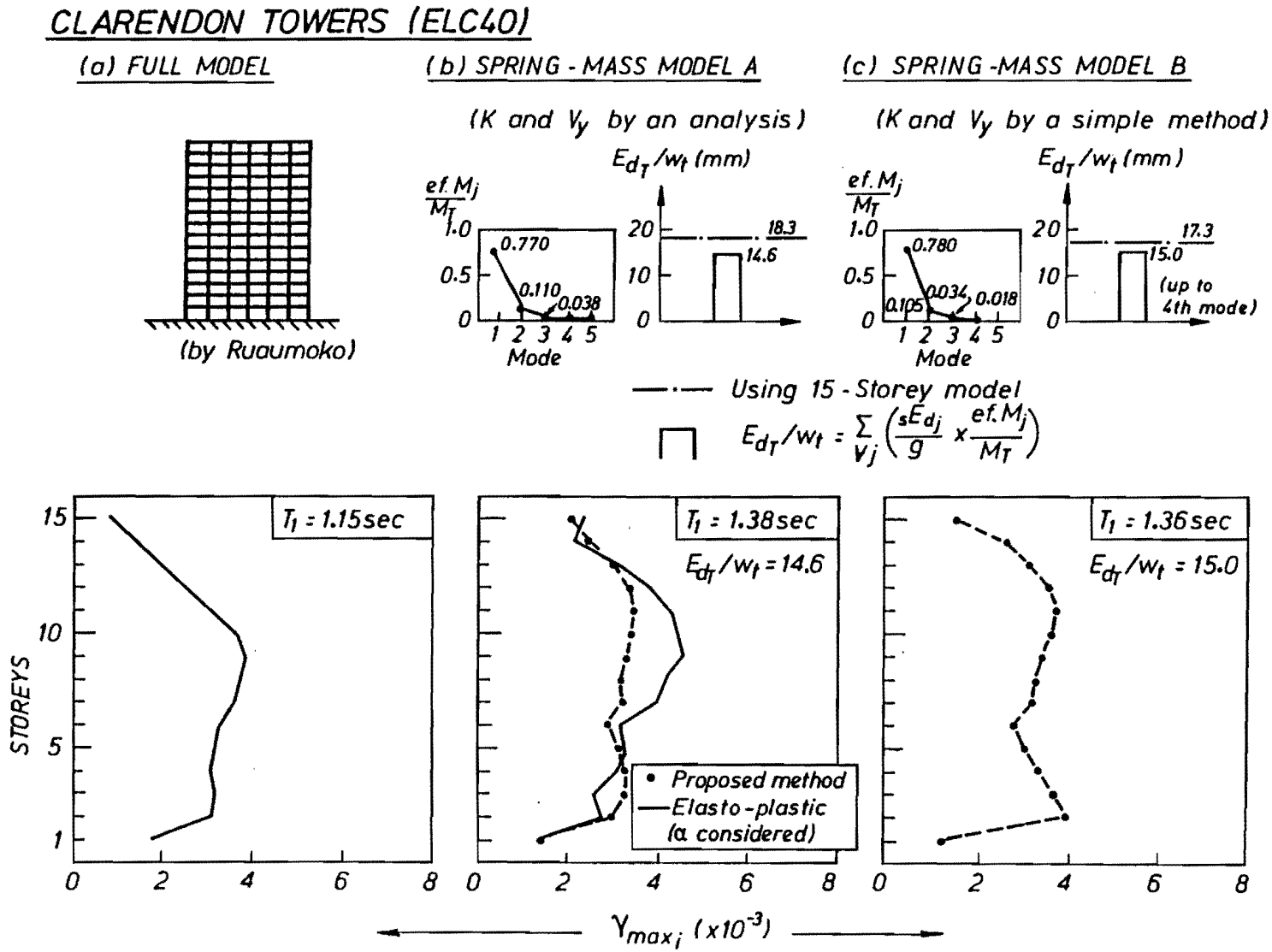

Fig. 6.5.1 Comparison of maximum storey deflection angles for three different models

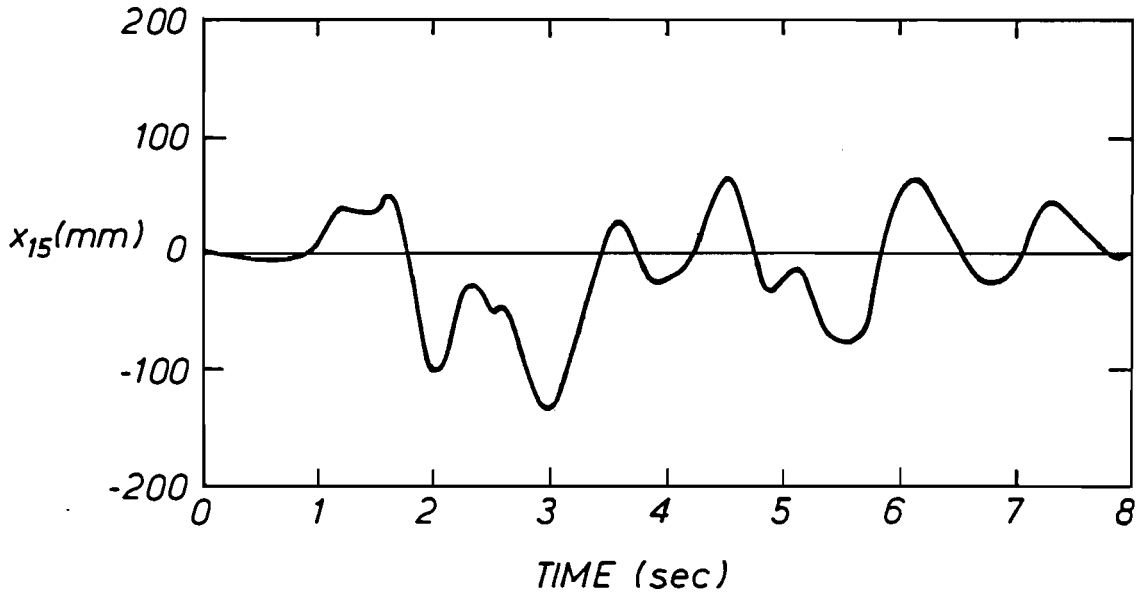

(a) Total Lateral Displacement at the Top

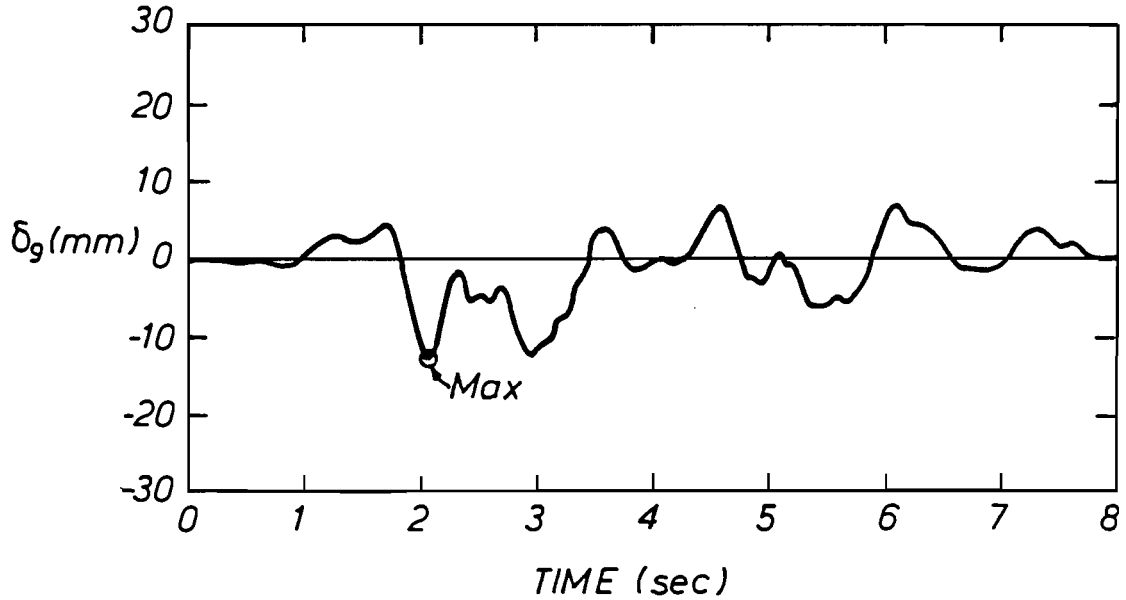

(b) Storey Drift of the 9th Storey

Clarendon Towers (Ruaumoko, ELC40)

Fig. 6.5.2 Time history results for Clarendon Towers

two analyses were carried out. The first was an inelastic time history analysis whose results can be regarded as target results as discussed in the previous section. The second used the proposed prediction approach. The maximum storey deflection angles γ_{max_i} are shown in Fig. 6.5.1(2).

For the spring-mass model B, the proposed prediction method for δ_{max_i} summarised in section 6.4.4 was used. The details of applying the method to the spring-mass model are given in Tables 6.5.1 and 6.5.2, and Fig. 6.5.3. In Table 6.5.1, using the mode shapes obtained by a modal analysis, the effective mass ratios in Eq. (6.3.20) for the first four modes were calculated. That is, the value of n_M in Eq. (6.4.15) was chosen as 4. Up to the fourth mode, about 94% of the total mass is involved. To calculate ${}_sE_{d_j}$ in Eq. (6.4.15), inelastic time history analyses with S.D.O.F. systems were carried out for 0.1 sec intervals of period T (see Fig. 6.5.3(1)). The S.D.O.F. systems have a unit mass and the same base shear coefficient as that of spring mass model B (C_d = 0.089). In estimating ${}_sE_{d_j}/g$, the corresponding values of ${}_sE_d/g$ in Fig. 6.5.3(1) were interpolated. Instead of doing so, of course, one could directly calculate the 4 values of ${}_sE_{d_j}/g$ (j = 1 - 4) using the S.D.O.F. systems for the corresponding modes. The total damage energy input E_{d_T} was then obtained by Eq. (6.4.15) (see Fig. 6.5.3(2)). Table 6.5.2 shows the results of Ω_{δ_i} and $\sigma^2_{\delta_i}$ using a random vibration approach and the calculation of δ_{max_i} from Eqs (6.4.7), (6.4.14), (6.3.43) and (6.3.44). The results are illustrated in Fig. 6.5.1(3) in terms of γ_{max_i}. The maximum of γ_{max_i} was 3.88×10^{-3}

Table 6.5.1 Calculation of effective mass ratios

	(1) Mode Shape				m_i	1st Mode		2nd Mode		3rd Mode		4th Mode	
	$U_{1,i}$	$U_{2,i}$	$U_{3,i}$	$U_{4,i}$	$(\frac{kN \cdot sec^2}{m})$	$U_{1,i} \cdot m_i$	$U_{1,i}^2 \cdot m_i$	$U_{2,i} \cdot m_i$	$U_{2,i}^2 \cdot m_i$	$U_{3,i} \cdot m_i$	$U_{3,i}^2 \cdot m_i$	$U_{4,i} \cdot m_i$	$U_{4,i}^2 \cdot m_i$
15	28.2	-8.91	5.88	-3.89	280	7896	222667	-2495	22229	1646	9681	-1089	4237
14	27.9	-7.99	4.23	-1.76	"	7812	217955	-2237	17875	1184	5010	- 493	867
13	27.2	-6.25	1.40	1.34	282	7670	208635	-1763	11016	395	553	378	506
12	26.2	-3.87	-1.82	3.68	"	7388	193576	-1091	4223	- 513	934	1038	3819
11	24.8	-1.09	-4.53	4.00	"	6994	173441	- 307	335	-1277	5787	1128	4512
10	23.1	1.80	-5.96	2.12	"	6514	150478	508	914	-1681	10017	598	1267
9	21.1	4.50	-5.72	-0.929	"	5950	125549	1269	5711	-1613	9227	- 262	243
8	19.0	6.74	-3.87	-3.47	"	5358	101802	1901	12811	-1091	4223	- 979	3396
7	16.5	8.29	-0.928	-4.10	"	4653	76775	2338	19380	- 262	243	-1156	4740
6	13.9	8.98	2.27	-2.48	300	4170	57963	2694	24192	681	1546	- 744	1845
5	11.5	8.73	4.38	0.094	"	3450	39675	2619	22864	1314	5755	28	3
4	8.99	7.68	5.40	2.62	"	2697	24246	2304	17695	1620	8748	786	2059
3	6.39	5.93	5.06	3.86	"	1917	12250	1779	10549	1518	7681	1158	4470
2	3.71	3.63	3.47	3.22	"	1113	4129	1089	3953	1041	3612	966	3111
1	1.0	1.0	1.0	1.0	312	312	312	312	312	312	312	312	312
				Σ	4346	73894	1609453	8920	174059	3274	73329	1669	35387
				(2) $ef.M_j = \frac{(U_{j,i} \cdot m_i)^2}{U_{j,i}^2 \cdot m_i}$		3392		456		146		79	
				(3) $\frac{ef.M_j}{M_T}$		0.780		0.105		0.034		0.018	

(1) Calculated by a modal analysis (Appendix C)

(2) $ef.M_J = \frac{(\{U_j\}^T[M]\{1\})^2}{\{U_j\}^T[M]\{U_j\}}$

(3) $M_T = \sum_i m_i$

Σ 0.937

(1) Calculation of $_sE_d/g$

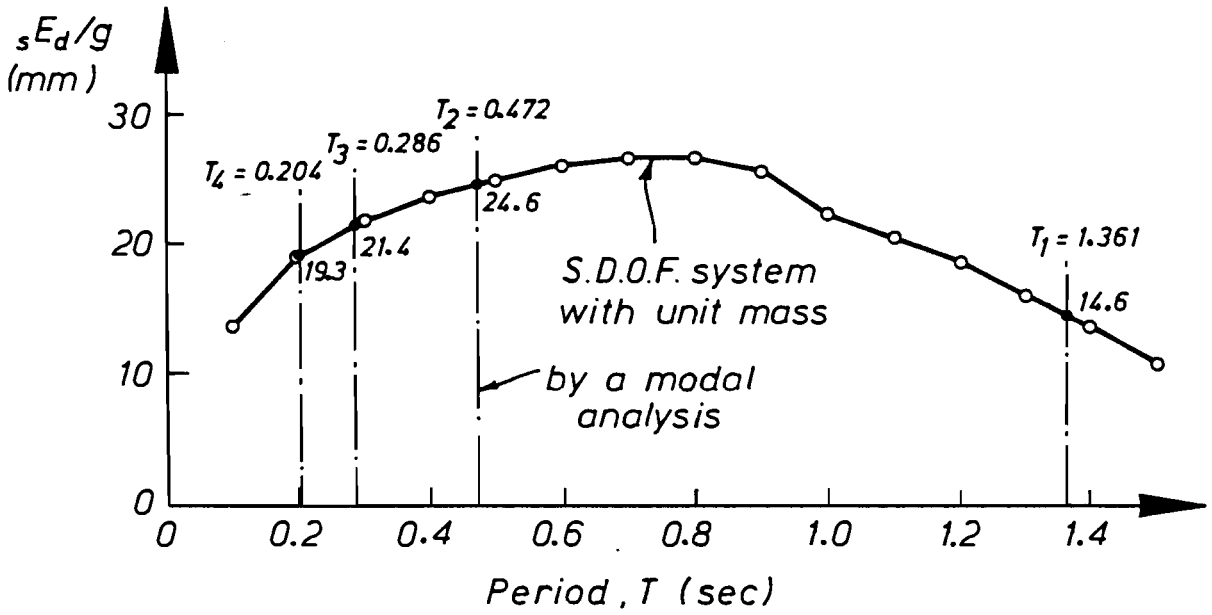

CLARENDON TOWERS (Frame A, Spring-mass model B)
ELC40, $h = 0.05$, $C_d = 0.089$

(2) Calculation of E_{d_T}

Mode	$_sE_{d_j}/g$ (mm)	$\frac{\text{ef.}M_j}{M_T}$	(1) x (2)
1	14.6	0.780	11.4
2	24.6	0.105	2.6
3	21.4	0.034	0.7
4	19.3	0.018	0.3
		E_{d_T}/w_t =	15.0 (mm)

$E_{d_T} = 15.0 \times 4346 \times 9.81 = \underline{639500\ (kN \cdot mm)}$

$$\left(\sum_{j=1}^{15} \left(\frac{_sE_{d_j}}{g} \times \frac{\text{ef.}M_j}{M_T} \right) = 15.9\ (mm) \right)$$

Fig. 6.5.3 Calculation of total damage energy

Table 6.5.2 Calculation of maximum inelastic storey drift

Storey	(1) Ω_δ (1/sec)	(1) σ_δ^2 (mm^2)	(2) k (kN/mm)	(2) V_y (kN)	(2) δ_y (mm)	(3) E_{e_i} (kN·mm)	(4) ${}_eE_{d_i}$ (kN·mm/sec)	(4) ${}_eE_{d_i} / \Sigma {}_eE_{d_i}$	(5) E_{d_T} (kN·mm)	(6) μ_i	(7) δ_{max_i} (mm)	(8) E_{d_T} (kN·mm)	(7) δ_{max_i} (mm)
15	13.7	1.61	483	474	0.981	232	7900	0.00906		5.16	5.06		4.05
14	12.1	5.80	"	916	1.90	870	24800	0.0284		4.48	8.51		6.93
13	10.7	11.3	485	1330	2.74	1820	42100	0.0483		3.83	10.5		8.59
12	9.91	17.2	"	1710	3.53	3020	57500	0.0659		3.33	11.7		9.80
11	9.30	22.6	"	2050	4.23	4340	68600	0.0787		2.93	12.4		10.1
10	8.45	26.8	"	2370	4.89	5790	70300	0.0806		2.48	12.1		10.4
9	7.42	30.0	"	2660	5.48	7290	65400	0.0750	639500	2.10	11.5	486000	10.1
8	6.45	32.8	"	2910	6.00	8730	59300	0.0680		1.83	11.0		9.79
7	5.72	35.9	"	3130	6.45	10090	55800	0.0640		1.68	10.8	(1st	9.77
6	5.56	28.1	579	3320	5.73	9510	50400	0.0578		1.65	9.44		8.56
5	5.89	31.7	"	3480	6.01	10460	61200	0.0702		1.72	10.3	mode	9.28
4	6.29	35.7	"	3610	6.23	11250	75500	0.0866		1.82	11.3		10.1
3	6.66	39.4	"	3700	6.39	11820	90500	0.1038		1.94	12.4	only)	10.9
2	6.98	42.1	"	3770	6.51	12270	102900	0.1180		2.03	13.2		11.6
1	7.11	5.85	1577	3800	2.41	4579	39900	0.0458		2.07	4.98		4.34
							Σ 872100	Σ 1.00					

(1) by Random Vibration method (Appendix C)

(2) See Appendix D ($\delta_y = V_y/k$)

(3) $E_e = 1/2 \cdot V_y \cdot \delta_y$

(4) ${}_eE_{d_i} = \Omega_{\delta_i} \cdot k_i \cdot \sigma_{\delta_i}^2 \cdot \exp\{-\delta_{y_i}^2/2\sigma_{\delta_i}^2\}$

$${}_eE_{d_T} = \sum_i {}_eE_{d_i}$$

(5) $$E_{d_T} = \sum_{j=1}^{4} \left(\frac{{}_sE_{d_j}}{g} \times {}_{ef.}\frac{M_j}{M_T}\right)$$

(6) $$\mu_i = \frac{1}{6\,E_{e_i}} \cdot E_{d_T} \cdot \frac{{}_eE_{d_i}}{{}_eE_{d_T}} + 1$$

(7) $\delta_{max_i} = \mu_i \cdot \delta_{y_i}$

(8) $E_{d_T} = {}_sE_{d_1}/g \times {}_{ef.} M_1/M_T$ (1st Mode Only)

Table 6.5.3(a) Comparison of maximum and mean values of storey deflection angle γ_{max_i} (Clarendon Towers)

Items	(1) Full Model	Spring-mass Models		
		A		B
		(2) Elasto-Plastic	(3) Proposed Method	(4) Proposed Method
Maximum $\max_i(\gamma_{max_i})$	3.83 (9th storey)	4.51 (9th storey)	3.44 (11th storey)	3.88 (2nd storey)
mean value $\overline{\gamma_{max_i}}$	2.79	3.25	2.95	3.03

Unit: $\times 10^{-3}$(rad)

Table 6.5.3(b) Mean and standard deviation of ratios $\gamma_{max_i}(j)/\gamma_{max_i}(1)$ (Clarendon towers)

Items	$\gamma_{max_i}(2)$ / $\gamma_{max_i}(1)$	$\gamma_{max_i}(3)$ / $\gamma_{max_i}(1)$	$\gamma_{max_i}(4)$ / $\gamma_{max_i}(1)$
mean	1.27	1.17	1.16
standard deviation	0.504	0.460	0.345

$\gamma_{max_i}(j)$ = γ_{max_i} calculated by jth model

(1) Full model
(2) Spring-mass model A (Elasto-plastic)
(3) Spring-mass model A (Proposed method)
(4) Spring-mass model B (Proposed method)

rad occurring in the 2nd storey. In order to obtain a comparison with the δ_{max_i} with $n_M = 4$, δ_{max_i} was also calculated in Table 6.5.2 when E_{d_T} was obtained only by the 1st mode ($n_M = 1$). The δ_{max_i} with $n_M = 1$ is about 80-90% of that with $n_M = 4$.

The maximum storey deflection angles γ_{max_i} obtained by the different analyses are compared in Fig. 6.5.1. Table 6.5.3(a) compares the maximum and mean values of γ_{max_i} for different models. The maximum value of γ_{max_i} is important for calculating a failure probability as will be shown by Eq. (7.5.1). The mean value of γ_{max_i} can be considered as a measure of average damage of the whole structure. Both the maximum and mean values are quite similar for the different models. The values calculated by the elasto-plastic time history analysis with the spring-mass model A are most different from those derived with the full model using Ruaumoko. However, the differences are less than 20%. The results obtained by the proposed method with spring-mass models A and B are within a range of about $\pm$10% of those derived by the full Ruaumoko analysis. Since the values of γ_{max_i} using Ruaumoko are considered more accurate, the ratio of γ_{max_i} using a spring-mass model to that obtained from the Ruaumoko analysis should indicate the deviation from the more accurate result. Table 6.5.3(b) shows the mean and standard deviation of these ratios for all storeys. When the mean is close to 1 and the standard deviation is small, the distribution of γ_{max_i} over the height of the building obtained by an analysis using spring-mass models will be similar to that obtained from

Ruaumoko. The mean values for the proposed methods with spring-mass models A and B are 1.17 and 1.16 respectively, and 1.27 for the elasto-plastic analysis. The standard deviation for the spring-mass model B is the smallest, about 0.35, and that for the elasto-plastic analysis the largest, about 0.5. Therefore in general the maximum value of γ_{max_i} and the pattern of its distribution over the height of the building are found to be similar using the different analyses.

6.5.2 Analytic Models and Results for 3, 7 and 30-Storey Frames

A similar comparison to that for Clarendon Towers is made for the 3, 7 and 30-storey models in Appendix A.

The computer program "Ruaumoko" was again used to check the accuracy of the spring-mass models. The modelling assumptions in using the program are all the same for Clarendon Towers except for the following:

1. One frame for each model was taken into account, because the frame was assumed to repeat infinitely with an interval of 6 m.

2. Rayleigh damping was applied for the 1st and 4th modes for the 3 and 7-storey models, with a critical damping ratio of 5% in both cases. For the 30-storey model, the same assumption was applied as for Clarendon Towers.

3. No rigid end blocks were allowed for at the ends of the beam and column elements.

To compare the results from Ruaumoko, three analyses, which are identical with those for Clarendon Towers, were carried out using spring-mass models A and B for each frames. The storey characteristics are shown in Tables A.1 and A.2 in Appendix A. The maximum storey deflection angles γ_{max_i} for the 3, 7 and 30-storey models are plotted in Fig. 6.5.4.

A comparison of the maximum and mean values of γ_{max_i} from the different analyses is given in Table 6.5.4(a). The results from Ruaumoko and the elasto-plastic analyses with spring-mass model A, are generally similar to those derived by the proposed method. The maximum difference between the results from Ruaumoko and the proposed methods is about 40% but most results are closer. Table 6.5.4(b) shows the mean and standard deviation of the ratios of γ_{max_i} obtained by spring-mass models to those given by Ruaumoko. The Table corresponds to Table 6.5.3(b) for Clarendon Towers. The differences of the mean values for the elasto-plastic analysis and the proposed method with spring-mass model B are within about $\pm$20%. The maximum of the mean value is 1.42 for the proposed method with the spring-mass model A. The values of the standard deviation vary from 0.19 to 0.65 and no special tendencies can be observed. Considering the inherent uncertainty in the calculation of values of γ_{max_i}, the differences are not significant.

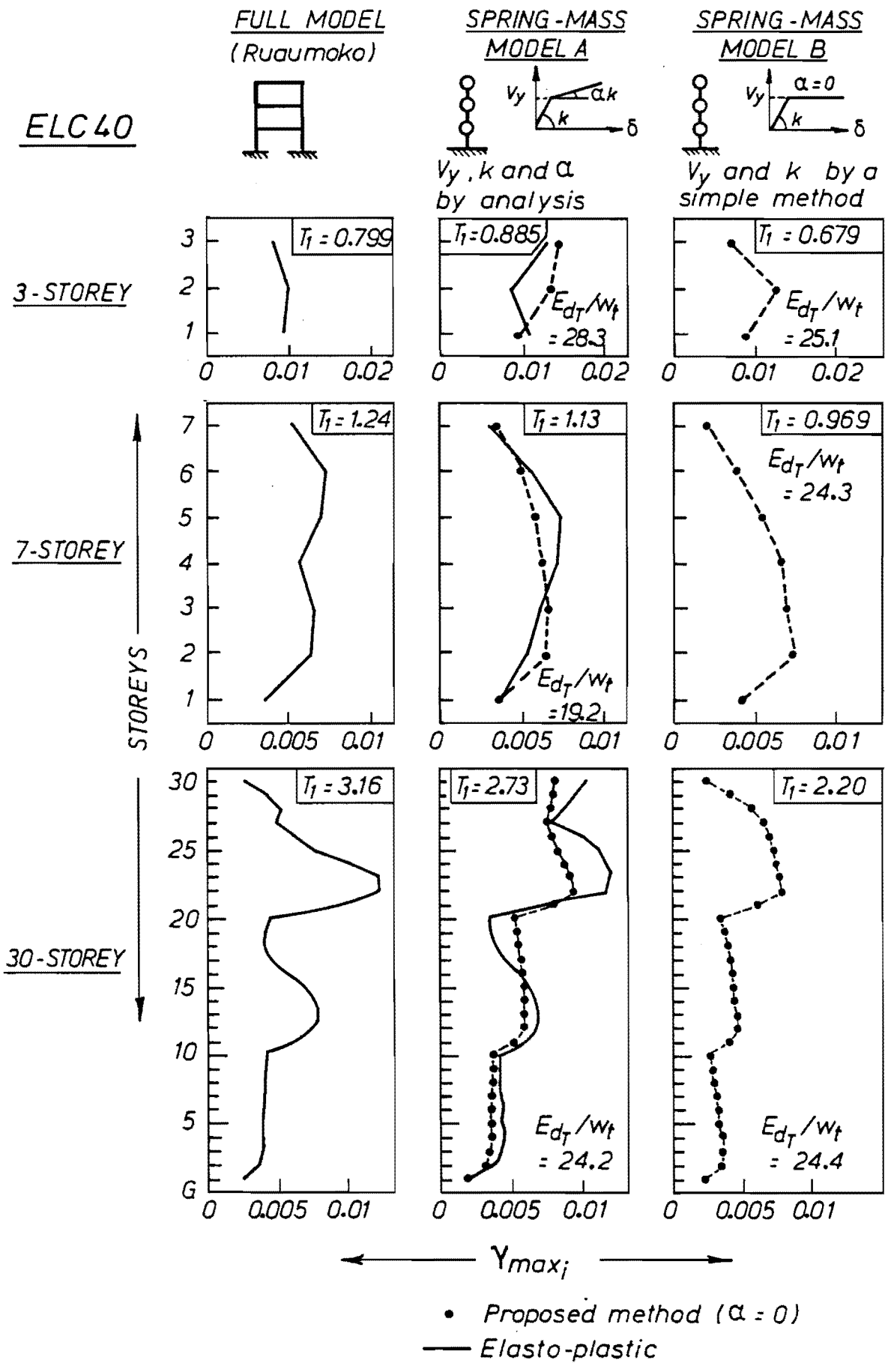

Fig. 6.5.4 Comparison of maximum storey deflection angles for three different models

Table 6.5.4(a) Comparison of maximum and mean values of storey deflection angle γ_{max_i} (3-, 7- and 30- storey frames)

Frames	Items	(1) Full Model	Spring-Mass Models		
			A		B
			(2) Elasto-Plastic	(3) Proposed Method	(4) Proposed Method
3-storey	$\frac{\text{Max}_i(\gamma_{max_i})}{\gamma_{max_i}}$	9.91 (2nd storey) 9.09	12.8 (3rd storey) 10.6	15.1 (3rd storey) 12.7	12.5 (2nd storey) 9.34
7-storey	$\frac{\text{Max}_i(\gamma_{max_i})}{\gamma_{max_i}}$	7.31 (6th storey) 6.00	7.20 (5th storey) 5.40	6.40 (2nd storey) 5.23	7.40 (2nd storey) 5.26
30-storey	$\frac{\text{Max}_i(\gamma_{max_i})}{\gamma_{max_i}}$	12.2 (22nd storey) 5.73	12.2 (23rd storey) 6.50	9.50 (22nd storey) 5.77	7.77 (22nd storey) 4.40

Unit: $\times 10^{-3}$

Table 6.5.4(b) Mean and standard deviation of ratios $\gamma_{max_i}(j)/\gamma_{max_i}(1)$ (3-, 7- and 30- storey frames)

Frames	Items	$\gamma_{max_i}(2)/\gamma_{max_i}(1)$	$\gamma_{max_i}(3)/\gamma_{max_i}(1)$	$\gamma_{max_i}(4)/\gamma_{max_i}(1)$
3-storey	mean	1.19	1.42	1.02
	standard deviation	0.374	0.429	0.215
7-storey	mean	0.909	0.885	0.894
	standard deviation	0.224	0.193	0.327
30-storey	mean	1.21	1.09	0.804
	standard deviation	0.649	0.497	0.186

$\gamma_{max_i}(j)$ = γ_{max_i} calculated by jth model

(1) Full model
(2) Spring-mass model A (Elasto-plastic)
(3) Spring-mass model A (Proposed method)
(4) Spring-mass model B (Proposed method)

In conclusion, the comparison shows that a spring-mass model a reasonably simple and appropriate model for general frame buildings designed to New Zealand code requirements.

6.6 CONCLUSION

One of the major barriers to the practical assessment of failure probability of structures subjected to earthquake has been to establish the performance function required for use in the F.O.S.M. method. A performance function for failure probability assessment must be expressed in terms of the basic demand and structural variables, and must involve a failure criterion. A failure criterion was introduced in terms of maximum storey deflection angle γ_{max}. Thus, for establishing a performance function, γ_{max} must be explicitly formulated in terms of basic variables. However, the inelastic seismic behaviour of structures is so complicated that it is not an easy task.

In order to resolve the problem, an invariant was needed which described the inelastic behaviour of the structure. The three requirements for the invariant were:

1. It must be able to be used in a performance function which can be used in a failure criterion.

2. It must be expressed in terms of the basic demand and structural variables.

3. It must be a function of only a relatively few basic variables, otherwise the F.O.S.M. approach becomes impractical.

Cumulative plastic strain energy was chosen as the appropriate invariant.

In the present chapter, an equation for predicting maximum storey drifts for multi-degree-of-freedom systems subjected to earthquake was established in terms of cumulative plastic strain energy (or simply damage energy). The main features in the development were:

1. Estimation of total damage energy for a multi-degree-of-freedom system, using the energy calculated for a single-degree-of-freedom system.

2. Estimation of the proportion of the total damage energy absorbed by a storey; and

3. Estimation of the maximum storey drift derived from the damage energy absorbed by that storey.

The applicability and usefulness of the proposed equation for predicting maximum storey drifts was examined using numerical studies. Using the proposed equation, a performance function in terms of damage energy was established (Eq. 6.4.11). Thus, the first two requirements for the invariant have been fulfilled.

The next chapter shows the development of a procedure for assessing failure probabilities, making use of the performance function. By eliminating unnecessary complexities, the procedure will be found to be reasonably simple and practical. Therefore, the last requirement to be derived from the introduction of the invariant will also be satisfied.

CHAPTER 7

DEVELOPMENT OF A SIMPLE METHOD FOR ESTIMATING FAILURE PROBABILITY OF MULTI-STOREY BUILDINGS SUBJECTED TO EARTHQUAKE

7.1 INTRODUCTION

In the previous chapter, a relationship was established between input and resistant energy in terms of cumulative plastic strain energy, viz damage energy. The input and resistant energy were explicity formulated using the basic demand and structural variables. A failure criterion was also formulated in terms of damage energy. Thus a performance function is now available to assess failure probabilities of structures subjected to earthquake. The aim of the present chapter is to develop a procedure for the calculation of failure probabilities, making use of the performance function.

The failure probability of a structure subjected to earthquake may be represented as an integral of the product of the following two terms:

1. probability of occurrence of an earthquake with certain characteristics; and

2. probability of failure of the structure considered, given that the earthquake occurs.

For the prediction of earthquake characteristics in practice, return periods expressed in terms of Modified Mercalli intensity are the only data available for seismic probabilistic studies at present. Therefore, earthquake characteristics should be predicted only by using the earthquake intensity scale. Because poor correlations have been observed between various measures of ground motion and the earthquake intensity scale, a large uncertainty must be expected in estimating the probability of occurrence of an earthquake of a certain intensity. The uncertainty is considered to be dominant in the uncertainty of the failure probability of a structure. In the present study a relationship between maximum ground acceleration and Modified Mercalli intensity is used. The probability of occurrence of an earthquake with a certain maximum ground acceleration is taken as a probability mass function corresponding to discrete Modified Mercalli intensities, rather than as a probability density function. Such a simplification is acceptable in view of the uncertainty involved.

Clearly, considerable uncertainty exists in developing a balanced code (see Section 5.2) as well as in predicting earthquake characteristics. Nevertheless, even if a great deal of uncertainty is involved, to establish a balanced code using probabilistic studies is still of great value, the author believes, because it must therefore be even more

difficult to justify the existing safety levels in codes, as described in Section 3.1.

For estimating the probability of failure of a structure, given that an earthquake with a certain maximum ground acceleration occurs, the equation in terms of damage energy established in the previous chapter is used. All items involved in the equation could be taken as random variables. However, all of them need not be considered as random variables, because randomness of some items dominates the results. Hence, items whose randomness does not strongly affect the results can remain as deterministic variables. It makes the procedure for estimating the failure probability simpler. In order to select such items, sensitivity studies were carried out.

In the next section, 7.2, the difficulties of predicting earthquake characteristics are discussed to give an understanding of the inherent uncertainty involved. The way in which the uncertainty affects code development is also considered. In section 7.3, a basic procedure for calculating failure probabilities is described consistent with the inherent uncertainty. Based on the probability distributions of total damage energy and other items assumed in section 7.4, sensitivity studies are carried out in 7.5 to select items which should be taken as random variables. Finally in section 7.6, the proposed procedure for obtaining failure probabilities of multi-storey buildings subjected to earthquake is summarised and details of the application to an existing building are explained.

7.2 DIFFICULTIES IN PREDICTING EARTHQUAKE CHARACTERISTICS

Uncertainty deriving from the difficulties involved in predicting earthquake characteristics is believed to dominate the total uncertainty in a procedure for estimating failure probabilities. According to the principle of consistent crudeness, explained in section 3.2.2, it is important to know the inherent uncertainty in a system being developed in order to avoid unnecessary complexity. Thus, before making reasonable assumptions for calculating failure probabilities, the difficulties in evaluating earthquake characteristics probabilistically and the resulting degree of uncertainty must first be clarified. The earthquake characteristics discussed in this section are (1) maximum ground motion amplitude, (2) spectral characteristics, and (3) time-domain intensity envelope (or characteristics of phase angles). The three measures are theoretically sufficient to characterise an earthquake motion.

First of all, an appropriate approach for predicting earthquake characteristics in harmony with the purpose of the present study must be discussed. The final aim of the study is to develop a balanced code. Two criteria exist for achieving a balanced code as described in section 3.3, (1) the lowest safety level of any structure designed according to the code must meet the failure criterion, and (2) the spread of safety levels between structures must be minimised. This means, an adequate code from the viewpoint

of safety can lead to designs whose safety levels vary considerably, but as long as the least safe of such structures meets the failure criterion, the code is satisfactory. However, the code may not be adequate economically as it may lead to overly conservative structures. A balanced code will achieve both the desired minimum safety level and also economical adequacy. Thus, in order to develop a balanced code, the assessment of structural safety or failure probability is essential. In practice, the safety levels of many existing buildings should be examined to obtain the least safety level and safety variation implied by a structural code. The reason for using existing buildings is to reduce the effects of uncertainties, modelling assumptions and so on (23) following the issue (b) in section 3.3.2.

Therefore, the prediction of earthquake characteristics required in this project is ideally required for each existing structure, considering individual local features as well as characteristics of the region. For instance, local conditions of surface soil and the embedded foundation of a structure are known to affect input earthquake motion, and the effect should be taken into account in estimating the earthquake characteristics of a structure. In designing nuclear power plants, local conditions have been carefully dealt with (87,88). However, though enormous efforts have been put into evaluating the input earthquake motion, the uncertainty is still considerable, as explained in section 2.4.4. Thus, a simpler prediction approach neglecting local conditions could be justified. It is particularly true when

a large degree of uncertainty is expected in predicting earthquake characteristics in a region. Moreover, since it is necessary to examine the safety of a number of structures, too detailed a prediction technique is not practical for developing a balanced code. Accordingly, a reasonably simple approach for predicting earthquake characteristics is required for this project.

A possible way of estimating earthquake characteristics could be based on theoretical concepts of seismology. Furthermore, it is useful to know some basic seismological ideas. Hence, first of all, the Fourier amplitude spectrum of far field shear waves is discussed from a seismological aspect (89,90). This is an important characteristic of an earthquake. The shearing rupture at the source of an earthquake gives rise to a complex set of seismic waves. The rupture mechanism is very complex and is not yet completely understood. However, simple models have been formulated that capture the gross properties of the rupture process, and study of these can yield valuable insight into the nature of strong ground shaking. Consider a shear dislocation with a simple ramp dislocation-time function as shown in Fig. 7.2.1; propagating in an infinite elastic medium. Let the dislocation occur simultaneously over the depth W of the fault and propagate unilaterally with velocity V in the direction of the length of the fault L, as shown in Fig. 7.2.2. From the simple source mechanism, the items which affect the Fourier amplitude spectrum of farfield shear waves are as follows.

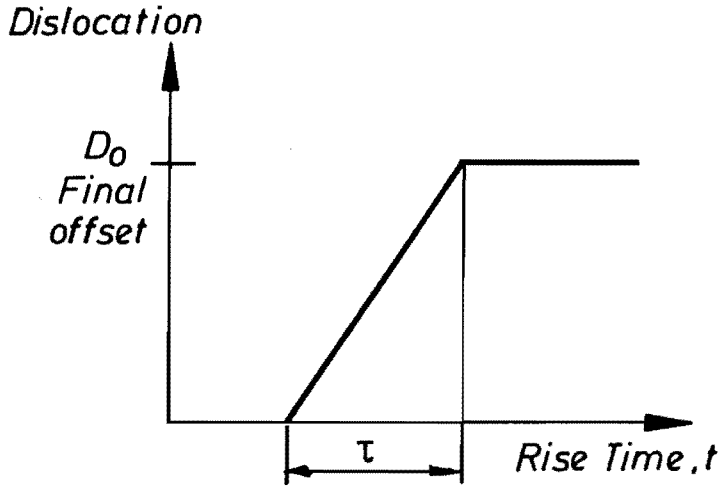

Fig. 7.2.1 Ramp dislocation (89)

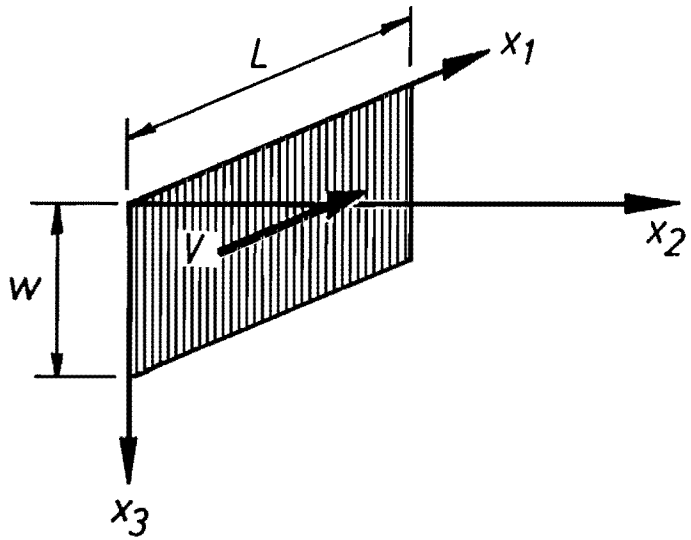

Fig. 7.2.2 Fault surface showing direction of rupture propagation (89)

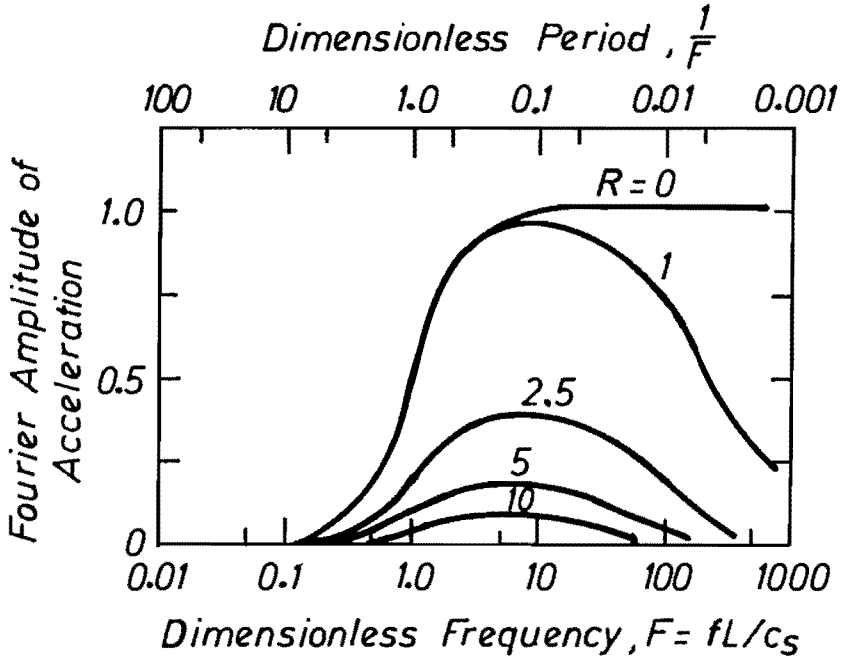

Fig. 7.2.3 Effect of material and geometric attenuation of body waves. Dimensionless distance, R = r/L where L = source dimension. Q = 320 is used in this plot (89)

1. Seismic Moment M_o:

$$M_o = \mu \cdot S \cdot \overline{D} \qquad (7.2.1)$$

where: S = fault area (= $L \cdot W$)

$\overline{D}$ = average offset

μ = material property

Because the Fourier amplitude spectrum increases linearly with M_o, M_o can be a fundamental measure of earthquake size.

2. Rise Time τ; the shorter the rise time (see Fig. 7.2.2), the stronger the high frequency amplitudes.

3. The Direction of Rupture Propagation; more energy is focussed in the direction of rupture propagation.

4. Source-to-Site Distance r; the term is related to the decay of wave amplitudes as seismic energy is spread over an increasing surface as waves propagate outwards from the source (geometric attenuation). In the case of the spherical spreading of body waves, the geometric attenuation is proportional to $1/r$, and in the case of surface waves, $1/\sqrt{r}$. Frictional losses also occur in which a fraction of a wave's energy is lost in each cycle of motion (material attenuation). Its effect can be described mathematically by multiplying wave amplitudes by the exponential factor:

$$\exp\left[-\frac{\pi \cdot f \cdot r}{Q \cdot C_s}\right]$$

where f is the frequency, C_s the shear wave velocity in the medium and Q a constant for a given material. The combined effect of the attenuations on acceleration amplitude is illustrated in Fig. 7.2.3.

Thus, even when simple models for rupture propagation are used, the Fourier amplitude spectrum of far field shear waves is related to several factors and the relationships are not simple. In addition difficulties may arise in predicting the factors probabilistically for a particular structure.

Though the basic relations between Fourier amplitude spectrum and the parameters are useful for predicting earthquake characteristics, they are not good enough to determine a complete earthquake motion. Additional information on phase angles (see ϕ_k in Eq. (6.3.24)) is required. However such information is not available. Because the phase angles in the frequency domain are related to an intensity envelope in the time domain, some research has been done to empirically determine the envelope (91,92). The unavailability of information on phase angles is an obstacle for predicting earthquake characteristics. Therefore, at present we do not have enough information on the distribution of regional values of the several source parameters mentioned above to be able to make use of theoretical source models in seismic risk analysis (89).

Another feasible way for predicting earthquake characteristics might be an empirical approach based on

seismological aspects, using empirical relationships between magnitude, epicentral or hypocentral distance, and various measures of ground motion amplitude (93). The relationships have been obtained by regression analyses on sets of strong motion data, mostly from the western United States and Japan. However, it is not straightforward to apply an empirical equation to a certain site. Some preliminary study would be necessary to estimate stochastically the occurrence of an earthquake with a certain magnitude and its epicentral distance to the site. Such a study, however, has not been done. Moreover, since the location of earthquake sources and magnitude has been determined from expert opinion in seismic hazard analysis for nuclear power plants (see section 2.4.1) the uncertainty involved in the estimation could be high.

The only data available for seismic probabilistic studies at present are return periods using Modified Mercalli intensity (M.M.I.) which is an earthquake intensity scale. Smith (58) estimated the likelihood of earthquake shaking throughout New Zealand using M.M. intensity as shown in Fig. 7.2.4. The M.M. intensity scale is probably the best single parameter for measuring earthquake damage. It can thus be said that return periods based on M.M.I. represent the most reasonable and practical modelling of earthquake prediction for developing a balanced code.

However, it is not easy to predict earthquake characteristics, such as maximum ground motion amplitude, spectral characteristics and time-domain intensity envelope,

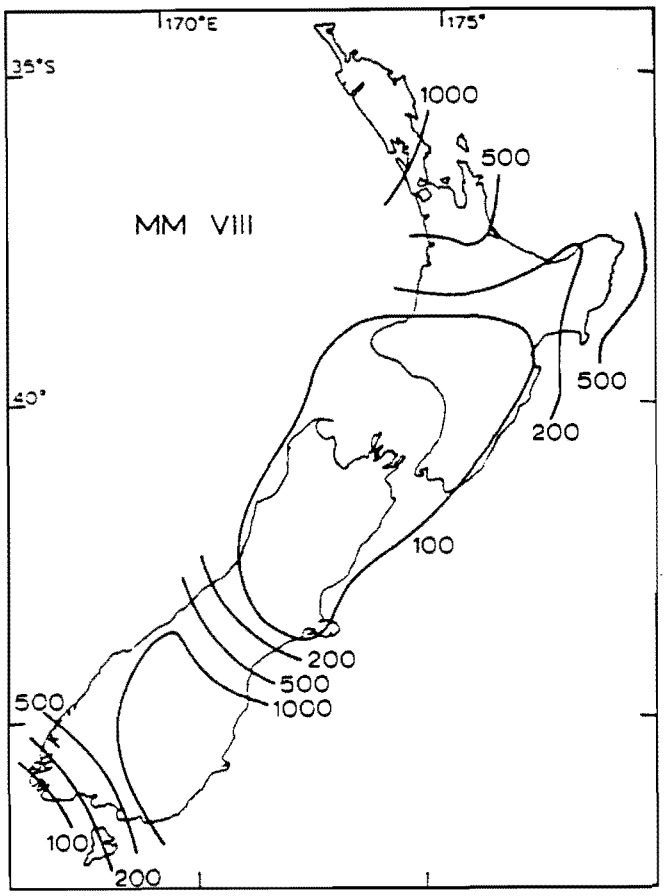

Fig. 7.2.4 Return periods (years) for intensity M.M.VIII and greater, based on the occurrence of large earthquakes between 1840 and 1975 (58)

Table 7.2.1 Relationship between M.M.I. and maximum ground acceleration

M.M.I / Bound	VII	VIII	IX	X
Upper	150~300	300~750	900~1500	2000↑
Lower	20~50	50~100	100~200	200~300

Unit: cm/sec^2

using M.M.I. alone. It is known that M.M.I. is only weakly correlated with maximum ground acceleration α_{max} (59,60). Upper and lower bounds of α_{max} estimation corresponding to M.M.I. proposed by researchers in different countries, are shown in Table 7.2.1. From the Table, it can be seen that the variation between different studies is surprisingly big. Other correlations have been attempted but these also are poorly correlated. No information is available on the relationships between M.M.I. and spectral characteristics, and between M.M.I. and time-domain intensity envelopes.

Since time-histories of earthquake acceleration are usually used in dynamic response analyses, if maximum acceleration α_{max} could be specified for a corresponding M.M.I., α_{max} would be the most convenient and simple measure. However, maximum acceleration itself is not a measure of earthquake intensity. Greater damage can sometimes be found for earthquakes with smaller values of α_{max}. Clearly, structural damage is not only related to the maximum acceleration of an earthquake but also to its spectral characteristics and time domain intensity envelope, whose relationship to M.M.I. again has not been obtained.

Nevertheless, in the light of the lack of data and the uncertainties involved, the following simple assumption is made for the present study: that the significant earthquake characteristics consist of maximum ground acceleration α_{max}, shape of spectral function with regard to period, and intensity envelope with regard to time. It is also assumed that:

(1) Maximum ground acceleration α_{max} is the basic measure of seismicity; and

(2) The shape of the spectral function and the intensity envelope differ from place to place even in the same seismic region.

These are the assumptions for predicting earthquake characteristics in a region. Because considerable uncertainty is expected in estimating them, it may not be necessary to consider local conditions such as conditions of surface soil or embedded foundations in predicting the earthquake motion input into a particular structure.

We must now consider how the uncertainty of predicting earthquake characteristics affects the precision of a balanced code. To achieve a balanced code, the two things needed to be accomplished in an earthquake provision as discussed earlier are:

(1) The code format should be revised such that the spread of failure probabilities among structures subjected to earthquake is minimised (format study) and

(2) The minimum safety level for all structures in an earthquake provision should coincide with that for other provisions (minimum safety study).

In the format study, when the distribution of failure probabilities is obtained, the amount each category in a code contributes to the total variability of the distribution needs to be calculated. Categories with a larger contribution to the variability should be divided further in order that each category has about the same variability. By modifying the safety levels of the categories such that each category meets a required minimum safety level, the total variability implied by the revised code can be much smaller than that for the former code (see Fig. 3.3.3).

Because the spread of failure probabilities is considered in the format study, the differences of failure probabilities between structures play an important role. Figure 7.2.5 shows a flow of obtaining failure probabilities, where the cross-hatched areas indicate uncertainties for corresponding assumptions. The differences of failure probabilities between structures are more or less influenced by all assumptions involved in the calculation. For example, uncertainties derived from the calculation method, definition of failure and assumptions of structural characteristics and earthquake intensity affect the differences. However, for instance, when the definition of failure is equally biased on structures, the relative differences between failure probabilities would not be affected very much. Similarly, though considerable uncertainty is involved in the expected values of earthquake intensity, only the relative intensity levels between different areas strongly affect the results. The

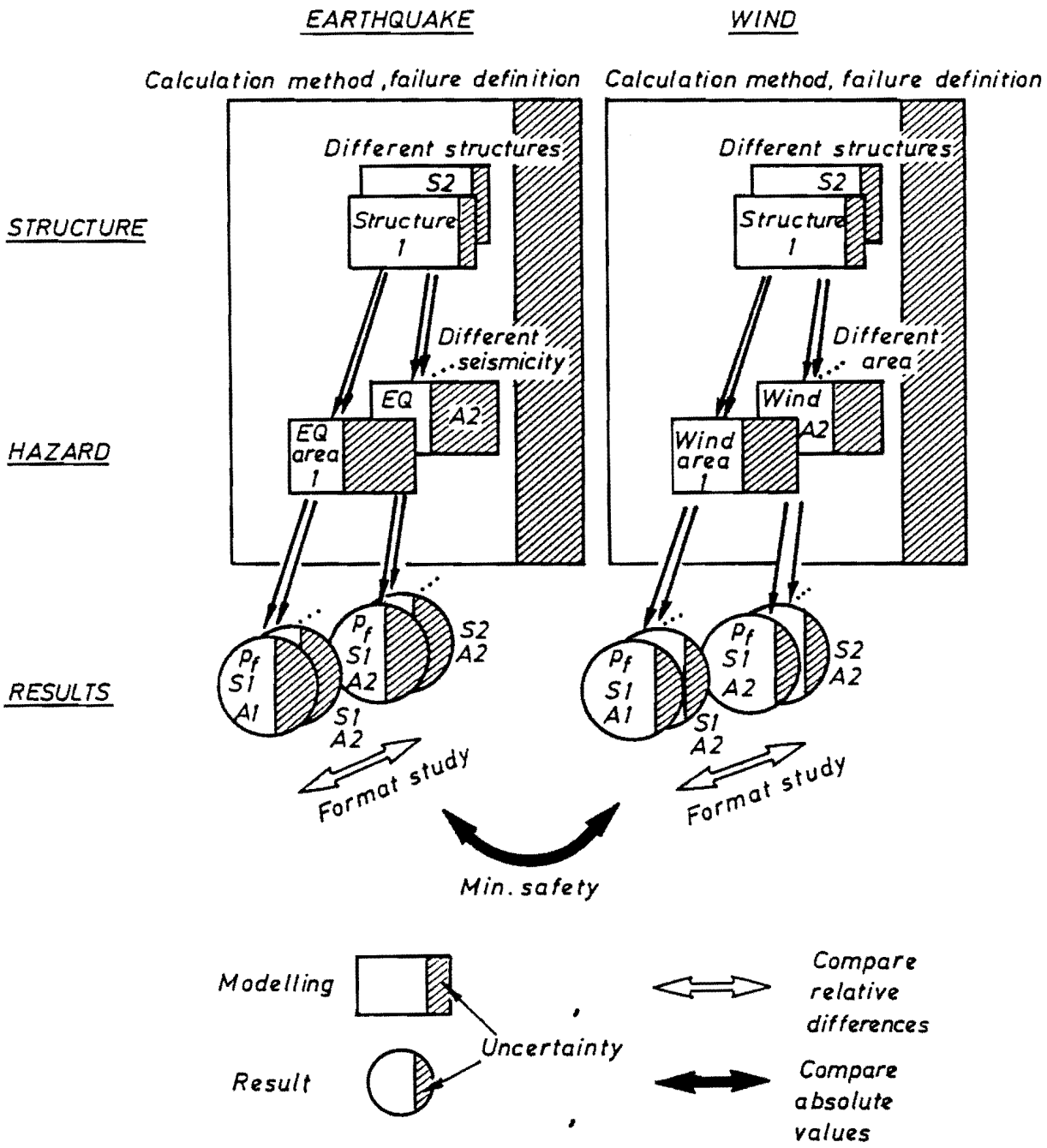

Fig. 7.2.5 Illustration of comparison among failure probabilities

uncertainty in the relative intensity levels is smaller than that for the absolute values. Therefore, the considerable uncertainty in estimating earthquake intensity does not markedly affect the format study.

On the other hand, in the minimum safety study, absolute minimum safety levels among different structures must be compared. Suppose that failure probabilities of many structures due to earthquake and wind were examined (see Fig. 7.2.5). The aim of the minimum safety study is to set resistance capacity of structures such that the minimum safety levels for the different loadings are the same and meet the required minimum safety level. Thus, the absolute value of failure probabilities is important rather than the relative safeties. The uncertainty involved in the calculation procedures both for earthquake and wind load affects the absolute value of failure probabilities. Thus, the considerable uncertainty in predicting earthquake characteristics rather directly influences the reliability of the results. Consequently, the uncertainty less affects the format study than it does the minimum safety study. This is because similar situations are compared in the format study, as stated in section 3.2.1(b).

7.3 CALCULATION PROCEDURE FOR FAILURE PROBABILITIES

The necessary preliminaries for developing a procedure for calculating failure probabilities of structures subjected to earthquake have now been completed. A failure probability, in general, can be calculated using Eq. (2.2.3) which

involved a performance function $g(\mathbf{X})$ and a joint probability density function $f_{\mathbf{X}}(\mathbf{X})$. A performance function for the present project was developed in Chapter 6 in terms of cumulative plastic strain energy. In this section, a practical form of joint probability density function is described using the simple assumptions for earthquake characteristics made in the previous section. Subsequently, the failure probability will be expressed as a summation of products of seismic risk and conditional failure probability. The seismic risk for the three main centres in New Zealand will also be considered.

The failure probability p_f of a structure subjected to earthquake can be expressed by:

$$p_f = \iiint_{g(\alpha_{max},s,r)<0} f(\alpha_{max},s,r)\,d\alpha_{max}\cdot dS.dR \qquad (7.3.1)$$

where: f = joint probability density function

α_{max} = maximum ground acceleration of an earthquake

S = shape functions of spectrum with regard to period and the intensity envelope with regard to time of an earthquake

R = structural resistance variables such as stiffness, yield strength and so on

g = performance function (failure region : $g < 0$)

The structural resistance variables R and the characteristics of an earthquake, α_{max} and S, are assumed to

be statistically independent. The earthquake characteristics, α_{max} and S, may not in fact be statistically independent because the source-to-site distance is a common parameter for both; α_{max} is large when the distance is small, and the shape of the spectral function also depends on the source-to-site distance, as shown in Fig. 7.2.3. However, because phase angles are uncertain, α_{max} will not always increase when the source-to-site distance decreases. Moreover, the shape of the spectral function can be also affected by local conditions such as surface soil, topography and so on. However, even if α_{max} and S are not statistically independent, the dependency is not obvious and would normally be small. Therefore, it is simply assumed here that α_{max} and S are statistically independent. Thus, Eq. (7.3.1) is transformed into:

$$p_f = \iiint_{g(\alpha_{max},s,r)<0} f_{\alpha_{max}}(\alpha_{max}) \cdot f_S(s) \cdot f_R(r) d\alpha_{max} \cdot dS \cdot dR \qquad (7.3.2)$$

where $f_{\alpha_{max}}(\alpha_{max})$, $f_S(s)$ and $f_R(r)$ are probability density functions of α_{max}, S and R respectively. Because in estimating $f_{\alpha_{max}}(\alpha_{max})$ and $F_S(s)$, a great deal of uncertainty is involved, the probability density functions can be changed into probability mass functions $p_{\alpha_{max}}(\alpha_{max})$ and $p_S(s)$, where α_{max} and S are discrete random variables ($p_X(x_i) = P[X = x_i]$). Hence:

$$p_f = \sum_{i=1}^{n_\alpha} \left[p_{\alpha_{max}}(\alpha_i) \times \sum_{j=1}^{n_s} \{ p_S(s_j) \times \right.$$

$$\int_{g(\alpha_i, s_j, r)<0} f_R(r)dR\}\Big] \qquad (7.3.3)$$

where n_α and n_s are the numbers of discrete variables for α_{max} and S respectively. Even though a probability mass function is used for S, it is still difficult to estimate the probability of occurrence of a certain value of S. By assuming that an occurrence of a certain value of S is completely random, a uniform mass function can be substituted for $p_S(s)$. Then:

$$P_f = \sum_{i=1}^{n_\alpha} \Big[p_{\alpha_{max}}(\alpha_i) \times \frac{1}{n_s} \sum_{j=1}^{n_s} \Big\{ \int_{g(\alpha_i, s_j, r)<0} f_R(r)dR \Big\} \Big] \qquad (7.3.4)$$

$$= \sum_{i=1}^{n_\alpha} \Big[\Big\{ \frac{1}{n_s} \sum_{j=1}^{n_s} P[F|EQ_{ij}] \Big\} \cdot p_{\alpha_{max}}(\alpha_i) \Big] \qquad (7.3.5)$$

in which:

$p_{\alpha_{max}}(\alpha_i)$ = seismic risk

$P[F|EQ_{ij}](=P[F|(\alpha_{max}=\alpha_i)\cap(S=s_j)])$ = conditional failure probability (failure probability given that $\alpha_{max} = \alpha_i$ and $S = s_j$)

Equation (6.4.11) in terms of cumulative plastic strain energy will be used as the performance function g, when the

conditional failure probability is evaluated. Equation (7.3.5) is then used for calculating failure probabilities.

In using Eq. (7.3.5) to obtain failure probabilities, a question arises as to the appropriate values of n_α and n_s for obtaining a reasonably accurate result in the light of the total uncertainty involved. The appropriate value of n_s will be examined in section 7.5. For the rest of the present section, the values of seismic risk to be used in Eq. (7.3.5), including the appropriate value of n_α are discussed following Elms and Silvester (94,95).

As described in the previous section, a practical way to estimate seismic risk for a region is to evaluate the relationship between α_{max} and Modified Mercalli intensity, for which return periods have been obtained for locations throughout New Zealand (58). To determine the relationship, three empirical equations relating earthquake parameters were used (95) as follows:

1. Gutenberg and Richter (96):

$$\log_{10} \alpha_{max} = I/3 - 0.5 \qquad (7.3.6)$$

where: α_{max} = maximum acceleration (cm/sec^2)
I = Modified Mercalli intensity

2. Whitman et al. (97):

$$\log_{10} \alpha_{max} = 0.38\ I - 0.73 \qquad (7.3.7)$$

3. Esteva and Rosenblueth (98):

$$I = 3.84 + 3.32 \log_{10} V \qquad (7.3.8)$$

where: V = maximum ground velocity (cm/sec)

Assuming that the peak velocity can be converted to peak acceleration by multiplying by the ratio 10.23 given by the El Centro 1940 NS record, a relationship between acceleration and M.M.I. can be derived, based on the three empirical equations. The average of the results resulted in the relation between α_{max} and M.M.I. are given in Table 7.3.1.

The probability of occurrence of an earthquake of intensity I in any one year is usually expressed by:

$$P[M.M.I. = I] = \frac{1}{T_I} \qquad (7.3.9)$$

in which:

T_I : return period of intensity I

However, Elms and Silvester assumed that on poor soil the return period for a particular intensity is closer to the figure for the next lower intensity level. The seismic risk for intensity I is then given by:

$$P[M.M.I. = I] = (1-q) \frac{1}{T_I} + q \frac{1}{T_{I-1}} \qquad (7.3.10)$$

Table 7.3.1 Maximum ground acceleration corresponding to M.M.I.

M.M.I.	VI	VII	VIII	IX	X
α_{max}/g	0.035	0.09	0.20	0.35	0.70

Unit: gal

Table 7.3.2 Approximate return periods

City \ M.M.I	VII	VIII	IX	X
Wellington	20	50	150	-
Christchurch	50	100	250	-
Auckland	300	900	-	-

Unit: Year

Table 7.3.3 Calculated seismic annual risk

City \ α_{max}	0.20g	0.35g	0.70g
Wellington	2.6×10^{-2}	9.33×10^{-3}	1.33×10^{-3}
Christchurch	1.2×10^{-2}	5.2×10^{-3}	8.0×10^{-4}
Auckland	1.56×10^{-3}	2.22×10^{-4}	-

($n_\alpha = 3$)

where: q = proportion of poor ground at a site

The proportion q was simply assumed to be 20%.

The assumptions used by Elms and Silvester are used in the present study because it is generally appropriate to New Zealand conditions. In addition, it is assumed that structures never collapse when α_{max} is less than 0.1 g. That is, only M.M.I. levels of VIII, IX and X, are considered here (i.e. $n_{\alpha} = 3$).

Auckland, Wellington and Christchurch are the three biggest cities in New Zealand, containing about 60% of the total population. These three cities are used as sample sites. Smith (58) suggested the return periods for the cities shown in Table 7.3.2. The values of VII are necessary in calculating seismic risks for VIII using Eq. (7.3.10). Hence, using Eq. (7.3.10) with q = 0.2, the seismic risk values set out in Table 7.3.3 are obtained.

7.4 ASSUMPTIONS FOR RANDOM VARIABLES IN CONDITIONAL FAILURE PROBABILITIES

7.4.1 Assumptions for Random Variables

In the previous section, a procedure to calculate failure probabilities was proposed, and values of seismic risk in three New Zealand centres were given. Therefore, the task remaining is to estimate the conditional failure probability

in Eq. (7.3.5). In this, the performance function proposed in Chapter 6 is used in terms of cumulative plastic strain energy. There are several basic random variables involved in the equation. The application of the performance function to the conditional failure probability and the distributions and their parameters for all random variables are discussed. Particular attention is paid to estimating a probability distribution for the damage energy input which is the most dominant term in terms of variability.

Let us denote the event that a failure occurs given an earthquake as:

$$E = [F|EQ] \tag{7.4.1}$$

The failure definition is that an entire structure collapses when the deflection angle of any storey reaches 1/50 (see Eq. (5.4.1)). Thus E is expressed by:

$$E = E_1 \cup E_2 \cup \ldots \cup E_n \tag{7.4.2}$$

where: E_i = failure of ith storey in an earthquake

$= [\gamma_{max_i} > 1/50|EQ]$

γ_{max_i} = maximum storey deflection angle of ith storey

n = total number of storeys

Therefore, the conditional failure probability given an earthquake, $p_{f|EQ}$ (= $P[F|EQ]$) is evaluated from:

$$p_{f|EQ} = P[E] = P[E_1 U E_2 U \ldots U E_n] \tag{7.4.3}$$

The conditional failure probability for the ith storey $p_{f_i|EQ}$ (= $P[E_i]$) can be expressed using Eq. (6.4.11) as:

$$p_{f_i|EQ} = P[g_i<0] \tag{7.4.4}$$

where:

$$g_i = \eta_{R_i} - \eta_{I_i} \cdot \frac{e^{E}d_i}{e^{E}d_T} \tag{7.4.5}$$

and the other quantities are those derived in section 6.4.4 namely:

$$\eta_{R_i} = 2\ C\ (1_i \cdot \gamma_u/\delta_{y_i} - 1) \tag{7.4.6}$$

$$\eta_{I_i} = \frac{w_t \cdot E_{d_t}/w_t}{\frac{1}{2} \cdot k_i \cdot \delta_{y_i}^2} \tag{7.4.7}$$

$$e^{E}d_i = \Omega_{\delta_i} \cdot k_i \cdot \sigma_{\delta_i}{}^2 \cdot \exp\{-\delta_{y_i}^2/2\sigma_{\delta_i}^2\} \tag{7.4.8}$$

$$e^{E}d_T = \sum_{m=1}^{n} e^{E}d_m \tag{7.4.9}$$

The notation is the same as that used in Section 6.4.4. Because the storey conditional probabilities are obviously not mutually exclusive, the probabilities of all joint events (e.g. $P[E_1 \cap E_2 \cap \ldots \cap E_1]$) or bounding operations (see section 2.3.2) are generally required in calculating $p_{f|EQ}$

in Eq. (7.4.3) using $p_{f_i|EQ}$. A practical means of calculation for a particular case is described in Section 7.5.2. Initially, we shall concentrate on the calculation of the probability of storey failure, $p_{f_i|EQ}$.

The storey failure probability $p_{f_i|EQ}$ can be calculated using Eq. (7.4.4), assuming the distributions and their parameters for all variables involved in the equation. There are 5 basic random variables and 2 dependent variables, as shown in Table 7.4.1. The assumptions concerning the basic random variables are briefly explained as follows, noting that the assumptions are necessary for the sensitivity studies discussed in Section 7.5.

(1) Coefficient C - the coefficient C varies about from 2 to 4 from Figs 6.4.4 and 6.4.5. A normal distribution with a mean of 3 and standard deviation of 0.775 is assumed. That is, it is presumed that the probabilities of C exceeding 4 or being less than 2 are both 10%.

(2) Weight of ith storey w_i - It is not easy to estimate the contribution of live load to the storey weight w_i during an earthquake. Thus, simply following the New Zealand code (49), the mean of w_i is taken as 1.1 x (Dead Load). From NBS577 (30), a normal distribution with coefficient of variation of 0.1 is assumed.

(3) Yield storey drift δ_{y_i} - The yield storey drift δ_{y_i} is assumed to be related to the initial stiffness k_i and yield shear force V_{y_i} for that storey alone, due to the use

Table 7.4.1 Variables involved in the assessment of failure probability

	Variables	Assumptions
Basic random variables	C	normal $\quad \overline{C} = 3, \quad \sigma_c = 0.775$
	w_i *1	normal $\quad \overline{w_i}$ = 1.1 x (dead load)*2; C.O.V. = 0.1
	δ_{y_i}	normal $\quad \overline{\delta_{y_i}}$ = (calculated value)*3, C.O.V. = 0.1
	γ_u	log-normal $\quad \lambda = -3.95, \quad \zeta = 0.30$
	E_{d_T}/w_t	(see Fig. 7.4.13)

(k_i : deterministic variable)

	Variables	Dependency
Dependent variables	Ω_{δ_i}	resonant periods (or w_i)
	σ_{δ_i}	

*1 $w_t = \sum_{i=1}^{n} w_i$

*2 See Appendix A

*3 See Appendix A ($\delta_{y_i} = V_{y_i}/k_i$)

of a spring mass model. Though some cracks in reinforced concrete members may exist in practice, the stiffness k_i is taken as the initial uncracked stiffness. The stiffness k_i is assumed to be a deterministic variable because the variability is considered smaller than that for the other structural characteristics. The assumptions on k_i affects the resonant periods and yield storey drifts. Instead, w_i and δ_{y_i} are assumed to be random variables. (The resonant periods are related to w_i.) The coefficient of variation of yield moment in a reinforced concrete section is about 0.15-0.20 according to a preliminary study. The coefficient of variation of the yield storey shear force V_{y_i} depends on the number of spans, but is simply assumed to be 0.1. The yield storey drift δ_{y_i} is assumed to be normally distributed with a coefficient of variation of 0.1. Its mean value is calculated from k_i and V_{y_i} as given in Appendix A.

(4) Ultimate storey deflection angle γ_u - The mean value of γ_u is 2/100 due to the definition of failure. It is assumed to be likely that collapse occurs for values of γ_u ranging between 1/100 to 4/100. Ultimate storey deflection angle γ_u is assumed to have a log-normal distribution with λ of -3.95 and ζ of 0.3 such that the probability of γ_u being less than 1/100 or exceeding 4/100 are both about 1%.

(5) Standard damage energy E_{d_T}/w_t - The standard damage energy E_{d_T}/w_t is an important quantity in calculating the storey failure probability $p_{f_i|EQ}$. It represents the earthquake intensity causing structural damage. The distributions and thus parameters corresponding to α_{max} values of 0.20, 0.35 and 0.70 g are given in the next two

subsections.

The variances assumed here are considered to arise from so-called "random errors" (see section 3.2). Other errors such as systematic and human errors can also affect the variances. Human error is not directly considered in the present study, as discussed in Section 3.2. Systematic errors, which are derived from for instance inadequacy of data and modelling limitations should theoretically be taken into account in the assumptions made for variances. However, in practice, variances caused by systematic errors cannot be easily estimated. It is generally true that systematic errors in earthquake characteristics are much greater than those for structural characteristics. However their quantitative estimation is hard. Therefore for practical reasons, only variances deriving from so-called random errors are considered in the sensitivity study presented in the next chapter.

7.4.2 Basic Assumptions and Preliminary Calculations for Estimating Input Damage Energy Distributions

The performance function, Eq. (7.4.5), contains 5 random variables. When assuming the distribution types and their parameters for all random variables, the conditional failure probability can be calculated using Eq. (7.4.4). In the previous subsection, these assumptions for resistance random variables were made. Thus, the distribution and parameters for standard damage energy derived from earthquake must be

determined. According to Eq. (7.3.5) and Table 7.3.1, the damage energy distributions corresponding to α_{max} values of 0.20, 0.35 and 0.70 g are required to be assessed. Since the damage energy distributions are considered to influence the conditional failure probability markedly, it is significant to reasonably estimate the distributions and parameters for the standard damage energy. However, it is not easy because considerable uncertainty is involved in the estimation, as explained in Section 7.2. In this subsection, for determining the damage energy distributions, basic assumptions and preliminary calculations are discussed.

For earthquake intensity, standard damage energy E_{d_T}/w_t is used rather than damage energy E_{d_T}. Equation (6.3.23) suggests that E_{d_T}/w_t is constant for systems with the same resonant periods and mode shapes. Thus, standard damage energy is only dependent on the modal characteristics of a system. Such a degree of independence is desirable. Moreover, from Eq. (6.2.1) the velocity response spectrum is written as:

$$S_V = \sqrt{2E_T/M_T} \tag{7.4.10}$$

where: E_T = total energy input

Kobayashi and Nagahashi (99) made the assumptions for the seismic spectrum of bed rock motion, which does not include surface soil effects, that the velocity response spectrum was constant independent of period. Using this assumption,

though M_T is substituted for w_t by reason of the units used in the present study, E_{d_T}/w_t will thus be adequate to predict earthquake intensity related to damage and may be taken as constant regardless of period. In addition, it is known that the earthquake acceleration Fourier spectrum is approximately equal to the velocity response spectrum. Hence, the standard damage energy may also be related to the Fourier spectrum of earthquake acceleration as well as the velocity response spectrum. Accordingly E_{d_T}/w_t is an appropriate measure for predicting earthquake intensity.

To determine the distribution and parameters of the standard damage energy, a set of earthquake records must be chosen. In choosing them, there are two issues; (1) the sort of earthquake records to be chosen; and (2) the number of records necessary. One can consider the records selected as samples with a specified earthquake intensity scale. Figure 7.4.1 shows an example for a Modified Mercalli intensity (M.M.I.) of IX. Suppose that all available records were obtained for an intensity of IX. The earthquakes would, of course, have occurred in different places. Because of the poor correlation between M.M.I. and α_{max}, the samples are scattered vertically in Fig. 7.4.1. Moreover, for the different earthquake records there will be considerable variation in surface soil, topography and so on, which may cause differences in the shape function, S, between samples. In choosing the samples, the following assumptions are made:

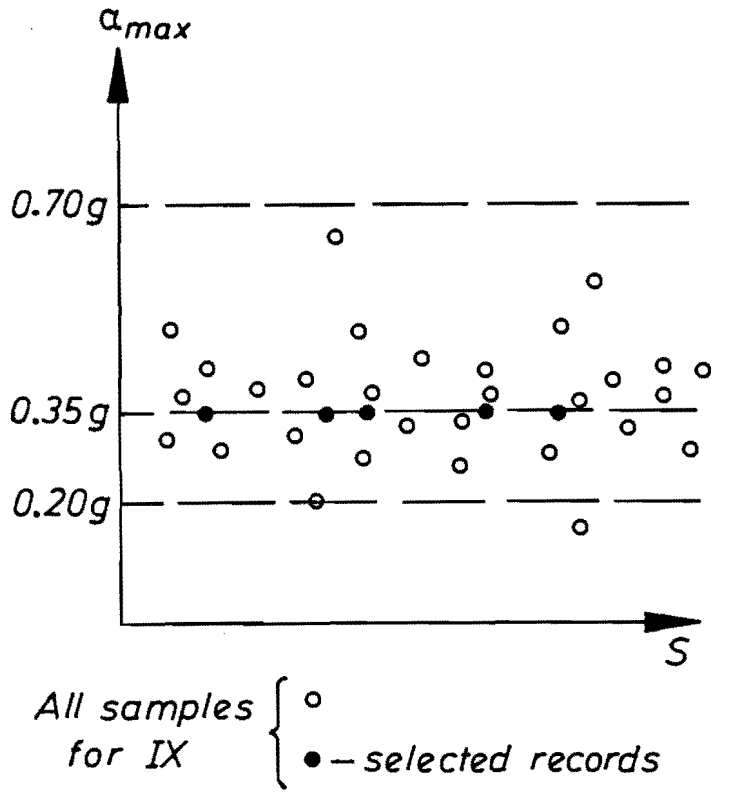

Fig. 7.4.1 Notional illustration concerning sampling of earthquake records for M.M.I. = IX

Table 7.4.2 Original values of maximum ground accelerations for the earthquake records chosen

EQ name	ELC40	PARKF	PACOI	BUCH	ELC79
α_{max}/g	0.314	0.489	1.17	0.206	0.213

Unit: gal

(1) α_{max} and S are statistically independent (see Eq. (7.3.2)).

(2) The α_{max} corresponding to each M.M.I. is fixed at the most probable value as given in Table 7.3.1.

(3) S is considered to have a lot of variability.

Because we do not have enough records for which α_{max} has the value specified in Table 7.3.1, it is necessary to scale the recorded waves up or down. This is not completely acceptable in general. The point is whether the shape function S is appropriate for the scaled record with a new value of α_{max}. Due to the above assumption (3), it can be acceptable. Thus, scaled records are assumed to be appropriate. This is the basic idea in choosing earthquake records, and perhaps almost all earthquake record in hand can be used for obtaining the relationship between E_{d_T}/w_t and α_{max}.

The appropriate sample size is determined by considering the balance between the degree to which the precision of the result is improved by increasing the sample size, and the computational effort. It is worthwhile to increase the sample size when the accuracy improves with only a small increase in effort for the calculation. However, in the present case, no matter how many earthquake waves are used, the accuracy of the prediction of the standard damage energy

will not improve because the inherent uncertainty is considerable. Therefore, a large sample size is not justified.

Arbitrarily, the five earthquake records in Appendix B were chosen to determine the distributions of E_{d_T}/w_t for α_{max} values of 0.20, 0.35 and 0.70 g. The original values of α_{max} are shown in Table 7.4.2. The five waves are used for the estimation of E_{d_T}/w_t for three centres in New Zealand, namely Wellington, Christchurch and Auckland, located in different seismic zones. It is not strictly correct to apply the same earthquake waves to different seismic regions. An area with low seismicity is usually at a longer distance from expected earthquake origins than one with high seismicity. Accordingly, even when the earthquake records observed in different seismic areas have the same value of α_{max}, other earthquake characteristics are generally different. However, such differences can be considered to be negligible, given the total uncertainty in predicting earthquake characteristics.

For the preliminary calculation to estimate the standard damage energy distributions, it must be examined how the standard damage energy input varies for different structures as well as for different levels of α_{max}. According to Eq. (6.3.23), the standard damage energy E_{d_T}/w_t can be calculated from the energy absorbed into a single-degree-of-freedom (S.D.O.F.) system with unit mass ${}_sE_d$. Hence to determine the distribution of E_{d_T}/w_t, values of ${}_sE_d$ were calculated by a non-linear time-history analysis

using the five earthquake records chosen. The six different values of base shear coefficient C_d of 0.05, 0.1, 0.2, 0.3, 0.4 and 0.5 and a range of natural periods T between 0.1 to 4.0 (sec) were selected as calculation points. All five earthquake records were scaled such that their maximum accelerations were adjusted to the specific values of α_{max} of 0.20, 0.35 and 0.70 g. The calculation results are shown in Figs 7.4.2-7.4.10.

Before discussing the general trends of the results, one can immediately observe that the values of $_sE_d$ from the Bucharest earthquake were much larger for the whole range of C_d and T values than those for the other four earthquake records. Though the records were chosen arbitrarily and can be justified as discussed above, it is necessary to make a comment on the Bucharest earthquake. Hartzell (100) explained the main characteristics of the earthquake as follows.

(1) The rupture propagated towards Bucharest and the focusing effect was large.

(2) The epicentral distance to source depth ratio was small.

(3) The type of dip-slip faulting was a thrust mechanism, which releases more energy than a normal fault mechanism.

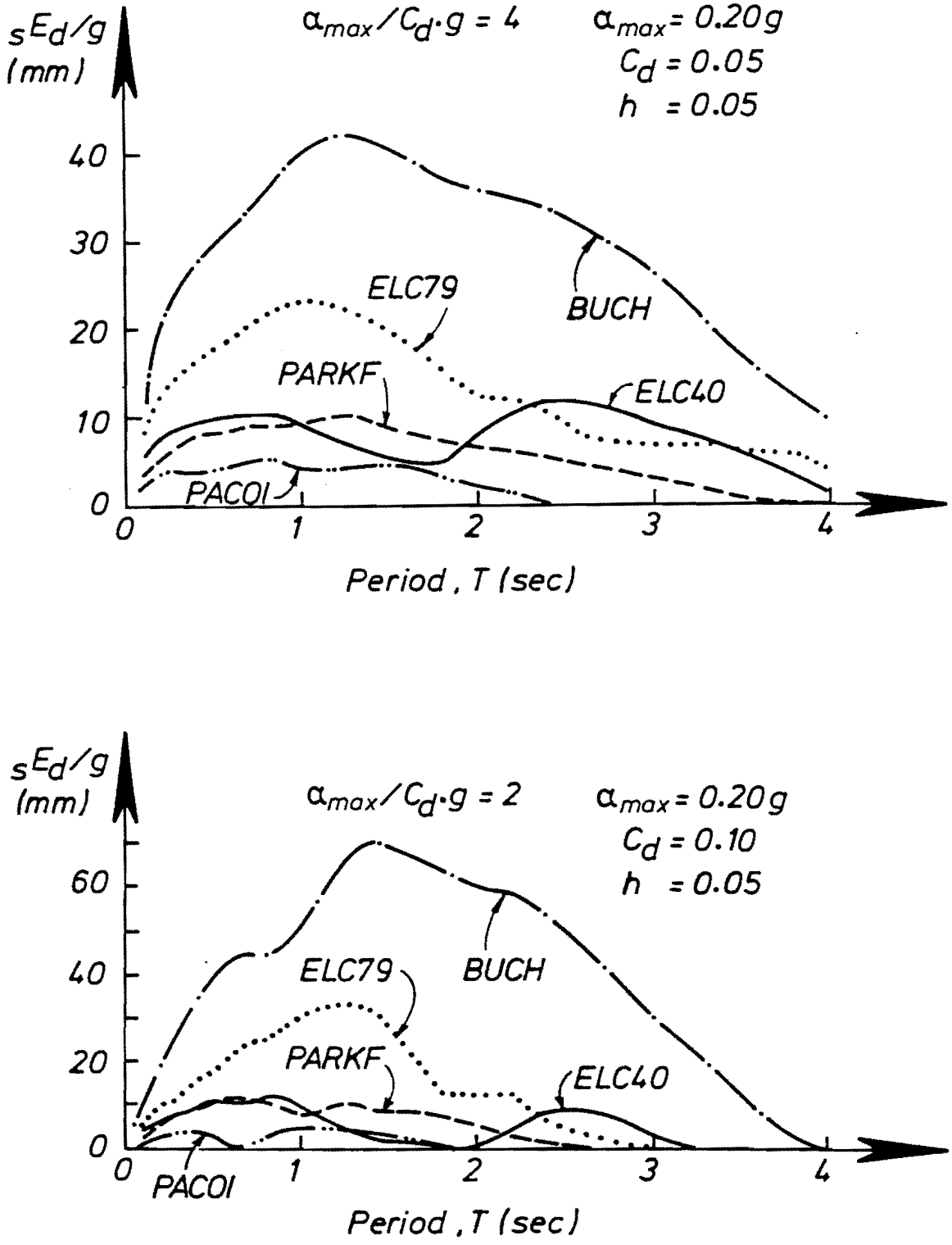

Fig. 7.4.2 Relationship between damage energy absorbed by a S.D.O.F. system and its resonant period

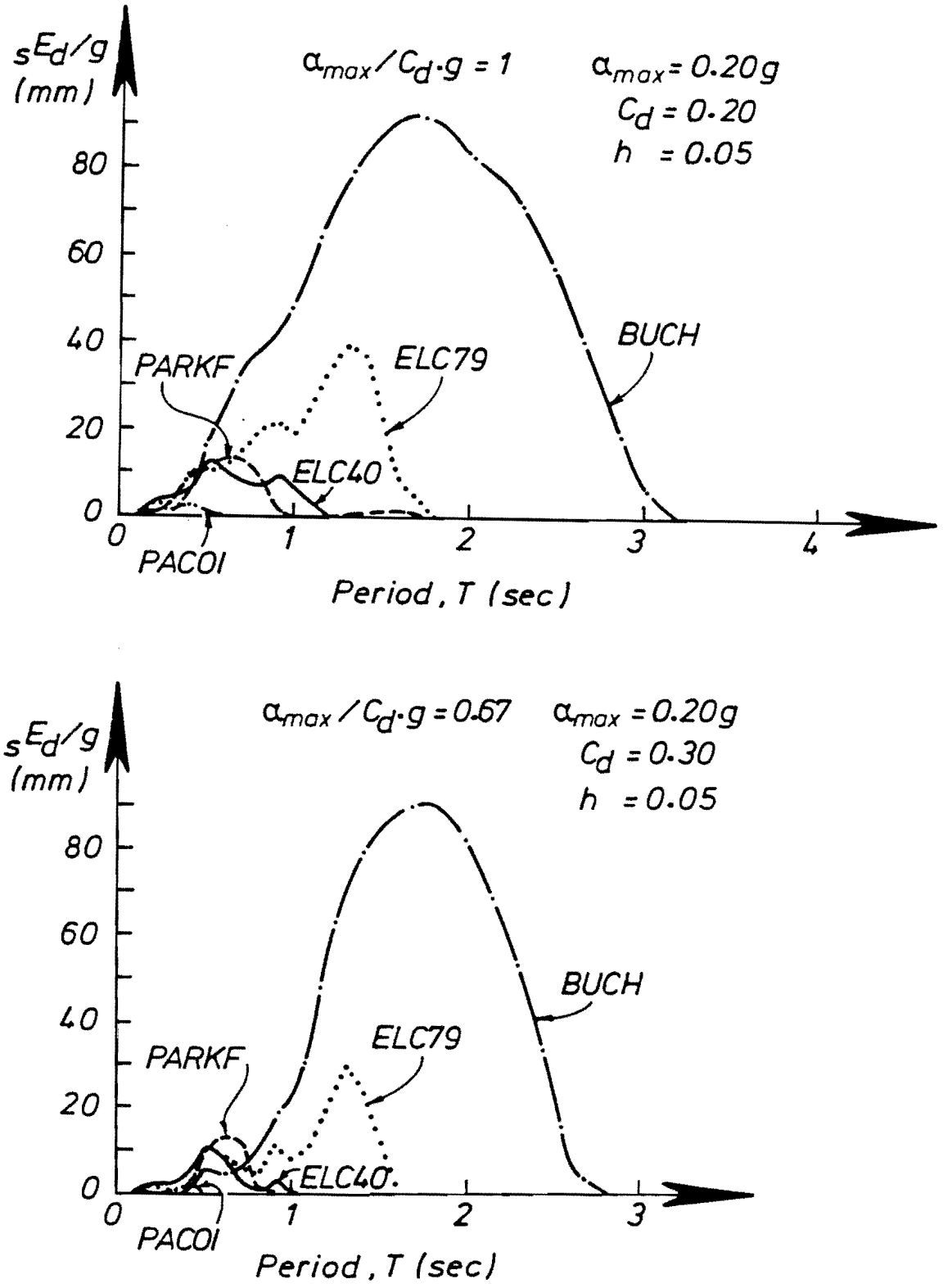

Fig. 7.4.3 Relationship between damage energy absorbed by a S.D.O.F. system and its resonant period

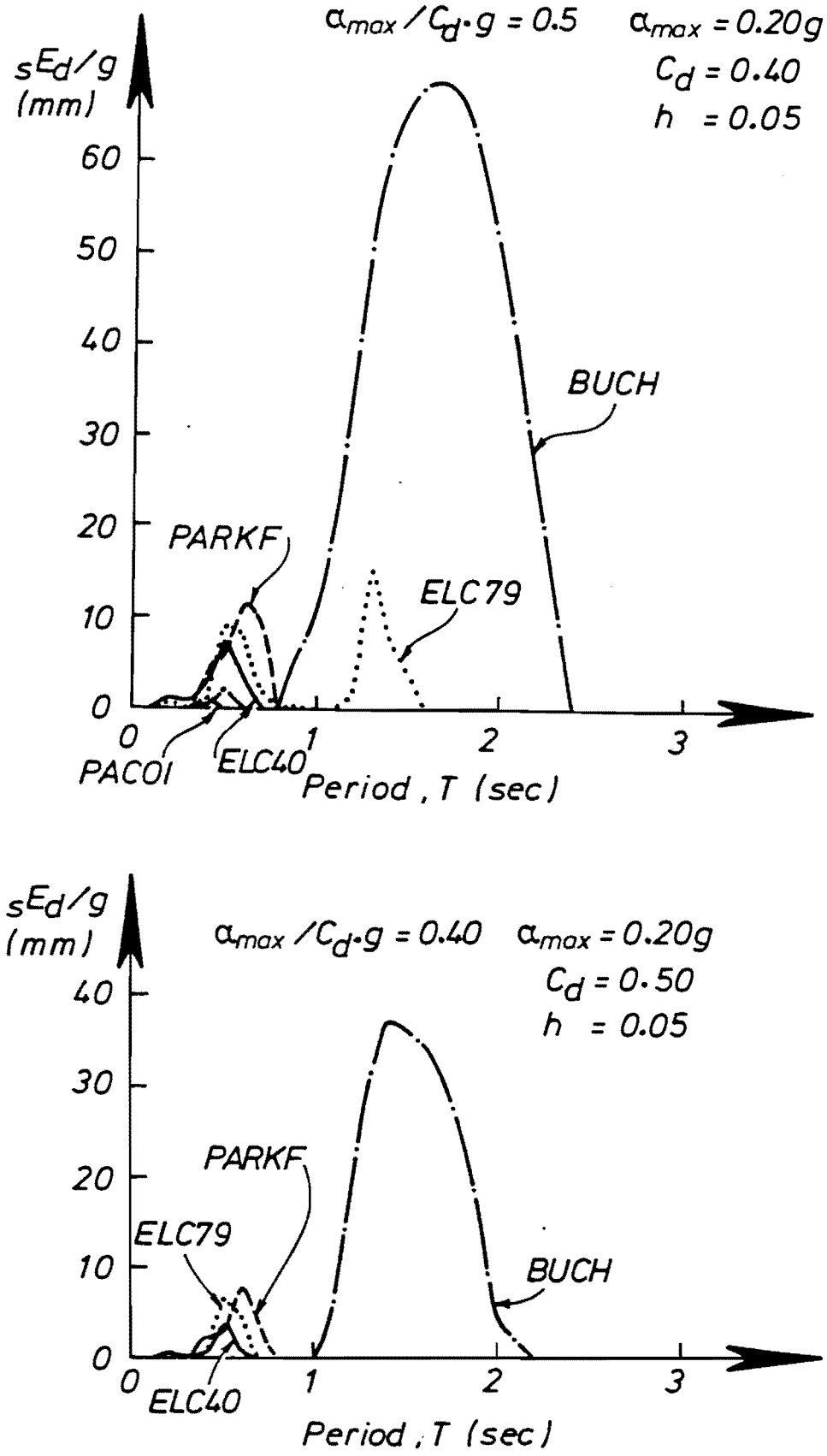

Fig. 7.4.4 Relationship between damage energy absorbed by a S.D.O.F. system and its resonant period

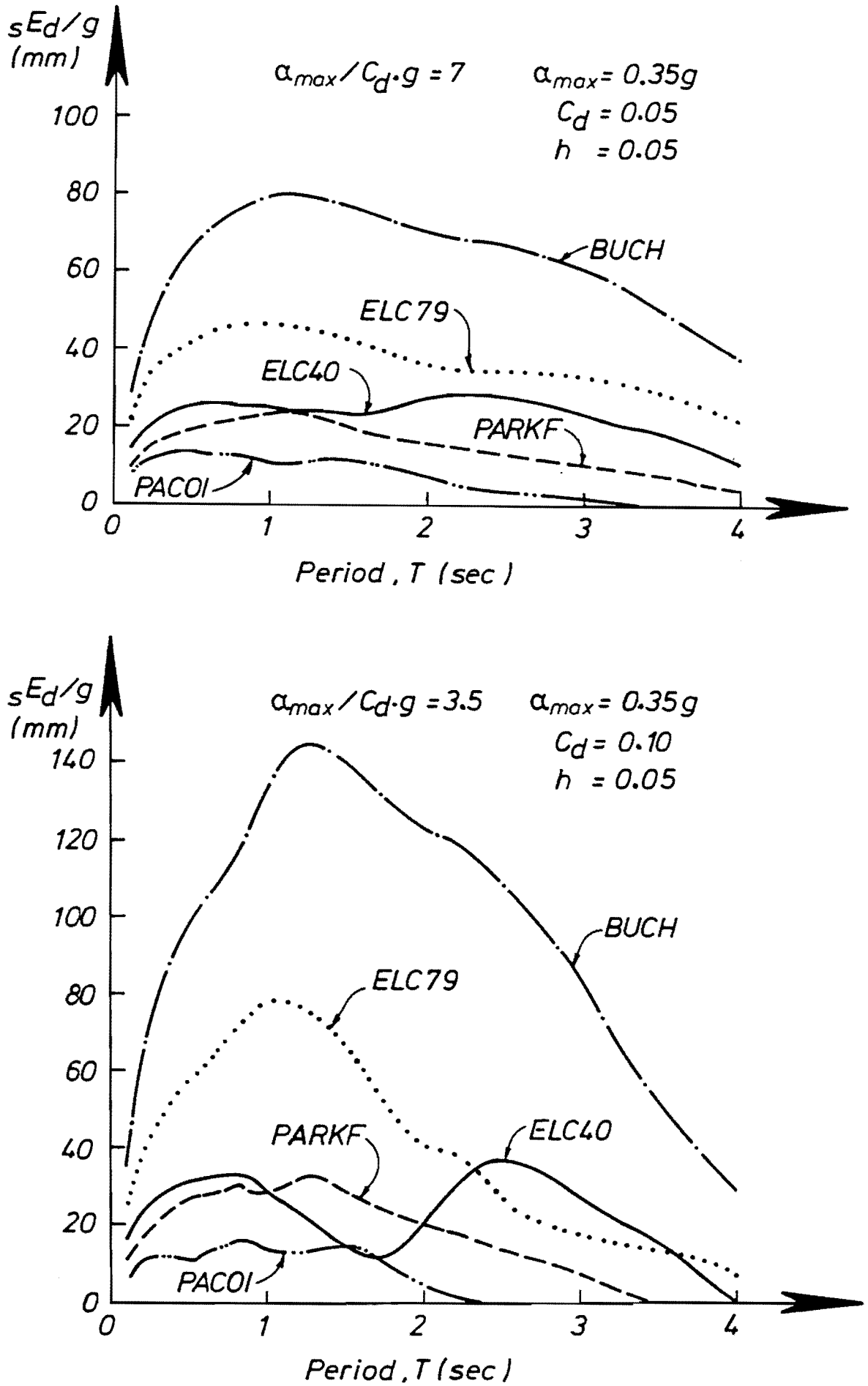

Fig. 7.4.5 Relationship between damage energy absorbed by a S.D.O.F. system and its resonant period

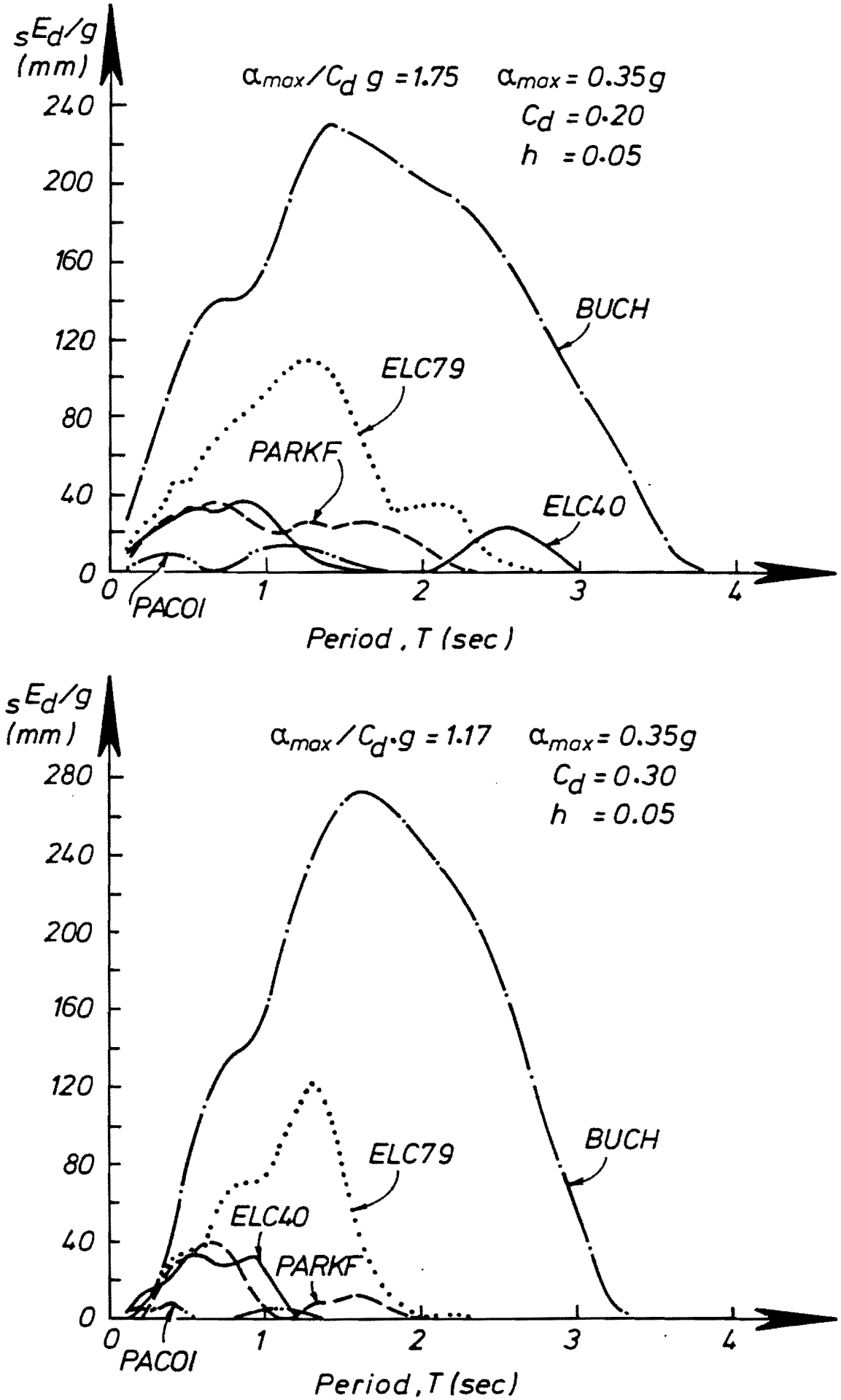

Fig. 7.4.6 Relationship between damage energy absorbed by a S.D.O.F. system and its resonant period

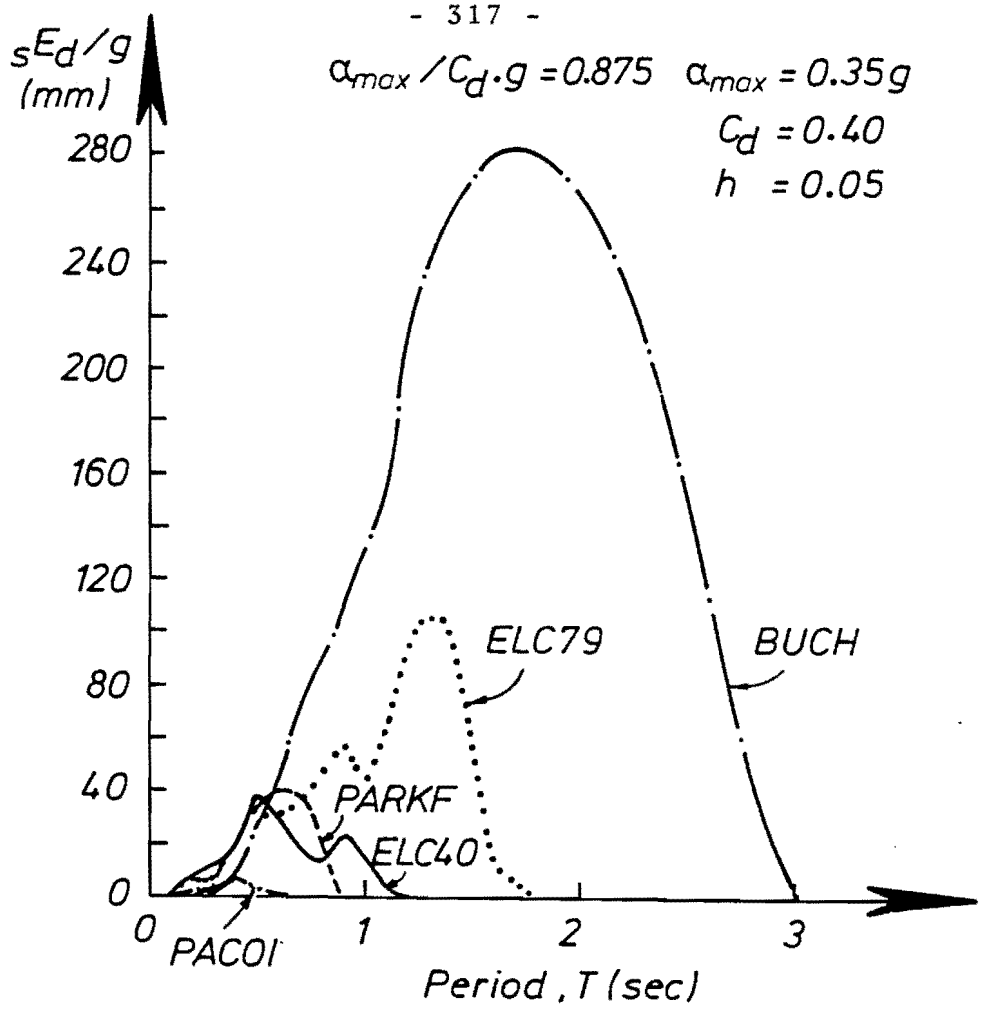

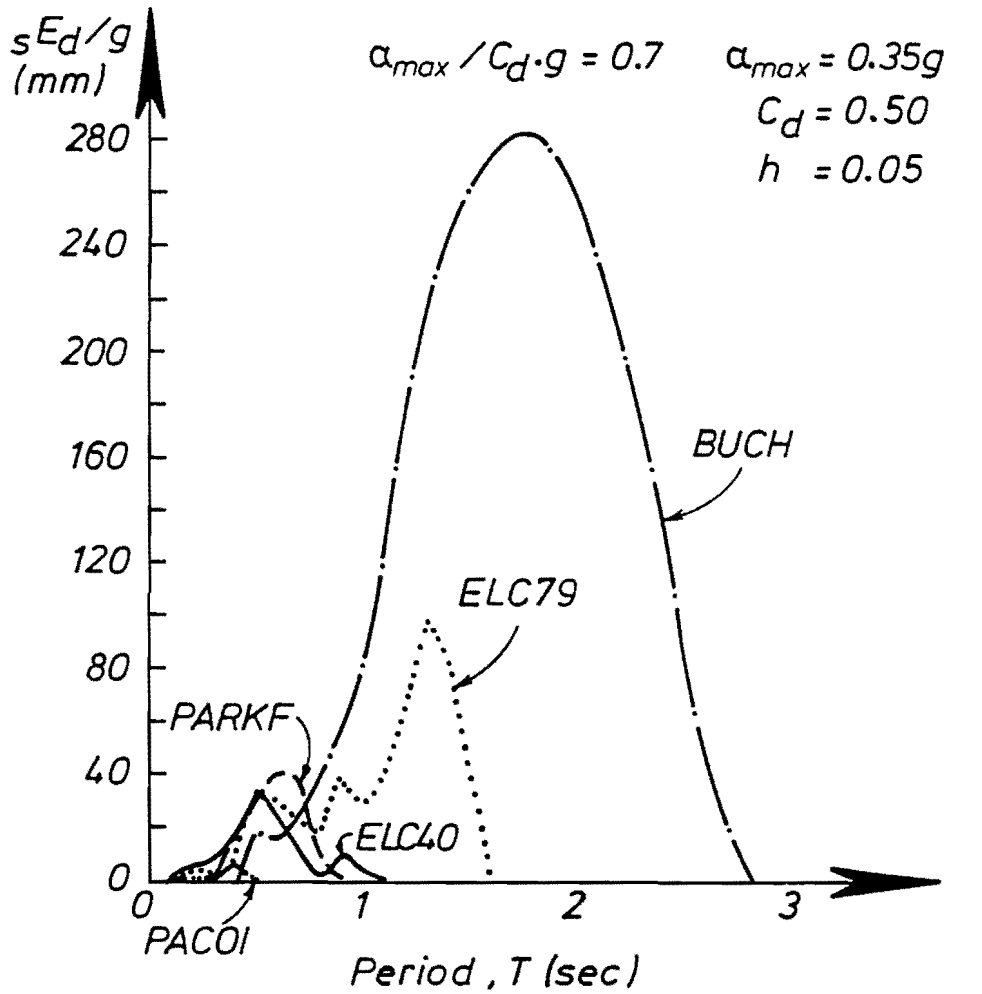

Fig. 7.4.7 Relationship between damage energy absorbed by a S.D.O.F. system and its resonant period

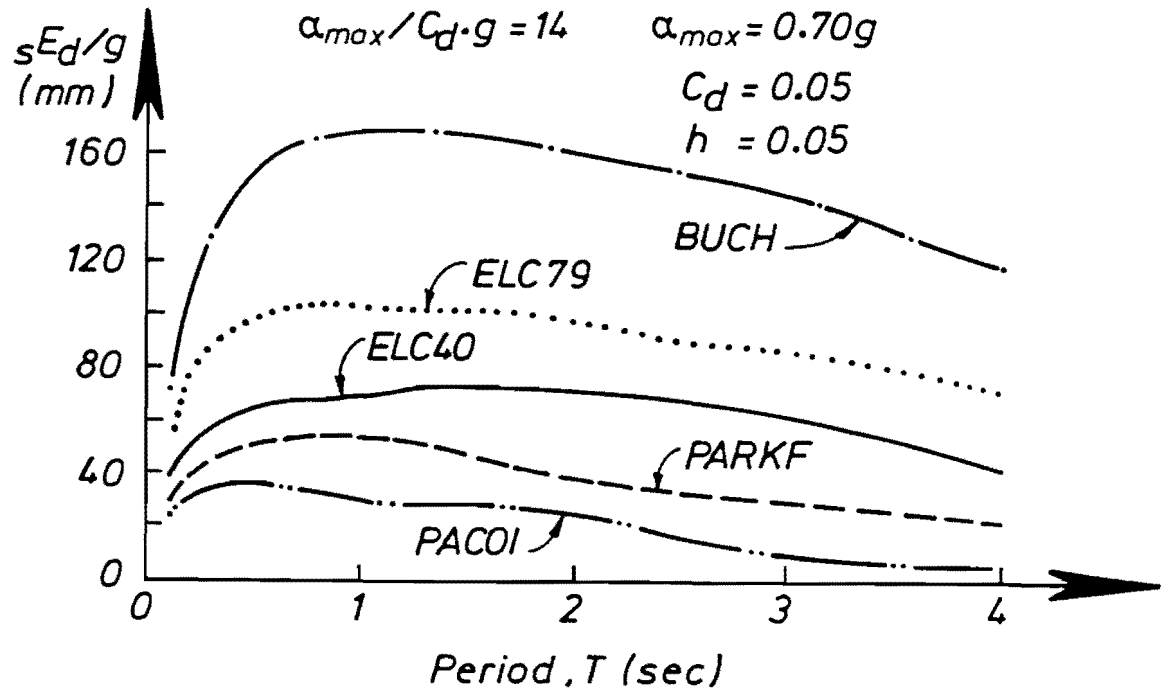

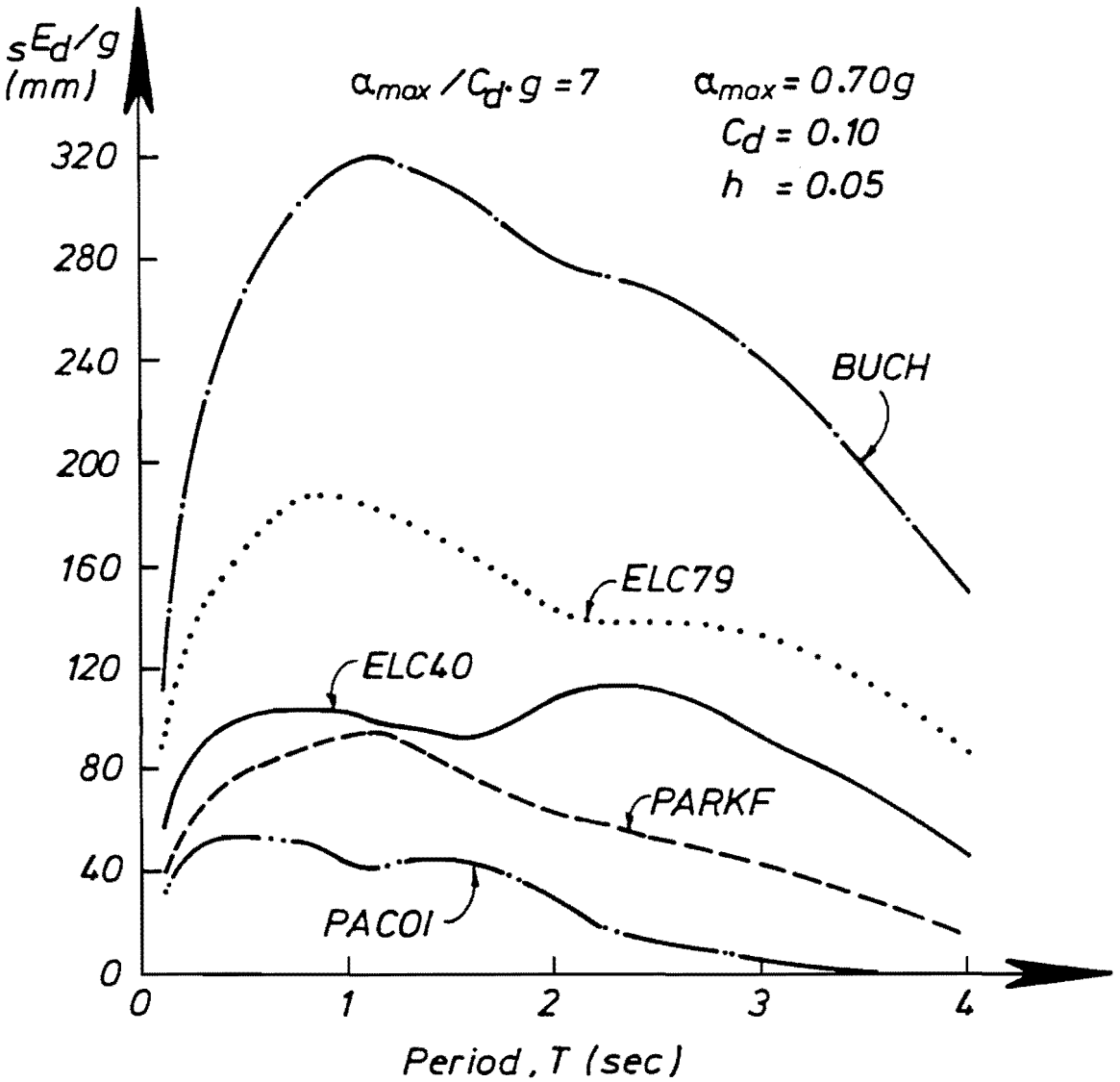

Fig. 7.4.8 Relationship between damage energy absorbed by a S.D.O.F. system and its resonant period

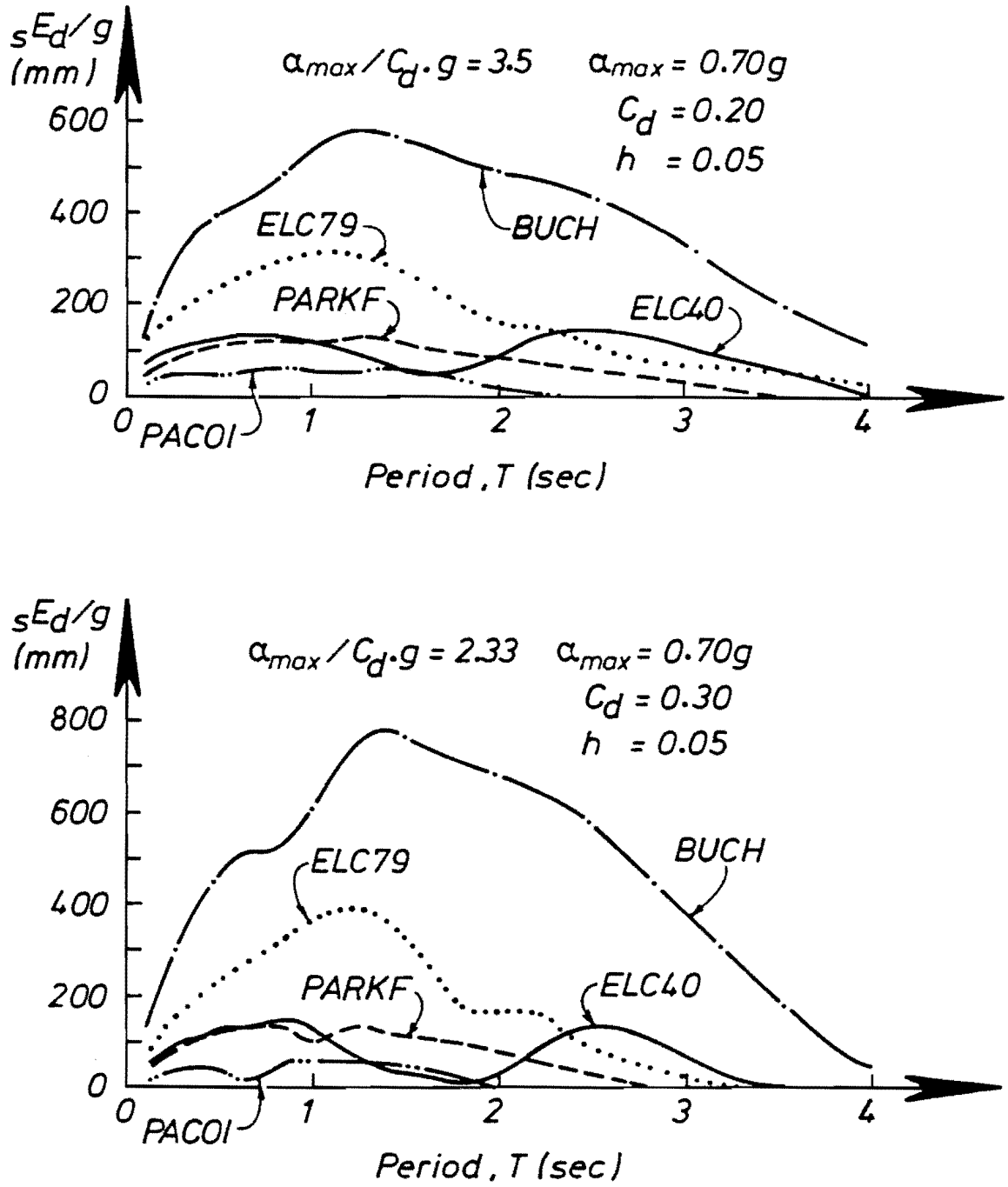

Fig. 7.4.9 Relationship between damage energy absorbed by a S.D.O.F. system and its resonant period

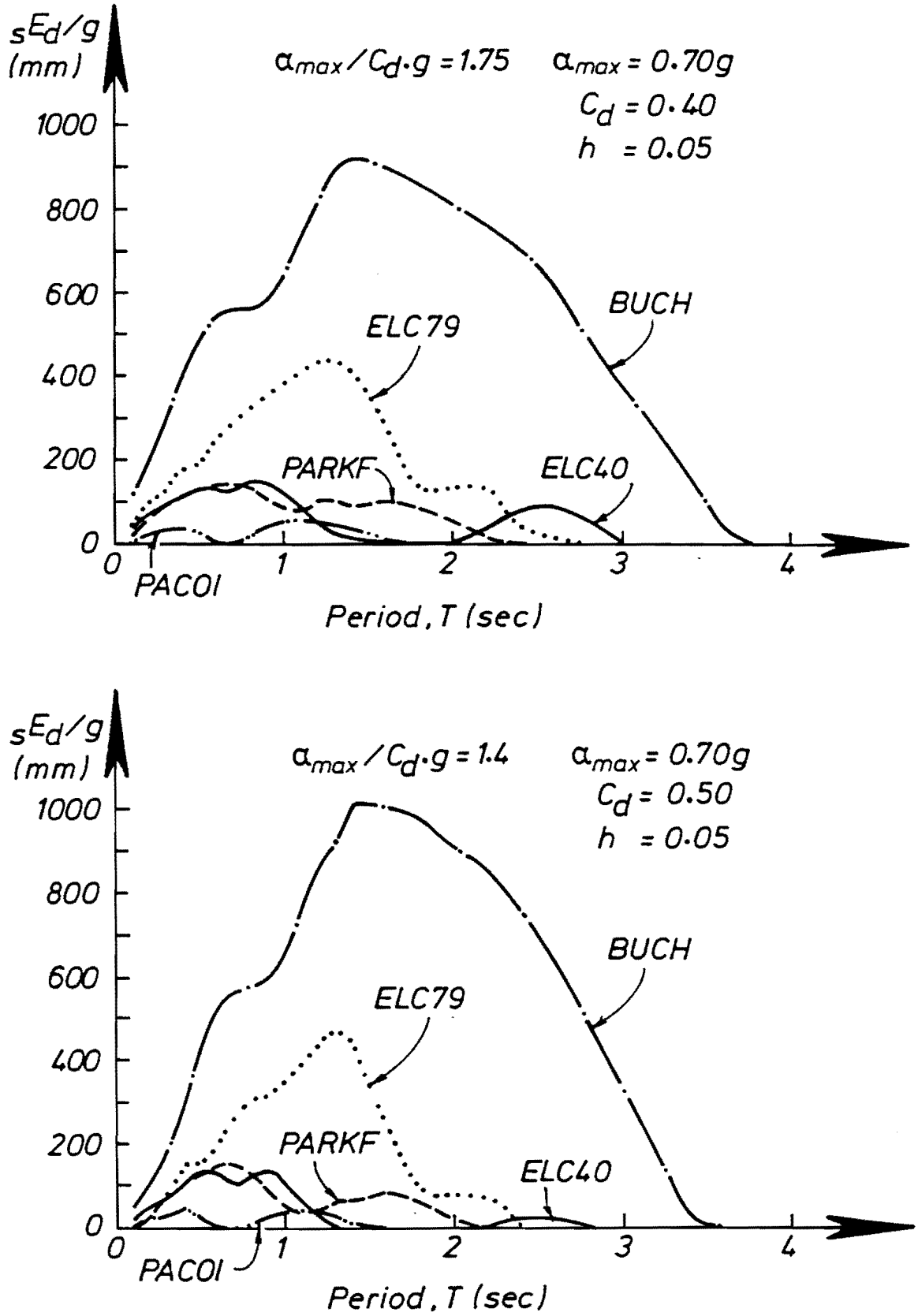

Fig. 7.4.10 Relationship between damage energy absorbed by a S.D.O.F. system and its resonant period

(4) The surface soil in Bucharest consisted of low rigidity sediments.

Such characteristics are not completely unlikely in New Zealand. Indeed, the northern part of the South Island around Nelson, which is not far from Wellington, has the possibility that an earthquake with at least the first three of the above conditions could occur (101,102). Thus, the Bucharest earthquake cannot be entirely eliminated.

In Figs 7.4.2-7.4.10, the following tendencies can be seen:

(1) The variance of ${}_sE_d$ - T relationship for a constant value of α_{max} caused by different earthquake records seems larger than that from different C_d values.

(2) The bigger the maximum acceleration, the larger the values of ${}_sE_d$.

(3) The shape of the ${}_sE_d$ - T relationship roughly depends on the ratio α_{max}/C_d. The bigger the ratio, the smaller the variation over T.

7.4.3 Distribution Parameters for Standard Damage Energy

In predicting damage energy input, it is important to know whether energy input is independent of structural characteristics. If the energy input markedly varies between structures with different values of T and C_d, the trend should be taken into account in its prediction. If not, the energy input can be simply assumed to be constant irrespective of differences in structural characteristics. In order to examine the dependency of ${}_sE_d$ on T and C_d, "Tests for significance of differences" (103), were carried out using the t table and the data in Figs 7.4.2-7.4.10. The test is used to tell whether there is a significant difference between two sample means, $\bar{x}$ and $\bar{y}$, where the standard deviations are unknown and believed to be different. In this case a set of samples both for x and y is five values of ${}_sE_d$ corresponding to different earthquakes. The variability of ${}_sE_d$ between different earthquake records is considered as inherent uncertainty since the maximum acceleration of the earthquakes was scaled to a specified value. For samples of x, values of ${}_sE_d$ with T = 0.4 (sec) and C_d = 0.1 for the five earthquakes were chosen for each value of α_{max}, which could be one possible combination of T and C_d for existing buildings. To compare with the samples of x, five values of ${}_sE_d$ for every other point of T and C_d corresponding to the same α_{max} as x were selected as samples of y. The procedure for examining a significant difference between the two samples is as follows.

(1) Calculate the mean values, $\bar{x}$ and $\bar{y}$, and squared deviations from mean, S_x and S_y, thus:

$$\bar{x} = \sum_{i=1}^{n_x} x_i / n_x \qquad (7.4.11)$$

$$\bar{y} = \sum_{i=1}^{n_y} y_i / n_y \qquad (7.4.12)$$

$$S_x = \sum_{i=1}^{n_x} (x_i - \bar{x})^2 \qquad (7.4.13)$$

$$S_y = \sum_{i=1}^{n_y} (y_i - \bar{y})^2 \qquad (7.4.14)$$

where: $n_x(n_y)$ = number of the x(y) samples ($n_x=n_y=5$)

$x_i(y_i)$ = ith sample of x(y)

(2) Read the value of t(f,0.05) from the t table where:

$$f = \left\{ \frac{C^2}{n_x-1} + \frac{(1-C)^2}{n_y-1} \right\}^{-1} \qquad (7.4.15)$$

$$C = \frac{S_x}{n_x(n_x-1)} \left\{ \frac{S_x}{n_x(n_x-1)} + \frac{S_y}{n_y(n_y-1)} \right\}^{-1} \qquad (7.4.16)$$

(3) Calculate the value of t_o from:

$$t_0 = \frac{\bar{x} - \bar{y}}{\sqrt{S_x/n_x(n_x-1) + S_y/n_y(n_y-1)}} \qquad (7.4.17)$$

(4) When t_o is less than t(f,0.05), the means of x and y, μ_x and μ_y are not significantly different with a 5% degree of risk.

The comparisons between x and y are shown in Fig. 7.4.11 for α_{max} values of 0.20, 0.35 and 0.70 g. A circle in the figures indicates that the mean value of ${}_sE_d$ at the point is not significantly different from that for T = 0.4 (sec) and C_d = 0.1. From the results, it is found that there are two regions, A and B as shown in Fig. 7.4.12, whose mean values of ${}_sE_d$ are significantly smaller than those for a T of 0.4 and C_d of 0.1. The regions become bigger when α_{max} is smaller.

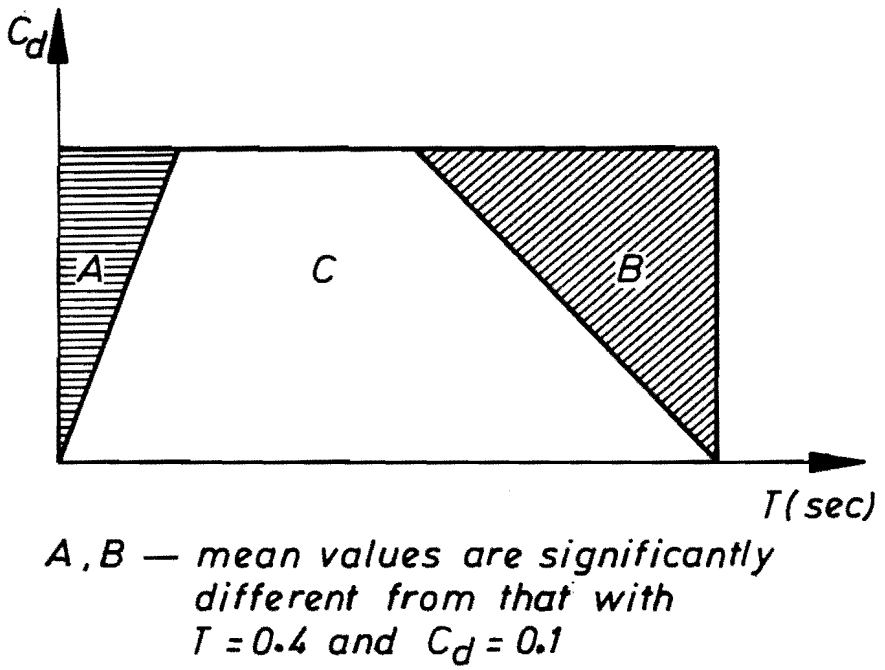

Fig. 7.4.12 Classification of T-Cd regions based on mean values of damage energy

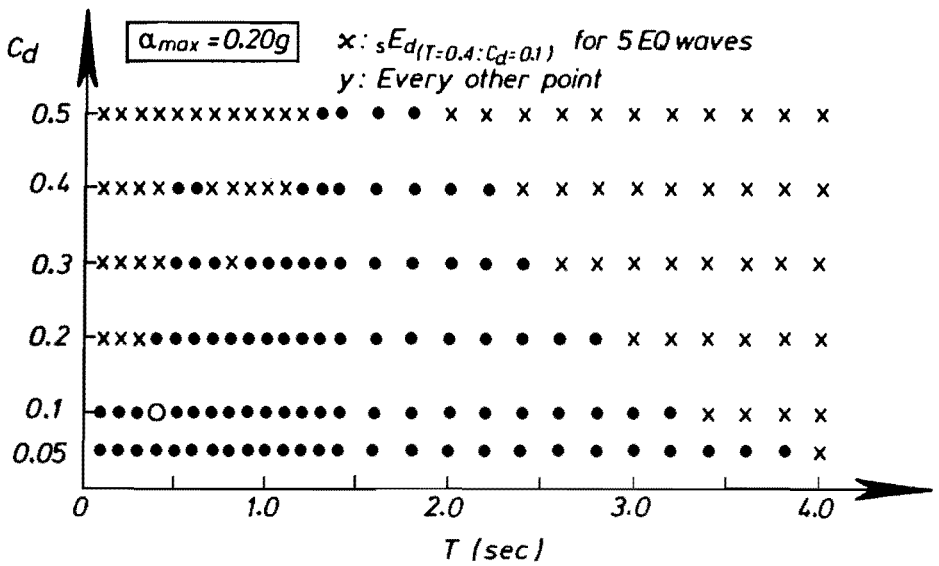

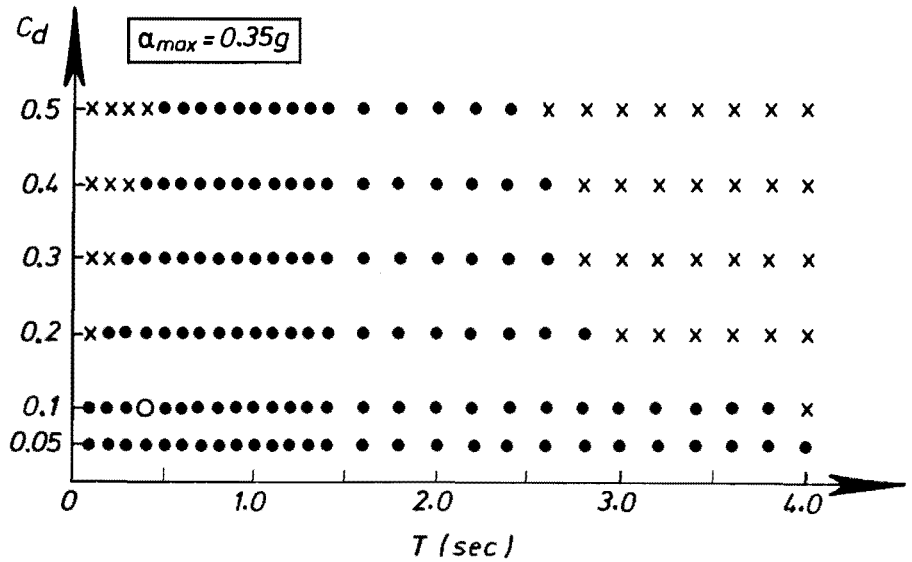

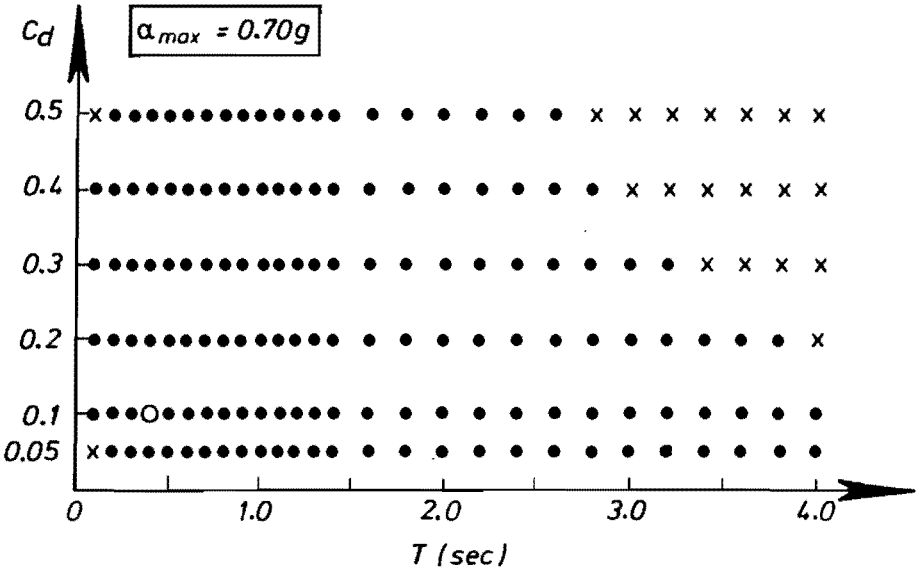

$$t_0 = \frac{\bar{x} - \bar{y}}{\sqrt{\frac{S_x}{n_x(n_x-1)} + \frac{S_y}{n_y(n_y-1)}}}$$

$$C = \frac{S_x/n_x(n_x-1)}{\frac{S_x}{n_x(n_x-1)} + \frac{S_y}{n_y(n_y-1)}}$$

$$\frac{1}{f} = \frac{C^2}{n_x-1} + \frac{(1-C)^2}{n_y-1}$$

× $t_0 \geq t(f, 0.05)$
• $t_0 < t(f, 0.05)$

Fig. 7.4.11 Results of test for significant difference

However, in predicting damage energy input for different structures, the realistic range of T - C_d combinations for existing buildings should be taken into account. It is generally true that C_d is not big when T is large. Thus, region B in Fig. 7.4.12 is a region we need not consider in predicting the energy input for existing buildings. In addition, the failure probability for a building with a small T and large C_d (region A) subjected to an earthquake would be considerably smaller than that due to gravity load. If so, the contribution of the earthquake-related failure probability to the total failure probability for that type of structures would be negligible. Hence, a rough assumption with regard to ${}_sE_d$ for structures in region A (see Fig. 7.4.12) would not significantly affect code development. Moreover, the inherent uncertainty involved in the prediction of ${}_sE_d$ is high. Therefore, for existing buildings, the damage energy input ${}_sE_d$ can be assumed to be stochastically identical regardless of the characteristics of the structures.

In order to determine the distribution and parameters of ${}_sE_d/g$ for a value of α_{max}, a histogram of ${}_sE_d$ must be obtained, using the computed results for ${}_sE_d/g$ given in Figs 7.4.2-7.4.10. (The item ${}_sE_d/g$ is rather convenient in estimating the distribution of E_{d_T}/w_t, see Eq. (7.4.18)). A point to be considered is what data should be taken into account. Following the discussion above, five different classifications (C-1)-(C-5) as shown in Fig. 7.4.13 were used; points indicated by circles in a T-C_d relationship were included in estimating a histogram. Each point has

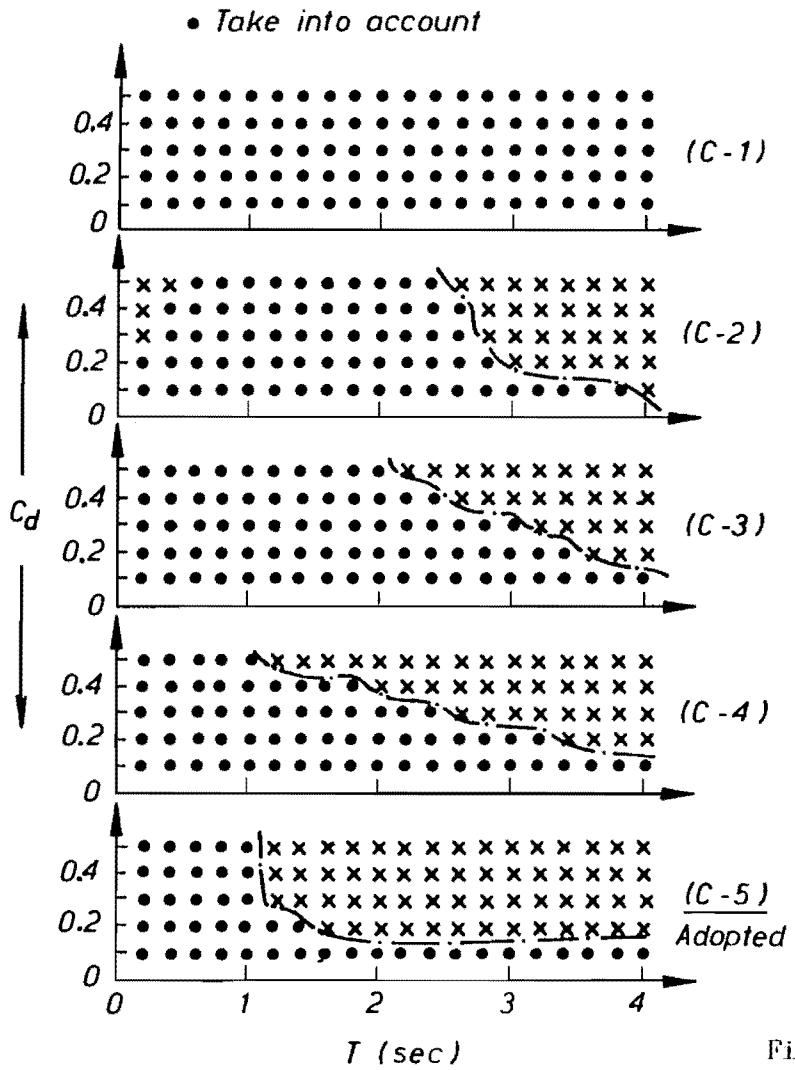

	α_{max}=0.20g		α_{max}=0.35g		α_{max}=0.70g	
	λ	ζ	λ	ζ	λ	ζ
(C-1)	-1.16	2.93	1.70	2.12	3.99	1.55
(C-2)	0.023	2.53	2.54	1.80	4.48	1.34
(C-3)	-0.34	2.69	2.30	1.91	4.45	1.31
(C-4)	-0.067	2.64	2.50	1.77	4.56	1.18
(C-5) Adopted	-0.30	2.30	2.82	1.40	4.60	1.10

λ, ζ - Parameters of log-normal distribution

Fig. 7.4.13 Classification of T-Cd regions and distribution parameters of damage energy

five values of ${}_sE_d/g$ corresponding different earthquakes for a value of α_{max}. The class of (C-1) involves all points, i.e. C_d = 0.1-0.5 (ΔC_d = 0.1) and T = 0.2-4.0 (sec) (ΔT = 0.2 (sec)). In (C-2), the areas corresponding to A and B in Fig. 7.4.12 were assumed and eliminates from the area for the data points. The classes of (C-3)-(C-5) were set by considering the range of T-C_d for existing buildings. The area of (C-5) is probably the most realistic range of T-C_d for existing buildings (62). The aim of the classification is to examine the sensitivity of failure probabilities to the classification in determining a distribution and parameters for damage energy input (see Section 7.5). If the influence of the classification on the results is negligibly small, much attention need not be paid to it.

A distribution of ${}_sE_d/g$ for each class can now be obtained. For instance, in the class of (C-5), 42 points were considered in T-C_d relations, and so 210 values of ${}_sE_d/g$ for each α_{max} value can be used to determine the distribution and parameters. Because ${}_sE_d$ is non-negative, a log-normal distribution is assumed to be appropriate rather than a normal distribution. Using the concept of probability paper (104) and regression analysis, the log-normal parameters, λ and ζ were calculated for the distributions corresponding to the five different classes and the three values of α_{max}. In the regression analysis, the points where ${}_sE_d$ equalled zero were neglected. The parameters obtained are also shown in Fig. 7.4.13. It is found that coefficients of variation of ${}_sE_d/g$ which are approximately the same as ζ, are much bigger than those normally expected for structural characteristics.

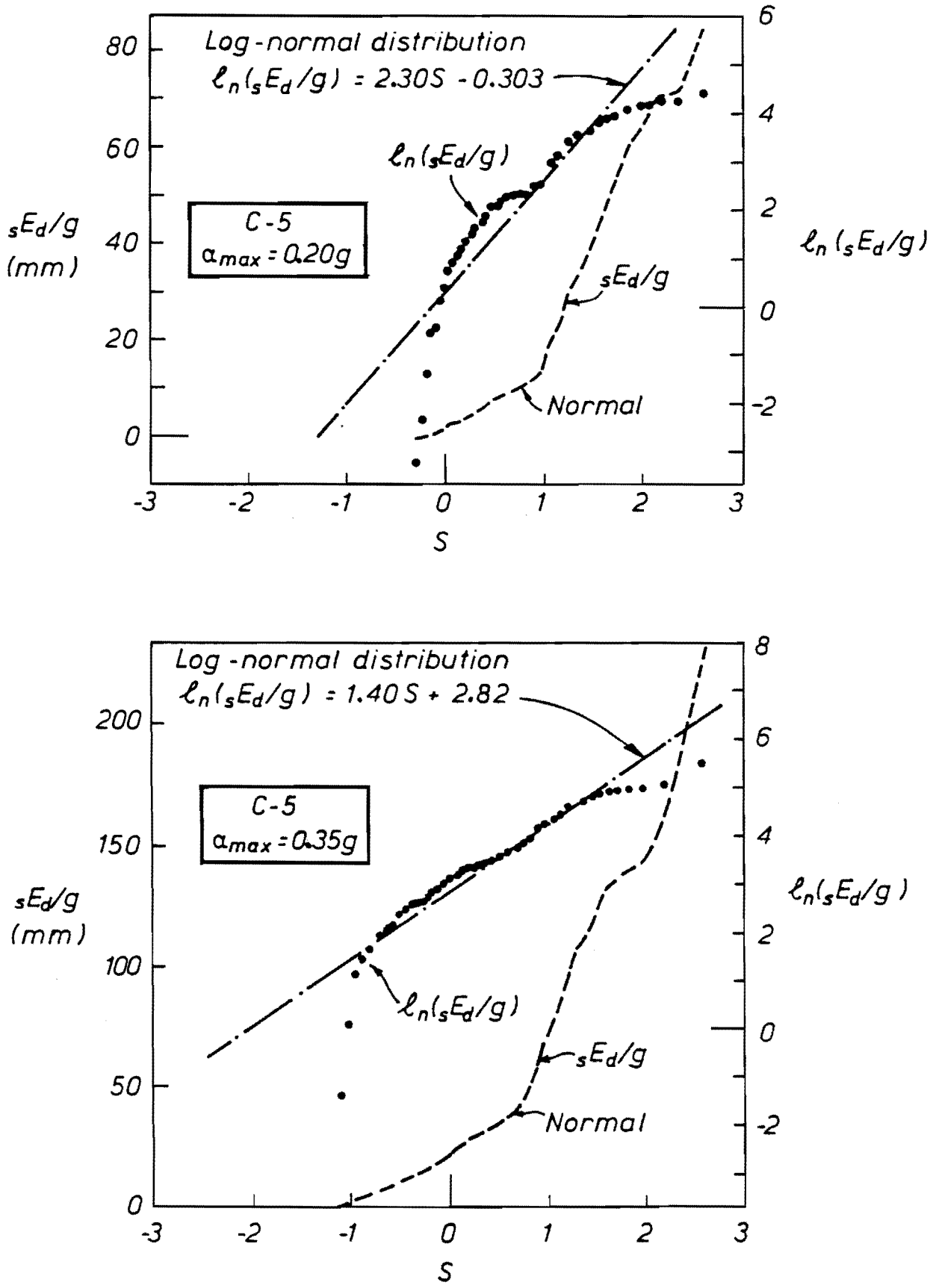

Fig. 7.4.14 Results of regression analysis for damage energy distribution

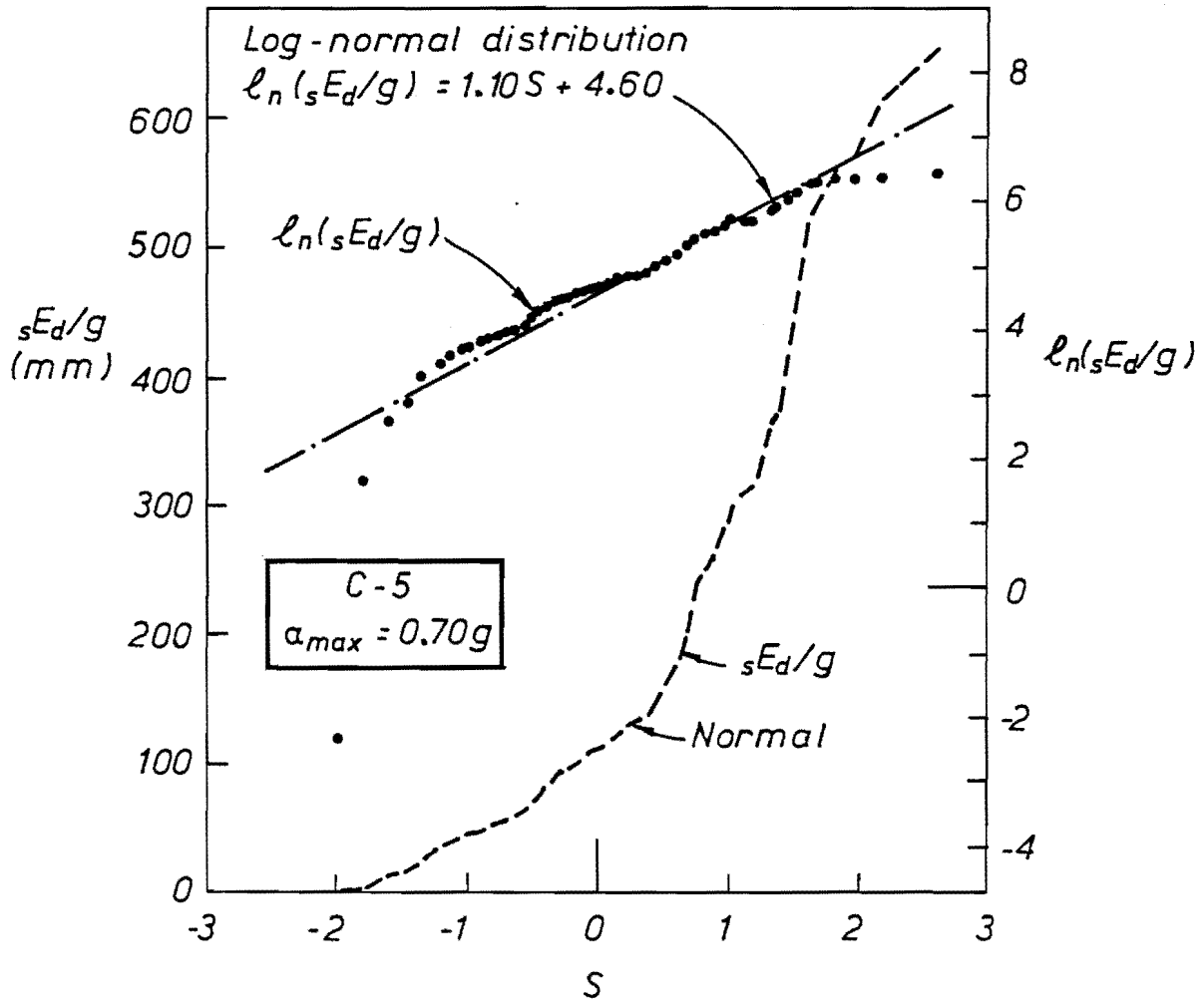

Fig. 7.4.15 Results of regression analysis for damage energy distribution

Figures 7.4.14 and 7.4.15 illustrate the fitting of ${}_sE_d/g$ to a log-normal distribution in the case of (C-5). It can be seen that the fit for larger values of α_{max} is better than that for smaller values. However, in general the distributions of ${}_sE_d/g$ seem to be satisfactorily fitted by a log-normal distribution.

Since the damage energy input ${}_sE_d$ is assumed to be stochastically identical regardless of the values of resonant period T and base shear coefficient C_d of structures, Eq. (6.3.23) can be rewritten as:

$$\frac{E_{d_T}}{w_t} = \frac{{}_sE_d}{g} \times \sum_{j=1}^{n} \frac{ef.M_j}{M_T} = \frac{{}_sE_d}{g} \qquad (7.4.18)$$

This means that the standard damage energy input E_{d_T}/w_t for M.D.O.F. systems has the same probability distribution as ${}_sE_d/g$ given in Fig. 7.4.13. Thus, the distributions and parameters of E_{d_T}/w_t is also independent of characteristics of structures and depends only on α_{max}.

We have thus made the required assumptions for all random variables used in calculating conditional failure probabilities, necessary for the sensitivity studies discussed in the next section.

7.5 SENSITIVITY STUDIES

7.5.1 Introduction

The necessary preliminaries for calculating failure probabilities are now almost complete. A basic calculation procedure and the appropriate assumptions concerning its variables have been determined. However, in order to refine the procedure, three problems must be resolved, which are dealt with by sensitivity studies.

Firstly, it is important to eliminate unnecessary complexity from the procedure. Several random variables are involved in the computation and each variable has a certain variability. But not all variability affects the results strongly. Some quantities which have only a slight influence on the results can be taken as deterministic variables. Such a simplification is acceptable on the basis of consistency with the total uncertainty involved in the procedure. To select the appropriate variables, the sensitivity of failure probability to variability of the variables must be examined. The sensitivity may vary from structure to structure. However, because the variability in predicting earthquake intensity is much bigger than that for structural characteristics, the variation of sensitivity between structures can be assumed to be small. Hence the number of buildings used in examining the sensitivity need not be large. The three frames described in Appendix A were used for the sensitivity studies.

As a result of the studies, it was found that all parameters except the standard damage input could be taken as deterministic variables. This has the considerable advantage that it makes the conditional failure probability of an entire structure, $p_{f|EQ}$ calculable from those for individual storeys, $p_{f_i|EQ}$ without using complicated bounding operations.

Secondly, it must be realised that the proportion of the standard damage energy introduced into each storey is dependent on earthquake records. (However, it is not required to specify an earthquake record for determining the standard damage energy E_{d_T}/w_t, which depends only on values of α_{max}.) Accordingly, we must consider the number of earthquake records necessary for obtaining an acceptable accuracy in the results. It is equivalent to determining an appropriate number for n_s (see section 7.3). This is also a problem of sensitivity. The variation of failure probabilities due to different earthquake records is examined and compared with the total uncertainty.

Thirdly, the sensitivity of failure probabilities to the classification for obtaining a distribution of E_{d_T}/w_t illustrated in Fig. 7.4.13 is necessary for confirming that the influence of the classification on the result is indeed negligible. An appropriate distribution of E_{d_T}/w_t for a value of α_{max} is then chosen.

7.5.2 Sensitivity Studies

In calculating the conditional failure probability $p_{f_i|EQ}$ of the ith storey using Eq. (7.4.4), there are five basic random variables as shown in Table 7.4.1. Of the five, the standard damage energy input E_{d_T}/w_t has the largest variance and might therefore be supposed to dominate the calculation. In order to confirm this, sensitivity studies must be carried out to examine the influence of the variance of each parameter on the results.

It is important to understand the relationship between E_{d_T}/w_t possessing the biggest variability and every other random variable. Therefore, firstly, the sensitivity of $p_{f_i|EQ}$ is discussed, assuming that E_{d_T}/w_t and another basic random variable are the only random variables, with the other variables being assigned their mean values. In the study a 3 storey-model is used with the distributions assumed in Table 7.4.1 to understand the basic relationship between two random variables. Afterwards, 3, 7 and 30-storey frames are used in the study for confirming whether only E_{d_T}/w_t can be taken as a random variable. For the distribution parameters of E_{d_T}/w_t, the class of (C-5) (see Fig. 7.4.13) is selected because it is finally adopted in the present study. The variance ζ for each value of α_{max} is the smallest for (C-5) compared with the variances for the other classes.

(1) Relationship between standard damage energy E_{d_T}/w_t and coefficient C

Figure 7.5.1 shows the failure surfaces for the 3rd storey of the 3-storey model in reduced coordinates (see 2.2.2), considering E_{d_T}/w_t and C. The El Centro 1940 NS earthquake record was used to calculate ${}_eE_{d_3}/{}_eE_{d_T}$ that is the proportion of E_{d_T}/w_t absorbed into the 3rd storey. The failure surfaces for three different values of α_{max} meet the axis of $(E_{d_T}/w_t)'$ at almost right angles. This implies that the failure surfaces are very sensitive to E_{d_T}/w_t but not to C. If E_{d_T}/w_t alone were a random variable and C were deterministic, the failure surface would be a straight line and cut the axis of $(E_{d_T}/w_t)'$ at right angles at the point of intersection between the original failure surface and the $(E_{d_T}/w_t)'$ axis. The failure region would not be very different from the failure surface shown in Fig. 7.5.1. Therefore, the effect of the variability of C on the probability of failure is negligible, compared with that for E_{d_T}/w_t.

(2) Relationship between standard damage energy E_{d_T}/w_t and yield storey drift δ_{y_i}

The failure surfaces with regard to E_{d_T}/w_t and δ_{y_i} (i = 1, 2 and 3) for α_{max} = 0.20 g are shown in Fig. 7.5.2(a). The same discussion as for the E_{d_T}/w_t - C relationship can be applied to this case. Though the failure surfaces are non-linear when $(E_{d_T}/w_t)'$ and δ_{y_i}' are large, they are far more sensitive to E_{d_T}/w_t than to δ_{y_i}, because they are almost vertical in the region close to the origin where the probability density is highest. Thus, the variability of

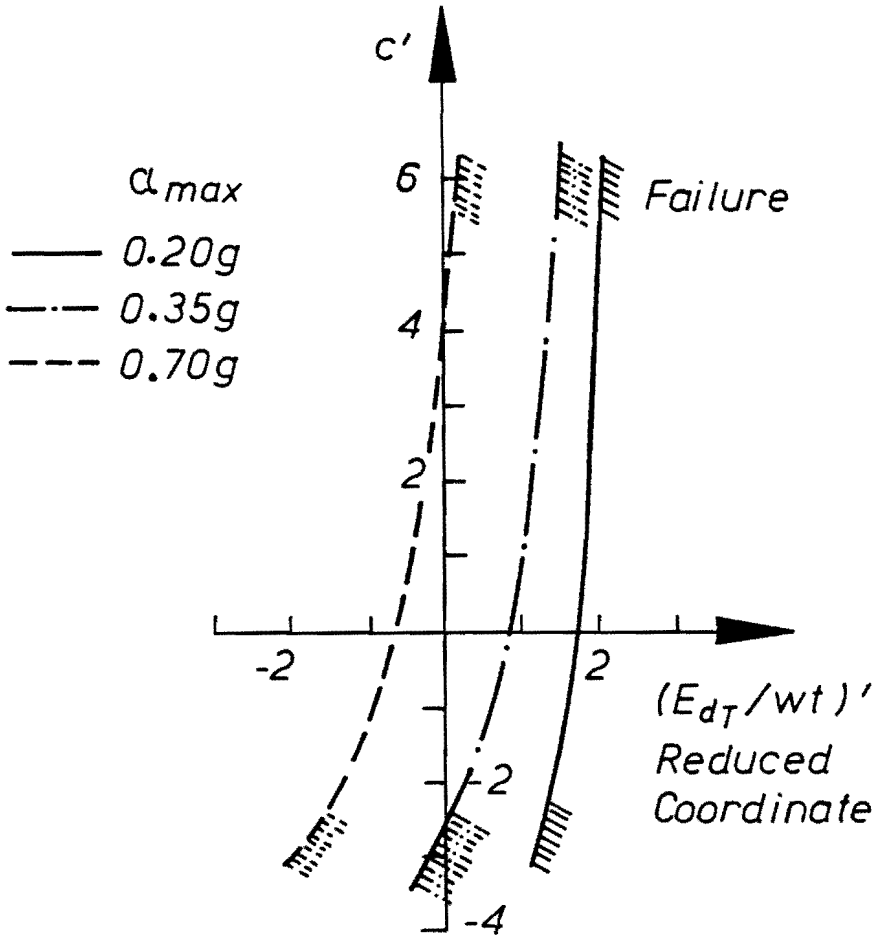

Fig. 7.5.1 Failure surfaces with regard to damage energy and a constant c

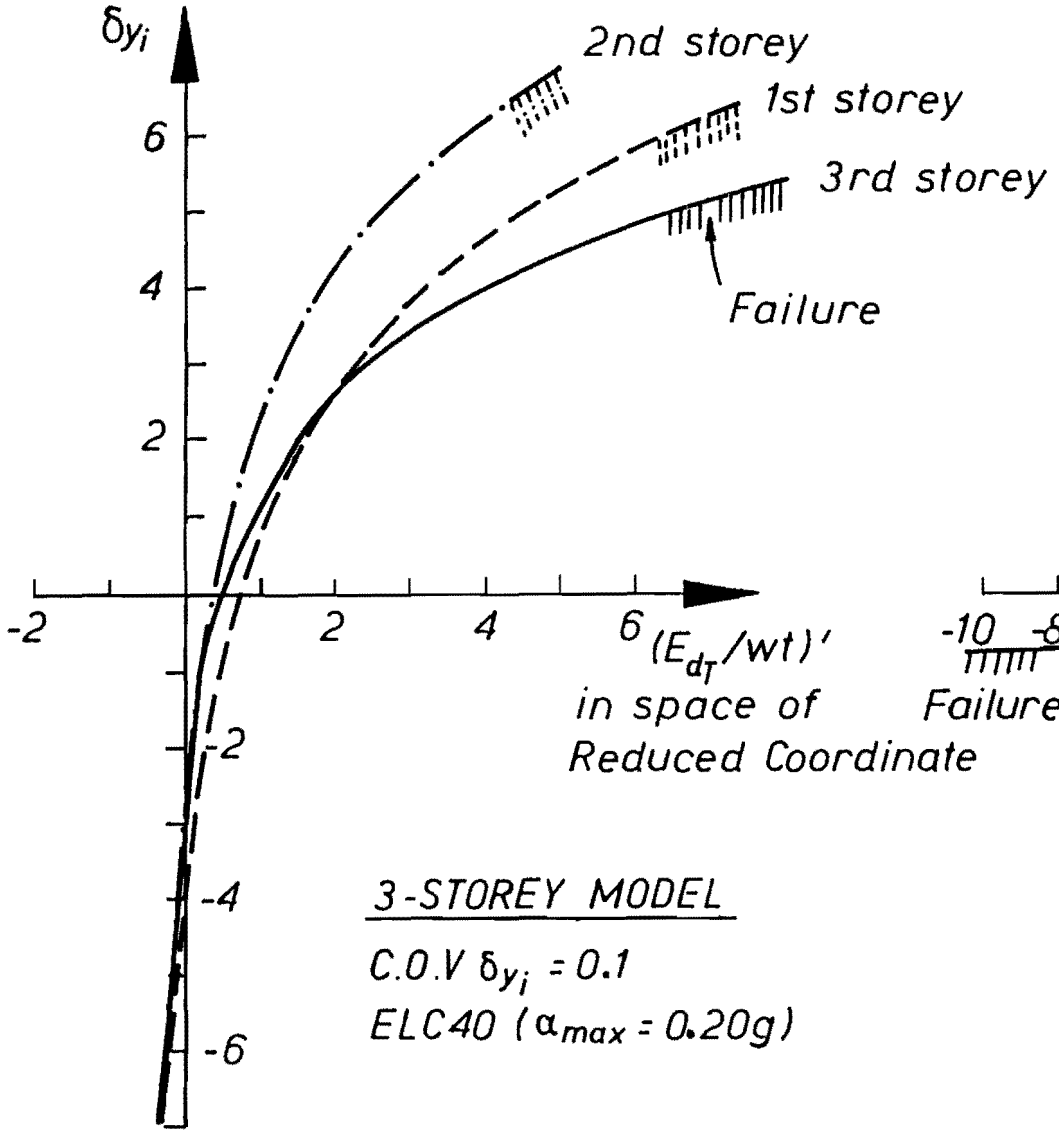

Fig. 7.5.2(a) Failure surfaces with regard to damage energy and yield storey drift

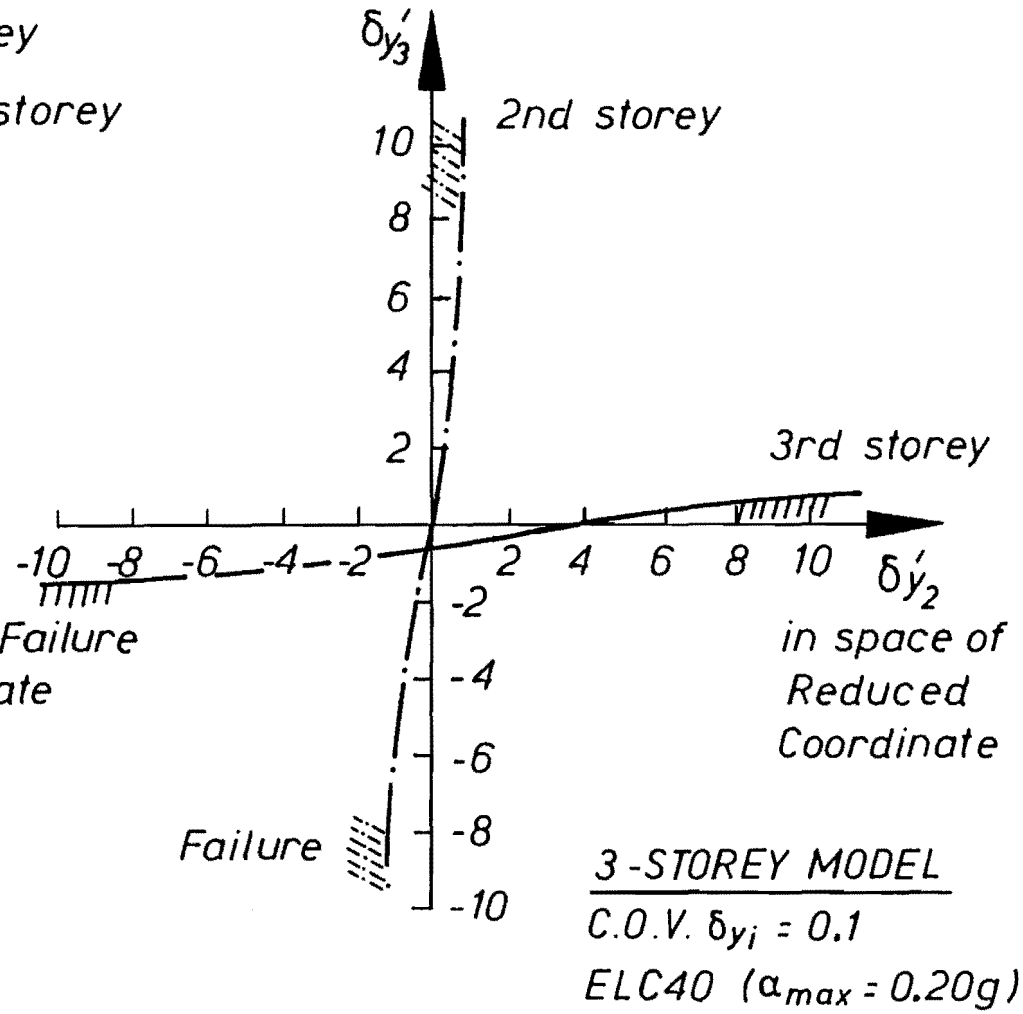

Fig. 7.5.2(b) Failure surfaces with regard to yield storey drifts of 2nd and 3rd storeys

δ_{y_i} is less important than that of E_{d_T}/w_t in calculating the ith storey conditional failure probability $p_{f_i|EQ}$. In addition, the jth yield storey drift δ_{y_j} $(j \neq i)$ is also involved in the calculation of $p_{f_i|EQ}$ for the ith storey. (According the Eqs (7.4.8) and (7.4.9), ${}_eE_{d_T}$ includes yield storey drifts of all storeys.) In order to examine the influence of δ_{y_j} $(j \neq i)$ on $p_{f_i|EQ}$, the failure surfaces for the 2nd and 3rd storeys of the 3-storey model are shown in Fig. 7.5.2(b), considering δ_{y_2} and δ_{y_3}. The figure indicates that in calculating the conditional failure probability of a storey, the yield storey drift of the storey affects the probability of failure more strongly than the yield storey drift of the other storeys because the failure surface for the ith storey is almost perpendicular to the axis corresponding to δ_{y_i}.

(3) Relationship between the standard damage energy E_{d_T}/w_t and the total weight w_t

The total weight w_t is explicitly related to $p_{f_i|EQ}$ as a product of E_{d_T}/w_t according to Eq. (7.4.7). However its coefficient of variation (C.O.V.) is at most 0.1 because the C.O.V. of w_i (weight of ith storey) is 0.1 as given in Table 7.4.1, while that of E_{d_T}/w_t varies between 1.1 and 2.3 ($\zeta \doteqdot$ C.O.V.). The variability of w_t is therefore negligible in comparison with that of E_{d_T}/w_t.

The other thing one should take into account concerning the variation of w_t is that it affects the resonant periods of a structure. That is, ${}^{\Omega}\delta_i$ and ${}^{\sigma}\delta_i$ in Eq. (7.4.8), which are

related to moments of the response spectral - density function, are implicitly concerned with the variation of w_t. For example, the dispersion of Ω_{δ_i} and σ_{δ_i} due to a C.O.V. of 0.1 of w_i using scaled El Centro 1940 NS records is illustrated in Figs 7.5.3 and 7.5.4. It is found from the figures that Ω_{δ_i} and σ_{δ_i} are dependent random variables on w_i. In order to deal with the effect, an equivalent C.O.V. of δ_y is assumed which is considered to contain the effect of the variability of both δ_y and w_i. The procedure for obtaining the equivalent coefficient of variation is as follows.

(i) The value of the C.O.V. of δ_y is fixed such that the distribution of ${}_eE_{d_i}/{}_eE_{d_T}$ when only the δ_y's are random variables is equal to that when both the δ_y's and w_i's are random variables. The latter distributions using a 3-storey model subjected to El Centro 1940 NS and Bucharest 1977 NS earthquakes have been obtained in Figs 6.3.15 and 6.3.16. For the comparison of the results obtained by the random vibration method, the distributions of ${}_eE_{d_i}/{}_eE_{d_T}$ with the δ_y's alone as random variables were calculated with a sample size of 100 as shown in Figs 7.5.5 and 7.5.6. In order to obtain almost the same distributions of ${}_eE_{d_i}/{}_eE_{d_T}$ illustrated in Figs 6.3.15 and 6.3.16, the C.O.V. of δ_{yi} in the case of the El Centro earthquake is 0.2, 0.2 and 0.5 for α_{max} values of 0.20, 0.35 and 0.70 g, respectively, and for the Bucharest earthquake 0.1, 0.2 and 0.3. To be on the conservative side, the C.O.V. of δ_{y_i} is assumed to be 0.2, 0.2 and 0.5 for the α_{max} values regardless of earthquake.

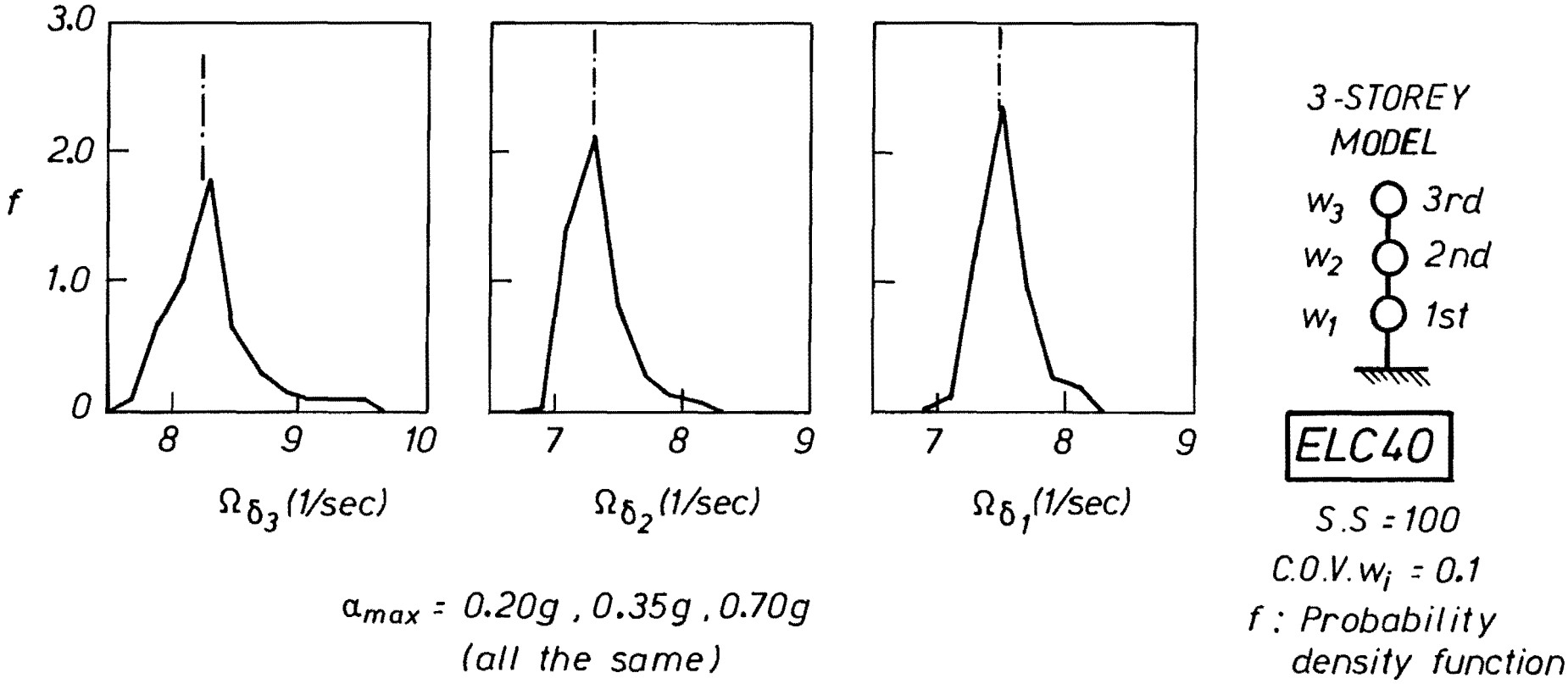

Fig. 7.5.3 Distribution of Ω_{δ_i} due to variation of weight of a structure

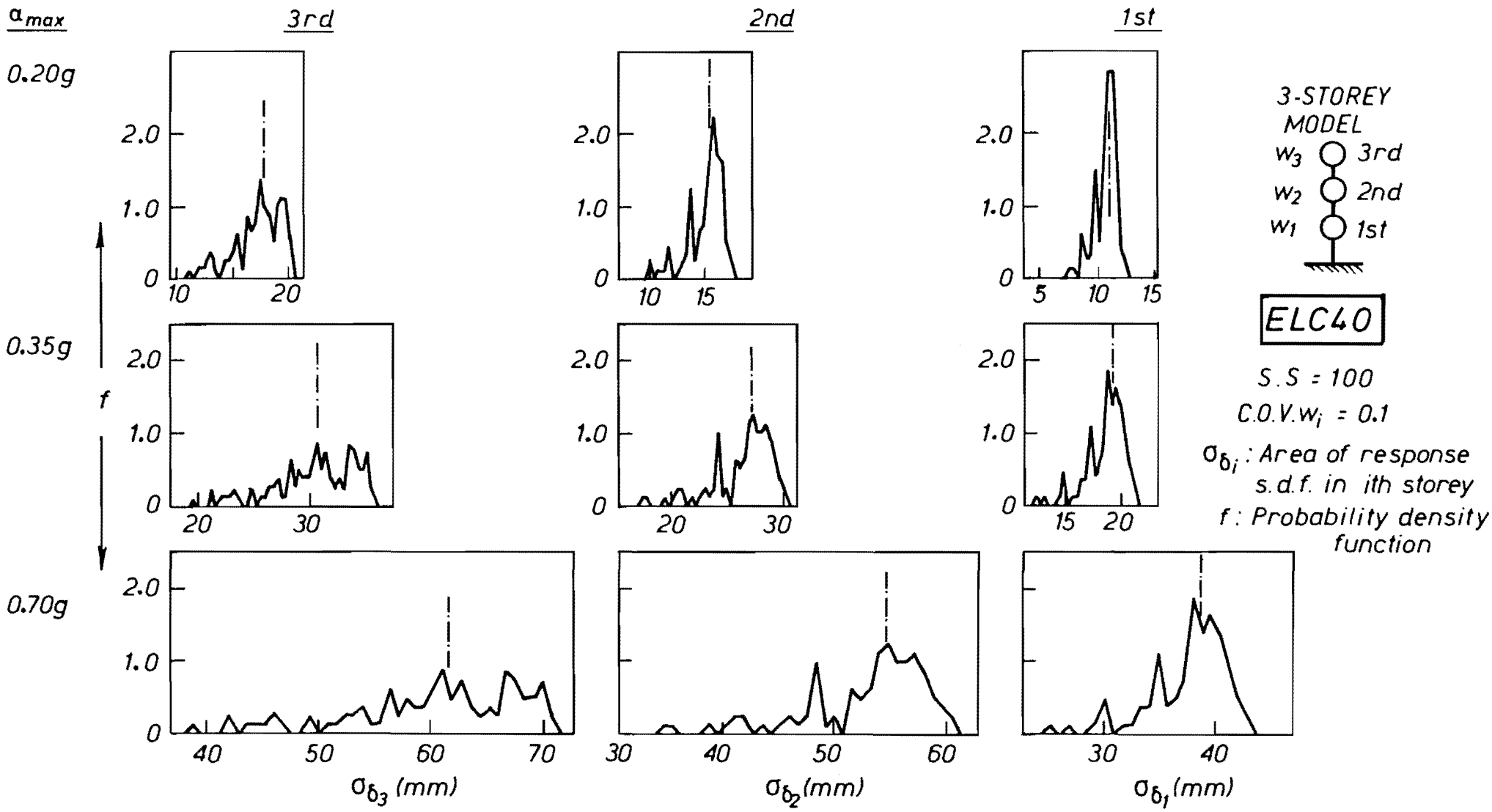

Fig. 7.5.4 Distribution of σ_{δ_i} due to variation of weight of a structure

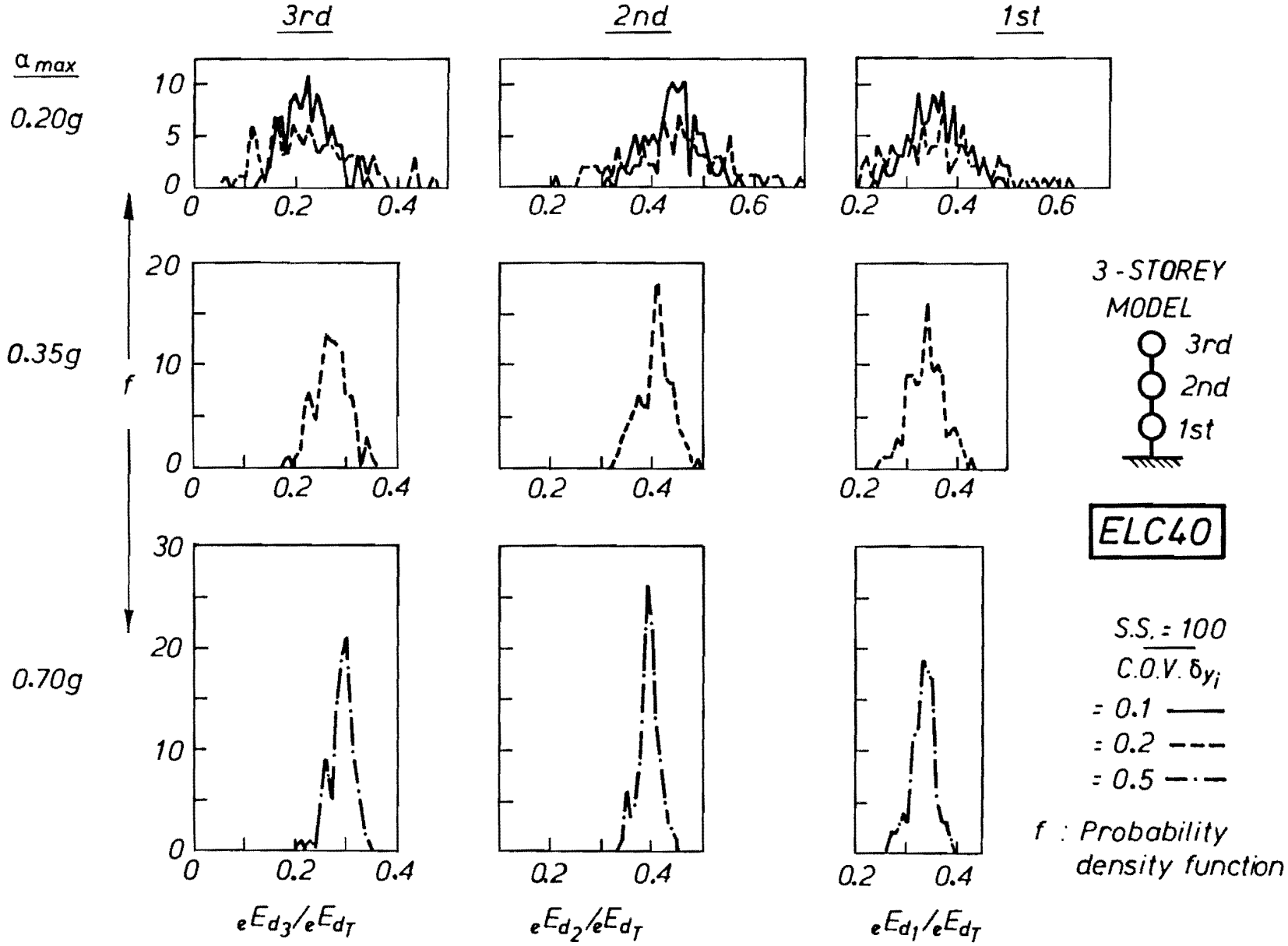

Fig. 7.5.5 Dispersion of proportion of damage energy absorbed by a storey due to variation of yield storey drifts (ELC40)

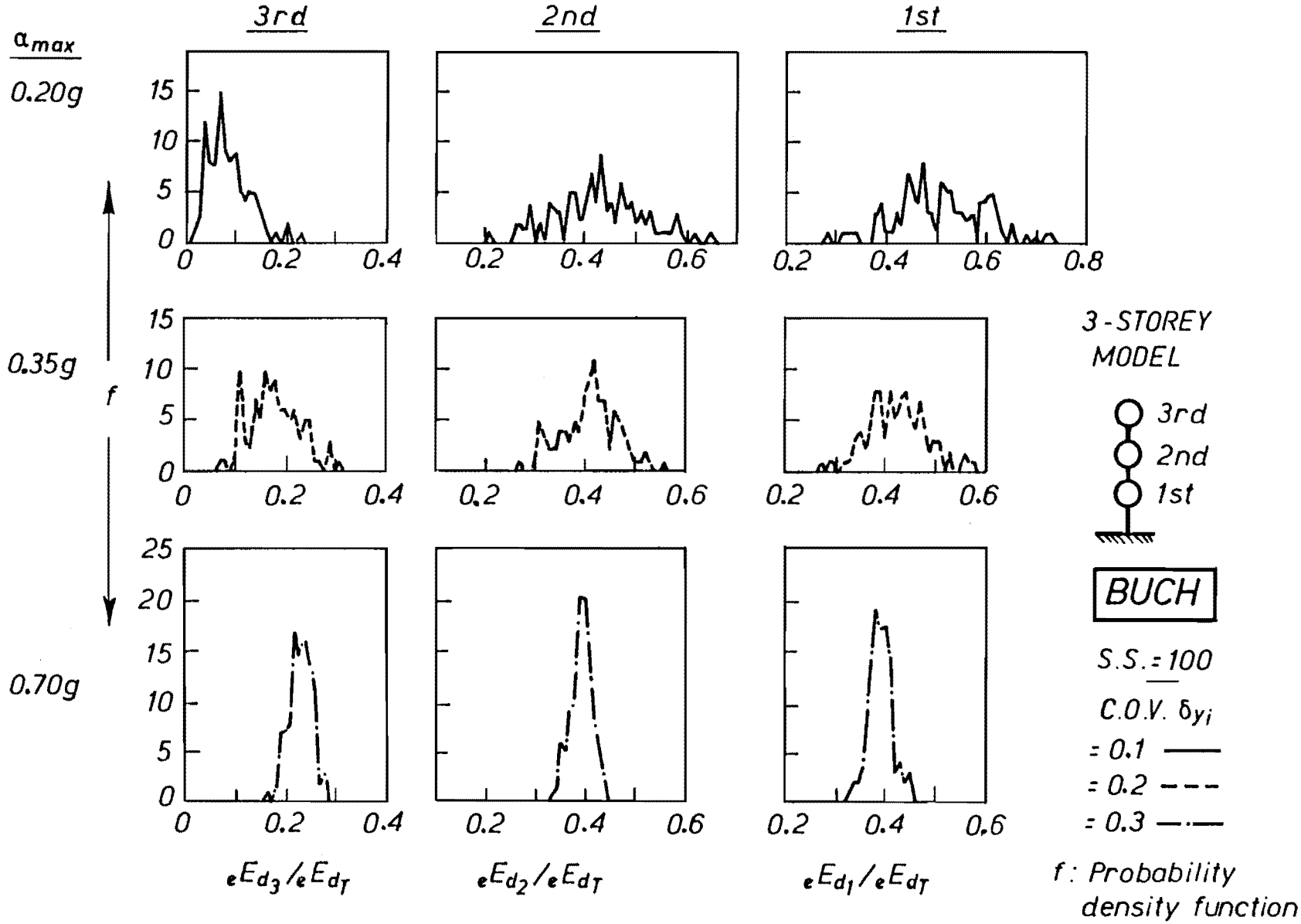

Fig. 7.5.6 Dispersion of proportion of damage energy absorbed by a storey due to variation of yield storey drifts (BUCH)

(ii) Next to be examined is the question of how the increment of the C.O.V. of the δ_y's in the ratio ${}_eE_{d_i}/{}_eE_{d_T}$ affects $p_{f_i|EQ}$. Note that δ_y is involved not only in ${}_eE_{d_i}/{}_eE_{d_T}$ but also in η_{R_i} and η_{I_i} in calculating $p_{f_i|EQ}$ (see Eqs (7.4.4)-(7.4.9)). Using the assumption that E_{d_T}/w_t and the δ_y's in ${}_eE_{d_i}/{}_eE_{d_T}$ are the only random variables, the advanced First-Order Second-Moment (F.O.S.M.) method (see section 2.2.2) was used to investigate the effect. The results are shown in the bottom diagrams of Figs 7.5.7 and 7.5.8. The shift of $p_{f_i|EQ}$ due to the gain of C.O.V. of the δ_y's in the ratio ${}_eE_{d_i}/{}_eE_{d_T}$ is very small.

(iii) The equivalent C.O.V. of δ_y is finally determined such that the difference on $p_{f_i|EQ}$ between using the original C.O.V. of the δ_y's (=0.1) and the equivalent C.O.V. is equal to the amount of shift in $p_{f_i|EQ}$ due to the increment of the C.O.V. of the δ_y's in ${}_eE_{d_i}/{}_eE_{d_T}$. The F.O.S.M. method was used to determine the equivalent C.O.V., assuming that the δ_y's and E_{d_T}/w_t are random variables. The equivalent C.O.V. of δ_y is 0.2 irrespective of α_{max} as shown in Figs 7.5.7 and 7.5.8.

In conclusion, the effect of the variation of resonant periods on the conditional failure probabilities due to changing w_i is found to be negligibly small. The equivalent C.O.V. of δ_y is 0.2, which includes the effect of the variability of both δ_y and w_i. The equivalent C.O.V. will be used later.

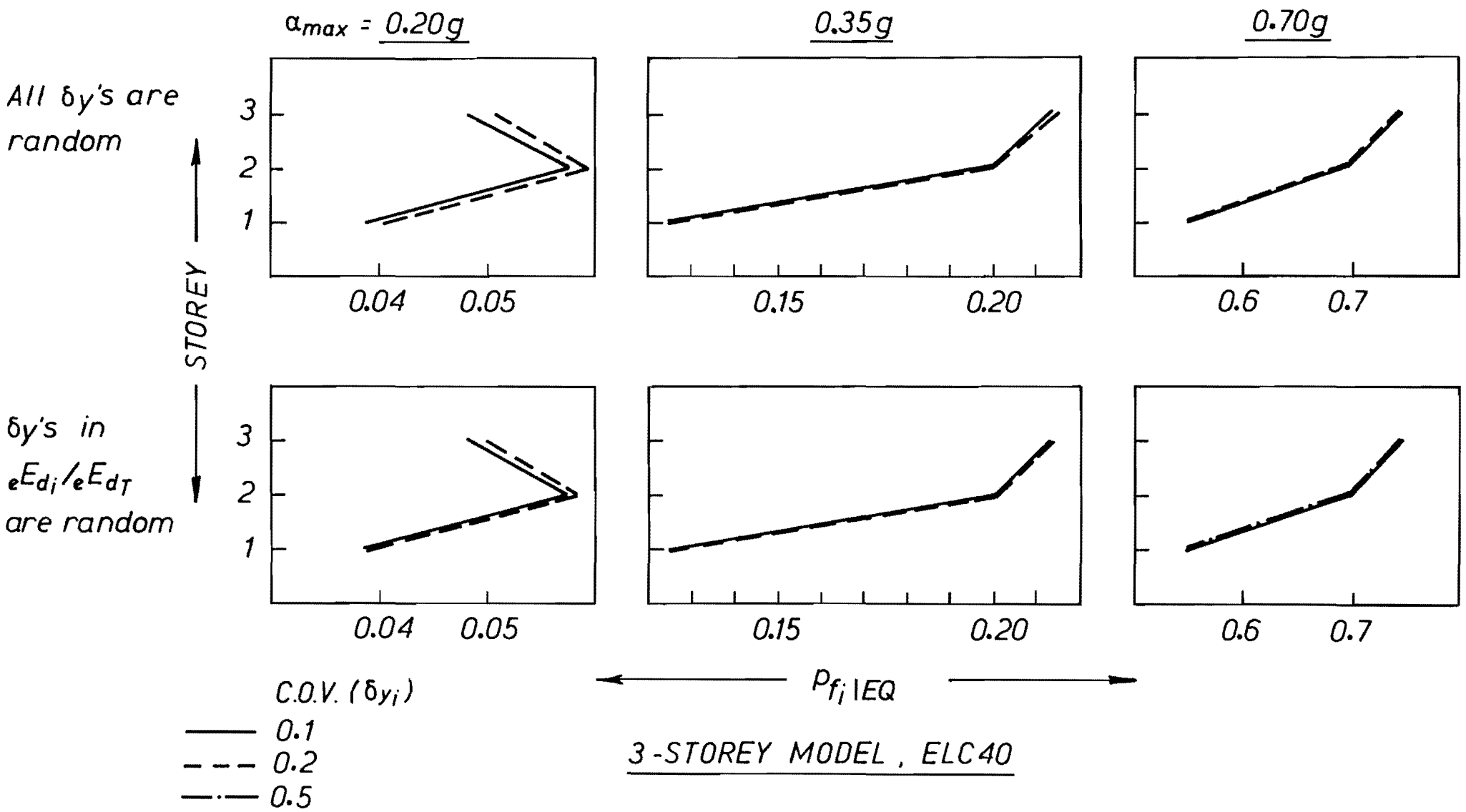

Fig. 7.5.7 Equivalent coefficient of variation of a yield storey drift (ELC40)

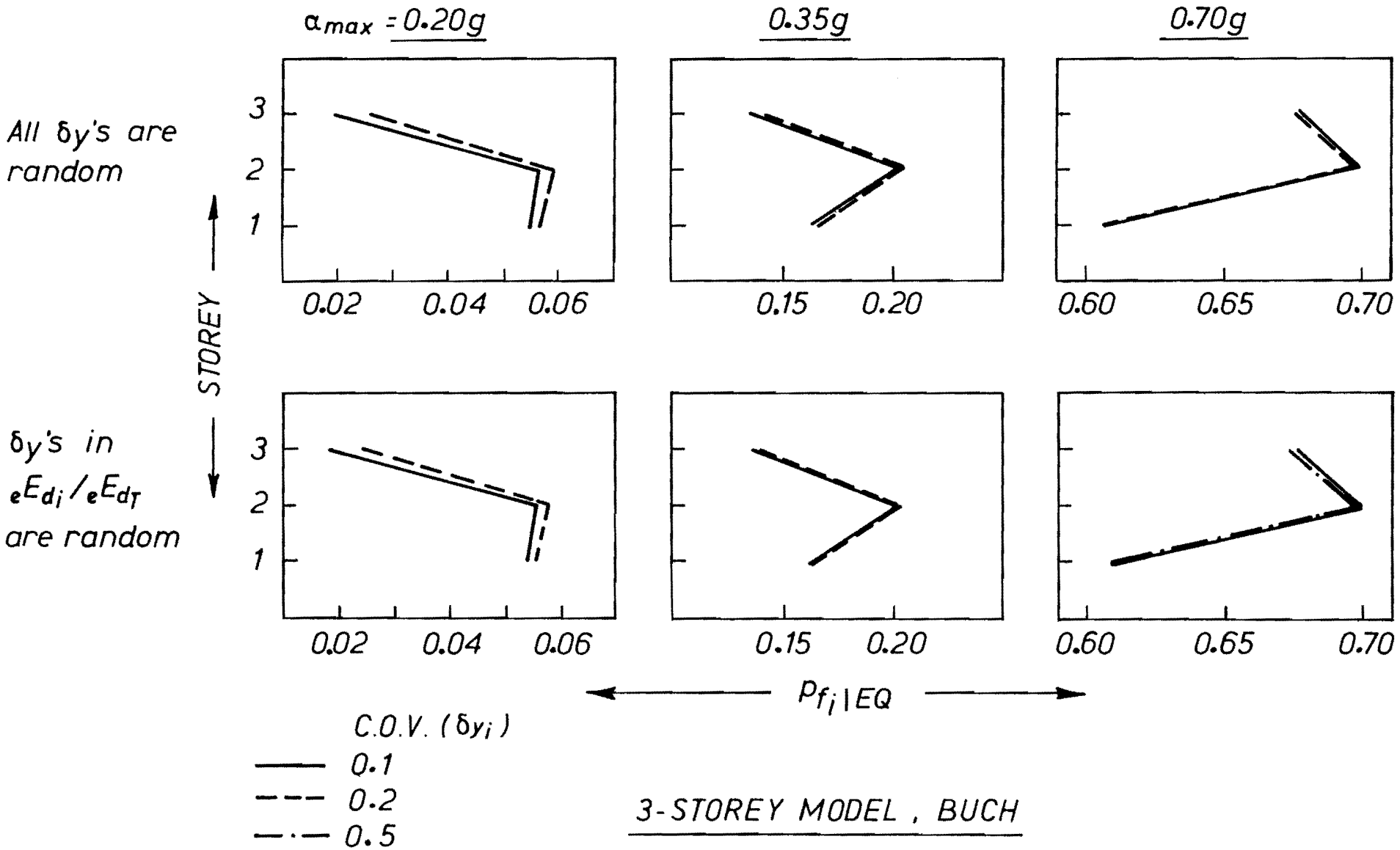

Fig. 7.5.8 Equivalent coefficient of variation of a yield storey drift (BUCH)

(4) Relationship between standard damage energy E_{d_T}/w_t and ultimate storey deflection angle γ_u

The failure surfaces relating the standard damage energy E_{d_T}/w_t and the ultimate storey deflection angle γ_u in reduced coordinates are shown in Fig. 7.5.9. In this case again the variability of E_{d_T}/w_t dominates the failure surfaces, and the variability of γ_u can be neglected.

The sensitivity studies have shown that $p_{f_i|EQ}$ is more sensitive to E_{d_T}/w_t than to any other single random variable as one would expect. Therefore, it seems reasonable that all random variables except E_{d_T}/w_t should be changed into deterministic variables because their individual variability only slightly affects $p_{f_i|EQ}$.

In order to confirm whether these variables should be treated as deterministic variables, $p_{f_i|EQ}$ was calculated based on two different assumptions that all five variables are dealt with random variables and that E_{d_T}/w_t only is taken as the random variable. For δ_y, the equivalent C.O.V. of 0.2 was used, as discussed earlier. The value of 0.2 was obtained from the 3-storey model but the figure was assumed to be applicable to the 7 and 30-storey models. In calculating $p_{f_i|EQ}$ with five random variables, the F.O.S.M. method was used. The comparative results for the 3, 7 and 30-storey models subjected to El Centro 1940 NS and Bucharest 1977 NS are shown in Fig. 7.5.10. Though small differences between the results based on the two assumptions

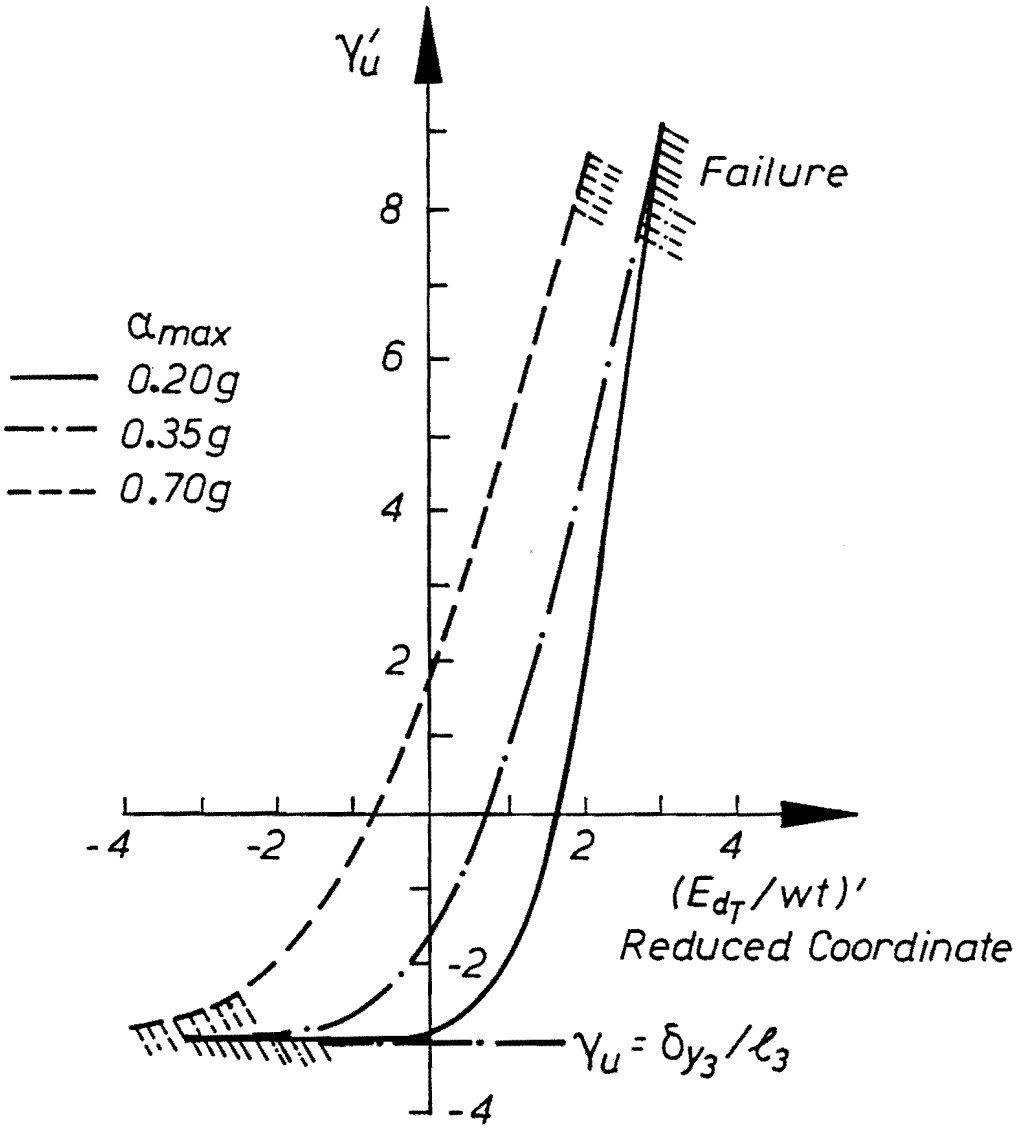

Fig. 7.5.9 Failure surfaces with regard to damage energy and ultimate storey deflection angle

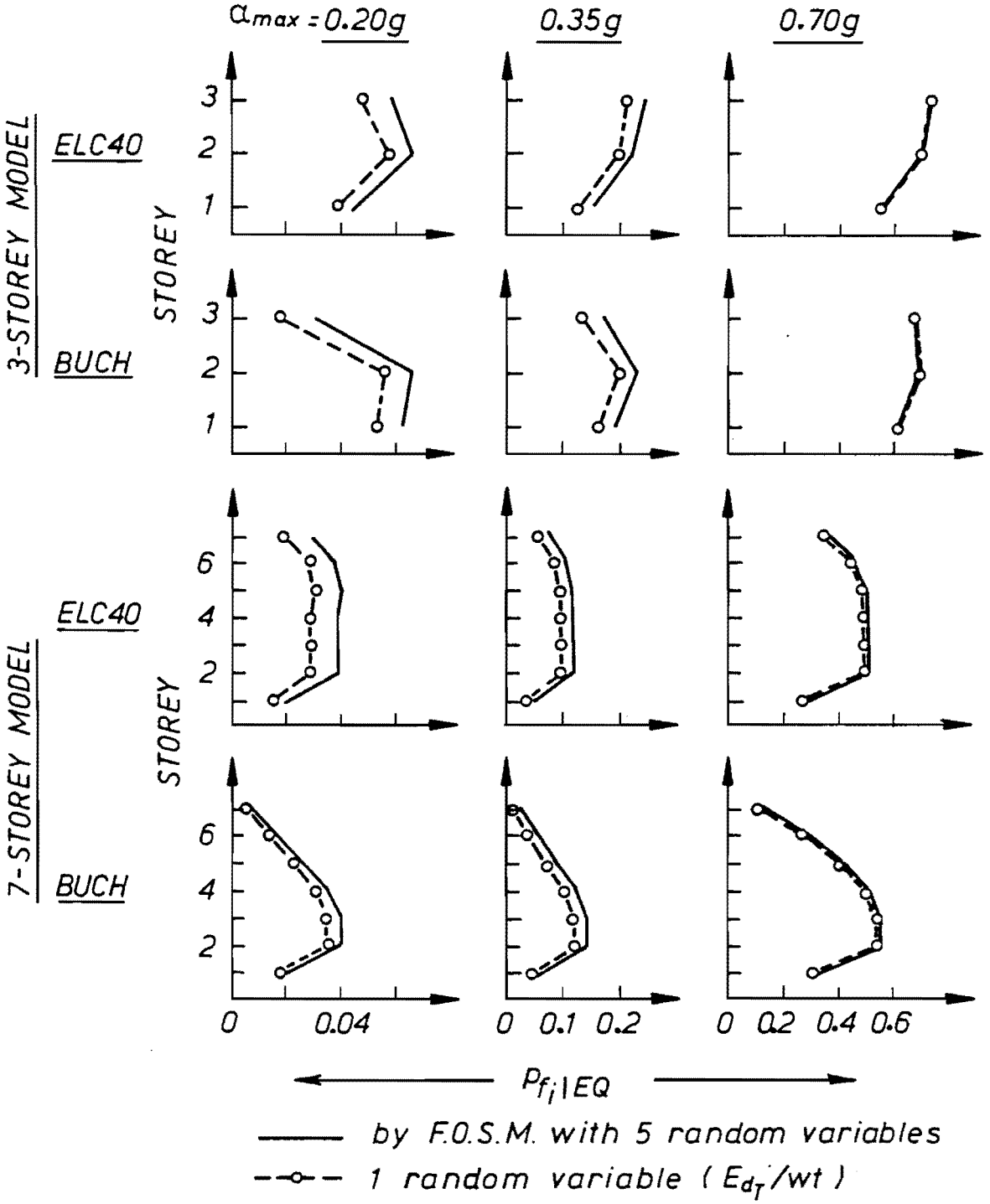

Fig. 7.5.10(a) Comparison of conditional failure probabilities (3 and 7-storey models)

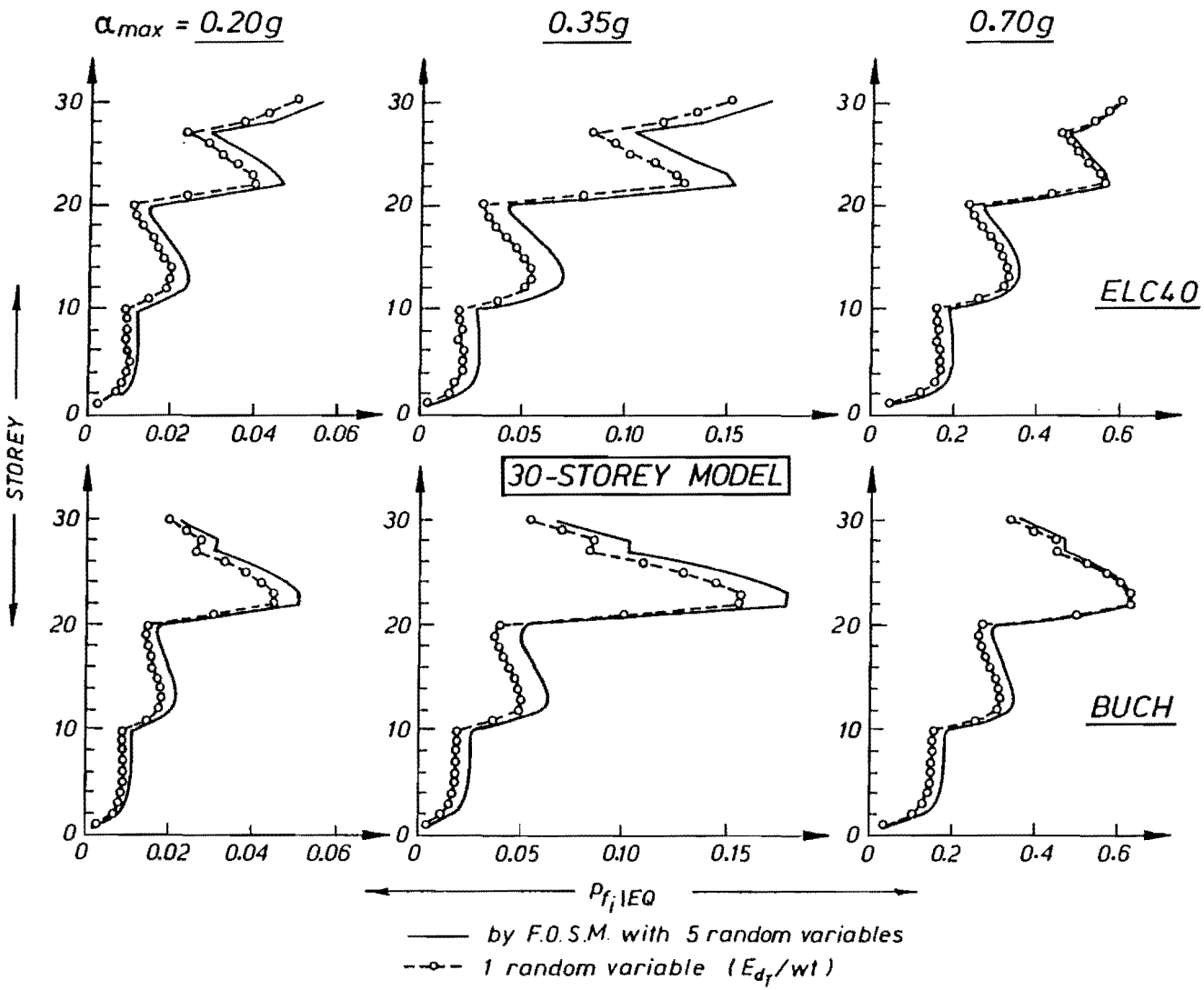

Fig. 7.5.10(b) Comparison of conditional failure probabilities (30-storey model)

are observed, they are considered to be satisfactorily close in the light of the underlying uncertainty characterising the input energy.

Thus the sensitivity studies show that reasonably accurate results are obtained by assuming that E_{d_T}/w_t is the sole random variable in calculating $p_{f_i|EQ}$.

This simplification enables the conditional failure probability for an entire structure, $p_{f|EQ}$ in Eq. (7.4.3), to be readily predictable from $p_{f_i|EQ}$ without using complicated bounding operations. Since only one common random variable E_{d_T}/w_t exists in the calculation of $p_{f_i|EQ}$, Eq. (7.4.3) can be transformed into:

$$p_{f|EQ} = \max_i p_{f_i|EQ} \qquad (i=1,2,\ldots,n) \qquad (7.5.1)$$

$$(P[F|EQ] = \max_i P[E_i])$$

Finally, therefore, using Eqs (7.3.5), (7.5.1) and (7.4.4) together with Table 7.3.3, failure probabilities p_f for multi storey buildings can be calculated using a reasonably simple procedure.

In order to complete the calculation procedure for obtaining the failure probabilities, it is necessary to discuss the appropriate value of n_s in Eq. (7.3.5), which is the number of selected earthquake records. The shape functions in the spectrum and intensity envelope affect the input energy absorbed into each storey. If the effect on probability of

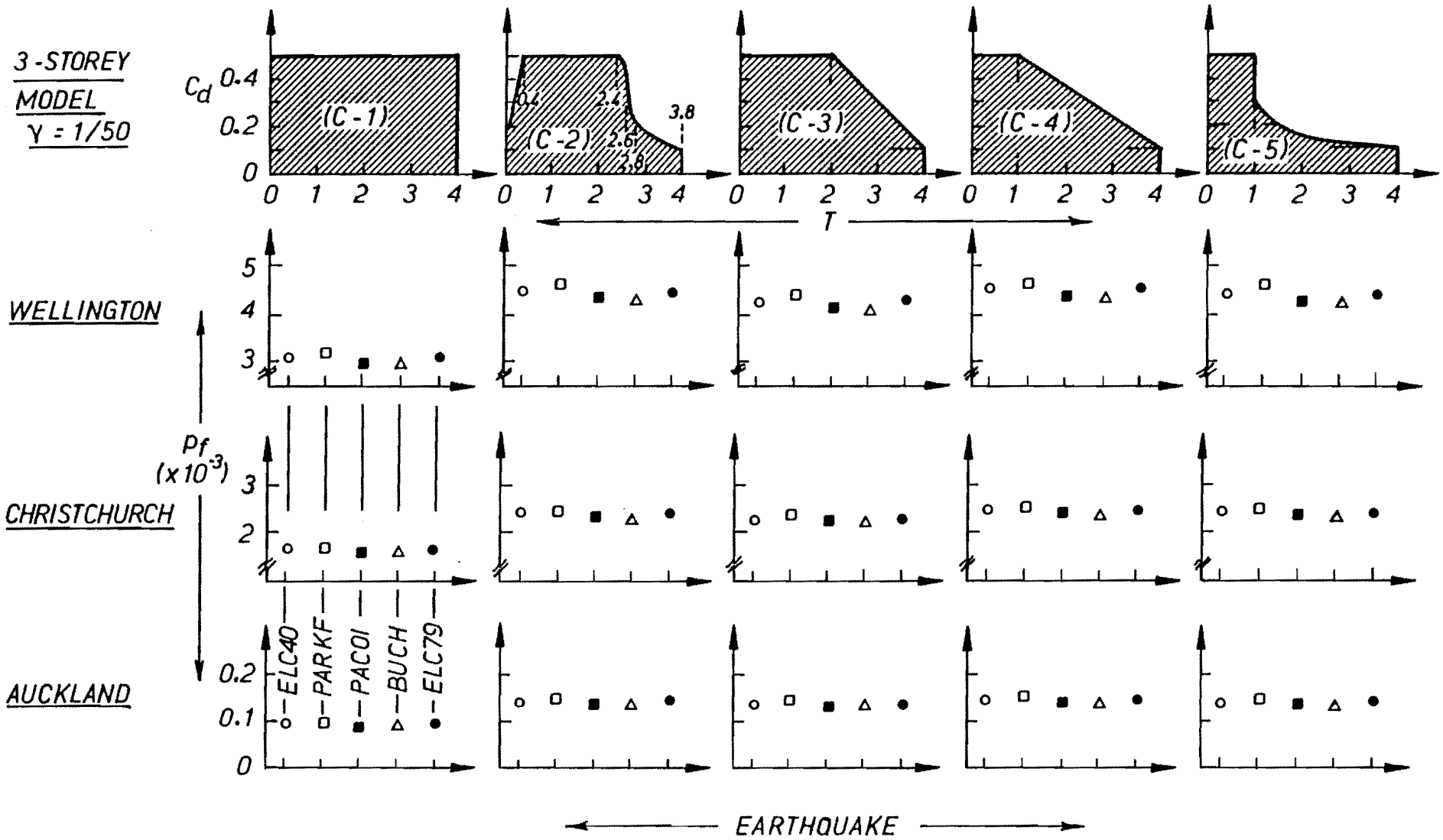

Fig. 7.5.11 Sensitivity of failure probability to choice of earthquake records and to different distributions of damage energy (3-storey model)

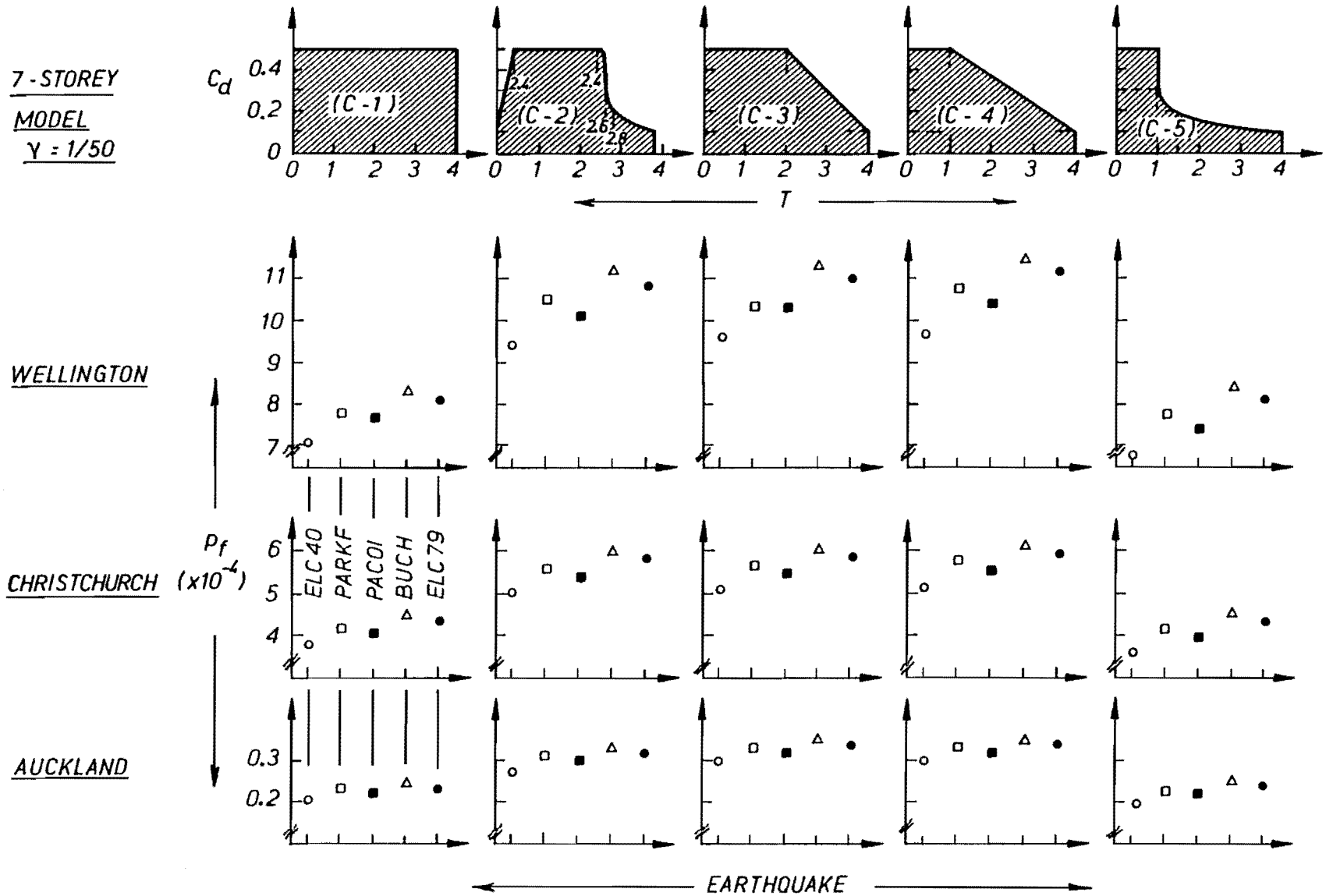

Fig. 7.5.12 Sensitivity of failure probability to choice of earthquake records and to different distributions of damage energy (7-storey model)

failure p_f is trivial, a small value of n_s will be enough for reasonable accuracy. To check the sensitivity of p_f to the choice of earthquake records, value of p_f obtained from different earthquake records are compared in Figs 7.5.11 and 7.5.12 for 3 and 7-storey models respectively. The figures also show the sensitivity of p_f to the choice of classification in determining the distribution parameters of E_{d_T}/w_t as illustrated in Fig. 7.4.13. From the results, it can be noted that the choice of earthquake record affects p_f only slightly. Thus, the appropriate value for n_s can be one, which is both the smallest sample size and the simplest. The choice of classification in Fig. 7.4.13 influences p_f more than the choice of earthquake records. However, the differences in p_f due to the classification choice are at most 50%. Considering the inherent uncertainty in predicting earthquake intensity and in a procedure for achieving a balanced code, it is thought to be small. Because the influence of the classification on p_f is not large, much attention need not be paid to it. The class of (C-5) is assumed to be appropriate because the area in the T-C_d region, given in Fig. 7.4.13, is the most realistic range for existing buildings.

7.6 SUMMARY AND DEMONSTRATION

A reasonably simple procedure for estimating failure probabilities for multi-storey frame buildings subjected to earthquake has now been developed. The procedure may be summarised as follows.

(1) The failure probability of a structure subjected to earthquake is expressed by:

$$P_f = \sum_{i=1}^{n_\alpha} \{P[F|EQ_{\alpha_{max}=\alpha_i}] \cdot P_{\alpha_{max}}(\alpha_i)\} \qquad (7.6.1)$$

where: $P[F|EQ_{\alpha_{max}=\alpha_i}]$ = failure probability given that an earthquake with a maximum acceleration of α_i occurs (conditional failure probability)

$P_{\alpha_{max}}(\alpha_i)$ = probability of occurrence of earthquake whose maximum acceleration is α_i (seismic risk)

n_α = number of discrete values of α_{max}

(2) The seismic risk is to be calculated for the seismic area being considered. Following Elms and Silvester (94,95) the seismic risk was obtained for three major centres in New Zealand as shown in Table 7.3.3 (n_α=3, α_1=0.20 g, α_2=0.35 g and α_3=0.70 g).

(3) The conditional failure probability is given by:

$$P[F|EQ_{\alpha_{max}=\alpha_i}]$$

$$= \max_j P[\gamma_{max_j} > 1/50|EQ_{\alpha_{max}=\alpha_i}] \qquad (7.6.2)$$

$$= \max_j P_{f_j|EQ_i} \qquad (j=1,2,\ldots,n)$$

where: n = total number of storeys of the building

γ_{max_j} = maximum storey deflection angle of the jth storey during an excitation.

One earthquake record can be arbitrarily chosen for the calculation. Its maximum acceleration α_{max} can be adjusted to α_i by scaling.

The conditional failure probability $P_{f_j|EQ_i}$ of the jth storey subjected to an earthquake with maximum acceleration of α_i is denoted by:

$$P_{f_j|EQ_i} = P[g_{j(\alpha_{max}=\alpha_i)} < 0] \tag{7.6.3}$$

in which:

$$g_{j(\alpha_{max}=\alpha_i)} = 3 \cdot k_j \cdot \delta_{y_j}^2 \cdot \left(\frac{l_j}{50 \cdot \delta_{y_j}} - 1\right) - w_t \cdot \left(\frac{E_{d_T}}{w_t}\right)_{\alpha_{max}=\alpha_i} \cdot \left(\frac{e^{E_{d_j}}}{e^{E_{d_T}}}\right)_{\alpha_{max}=\alpha_i}$$

E_{d_T}/w_t = the standard damage energy

w_t = total weight of a structure

k_j = jth storey initial stiffness

δ_{y_j} = yield storey drift of jth storey

l_j = height of jth storey

$$e^{E_{d_T}} = \sum_{m=1}^{n} e^{E_{d_m}} \tag{7.6.4}$$

$$e^{E_{d_j}} = \Omega_{\delta_j} \cdot k_j \cdot \sigma_{\delta_j}^2 \cdot \exp\{-\delta_{y_j}^2 / 2\sigma_{\delta_j}^2\} \tag{7.6.5}$$

$$\sigma_{\delta_j}^2 = \lambda_{0,\delta_j} \tag{7.6.6}$$

$$\Omega_{\delta_i} = \sqrt{\lambda_{2,\delta_j}/\lambda_{0,\delta_j}} \tag{7.6.7}$$

λ_{m,δ_j} = mth moment of the response spectral-density function of storey drift δ_j

$$\lambda_{m,\delta_j} = \int_0^\infty \omega^m \cdot G_{\delta_j}(\omega)\, d\omega \tag{7.6.8}$$

$G_{\delta_j}(\omega)$ = spectral-density function of response storey drift δ_j

All variables except E_{d_T}/w_t can be taken as deterministic. The probability distribution of E_{d_T}/w_t corresponding to α_i must be estimated. In the present study to apply the procedure to buildings in New Zealand, a log-normal distribution was chosen for E_{d_T}/w_t with parameters shown in classification (C-5) of Fig. 7.4.13, which can be denoted as λ_{α_i} and ζ_{α_i} for α_i. Therefore, Eq. (7.6.3) is transformed to:

$$P_{f_j|EQ_i} = 1 - \Phi\left[\frac{\ln(E_{d_T}/w_t)_{g_{j(\alpha_{max}=\alpha_j)=0}} - \lambda_{\alpha_i}}{\zeta_{\alpha_i}}\right] \tag{7.6.9}$$

where: Φ = cumulative distribution function of the standard normal variable.

Therefore, in order to calculate the probability of failure p_f of a building at three major centres in New Zealand, only the following preparatory analyses are required.

(1) Estimate structural storey characteristics, w_j, k_j, δ_{y_j} and l_j.

(2) Calculate the 0th and 2nd moments of the response spectral density function for the drift of each storey using an elastic dynamic analysis. An earthquake record with a specified maximum acceleration used in computing the moments can be chosen arbitrarily. Once the moments for the maximum acceleration are obtained, it is straightforward to calculate the moments for the same earthquake record scaled to a different maximum acceleration, which is given by:

$$\lambda_{m,\delta_j(\text{scaled})} = r^2 \cdot \lambda_{m,\delta_j(\text{original})} \tag{7.6.10}$$

where: $r = \alpha_{\max\ (\text{scaled})} / \alpha_{\max\ (\text{original})}$

In order to demonstrate an application procedure, a reinforced concrete frame building located in Christchurch, Clarendon Towers, was chosen as a sample building. The building is described in Section 6.5 as well as in Appendix D. Details of calculating the conditional failure probability $p_{f_i|EQ}$ for α_{max} values of 0.20, 0.35 and 0.70 g are given in Tables 7.6.1 and 7.6.2. As mentioned above, evaluation of structural storey characteristics and moments of the response spectral density function is required to obtain $p_{f_i|EQ}$. The storey characteristics used in the demonstration are tabulated in Table D.1(2) and the details of obtaining them are discussed in Appendix D (see Figs D.9-D.11 and Tables D.2 and D.3). In calculating 0th and

Table 7.6.1 Calculation of conditional failure probabilities (α_{max} = 0.20g)

Storey	(1) EQ=ELC40 (α_{max}=0.314g) Ω_δ (1/sec)	(1) σ_δ^2 (mm²)	(2) α_{max}=0.2g σ_δ^2 (mm²)	(3) k (kN/mm)	(3) V_y (kN)	(3) δ_y (mm)	(4) ${}_eE_{d_i}$ (kN·mm/sec)	(4) ${}_eE_{d_i}/{}_eE_{d_T}$	(5) w_t (kN)	(6) ℓ_i (mm)	(7) ${}_{E_{d_T}}/w_t$ (mm)	(8) $p_{f_i\|EQ}$
15	13.7	1.61	0.653	483	474	0.981	2068	0.0118		3400	189	0.0158
14	12.1	5.80	2.35	"	916	1.90	6371	0.0364		"	117	0.0264
13	10.7	11.3	4.58	485	1330	2.74	10472	0.0599		"	103	0.0299
12	9.91	17.2	6.98	"	1710	3.53	13741	0.0785		"	97.9	0.0313
11	9.30	22.6	9.17	"	2050	4.23	15591	0.0891		"	103	0.0298
10	8.45	26.8	10.9	"	2370	4.89	14916	0.0853		"	124	0.0247
9	7.42	30.0	12.2	"	2660	5.48	12823	0.0733		"	160	0.0190
8	6.45	32.8	13.3	"	2910	6.00	10749	0.0614	42650	"	207	0.0144
7	5.72	35.9	14.6	"	3130	6.45	9744	0.0557		"	245	0.0119
6	5.56	28.1	11.4	579	3320	5.73	8695	0.0497		"	291	0.0098
5	5.89	31.7	12.9	"	3480	6.01	10848	0.0620		"	247	0.0118
4	6.29	35.7	14.5	"	3610	6.23	13850	0.0792		"	199	0.0150
3	6.66	39.4	16.0	"	3700	6.39	17223	0.0985		"	163	0.0187
2	6.98	42.1	17.1	"	3770	6.51	20015	0.1144		"	142	0.0215
1	7.11	5.85	2.37	1577	3800	2.41	7831	0.0448		4000	463	0.0055
							Σ 174937	Σ 1.00				

$P[F|EQ_{\alpha_{max}=0.20g}]=0.0313$

(1) by Random Vibration method (Appendix C)

(2) $\sigma_\delta^2(\alpha_{max}=0.20g) = (\frac{0.2}{0.314})^2 \cdot \sigma_\delta^2(\alpha_{max}=0.314g)$

$\Omega_\delta(\alpha_{max}=0.20g) = \Omega_\delta(\alpha_{max}=0.314g)$

(3) See Appendix D ($\delta_y = V_y/k$)

(4) ${}_eE_{d_i} = \Omega_{\delta_i} \cdot k_i \cdot \sigma_{\delta_i}^2 \cdot \exp\{-\delta_{y_i}^2/2\sigma_{\delta_i}^2\}$

${}_eE_{d_T} = \sum_i {}_eE_{d_i}$

(5) See Appendix D

(6) See Appendix D

(7) ${}_{E_{d_T}}/w_t = 3 \cdot k_i \cdot \delta_{y_i}^2 \cdot (\frac{\ell_i}{50\,\delta_{y_i}} - 1)/\{w_t \cdot (\frac{{}_eE_{d_i}}{{}_eE_{d_T}})\}$

(8) $p_{f_i|EQ} = 1 - \Phi\left(\frac{\ln({}_{E_{d_T}}/w_t) - \lambda}{\zeta}\right)$

($\lambda = 0.303$ & $\zeta = 2.3$ for $\alpha_{max}=0.20g$)

Table 7.6.2 Calculation of conditional failure probabilities (α_{max} = 0.35 & 0.70g)

Storey	(2) α_{max}=0.35g σ_δ^2 (mm^2)	(4) $e^{E_{d_i}}$ (kN.mm/sec)	(4) $\frac{e^{E_{d_i}}}{e^{E_{d_T}}}$	(7) E_{d_T}/w_t (mm)	(8) $P_{f_i}\|EQ$
15	2.00	10400	0.00874	256	0.0258
14	7.21	32700	0.0275	155	0.0562
13	14.0	55500	0.0466	131	0.0710
12	21.4	76800	0.0645	120	0.0802
11	28.1	92000	0.0773	119	0.0812
10	33.3	95100	0.0799	132	0.0706
9	37.3	89500	0.0752	156	0.0561
8	40.8	81800	0.0687	185	0.0434
7	44.6	77500	0.0651	208	0.0362
6	34.9	70200	0.0590	246	0.0276
5	39.4	84800	0.0712	213	0.0348
4	44.4	104100	0.0874	179	0.0455
3	49.0	124400	0.1045	153	0.0571
2	52.3	141000	0.1184	138	0.0666
1	7.27	54700	0.0459	452	0.0092
		Σ 1190500	Σ 1.00		

$P[F|EQ\ \alpha_{max}=0.35g] = 0.0812$

(2) $\sigma_\delta^2(\alpha_{max}=0.35g) = (\frac{0.35}{0.314})^2 \cdot \sigma_\delta^2(\alpha_{max}=0.314g)$

(4) $e^{E_{d_i}} = \Omega_{\delta_i} \cdot k_i \cdot \sigma_{\delta_i}^2 \cdot \exp\{-\delta_{y_i}^2/2\sigma_{\delta_i}^2\}$

$e^{E_{d_T}} = \sum_i e^{E_{d_i}}$

(7) $E_{d_T}/w_t = 3 \cdot k_i \cdot \delta_{y_i}^2 (\frac{\ell i}{50 \cdot \delta_{y_i}}) - 1)/\{w_t \cdot (\frac{e^{E_{d_i}}}{e^{E_{d_T}}})\}$

(8) $P_{f_i}|EQ = 1 - \Phi\ (\frac{\ell n(E_{d_T}/w_t) - \lambda}{\zeta})$

(λ = 2.82 & ζ = 1.40 for α_{max} = 0.35g)

Storey	(2) α_{max}=0.70g σ_δ^2 (mm^2)	(4) $e^{E_{d_i}}$ (kN.mm/sec)	(4) $\frac{e^{E_{d_i}}}{e^{E_{d_T}}}$	(7) E_{d_T}/w_t (mm)	(8) $P_{f_i}\|EQ$
15	8.00	49700	0.00776	288	0.167
14	28.8	157600	0.0246	173	0.308
13	56.2	271700	0.0424	144	0.368
12	85.5	381800	0.0596	130	0.405
11	112	467400	0.0730	126	0.416
10	133	498400	0.0778	135	0.390
9	149	484600	0.0757	155	0.345
8	163	456100	0.0712	178	0.298
7	178	440000	0.0687	197	0.268
6	140	399600	0.0624	233	0.220
5	158	478800	0.0748	203	0.259
4	177	578800	0.0904	174	0.307
3	196	680100	0.1062	151	0.353
2	209	763900	0.1193	137	0.387
1	29.1	295200	0.0461	450	0.084
		Σ 6403700	Σ 1.00		

$P[F|EQ\ \alpha_{max}=0.70g] = 0.416$

(2) $\sigma_\delta^2(\alpha_{max}=0.70g) = (\frac{0.70}{0.314})^2 \cdot \sigma_\delta^2(\alpha_{max}=0.314g)$

(4) & (7) same as the note of the left table

(8) $P_{f_i}|EQ = 1 - \Phi\ (\frac{\ell n(E_{d_T}/w_t) - \lambda}{\zeta})$

(λ = 4.60 & ζ = 1.10 for α_{max} = 0.70g)

2nd moments of the response spectral density function for the drift of each storey, the El Centro 1940 NS record was chosen whose observed maximum acceleration is 0.314 g. Using the spectral moments, σ_δ^2 and Ω_δ were computed by Eqs (7.6.6) and (7.6.7) and the results are given in column (1) of Table 7.6.1. The values of σ_δ^2 were used in obtaining σ_δ^2 for α_{max} values of 0.20, 0.35 and 0.70 g. Column (2) in Tables 7.6.1 and 7.6.2 shows the values of σ_δ^2 for the scaled El Centro record (Ω_δ does not change due to scaling). Based on the data, the conditional failure probability $p_{f_i|EQ}$ for each storey was calculated by Eq. (7.6.9) and the results are given in column (8) in the Tables. Figure 7.6.1 shows the results for α_{max} of 0.20, 0.35 and 0.70 g. Using Eq. (7.6.2), the conditional failure probability $p_{f,1}$ for each α_{max} value was then obtained. Finally, the failure probability of Clarendon Towers in periods of a year due to earthquake was calculated using Eq. (7.6.1) and Table 7.3.3 to give a result of:

$$\begin{aligned} p_{f,1} &= 0.031 \times 1.2 \times 10^{-2} + 0.081 \times 5.2 \times 10^{-3} \\ &\quad + 0.42 \times 0.8 \times 10^{-4} \\ &= 1.1 \times 10^{-3} \quad \text{(per year)} \end{aligned}$$

The annual failure probabilities of the 3, 7 and 30-storey frames located in Wellington as well as of Clarendon Towers in Christchurch are shown in Fig. 7.6.2. The 3, 7 and 30-storey frames were designed for a high seismicity region, while Christchurch is classified as medium. The calculated failure probabilities are of the order of 10^{-3}. This is far higher than the order of magnitude often quoted for

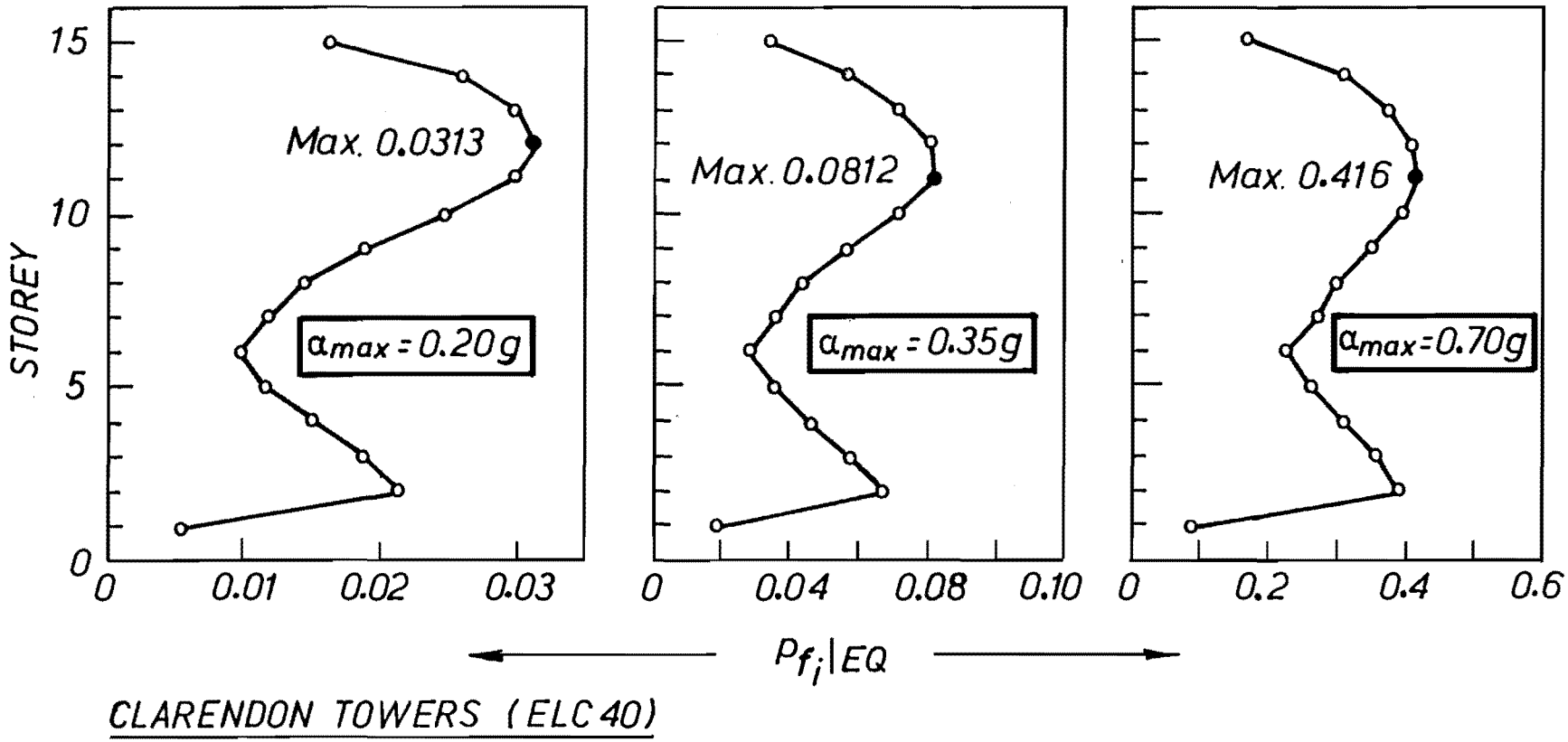

Fig. 7.6.1 Conditional failure probabilities for α_{max} values of 0.2, 0.35 & 0.70g

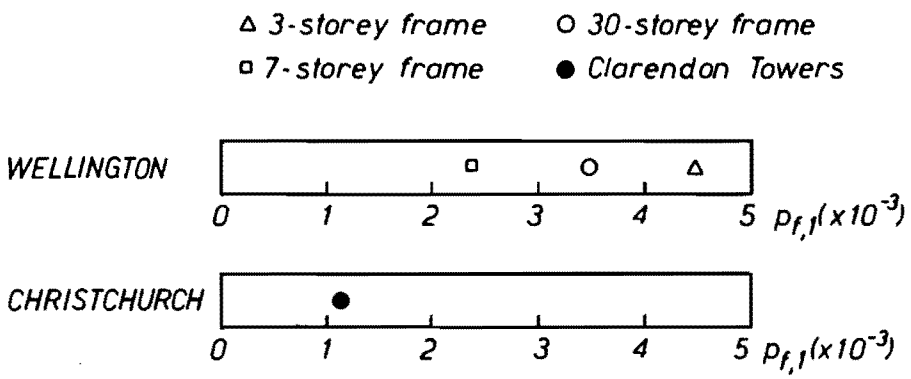

Fig. 7.6.2 Annual failure probabilities

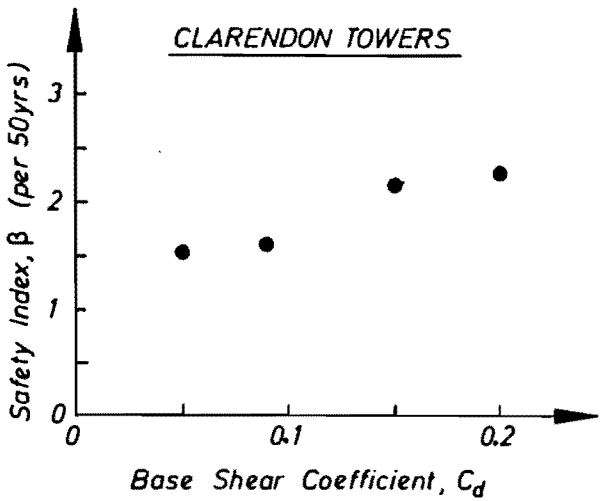

Fig. 7.6.4 Relationship between safety index and base shear coefficient

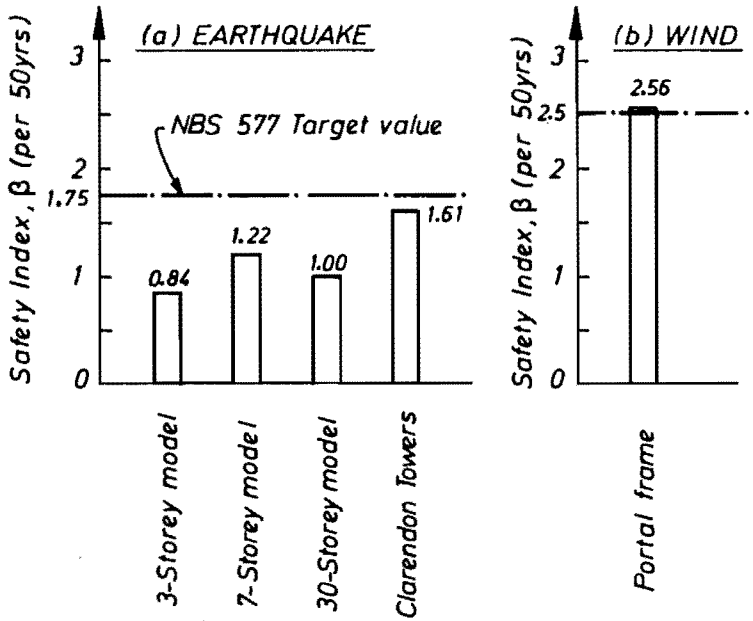

Fig. 7.6.3 Comparison of safety indices obtained by the present study with NBS577 target value

structural failure. For example, according to references (105,106), calculated failure probabilities for a member, i.e. a beam or column, are of the order of 10^{-5} to 10^{-12}. However, such references have primarily dealt with member failure due to gravity load whereas failure of an entire structure due to earthquake has been focussed on in the present study.

It is of interest to compare the results with the target values of the reliability index given in NBS577 (30). In that report, structural failure was based on member failure alone, and its target reliability levels were 50-year values in contrast to the annual levels adopted in the present work. Values for annual probability of failure $p_{f,1}$ may be transformed into a 50-year safety index β by:

$$\beta = \Phi^{-1}(1 - p_{f,50}) \qquad (7.6.11)$$

where: $p_{f,50} = 1 - (1 - p_{f,1})^{50}$

Φ = the cumulative distribution function of the standard normal distributon

Figure 7.6.3(a) shows the comparison of the 50-year safety index β due to earthquake for the 3, 7 and 30-storey models and Clarendon Towers with the NBS577 target value of 1.75. The safety indices for all four models are lower than the target values. Note that the 3-storey model may not be realistic because it was designed only to the earthquake load combination, while gravity load usually dominates this type of frame. For the wind load case, the NBS577 target

value of β was 2.5. The issue of taking different values of target safety index for different loading types was discussed but not resolved in NBS577. The failure probability of the portal frame discussed in Chapter 4 was dominated by wind load. Figure 7.6.3(b) compares the safety index of the portal frame due to wind with the corresponding target value in NBS577. These values are quite similar. Therefore, in general, the calculated safety levels obtained by the present study are not very different from the specified target values of safety in NBS577. However, the minimum safety level among structures and structural types is taken as the criterion for a balanced code in this study, while the target values in NBS577 are average values. Thus, for developing a balanced code, the relationship between the minimum and average safety levels should be more carefully examined. Moreover, as explained in Section 3.3, it is difficult to determine the appropriate level of minimum safety, because calculated failure probability using tractable information does not dominate observed failure probability. These problems are left for future research.

Finally, it is important to know the sensitivity of the safety index to changes in the base shear coefficient C_d. The base shear coefficient can be considered to be a representative value for the resistance of structures. If the existing safety level was too high or too low, the base shear coefficient C_d should decrease or increase. The Clarendon Towers analysis was used to examine the sensitivity; the original C_d was 0.089 (see Table D.1(2) C_{d_1}). Assuming that larger member sizes are required when

C_d becomes larger, both the initial stiffness and yield shear strength for each storey were magnified or reduced by a certain factor such that the modified base shear coefficient was 0.05, 0.15 and 0.20. The safety indices for the models with C_d = 0.05, 0.15 and 0.20 were calculated using the El Centro 1940 NS record and are shown in Fig. 7.6.4. The relationship between C_d and β is not linear since the proportion of damage energy absorbed by a storey varies in a complex way due to changing the initial storey stiffnesses. It is found for this particular case that by modifying C_d by about 70% from 0.089 to 0.15, the safety index improves from 1.6 to 2.2. This means, the safety level would be improved by a factor of about 3.5 as a result of the modification. Thus a large increase in base shear coefficient would be required to increase the safety of a structure by an order of magnitude; which is to say that structural safety is relatively insensitive to changes in base shear coefficient.

CHAPTER 8

SUMMARY, CONCLUSIONS AND RECOMMENDATIONS FOR FUTURE RESEARCH

8.1 SUMMARY

Structural codes are necessary for optimising safety and economy within a society. Though studies have been made towards rationalising codes by the limit states concept and similar approaches, the resulting codes are still not fully rational as they do not achieve an optimal balance of relative risk between different structural types and, particularly, given loading types. The reason for this is primarily that it has not been possible to compute failure probabilities with any degree of confidence, particularly for earthquake loadings where the behaviour of a total structure must be considered.

We need to proceed towards a more rational code. Such a code may be called a "balanced code" as it is based on the concept of balanced risk. This indicates that risks due to general social accidents and due to structural failure should be balanced with regard to each other. Because fundamental difficulties in the application of this approach lie in obtaining the expectation of structural risks consistent with those of social accidents, criteria for a

balanced code may be expressed in terms of structural safety rather than structural risks. In this, the following two precepts are followed:

(1) The minimum safety levels for different loadings are the same for all structural types.

(2) The spread of reliability between structures is minimised.

To achieve these criteria, many different structures have to be analysed. Therefore, the most urgent need in moving towards a balanced code is to develop a procedure for assessing probabilities of failure due to earthquake which is at the same time sufficiently simple that many calculations can be carried out without undue effort.

This thesis has therefore been primarily concerned with developing a simplified procedure for computing earthquake failure probabilities. Because of time limitations, the development has been restricted to reinforced concrete frame buildings, but the principles are applicable to a wider range of structures.

Since many structures need to be analysed, the procedure for assessment must be simple. The only practical approach for developing such a procedure is to use the advanced First-Order Second-Moment method. In order to examine its applicability and limitations, failure probabilities of the simplest possible structure, a portal frame, were calculated

by the First-Order Second-Moment method. Even for such a structure, a large number of random variables were involved and the performance functions (or limit state functions) for some failure modes were very complicated. The First Order Second-Moment method was found to be practical only when applied to a simple performance function.

Development of a procedure for assessing the failure probabilities of structures due to earthquake using the First-Order Second-Moment method has three steps.

Firstly, a failure criterion was defined. Collapse was chosen as the most appropriate limit state for the definition of failure, because the collapse criterion generally dominates a design in areas of high seismic risk. In studying mechanisms of collapse, two factors were considered:

(1) the so-called P-δ effect; and

(2) deterioration of strength due to large deformations and cyclic loading effects.

Quantifying these effects with some difficulty, a failure criterion was defined as a limitation of storey drift.

Secondly, a performance function was developed. Cumulative plastic strain energy was chosen as the performance measure, since it was considered to be :

(1) the most suitable quantity in the context of dynamic equilibrium to express structural damage; and

(2) a scalar and cumulative quantity which can simply express the total magnitude of damage during the bi-directional cyclic excitations in an earthquake.

Hence, cumulative plastic strain energy was referred to as damage energy. In order to relate damage energy to maximum storey drift, which was adopted as the failure criterion, three separate analytic procedures were used as follows:

(1) The total damage energy for an entire structure was computed approximately. For this, a series of inelastic dynamic analyses of a single-degree-of-freedom system, together with a modal analysis of a multi-degree-of-freedom system were used.

(2) The proportion of total damage energy absorbed by each storey was estimated using a random vibration approach.

(3) The maximum storey drift developed in the process of absorbing the damage energy in each storey was then evaluated in terms of basic seismic and structural variables.

Subsequently, a performance function based on damage energy was obtained.

Thirdly, using the performance function, a procedure to assess failure probabilities due to earthquake was established. The procedure consists of the estimation of seismic risks and conditional failure probabilities for different levels of maximum ground accelerations. Seismic risks for three major centres in New Zealand were introduced. For conditional failure probabilities, the advanced First-Order Second-Moment method was used with the proposed performance function, assuming probability distributions of total damage energy for different levels of maximum ground acceleration. As a result of sensitivity studies for parameters involved in the performance function, only the variability of the total damage energy was found to affect strongly the probability of failure. As a consequence, the procedure to assess failure probabilities could be made simple as well as practical.

Trial application of the proposed procedure to four reinforced concrete frame buildings was carried out. The calculated safety levels were not very different from the specified target values of safety in NBS577 (30), but the seismic reliability was slightly lower.

8.2 CONCLUSIONS

A number of conclusions may be made from the present study as follows:

(1) The underlying approximations and assumptions are rational and consistent, being based on careful

investigations, comparisons with complex time - history dynamic analyses and sensitivity studies.

(2) The results appear to be of the right order of magnitude, in that the probabilities of failure computed for four trial structures give reliability indices similar to though slightly lower than the target value suggested by National Bureau of Standards Publication NBS577 (30).

(3) The assessment procedure has certain limitations. Firstly, the estimation of failure probability is based only on tractable information and the effect of intractable information (human error and so on) is not taken into account. Therefore, the calculated safety level cannot be used as a prediction of observed failure probability but only on a comparative basis. Moreover, the calculated failure probability is only a minor part of the observed failure probability. This leads to the question of how much the calculated failure probability should be changed in order to obtain a certain intended level of observed failure probability. However, it is difficult to allow for the effect of intractable information in assessing failure probabilities, because of the limited present state of the art. Secondly, the inherent uncertainty involved in this procedure is dominated by that in predicting input damage energy induced by an earthquake. Such a prediction involves considerable uncertainly. Hence, the inherent uncertainty of the total assessment is also considerable.

(4) Failure probabilities appear to be relatively insensitive to changes in seismic base shear coefficient.

(5) Preliminary indications are that the New Zealand Loadings Code seismic provisions may be somewhat unconservative. However, too few trials have as yet been carried out to give much weight to this observation.

8.3 RECOMMENDATIONS FOR FUTURE WORK

For future research related to the topic of this project, the study of the following issues is recommended:

(1) Extensions Leading Towards a Balanced Code: Three areas remain which a balanced code should also consider. Firstly, the assessment of failure probabilities for earthquakes should be extended to cover other types of concrete structures such as structural walls and hybrid structures, as well as steel structures. Secondly, although the earthquake load case is the most difficult case for the estimation of failure probabilities, compatible procedures for other load cases should also be established. Thirdly, using the proposed assessment procedures, failure probabilities for different types of building should be evaluated, while considering additional parameters such as different site conditions, occupancies, scales and so on.

(2) The Influence of Brittleness: The probability of the occurrence of brittle mechanisms should also be examined for further development of a balanced code. Using

probabilistic techniques, it should be possible to confirm whether the probability of failure based on brittle mechanisms is acceptably small.

(3) Improving Reliability: A more reliable approach to estimate the total damage energy induced by an earthquake is desirable becausethe uncertainty in predicting damage energy dominates the total uncertainty of assessing failure probabilities. Thus, by improving the quality of the prediction, the reliability of the results should also increase. In the present study, a relationship between Modified Mercalli intensity and maximum ground acceleration was used for estimating the total damage energy. Unfortunately, considerable uncertainty is involved in this. Thus, by making greater use of seismological data, it should be possible to improve the prediction of damage energy.

APPENDIX A

DETAILS OF 3, 7 AND 30-STOREY FRAMES AND THEIR MODELS

For the numerical studies, 3, 7 and 30-storey reinforced concrete frames were designed according to New Zealand codes (49,50). For the purposes of the study a detailed design is not required. Since only earthquake behaviour is considered in this report, the frames were designed only for the load combination $D + 1.3\ L_R + E$. It is likely that gravity load requirements are less critical. Details of the frames are shown in Figs A.1-A.3.

Because a spring-mass model is used, an initial stiffness k, yield shear strength V_y and ratio α of post yield stiffness to the initial stiffness for each storey must be determined for the bi-linear model. A non-linear static analysis of the whole frame model is required to obtain the storey characteristics. For this a lateral load distribution needs to be assumed. This in fact determines the failure mode before the start of analysis. The storey shear - drift relationship for a particular level is also affected by other storeys. This means that it is impossible to determine the characteristics for each storey independently. Therefore, the problem of the load distribution appropriate for obtaining the storey characteristics cannot be solved (84). In the present study, the commonly used inverted

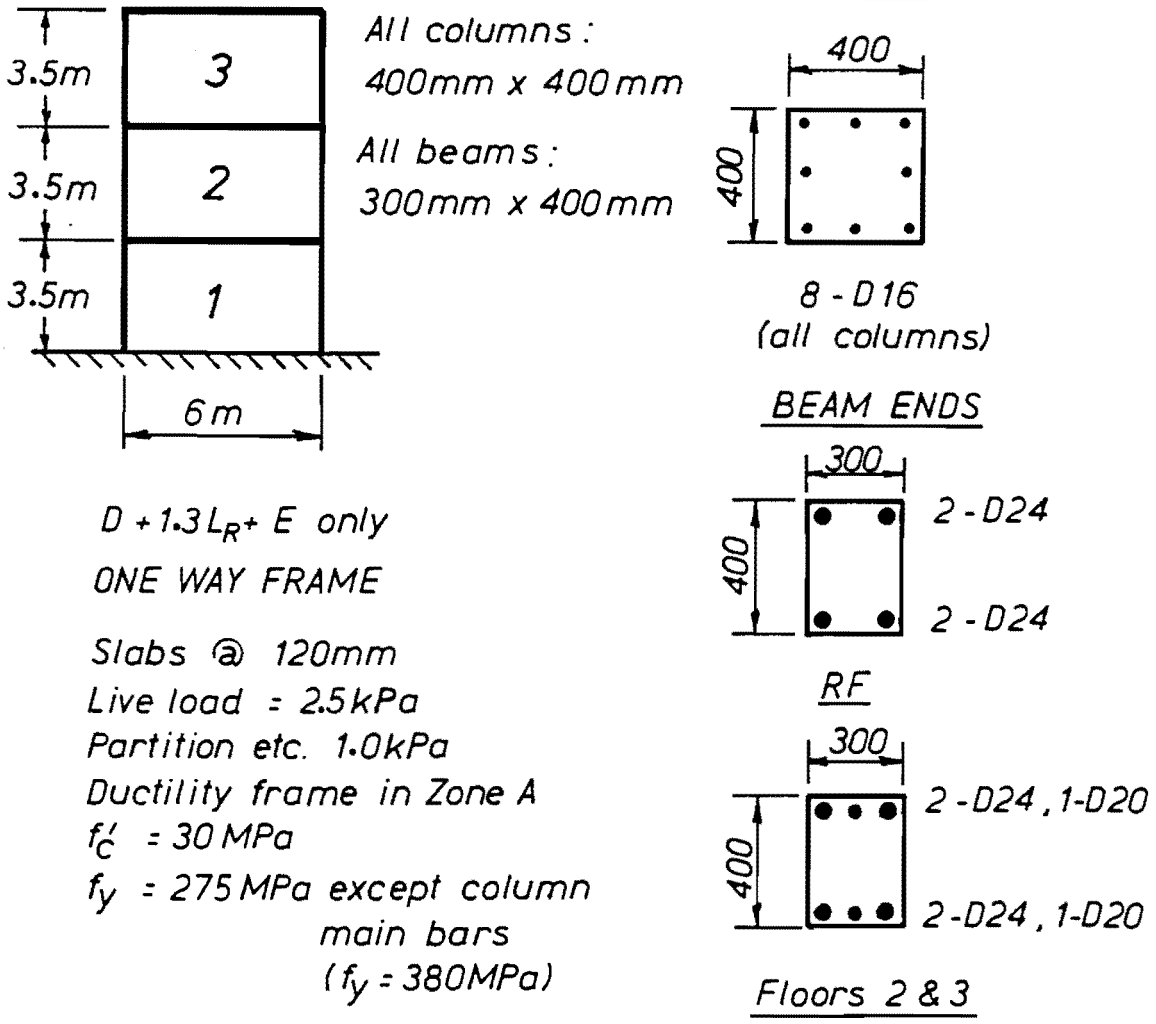

Fig. A.1 Details of 3-storey frame

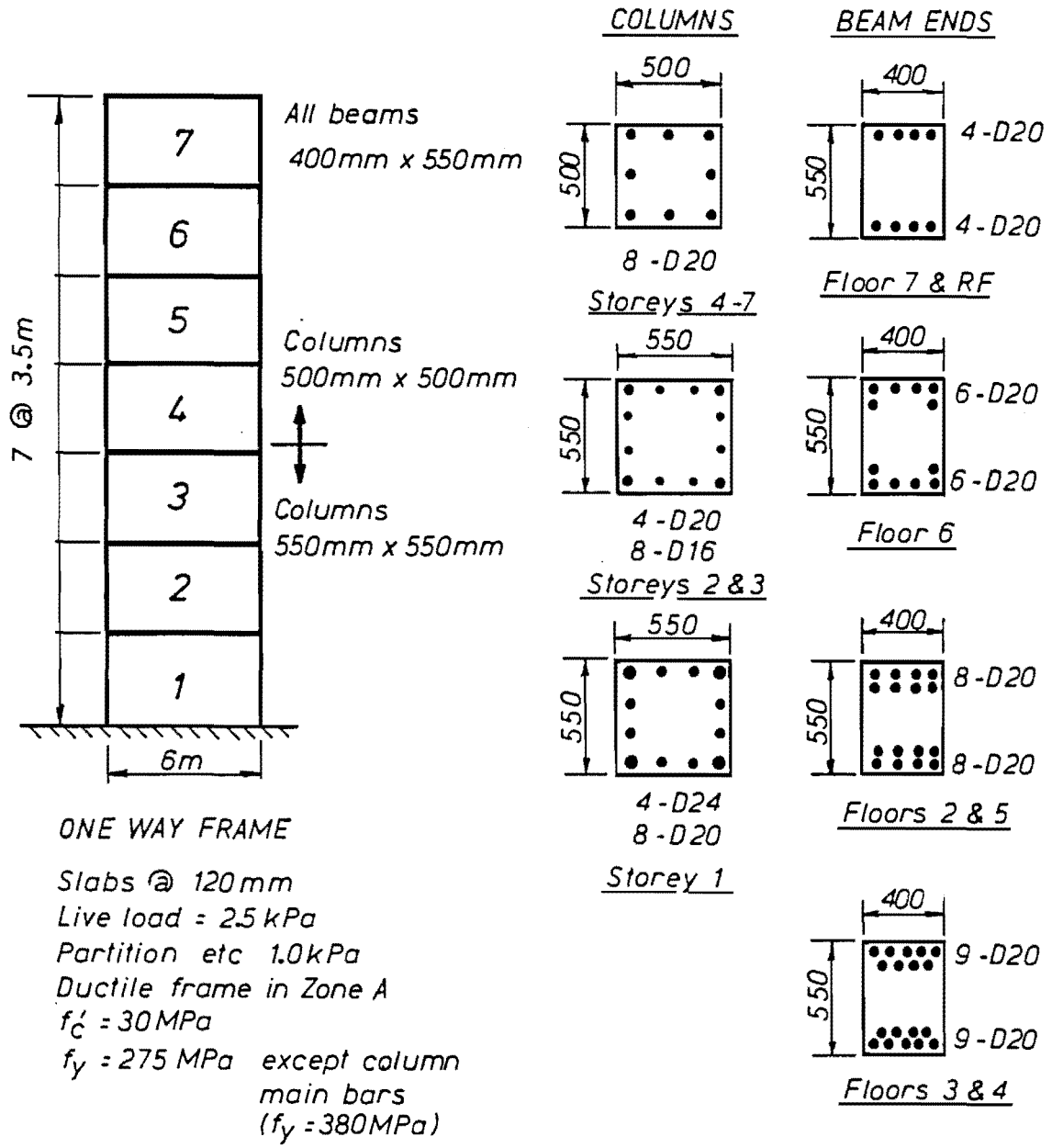

Fig. A.2 Details of 7-storey frame

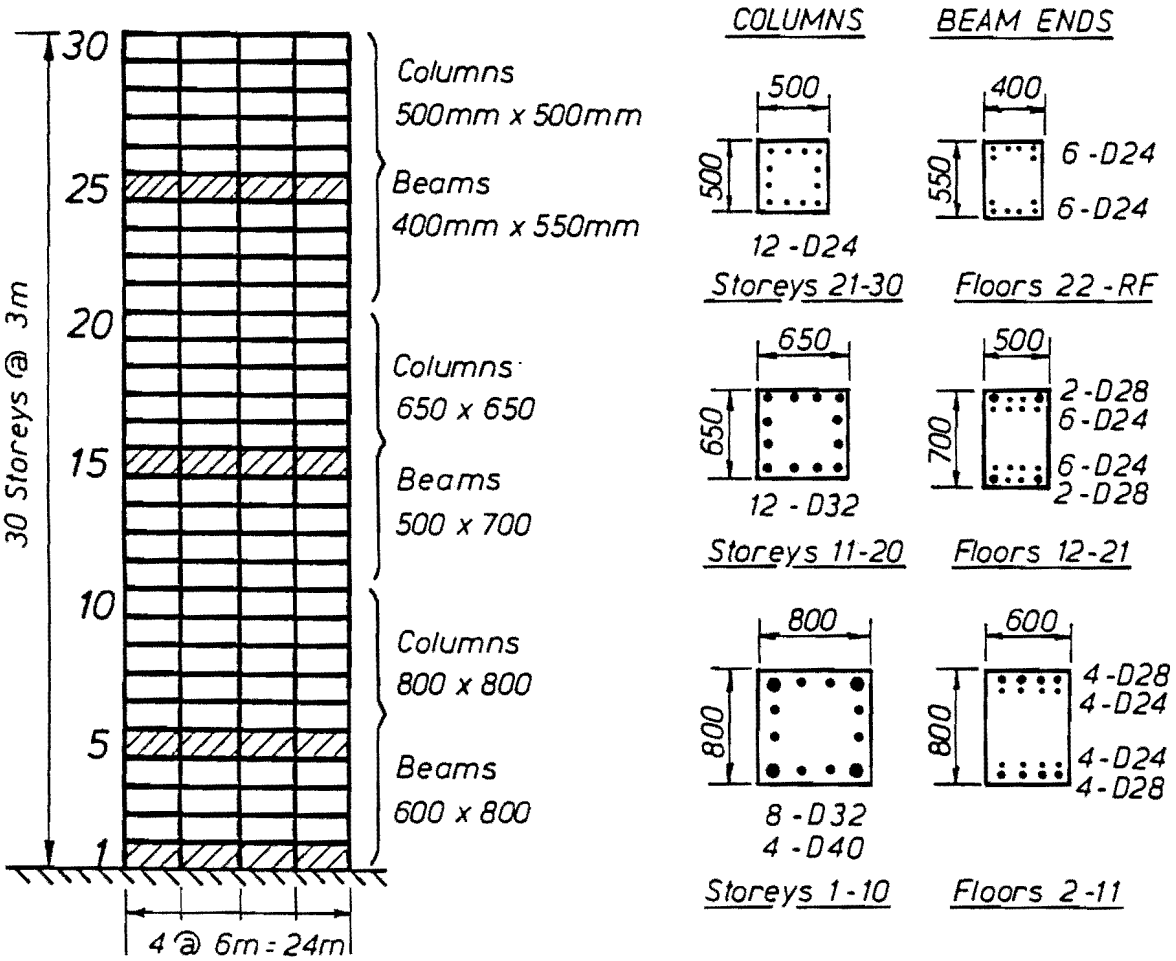

//// Storey designed

$D + 1.3L_R + E$ only

ONE WAY FRAME

Slabs @ 120 mm
Live load = 2.5 kPa
Partition etc. 1.0 kPa
Ductile frame in Zone A
f'_c = 30 MPa
f_y = 275 MPa except column main bars (f_y = 380 MPa)

Fig. A.3 Details of 30-storey frame

triangular pattern of lateral load distribution was assumed. The storey characteristics, k, V_y and α were then calculated such that a bi-linear storey shear-drift relationship by a non-linear static analysis was obtained. Table A.1 shows the storey characteristics. The term C_{d_i} in the Table is defined as a ratio of yield strength of the ith storey to weight of the structure sustained by the ith storey. These were mainly used in this study for a spring-mass model. The building was assumed to consist of identical frames, spaced 6 m apart. Therefore, the floor masses were computed for one frame only. To allow for the presence of some live load during the earthquake, floor mass was based on 1.1 times dead load.

A non-linear static analysis may not be necessary to obtain the storey characteristics used in a simple method for predicting failure probability. Thus, a more straightforward approach to obtain them is desirable. Since an elasto-fully-plastic model (α=0) was adopted in the prediction method, a possible simpler approach for estimating k and V_y for frame structures is also considered in the following. This is based on the suggestion of Umemura (84).

(1) Calculation of a Storey Initial Stiffness k_i

In calculating a storey initial stiffness k_i, Muto's method (86) is used. it is considered to be one of the most accurate and versatile techniques to estimate frame actions due to lateral load. The stiffness of jth column in ith

Table A.1 Storey characteristics of 3,7 & 30 storey models (spring-mass model A)

3-storey model

Storey	w_t (kN)	k (kN/mm)	α	V_y (kN)	C_{d_i}
3	210	2.77	0.249	75.0	0.358
2	247	5.15	0.273	100.0	0.219
1	"	8.68	0.247	120.0	0.170

7-storey model

Storey	w_t (kN)	k (kN/mm)	α	V_y (kN)	C_{d_i}
7	243	12.7	0.217	67.5	0.277
6	292	15.1	0.197	126	0.234
5	"	15.8	0.178	174	0.210
4	"	16.1	0.179	212	0.189
3	"	17.3	0.193	241	0.171
2	"	19.4	0.197	260	0.152
1	"	37.1	0.165	270	0.135

30-storey model

Storey	w_t (kN)	k (kN/mm)	α	V_y (kN)	C_{d_i}
30	1001	28.2	(0.35)	(168)	0.168
29	"	42.8	(0.35)	(330)	0.165
28	"	51.0	(0.35)	(486)	0.162
27	"	56.3	0.32	740	0.185
26	"	60.1	0.32	790	0.158
25	"	63.0	0.27	860	0.143
24	"	65.3	0.24	930	0.133
23	"	67.5	0.23	991	0.124
22	"	71.0	0.23	1079	0.120
21	"	87.6	0.18	1383	0.138
20	1227	146	0.20	1579	0.141
19	"	154	0.19	1678	0.135
18	"	159	0.19	1707	0.125
17	"	163	0.20	1717	0.115
16	"	166	0.19	1746	0.108
15	"	170	0.19	1756	0.101
14	"	174	0.20	1766	0.095
13	"	178	0.19	1825	0.092
12	"	185	0.19	1893	0.090
11	"	215	0.18	2011	0.090
10	1461	308	0.16	2099	0.088
9	"	321	0.16	2158	0.086
8	"	331	0.16	2178	0.082
7	"	341	0.15	2246	0.080
6	"	351	0.15	2256	0.076
5	"	363	0.16	2286	0.074
4	"	376	0.16	2305	0.071
3	"	394	0.17	2394	0.070
2	"	440	0.19	2492	0.070
1	"	760	0.27	2619	0.071

( ) - not obtained and arbitrarily determined

Table A.2 Storey characteristics of 3,7 & 30 storey models (spring-mass model B)

3-storey model

Storey	w_t (kN)	k (kN/mm)	V_y (kN)	C_{d_i}
3	210	7.74	49.7	0.237
2	247	"	82.9	0.181
1	"	13.2	99.1	0.141

7-storey model

Storey	w_t (kN)	k (kN/mm)	V_y (kN)	C_{d_i}
7	243	22.7	66.0	0.272
6	292	"	123	0.230
5	"	"	170	0.206
4	"	"	207	0.185
3	"	25.1	235	0.167
2	"	"	255	0.150
1	"	45.4	264	0.132

30-storey model

Storey	w_t (kN)	k (kN/mm)	V_y (kN)	C_{d_i}
30	1001	106	168	0.168
29	"	"	330	0.165
28	"	"	486	0.162
27	"	"	637	0.159
26	"	"	782	0.157
25	"	"	921	0.153
24	"	"	1059	0.151
23	"	"	1187	0.148
22	"	"	1305	0.145
21	"	142	1422	0.142
20	1227	272	1540	0.137
19	"	"	1638	0.131
18	"	"	1746	0.128
17	"	"	1834	0.123
16	"	"	1923	0.119
15	"	"	2011	0.116
14	"	"	2090	0.112
13	"	"	2158	0.109
12	"	"	2227	0.106
11	"	328	2286	0.103
10	1461	507	2345	0.099
9	"	"	2394	0.095
8	"	"	2443	0.092
7	"	"	2482	0.088
6	"	"	2511	0.085
5	"	"	2541	0.082
4	"	"	2560	0.079
3	"	"	2580	0.076
2	"	"	2590	0.073
1	"	854	2600	0.070

storey $S_{i,j}$ is:

$$S_{i,j} = D_j \cdot \frac{12E}{h_i^2} \qquad (A.1)$$

in which:

h_i = height of the ith storey

E = young modulas

D_j = D value of the Muto method

D value is expressed by:

$$D_j = a_{i,j} \cdot k_j \qquad (A.2)$$

where: $a_{i,j} = \frac{\overline{k_j}}{2+\overline{k_j}}$ $\left(a_{1,j} = \frac{0.5+\overline{k_j}}{2+\overline{k_j}} \text{ at basement}\right)$

K_j = defined in Fig. A.4

K_j = I_j/h_j (relative stiffness for columns)

$K_{j,n}$ = $I_{j,n}/h_{j,n}$ (relative stiffness for beams)

I_j = moment of inertia

The stiffness of the column $S_{i,j}$ can be rewritten as:

$$S_{i,j} = \frac{V_{i,j}}{\delta_{i,j}} \qquad (A.3)$$

where: $V_{i,j}$ = shear force sustained by the jth column in the ith storey

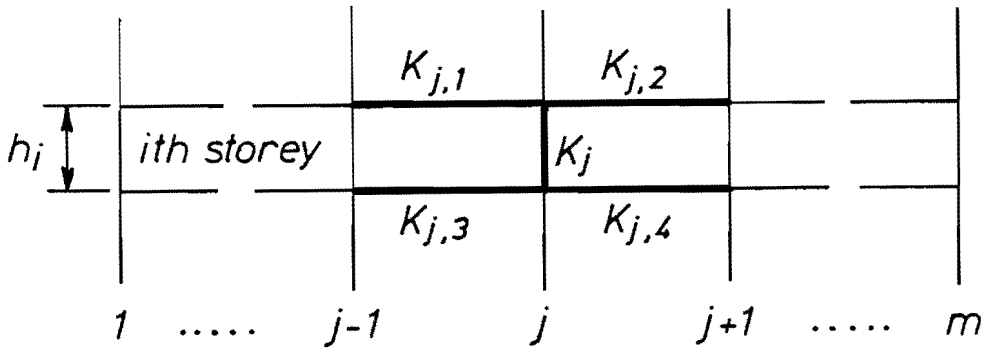

$$\bar{K}_j = \frac{K_{j,1} + K_{j,2} + K_{j,3} + K_{j,4}}{2K_j}$$

Fig. A.4 Calculation of value of $\bar{K}_j$

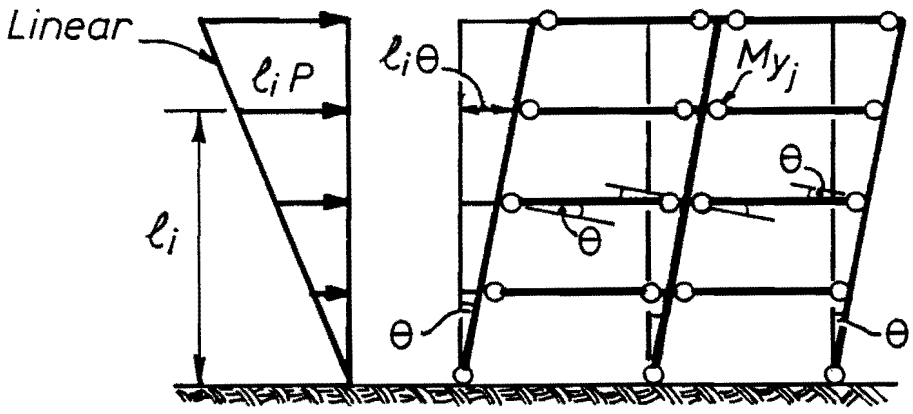

Fig. A.5 Assumption of a yield hinge formation and a load distribution

$\delta_{i,j}$ = deformation of the jth column in the ith storey

Assuming that deformations of columns in a storey are all the same, the relationship between a storey shear and drift is:

$$V_i = \sum_{j=1}^{m} V_{i,j}$$

$$= \delta_i \cdot \left(\sum_{j=1}^{m} S_{i,j} \right) \qquad (A.4)$$

in which:

m = the number of columns in the ith storey

V_i = total shear force sustained by all columns in the ith storey

δ_i = storey drift in the ith storey

Hence, the initial stiffness k_i of the ith storey can be expressed as:

$$k_i = \sum_{j=1}^{m} S_{i,j} \qquad (A.5)$$

(2) Calculation of a Yield Shear Strength V_{y_i}

A yield shear strength V_{y_i} may be obtained by using virtual work theory assuming a plastic hinge formation of a structure and a load distribution. In the present study, plastic hinges were assumed to develop at beam ends and at the base of the first storey columns under the action of the

lateral load with an inverted triangular distribution (see Fig. A.5). From virtual work theory, the following equation must be satisfied:

$$\sum_{i=1}^{n} l_i \cdot P \cdot l_i \cdot \theta = \sum_{\forall j} M_{y_j} \cdot \theta$$

or:

$$P \cdot \sum_{i=1}^{n} l_i^2 = \sum_{\forall j} M_{y_i} \tag{A.6}$$

where: n = number of storeys

l_i = height of the (i+1)th floor

$l_i.P$ = applied load at the (i+1)th floor

M_{y_j} = ideal flexural strength of jth plastic hinge

Thus:

$$P = \frac{\sum_{\forall j} M_{y_j}}{\sum_{i=1}^{n} l_i^2} \tag{A.7}$$

Accordingly, a yield shear strength V_{y_i} of the ith storey can be written as:

$$V_{y_i} = P \cdot \sum_{j=i}^{n} l_j \tag{A.8}$$

From Eqs (A.5) and (A.8), the initial stiffness and yield shear strength of any storey are relatively simply calculated. The storey characteristics by this simple approach are shown in Table A.2. The comparison of dynamic responses using the storey characteristics shown in Tables A.1 and A.2 was discussed in Section 6.5.

Details of the calculation of k_i and V_{y_i} from Eqs (A.5) and (A.8) for an existing building, Clarendon Towers, are described in Appendix D.

APPENDIX B

EARTHQUAKE RECORDS USED IN THIS REPORT

Five earthquake records were used in the present study.

The time-history and Fourier spectrum for each earthquake acceleration are shown in Figs B.1 - B.5.

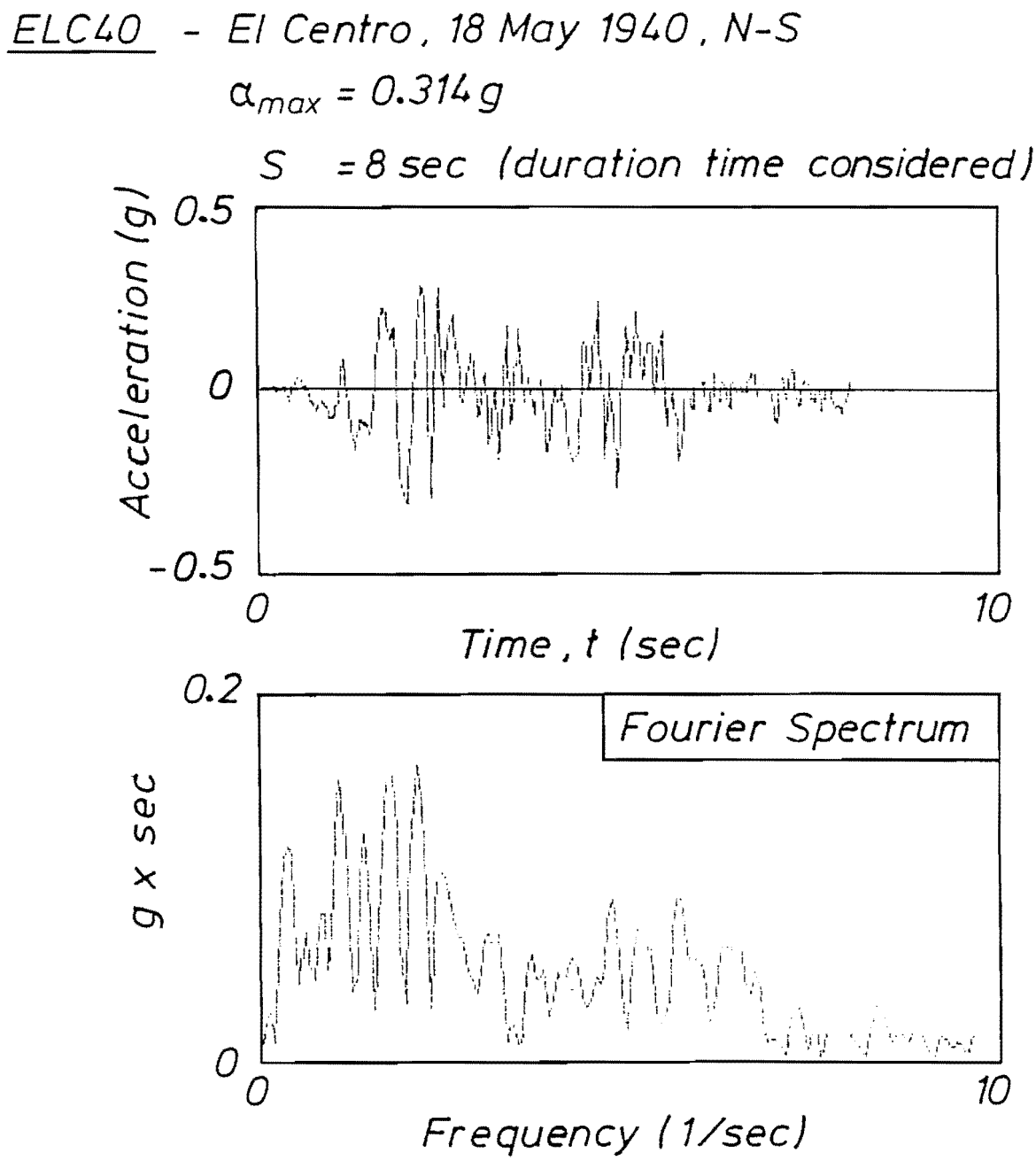

Fig. B.1 Time-history of acceleration and its Fourier spectrum

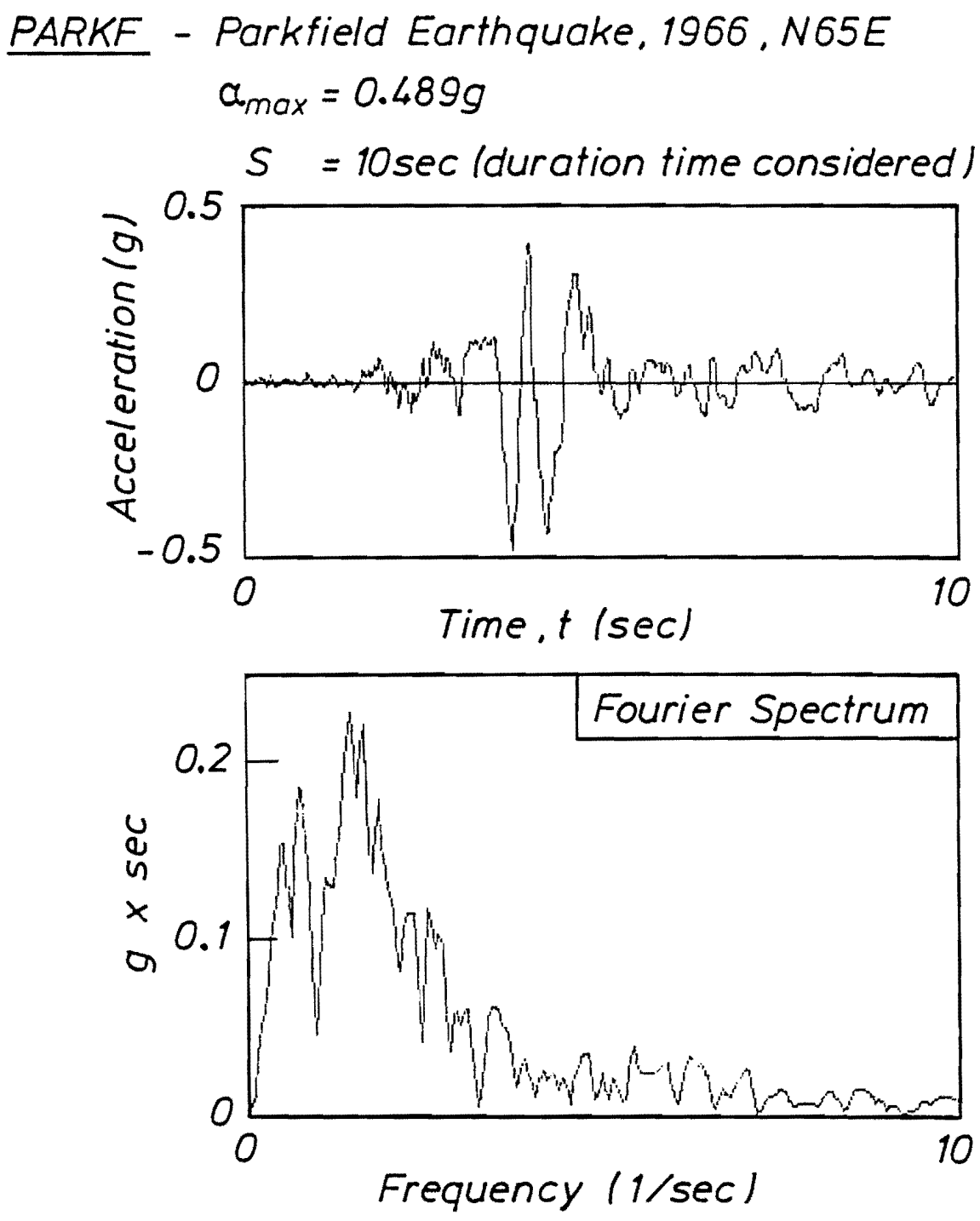

Fig. B.2 Time-history of acceleration and its Fourier spectrum

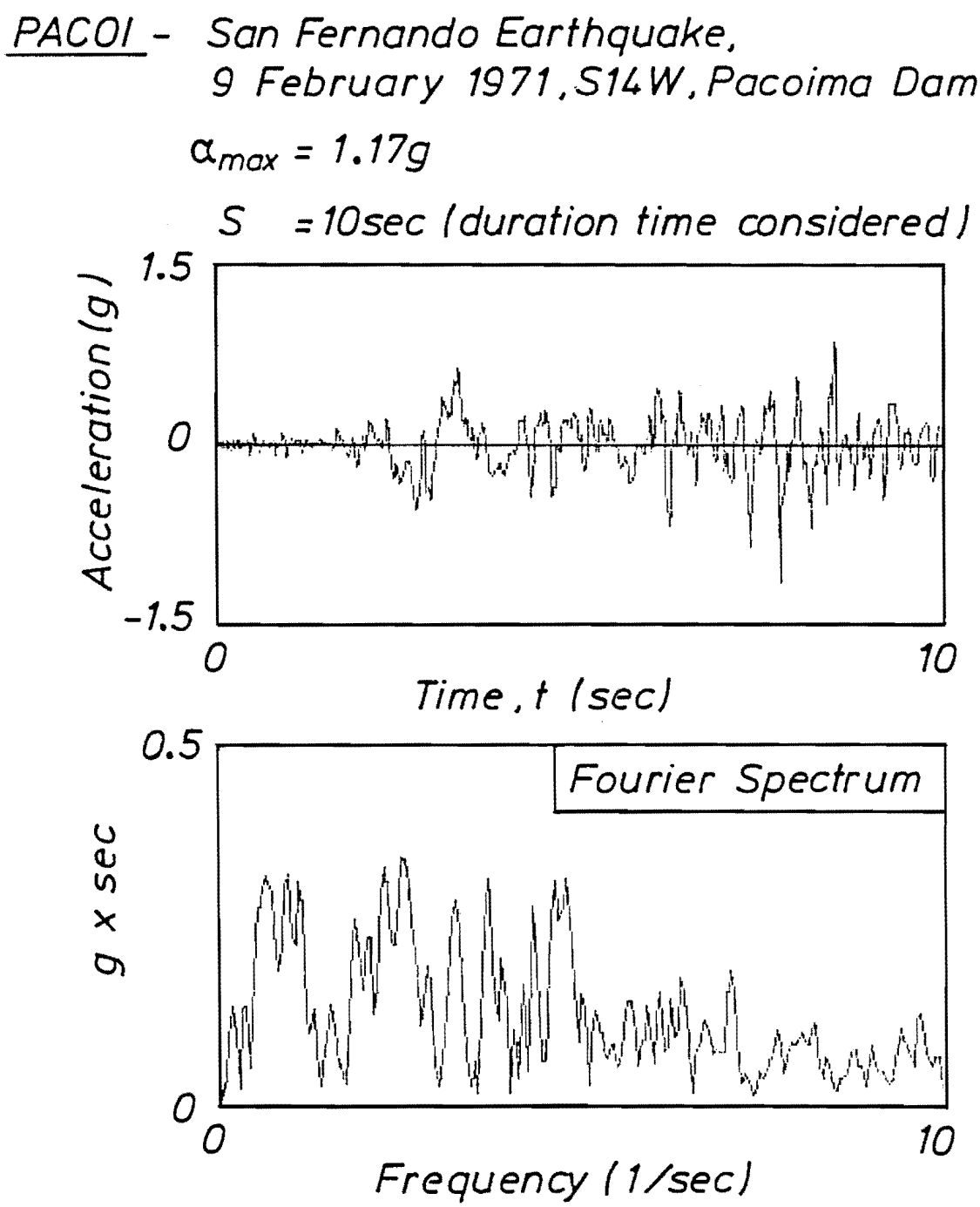

Fig. B.3 Time-history of acceleration and its Fourier spectrum

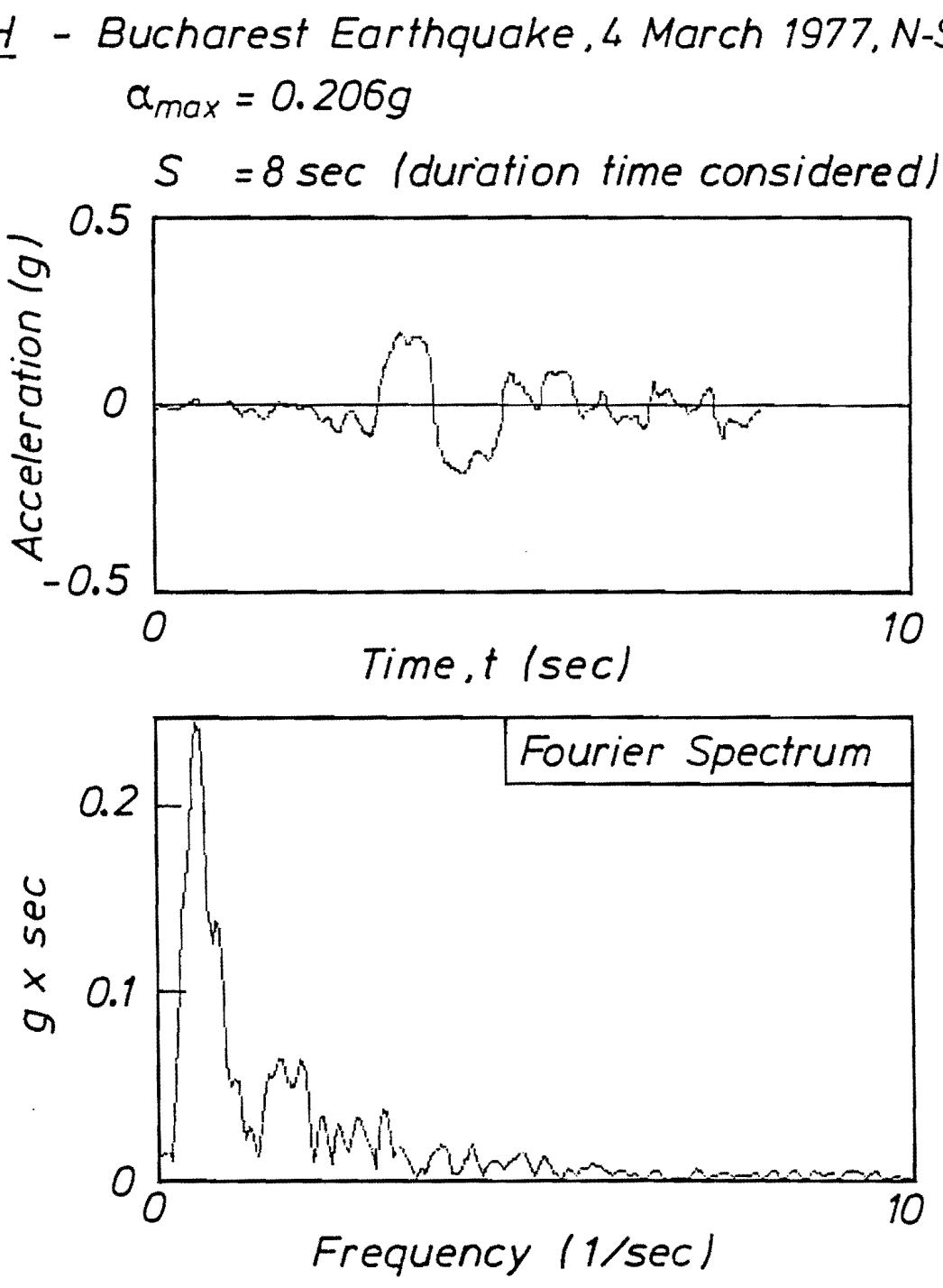

Fig. B.4 Time-history of acceleration and its Fourier spectrum

ELC79 - El Centro, 15 October 1979, N-S
Imperial County Services Bldg.
$\alpha_{max} = 0.213g$

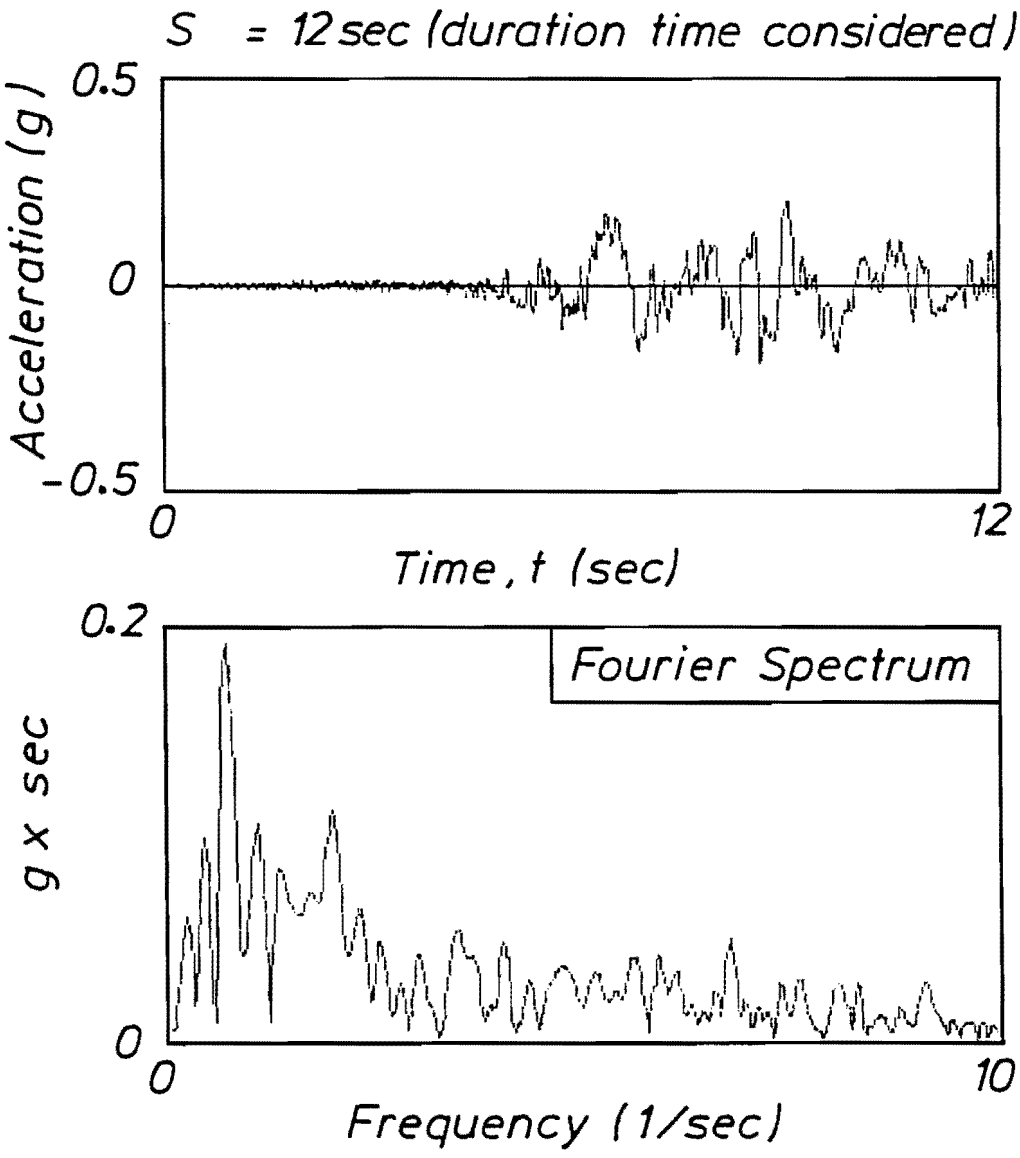

Fig. B.5 Time-hisroty of acceleration and its Fourier spectrum

APPENDIX C

A PROGRAM FOR MODAL ANALYSIS AND OBTAINING 0th AND 2nd MOMENTS OF SPECTRAL-DENSIYT FUNCTION

```
CCCCCCCCCCCCCCCCCCCCCCCCCCCCCCCCCCCCCCCCCCCCCCCCCCCCCCCCCCCCCCCCCCCCCCCCCCCCCCC
C                                                                              C
C  --- AIMS OF THIS PROGRAM ---                                                C
C                                                                              C
C   (1)  MODAL ANALYSIS , and                                                  C
C   (2)  0th AND 2nd MOMENTS OF THE SPECTRAL DENSITY FUNCTION                  C
C        FOR STOREY DRIFTS SUBJECTED TO A GIVEN EARTHQUAKE ,                   C
C   FOR A M.D.O.F. SYSTEM                                                      C
C                                                                              C
C                                          CODED BY   S. OGAWA                 C
C                                                                              C
CCCCCCCCCCCCCCCCCCCCCCCCCCCCCCCCCCCCCCCCCCCCCCCCCCCCCCCCCCCCCCCCCCCCCCCCCCCCCCC
C                                                                              C
C   -- LIMITATION --                                                          C
C                                                                              C
C         MAX. DEGREE OF FREEDOM              -- 30                            C
C         MAX. NUMBER OF DISCRETE DATA POINTS -- 4096                          C
C              ( INC. ADDITIONAL '0's )                                        C
C         INPUT EQ. FORMAT                    -- BERG FORMAT                   C
C                                                                              C
C  -- EXPLANATION OF ITEMS --                                                  C
C                                                                              C
C   IRATIO --- 'NT' IS MINIMUM REQUIRED NUMBER OF DATA WHICH MUST              C
C              BE INTEGER POWER OF 2. ( EX. WHEN TIME INCREMENT                C
C              = 0.01 sec. & TIME DURATION = 8 sec. THEN NT = 1024)            C
C              BUT, IN GENERAL, IT IS NOT BIG ENOUGH TO GET A                  C
C              REASONABLE RESULT. 'IRATIO' IS USED TO INCREASE THE             C
C              NUMBER SUCH THAT NT = NT * IRATIO.                              C
C   AM -------  STOREY MASS ( SPRING-MASS MOLEL )                              C
C   Wt -------  STOREY WEIGHT ( KN )                                           C
C   AH(I) ----  CRITICAL DAMPING RATIO OF ith MODE                             C
C   STIFF ----  STOREY STIFFNESS ( SPRING-MASS MODEL ; KN/MM )                 C
C   TIMEM ----  DURATION OF EARTHQUAKE ( SEC. )                                C
C   DT -------  INTEGRATION TIME STEP ( SEC. )                                 C
C   WN -------  RESONANT CIRCULAR FREQUENCY                                    C
C   U --------  MODAL SHAPE                                                    C
C   COEFT ----  RATIO OF TIMEM TO DT*NT ( POWER MUST BE INDEPENDENT            C
C               ON THE NUMBER OF ADDITIONAL ZERO. )                            C
C                                                                              C
C  -- NOTE --                                                                 C
C               INPUT DATA FOR A STRUCTURE MUST BE ENTERED FROM THE            C
C               TOP STOREY DOWN. ( EX. Wt(IDOF), - - , Wt(2),Wt(1) )           C
C                                                                              C
CCCCCCCCCCCCCCCCCCCCCCCCCCCCCCCCCCCCCCCCCCCCCCCCCCCCCCCCCCCCCCCCCCCCCCCCCCCCCCC
      DIMENSION NAME(10),TIME1(2000),GP(30,4096),
     1          WVIN1(2000),AM(30,30),AK(30,30),AH(30),WN(30),
     2          PHAI(30,30),BETA(30),AMN(30),WORK(30),CM(30,30),
     3          DUMY(30,30),STIF(30)
      REAL TIME(4096),WV(4096)
      COMPLEX   G(30,2,4096),Z1,GCH(4096),TEMP
      REAL*8 AAM(30,30),AAK(30,30),EIGV(30),EIGVEC(30,30),TEMP1(30),
     1       TEMP2(30,30),VMIN
      DATA NAME/10*'    '/
C=============================================================
C=== INPUT DATA ==============================================
C=============================================================
C
      READ(5,90) IDOF,IRATIO
   90 FORMAT(16I5)
C
      IF(IDOF.LE.30) GO TO 10
      WRITE(6,20)
   20 FORMAT(1H ,'THE NUMBER OF FREEDOM IS OVER THE LIMITATION.')
      STOP
   10 CONTINUE
C
      WRITE(6,95) IDOF,IRATIO
   95 FORMAT(1H ,'***** INPUT DATA *****'/1H ,2X,
     1       'DEGREE OF FREEDOM = ',I5/1H ,2X,'NT = NT * ',I3)
C
      DO 60 I=1,IDOF
      DO 60 J=1,IDOF
      AM(I,J)=0.0
      AAM(I,J)=0.0
   60 CONTINUE
C
      READ(5,70) (AM(I,I),I=1,IDOF)
   70 FORMAT(8F10.0)
      WRITE(6,75) (AM(I,I),I=1,IDOF)
   75 FORMAT(1H ,2X,'Weight(KN)=',5F12.1)
C
      DO 77 I=1,IDOF
      AM(I,I)=AM(I,I)/9810.
   77 CONTINUE
C
      READ(5,70) (AH(I),I=1,IDOF)
      WRITE(6,78) (AH(I),I=1,IDOF)
   78 FORMAT(1H ,2X,'Crit. Damp= ',5F12.4)
C
      READ(5,70) (STIF(J),J=1,IDOF)
      WRITE(6,85) (STIF(J),J=1,IDOF)
   85 FORMAT(1H ,2X,'STIF(KN/MM)=',5F12.1)
C
      CALL STIFM(IDOF,STIF,AK)
C
      READ(5,120) TIMEM,DT,(NAME(I),I=1,10)
  120 FORMAT(2F10.0,10A4)
      WRITE(6,130) TIMEM,DT,(NAME(I),I=1,10)
  130 FORMAT(/1H ,2X,'MAX. TIME = ',F10.1,' (SEC.)  ;  D-TIME = ',
     1       F10.4,' (SEC.)'/1H ,2X,' EQ NAME = ',10A4)
C
C--- INPUT WAVE ----
C
      DO 210 I=1,4096
      WV(I)=0.0
  210 CONTINUE
C
      II=-3
      READ(10,145) PP
  145 FORMAT(A4)
C
  150 CONTINUE
```

```
      II=II+4
      IF(II.EQ.1) GO TO 170
      IF(TIMEM.LT.TIME1(II-1)) GO TO 180
      IF(II.LT.1996) GO TO 170
      WRITE(6,160)
  160 FORMAT(1H ,'INPUT WAVE DIMENSION IS TOO SMALL.')
      STOP
C
  170 CONTINUE
      READ(10,140,END=180) J,TIME1(II),WVIN1(II),TIME1(II+1),
     1   WVIN1(II+1),TIME1(II+2),WVIN1(II+2),TIME1(II+3),WVIN1(II+3)
  140 FORMAT(I3,4(F8.4,F9.6))
C
      GO TO 150
C
  180 CONTINUE
C
C--- REARRANGE INPUT WAVE  ---
C
      CALL INTPL(TIME1,WVIN1,TIME,WV,DT,II,TIMEM)
C
      IF(WV(1).EQ.0.0) GO TO 241
      DO 242 I=1,II
      J=II-I+2
      TIME(J)=TIME(J-1)
      WV(J)=WV(J-1)
  242 CONTINUE
      TIME(1)=0.0
      WV(1)=0.0
      II=II+1
  241 CONTINUE
      NUMRE=II
C
      NT=2
  240 CONTINUE
      IF(NT.GE.II) GO TO 230
      NT=NT*2
      GO TO 240
  230 CONTINUE
C
      NT=NT*IRATIO
      WRITE(6,233) NT
  233 FORMAT(/1H ,2X,'TOTAL NUMBER ( FOURIER ) = ',I5)
C
      IF(NT.LE.4096) GO TO 250
      WRITE(6,165) NT,II
  165 FORMAT(1H ,'WAVE DIMENSION IS OVER 4096. NT= ',I6,' II=',I5)
      STOP
C
  250 CONTINUE
C
C--- EIGEN VALUE ( JACOBI METHOD ) ---
C
      DO 113 I=1,IDOF
      AAM(I,I)=AM(I,I)
      DO 113 J=1,IDOF
      AAK(I,J)=AK(I,J)
  113 CONTINUE
C
      CALL JACOBI(AAK,AAM,TEMP2,TEMP1,IDOF)
C
C--- REARRANGING BASED ON INCREASING ORDER ---
C
      DO 513 I=1,IDOF
      VMIN=100000000.
C
      DO 514 J=1,IDOF
      IF(TEMP1(J).GE.VMIN) GO TO 514
      VMIN=TEMP1(J)
      IJ=J
  514 CONTINUE
C
      EIGV(I)=TEMP1(IJ)
      TEMP1(IJ)=10000000.
C
      DO 516 J=1,IDOF
      EIGVEC(J,I)=TEMP2(J,IJ)
  516 CONTINUE
C
  513 CONTINUE
C
      DO 114 I=1,IDOF
      WN(I)=SQRT(EIGV(I))
      DO 114 J=1,IDOF
      PHAI(I,J)=EIGVEC(I,J)/EIGVEC(IDOF,J)
  114 CONTINUE
C
      WRITE(6,351)
  351 FORMAT(/1H ,'***** MODAL ANLYSIS RESULTS *****')
      WRITE(6,115) (WN(I),I=1,IDOF)
  115 FORMAT(1H ,2X,'Wn(I) = ',5F12.5)
C
      DO 117 I=1,IDOF
      WRITE(6,116) I
  116 FORMAT(1H ,2X,'-- MODE = ',I5,' --')
      WRITE(6,118) (PHAI(J,I),J=1,IDOF)
  118 FORMAT(1H ,2X,'U(I) = ',5F12.5)
  117 CONTINUE
C
C--- MODAL COEFFICIENTS ---
C
      DO 700 I=1,IDOF
      UP=0.0
      DN=0.0
      DO 705 J=1,IDOF
      UP=UP+AM(J,J)*PHAI(J,I)
      DN=DN+AM(J,J)*PHAI(J,I)**2
  705 CONTINUE
      BETA(I)=UP/DN
  700 CONTINUE
C
      WRITE(6,709)
  709 FORMAT(/1H ,2X,'-- MODAL PARTICIPATION FACTOR --')
      WRITE(6,708) (BETA(I),I=1,IDOF)
  708 FORMAT(1H ,2X,5E12.4)
C
C--- MODAL MASS ---
C
      DO 710 I=1,IDOF
      DO 715 J=1,IDOF
```

```
        WORK(J)=AM(J,J)*PHAI(J,I)
  715   CONTINUE
        AMN(I)=0.0
        DO 716 J=1,IDOF
        AMN(I)=AMN(I)+WORK(J)*PHAI(J,I)
  716   CONTINUE
  710   CONTINUE
C
C--- C MATRIX (USING MODAL DAMPING) ---
C
        DO 740 MODE=1,IDOF
        COEF=2.0*AH(MODE)*WN(MODE)/AMN(MODE)
        DO 741 I=1,IDOF
        DO 741 J=1,IDOF
        CM(I,J)=CM(I,J)+PHAI(I,MODE)*PHAI(J,MODE)*COEF
  741   CONTINUE
  740   CONTINUE
C
        DO 742 I=1,IDOF
        DO 742 J=1,IDOF
        DUMY(I,J)=0.0
        DO 742 K=1,IDOF
        DUMY(I,J)=DUMY(I,J)+CM(I,K)*AM(K,J)
  742   CONTINUE
C
        DO 747 I=1,IDOF
        DO 747 J=1,IDOF
        CM(I,J)=0.0
        DO 747 K=1,IDOF
        CM(I,J)=CM(I,J)+AM(I,K)*DUMY(K,J)
  747   CONTINUE
C
C=============================================================
C=== FOURIER TRANSFORM FOR INPUT WAVE ========================
C=============================================================
        NTF=NT/2+1
C
        DO 270 I=1,NT
        GCH(I)=CMPLX(WV(I),0.0)
  270   CONTINUE
C
        CALL FAST(NT,GCH,4096,-1)
C
        DO 280 I=1,NT
        G(1,1,I)=GCH(I)/FLOAT(NT)
  280   CONTINUE
C
C=============================================================
C=== FREQUENCY DOMAIN ANALYSIS ===============================
C=============================================================
C
        DO 282 I=1,IDOF
        DO 282 K=1,NTF
        G(I,2,K)=CMPLX(0.0,0.0)
  282   CONTINUE
C
        DO 290 MODE=1,IDOF
C
        HWW=2.0*AH(MODE)*WN(MODE)
C
        DO 290 IFREQ=1,NTF
        J=IFREQ-1
        WW=2.0*3.141593/FLOAT(NT)/DT*FLOAT(J)
        RE=WN(MODE)**2-WW**2
        BI=HWW*WW
        Z1=CMPLX(-1.0,0.0)/CMPLX(RE,BI)
        G(MODE,2,IFREQ)=G(1,1,IFREQ)*Z1
  290   CONTINUE
C
C=== POWER SPECTRUM ===
C
        TOT=FLOAT(NT)*DT
        RET=FLOAT(NT)/FLOAT(NUMRE)
        COEFT=RET*TOT
C
        DO 800 NODE=1,IDOF
C
        DO 805 I=1,NTF
        TEMP=0.0
C
        DO 810 M=1,IDOF
        TEMP=TEMP+CMPLX(PHAI(NODE,M)*BETA(M),0.0)*G(M,2,I)
  810   CONTINUE
C
        IF(NODE.EQ.IDOF) GO TO 825
C
        DO 815 M=1,IDOF
        TEMP=TEMP-CMPLX(PHAI(NODE+1,M)*BETA(M),0.0)*G(M,2,I)
  815   CONTINUE
C
  825   CONTINUE
        IF(I.NE.1) GO TO 820
        GP(NODE,I)=CABS(TEMP)**2*COEFT
        GO TO 805
  820   CONTINUE
        IF(I.EQ.NTF) GO TO 830
        GP(NODE,I)=2.0*CABS(TEMP)**2*COEFT
        GO TO 805
  830   CONTINUE
        GP(NODE,I)=CABS(TEMP)**2*COEFT
C
  805   CONTINUE
C
  800   CONTINUE
C
        WRITE(6,350)
  350   FORMAT(/1H ,'***** 0th AND 2nd MOMENTS OF S.D.F. *****')
C
        CALL RAND(GP,NT,NTF,DT,IDOF)
C
        STOP
        END
        SUBROUTINE RAND(G,NT,NTF,DT,IDOF)
CCCC
```

```
      DO 100 NEL=1,IDOF
C
      T=DT*FLOAT(NT)
      DW=2.0*3.141593/T
C
      DO 130 I=1,3,2
      RAM(I)=0.0
      N=I-1
C
      DO 130 J=1,NTF
      IF(J.NE.1) GO TO 140
      RAM(I)=DW/2.0*(DW/4.0)**N*G(NEL,J)/6.2832
      GO TO 130
C
  140 CONTINUE
      IF(J.NE.NTF) GO TO 150
      RAM(I)=RAM(I)+DW/2.0*(DW*(FLOAT(NTF-1)-0.25))**N*G(NEL,J)/
     1       6.2832
      GO TO 130
C
  150 CONTINUE
      RAM(I)=RAM(I)+DW*(DW*(FLOAT(J-1)))**N*G(NEL,J)/6.2832
C
  130 CONTINUE
C
      OME=SQRT(RAM(3)/RAM(1))
C
      INV=IDOF+1-NEL
      WRITE(6,170) INV,OME,RAM(1)
  170 FORMAT(1H ,'STOREY = ',I3,'   OME = ',F8.3,
     1       ' (1/SEC.)    SIG**2 = ',F10.5,' (MM**2)')
C
  100 CONTINUE
C
      RETURN
      END
      SUBROUTINE FAST(N,X,ND,IND)
CCCCCCCCCCCCCCCCCCCCCCCCCCCCCCCCCCCCCCCCCCCCCCCCCCCCCCCCCCCCCCCCCCCCCCC
C                                                                      C
C              FAST FOURIER TRANSFORM             CODED BY OHSAKI      C
C                                                                      C
CCCCCCCCCCCCCCCCCCCCCCCCCCCCCCCCCCCCCCCCCCCCCCCCCCCCCCCCCCCCCCCCCCCCCCC
      COMPLEX X(ND),TEMP,THETA
C
      J=1
      DO 140 I=1,N
      IF(I.GE.J) GO TO 110
      TEMP=X(J)
      X(J)=X(I)
      X(I)=TEMP
  110 M=N/2
  120 IF(J.LE.M) GO TO 130
      J=J-M
      M=M/2
      IF(M.GE.2) GO TO 120
  130 J=J+M
  140 CONTINUE
C
      KMAX=1
  150 IF(KMAX.GE.N) RETURN
      ISTEP=KMAX*2
      DO 170 K=1,KMAX
      THETA=CMPLX(0.0,3.141593*FLOAT(IND*(K-1))/FLOAT(KMAX))
      DO 160 I=K,N,ISTEP
      J=I+KMAX
      TEMP=X(J)*CEXP(THETA)
      X(J)=X(I)-TEMP
      X(I)=X(I)+TEMP
  160 CONTINUE
  170 CONTINUE
      KMAX=ISTEP
      GO TO 150
      END
      SUBROUTINE INTPL(T1,W1,T,W,DT,II,BNMAX)
CCCCCCCCCCCCCCCCCCCCCCCCCCCCCCCCCCCCCCCCCCCCCCCCCCCCCCCCCCCCCCCCCCCCCCC
C                                                                      C
C         RE-ARRANGE INPUT WAVE BASED ON SPECIFIED D-TIME              C
C                                                                      C
CCCCCCCCCCCCCCCCCCCCCCCCCCCCCCCCCCCCCCCCCCCCCCCCCCCCCCCCCCCCCCCCCCCCCCC
      DIMENSION T1(2000),W1(2000),T(4096),W(4096)
C
      GAL=9810.
      N=0
      ANMAX=BNMAX/DT
      MAX=IFIX(ANMAX)+1
      K1=1
C
   10 CONTINUE
      N=N+1
      IF(N.GT.MAX) GO TO 200
C
      TM=DT*(FLOAT(N)-1.0)
   30 CONTINUE
      IF(T1(K1).LE.TM.AND.T1(K1+1).GT.TM) GO TO 20
      K1=K1+1
      GO TO 30
C
   20 CONTINUE
      T(N)=TM
      W(N)=((TM-T1(K1))/(T1(K1+1)-T1(K1))*(W1(K1+1)
     1              -W1(K1))+W1(K1))*GAL
C
      GO TO 10
C
  200 CONTINUE
C
      II=MAX
C
      DO 250 I=MAX+1,4096
      W(I)=0.0
  250 CONTINUE
C
      IF(II.LE.4096) RETURN
      WRITE(6,100)
  100 FORMAT(1H ,'*** SUB-INTPL *** WAVE DIMENSION IS OVER.')
      STOP
      END
      SUBROUTINE STIFM(IDOF,STIF,AK)
CCCCCCCCC1CCCCCCCCC1CCCCCCCCC1CCCCCCCCC1CCCCCCCCC1CCCCCCCCC1CCCCCCCCC1CC
C                                                                      C
```

```
C              CREATE STIFFNESS MATRIX FOR SPRING-MASS MODEL             C
C                                                                        C
CCCCCCCCCCCCCCCCCCCCCCCCCCCCCCCCCCCCCCCCCCCCCCCCCCCCCCCCCCCCCCCCCCCCCCCCC
      DIMENSION STIF(30),AK(30,30)
C
      DO 50 I=1,IDOF
      DO 50 J=1,IDOF
      AK(I,J)=0.0
   50 CONTINUE
C
      IF(IDOF.GE.2) GO TO 120
      AK(1,1)=STIF(1)
      RETURN
  120 CONTINUE
C
      AK(1,1)=STIF(1)
      AK(1,2)=-STIF(1)
C
      AK(IDOF,IDOF-1)=-STIF(IDOF-1)
      AK(IDOF,IDOF)=STIF(IDOF)+STIF(IDOF-1)
C
      IF(IDOF.EQ.2) RETURN
C
      DO 130 I=2,IDOF-1
      AK(I,I-1)=-STIF(I-1)
      AK(I,I)=STIF(I)+STIF(I-1)
      AK(I,I+1)=-STIF(I)
  130 CONTINUE
C
      RETURN
      END
      SUBROUTINE JACOBI(A,B,X,EIGV,N)
CCCCCCCCC1CCCCCCCCC2CCCCCCCCC3CCCCCCCCC4CCCCCCCCC5CCCCCCCCC6CCCCCCCCC7CC
C                                                                        C
C     TO SOLVE THE GENERALIZED EIGENPROBLEM                              C
C                              USING THE JACOBI ITERATION                C
C                                                   CODED BY WILSON      C
C                                                                        C
CCCCCCCCCCCCCCCCCCCCCCCCCCCCCCCCCCCCCCCCCCCCCCCCCCCCCCCCCCCCCCCCCCCCCCCCC
      IMPLICIT REAL*8(A-H,O-Z)
      DIMENSION A(30,30),B(30,30),X(30,30),EIGV(30),D(30)
C
      RTOL=1.0E-15
      NSMAX=20
C
      DO 10 I=1,N
      IF(A(I,I).GT.0.0.AND.B(I,I).GT.0.0) GO TO 4
      WRITE(6,2020)
      STOP
    4 D(I)=A(I,I)/B(I,I)
   10 EIGV(I)=D(I)
      DO 30 I=1,N
      DO 20 J=1,N
   20 X(I,J)=0.0
   30 X(I,I)=1.0
      IF(N.EQ.1) RETURN
C
      NSWEEP=0
      NR=N-1
   40 NSWEEP=NSWEEP+1
C
      EPS=(0.01**NSWEEP)**2
      DO 210 J=1,NR
      JJ=J+1
      DO 210 K=JJ,N
      EPTOLA=(A(J,K)*A(J,K))/(A(J,J)*A(K,K))
      EPTOLB=(B(J,K)*B(J,K))/(B(J,J)*B(K,K))
      IF((EPTOLA.LT.EPS).AND.(EPTOLB.LT.EPS)) GO TO 210
C
      AKK=A(K,K)*B(J,K)-B(K,K)*A(J,K)
      AJJ=A(J,J)*B(J,K)-B(J,J)*A(J,K)
      AB=A(J,J)*B(K,K)-A(K,K)*B(J,J)
      CHECK=(AB*AB+4.*AKK*AJJ)/4.
      IF(CHECK) 50,60,60
   50 WRITE(6,2020)
      STOP
   60 SQCH=DSQRT(CHECK)
      D1=AB/2.+SQCH
      D2=AB/2.-SQCH
      DEN=D1
      IF(DABS(D2).GT.DABS(D1)) DEN=D2
      IF(DEN) 80,70,80
   70 CA=0.0
      CG=-A(J,K)/A(K,K)
      GO TO 90
   80 CA=AKK/DEN
      CG=-AJJ/DEN
C
   90 IF(N-2) 100,190,100
  100 JP1=J+1
      JM1=J-1
      KP1=K+1
      KM1=K-1
      IF(JM1-1) 130,110,110
  110 DO 120 I=1,JM1
      AJ=A(I,J)
      BJ=B(I,J)
      AK=A(I,K)
      BK=B(I,K)
      A(I,J)=AJ+CG*AK
      B(I,J)=BJ+CG*BK
      A(I,K)=AK+CA*AJ
  120 B(I,K)=BK+CA*BJ
  130 IF(KP1-N) 140,140,160
  140 DO 150 I=KP1,N
      AJ=A(J,I)
      BJ=B(J,I)
      AK=A(K,I)
      BK=B(K,I)
      A(J,I)=AJ+CG*AK
      B(J,I)=BJ+CG*BK
      A(K,I)=AK+CA*AJ
  150 B(K,I)=BK+CA*BJ
  160 IF(JP1-KM1) 170,170,190
  170 DO 180 I=JP1,KM1
      AJ=A(J,I)
      BJ=B(J,I)
      AK=A(I,K)
      BK=B(I,K)
      A(J,I)=AJ+CG*AK
      B(J,I)=BJ+CG*BK
```

```
      A(I,K)=AK+CA*AJ
  180 B(I,K)=BK+CA*BJ
  190 AK=A(K,K)
      BK=B(K,K)
      A(K,K)=AK+2.0*CA*A(J,K)+CA*CA*A(J,J)
      B(K,K)=BK+2.0*CA*B(J,K)+CA*CA*B(J,J)
      A(J,J)=A(J,J)+2.0*CG*A(J,K)+CG*CG*AK
      B(J,J)=B(J,J)+2.0*CG*B(J,K)+CG*CG*BK
      A(J,K)=0.0
      B(J,K)=0.0
C
      DO 200 I=1,N
      XJ=X(I,J)
      XK=X(I,K)
      X(I,J)=XJ+CG*XK
  200 X(I,K)=XK+CA*XJ
  210 CONTINUE
C
      DO 220 I=1,N
      IF(A(I,I).GT.0.0.AND.B(I,I).GT.0.0) GO TO 220
      WRITE(6,2020)
      STOP
  220 EIGV(I)=A(I,I)/B(I,I)
C
      DO 240 I=1,N
      TOL=RTOL*D(I)
      DIF=DABS(EIGV(I)-D(I))
      IF(DIF.GT.TOL) GO TO 280
  240 CONTINUE
C
      EPS=RTOL**2
      DO 250 J=1,NR
      JJ=J+1
      DO 250 K=JJ,N
      EPSA=(A(J,K)*A(J,K))/(A(J,J)*A(K,K))
      EPSB=(B(J,K)*B(J,K))/(B(J,J)*B(K,K))
      IF((EPSA.LT.EPS).AND.(EPSB.LT.EPS)) GO TO 250
      GO TO 280
  250 CONTINUE
C
  255 DO 260 I=1,N
      DO 260 J=1,N
      A(J,I)=A(I,J)
  260 B(J,I)=B(I,J)
      DO 270 J=1,N
      BB=DSQRT(B(J,J))
      DO 270 K=1,N
  270 X(K,J)=X(K,J)/BB
      RETURN
C
  280 DO 290 I=1,N
  290 D(I)=EIGV(I)
      IF(NSWEEP.LT.NSMAX) GO TO 40
      GO TO 255
 2000 FORMAT(1H ,'SWEEP NUMBER IN JACOBI = ',I4)
 2010 FORMAT(1H ,6E20.12)
 2020 FORMAT(1H ,'*** ERROR OCCURS IN JACOBI ***')
 2030 FORMAT(1H ,'CURRENT EIGENVALUES IN JACOBI ')
      END
```

```
C                                                                       C
C                    INPUT DAT   ( CLARENDON TOWERS )                   C
C                                                                       C
ccccccccccccccccccccccccccccccccccccccccccccccccccccccccccccccccccccccc
   15    4
  2750.     2750.     2770.     2770.     2770.     2770.     2770.     2770.
  2770.     2940.     2940.     2940.     2940.     2940.     3060.
  0.05      0.05      0.05      0.05      0.05      0.05      0.05      0.05
  0.05      0.05      0.05      0.05      0.05      0.05      0.05
  483.      483.      485.      485.      485.      485.      485.      485.
  485.      579.      579.      579.      579.      1577.
  8.0       0.01      ELCNT40
ccccccccccccccccccccccccccccccccccccccccccccccccccccccccccccccccccccccc
C                                                                       C
C                              OUTPUT  LIST                            C
C                                                                       C
ccccccccccccccccccccccccccccccccccccccccccccccccccccccccccccccccccccccc
 ***** INPUT DATA *****
   DEGREE OF FREEDOM =    15
   NT = NT *   4
   Weight(KN)=      2750.0      2750.0      2770.0      2770.0      2770.0
   Weight(KN)=      2770.0      2770.0      2770.0      2770.0      2940.0
   Weight(KN)=      2940.0      2940.0      2940.0      2940.0      3060.0
   Crit. Damp=       0.0500      0.0500      0.0500      0.0500      0.0500
   Crit. Damp=       0.0500      0.0500      0.0500      0.0500      0.0500
   Crit. Damp=       0.0500      0.0500      0.0500      0.0500      0.0500
   STIF(KN/MM)=       483.0       483.0       485.0       485.0       485.0
   STIF(KN/MM)=       485.0       485.0       485.0       485.0       579.0
   STIF(KN/MM)=       579.0       579.0       579.0       579.0      1577.0

   MAX. TIME =        8.0 (SEC.)  ;  D-TIME =     0.0100 (SEC.)
   EQ NAME =   ELCNT40

   TOTAL NUMBER ( FOURIER ) =  4096

 ***** MODAL ANLYSIS RESULTS *****
   Wn(I) =      4.61918     13.31718     21.97712     30.73529     38.60844
   Wn(I) =     46.36480     53.80975     60.10911     66.13387     71.57182
   Wn(I) =     75.61926     79.01500     81.74244     84.31084     90.01931
   -- MODE =      1 --
   U(I) =      28.20621     27.85692     27.16265     26.13383     24.78037
   U(I) =      23.11908     21.17060     18.95914     16.51216     13.86006
   U(I) =      11.48546      8.98401      6.38334      3.71217      1.00000
   -- MODE =      2 --
   U(I) =      -8.90020     -7.98410     -6.24620     -3.87055     -1.09525
   U(I) =       1.79313      4.49636      6.73535      8.27890      8.96765
   U(I) =       8.72139      7.67454      5.92319      3.62812      1.00000
   -- MODE =      3 --
   U(I) =       5.87866      4.23074      1.39684     -1.81815     -4.52189
   U(I) =      -5.95408     -5.71201     -3.86373     -0.92899      2.26698
   U(I) =       4.37735      5.39337      5.06105      3.46346      1.00000
   -- MODE =      4 --
   U(I) =      -3.88372     -1.75441      1.33678      3.68003      3.99935
   U(I) =       2.11912     -0.92657     -3.46267     -4.09439     -2.47429
   U(I) =       0.09262      2.61424      3.85760      3.21474      1.00000
   -- MODE =      5 --
   U(I) =       2.77495      0.37426     -2.35021     -3.02387     -1.07333
   U(I) =       1.80867      3.12106      1.72490     -1.16817     -3.04747
   U(I) =      -2.27040      0.25841      2.58783      2.92062      1.00000
   -- MODE =      6 --
```

```
 U(I) =     -2.45753     0.60861     2.91542     1.56394    -1.74488
 U(I) =     -2.86991    -0.40313     2.56818     2.32530    -0.82779
 U(I) =     -2.54791    -1.43297     1.27642     2.56555     1.00000
 -- MODE =     7 --
 U(I) =      1.78978    -1.21795    -2.17892     0.53717     2.34773
 U(I) =      0.20062    -2.28468    -0.91860     1.99600     1.54586
 U(I) =     -1.14802    -2.12134     0.08464     2.16376     1.00000
 -- MODE =     8 --
 U(I) =     -1.40301     1.53909     1.25373    -1.66772    -1.08106
 U(I) =      1.77964     0.89680    -1.87249    -0.70294     1.94527
 U(I) =      0.52556    -1.87704    -0.76927     1.77716     1.00000
 -- MODE =     9 --
 U(I) =      1.35490    -2.08441    -0.23260     2.20385    -0.97146
 U(I) =     -1.67310     1.88554     0.64295    -2.23681     0.57912
 U(I) =      1.62685    -1.00837    -1.36079     1.36741     1.00000
 -- MODE =    10 --
 U(I) =     -0.96516     1.90430    -0.88780    -1.02069     1.89044
 U(I) =     -0.83631    -1.06892     1.88632    -0.78404    -1.11615
 U(I) =      1.56508     0.09657    -1.62799     0.96399     1.00000
 -- MODE =    11 --
 U(I) =      0.68434    -1.58684     1.40840    -0.29748    -1.01300
 U(I) =      1.64391    -1.17201    -0.08612     1.28648    -1.62381
 U(I) =      0.74456     0.90917    -1.61720     0.64304     1.00000
 -- MODE =    12 --
 U(I) =     -0.73663     1.93260    -2.40106     2.01068    -0.88612
 U(I) =     -0.56199     1.80490    -2.38877     2.10042    -1.04512
 U(I) =     -0.30256     1.41776    -1.44356     0.36015     1.00000
 -- MODE =    13 --
 U(I) =      0.66397    -1.91092     2.92480    -3.63728     3.95014
 U(I) =     -3.82899     3.28716    -2.38417     1.21923     0.07966
 U(I) =     -1.15042     1.59828    -1.18077     0.12394     1.00000
 -- MODE =    14 --
 U(I) =     -0.01483     0.04634    -0.08368     0.13314    -0.20102
 U(I) =      0.29674    -0.43353     0.63034    -0.91440     1.32505
 U(I) =     -1.67435     1.48670    -0.82228    -0.10583     1.00000
 -- MODE =    15 --
 U(I) =      0.00003    -0.00010     0.00023    -0.00054     0.00123
 U(I) =     -0.00281     0.00640    -0.01458     0.03324    -0.07575
 U(I) =      0.15069    -0.25492     0.40871    -0.64195     1.00000

 -- MODAL PARTICIPATION FACTOR --
   0.4593E-01  0.5118E-01  0.4459E-01  0.4726E-01  0.5089E-01
   0.4303E-01  0.4812E-01  0.4997E-01  0.3862E-01  0.4400E-01
   0.4791E-01  0.2529E-01  0.1034E-01  0.7415E-01  0.3787E+00

***** 0th AND 2nd MOMENTS OF S.D.F. *****
STOREY =  15   OME =   13.657 (1/SEC.)    SIG**2 =    1.60420 (MM**2)
STOREY =  14   OME =   12.065 (1/SEC.)    SIG**2 =    5.78949 (MM**2)
STOREY =  13   OME =   10.686 (1/SEC.)    SIG**2 =   11.30930 (MM**2)
STOREY =  12   OME =    9.912 (1/SEC.)    SIG**2 =   17.21754 (MM**2)
STOREY =  11   OME =    9.305 (1/SEC.)    SIG**2 =   22.56556 (MM**2)
STOREY =  10   OME =    8.449 (1/SEC.)    SIG**2 =   26.79330 (MM**2)
STOREY =   9   OME =    7.422 (1/SEC.)    SIG**2 =   30.00715 (MM**2)
STOREY =   8   OME =    6.448 (1/SEC.)    SIG**2 =   32.81025 (MM**2)
STOREY =   7   OME =    5.726 (1/SEC.)    SIG**2 =   35.89048 (MM**2)
STOREY =   6   OME =    5.560 (1/SEC.)    SIG**2 =   28.07160 (MM**2)
STOREY =   5   OME =    5.894 (1/SEC.)    SIG**2 =   31.71366 (MM**2)
STOREY =   4   OME =    6.285 (1/SEC.)    SIG**2 =   35.67393 (MM**2)
STOREY =   3   OME =    6.664 (1/SEC.)    SIG**2 =   39.35665 (MM**2)
STOREY =   2   OME =    6.985 (1/SEC.)    SIG**2 =   42.10743 (MM**2)
STOREY =   1   OME =    7.109 (1/SEC.)    SIG**2 =    5.85314 (MM**2)
```

APPENDIX D

DETAILS OF CLARENDON TOWERS AND ITS MODEL

Clarendon Towers is a 19 storey reinforced concrete frame building located in central Christchurch. It was designed in accordance with New Zealand codes (49,50). The building is now under construction. An elevation of the building is shown in Fig. D.1. The facade of the old Clarendon Hotel over the lower 3 storeys of the building was retained. The upper 3 storeys are set back. Figures D.2 and D.3 show a typical floor plan and the elevation of the frame A, respectively. Typical floor height is 3.4 m. The peripheral frames are used to resist lateral loads. Internal beams and columns are designed to sustain only gravity loads. No structural walls exist even around the core. For frame A, plastic hinges are assumed to occur at the beam ends and at the base of the 1st storey columns. In order to avoid the placing of concrete in the congested beam-column joint core region on the site, precast beams are used. Columns are cast in situ.

Because of the irregularity in the 1st storey and above 17 storey shown in Fig. D.3, the frames between 2nd and 16th storeys are considered in this study. The analytical models for the frames, A and D, are shown in Fig. D.4. Figures D.5-D.8 show the sectional details of the frame members as

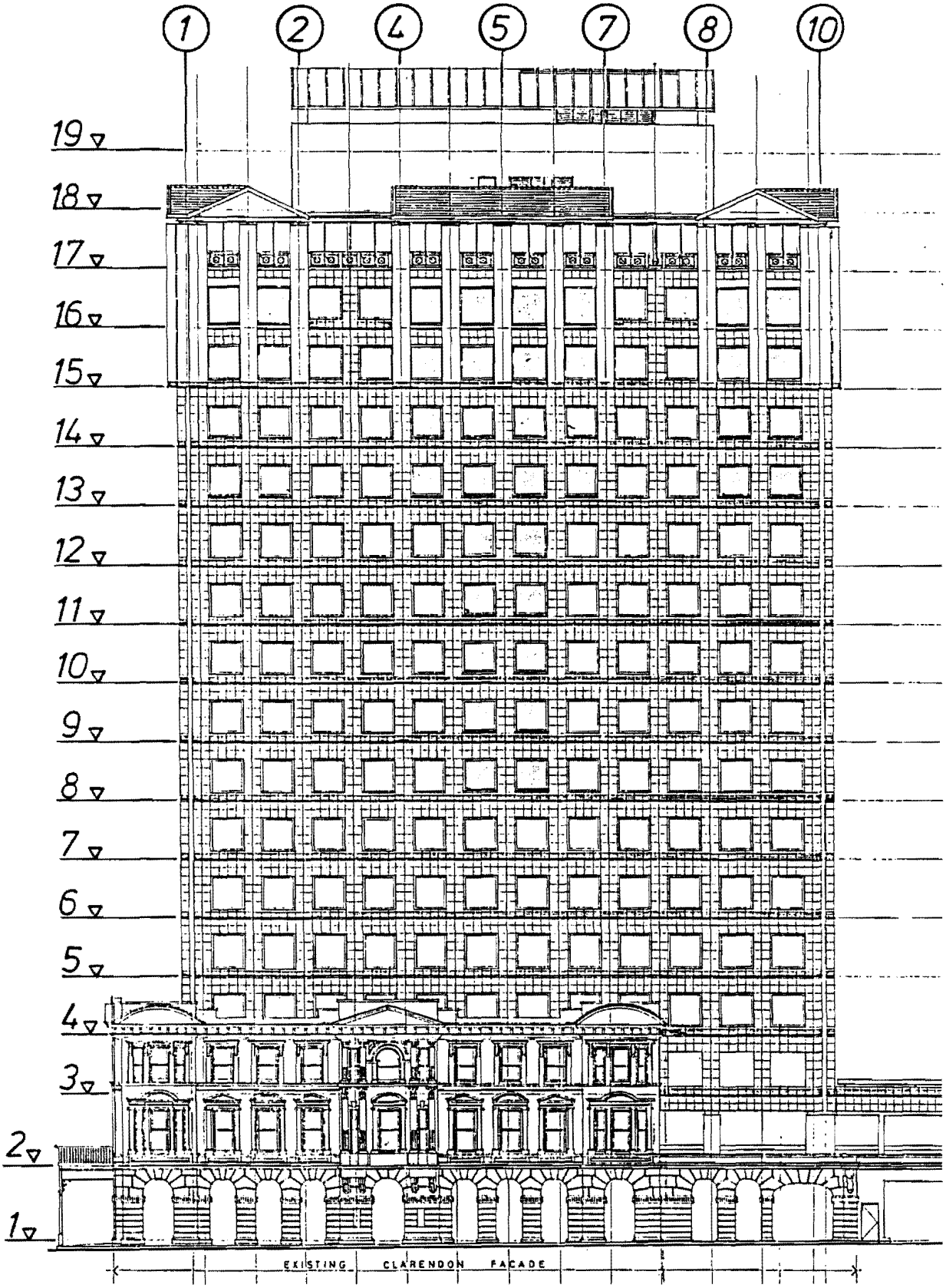

Fig. D.1 Elevation of Clarendon Towers

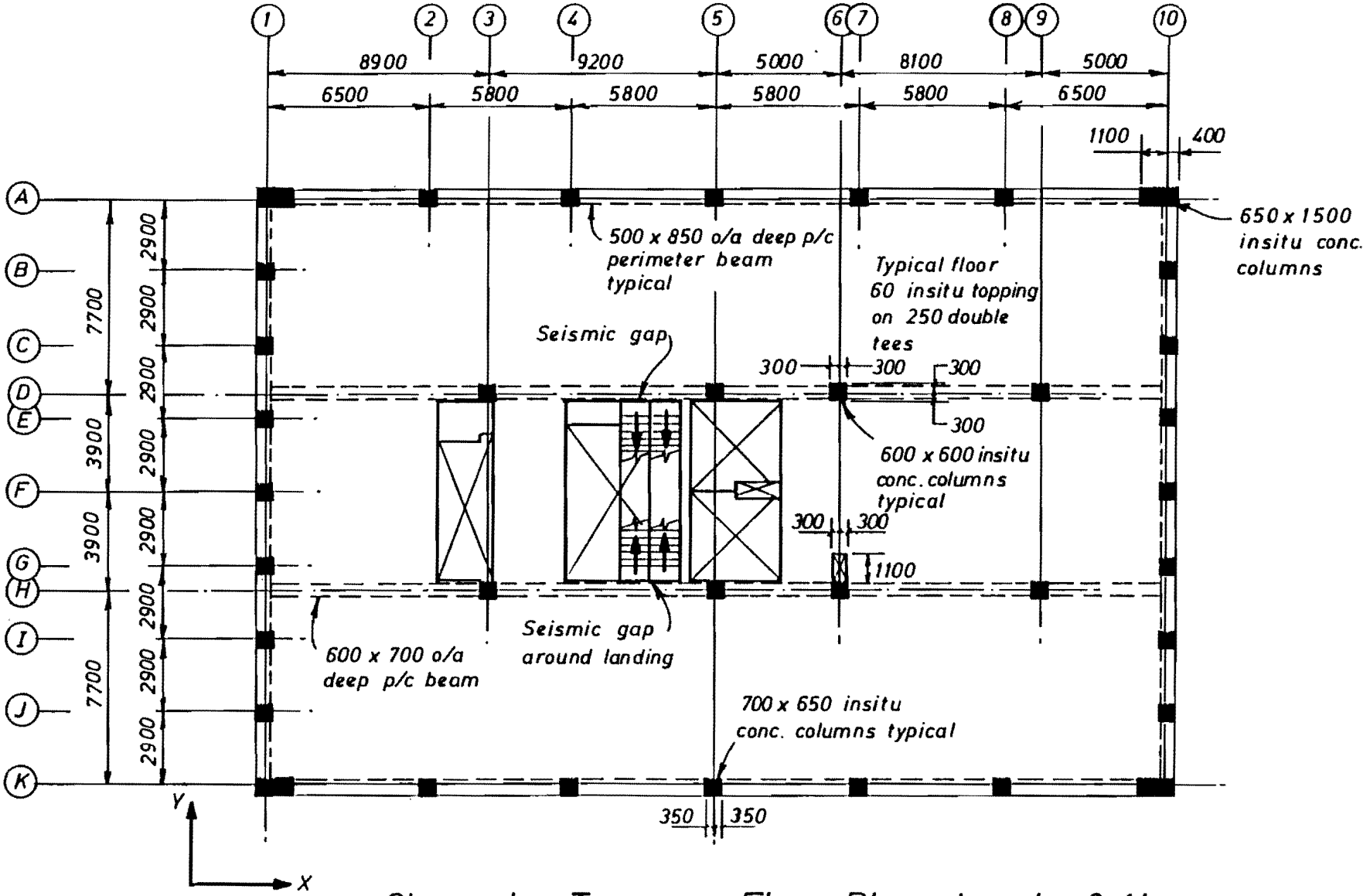

Clarendon Towers - Floor Plan , Levels 8-14

Fig. D.2 Typical floor plan of Clarendon Towers

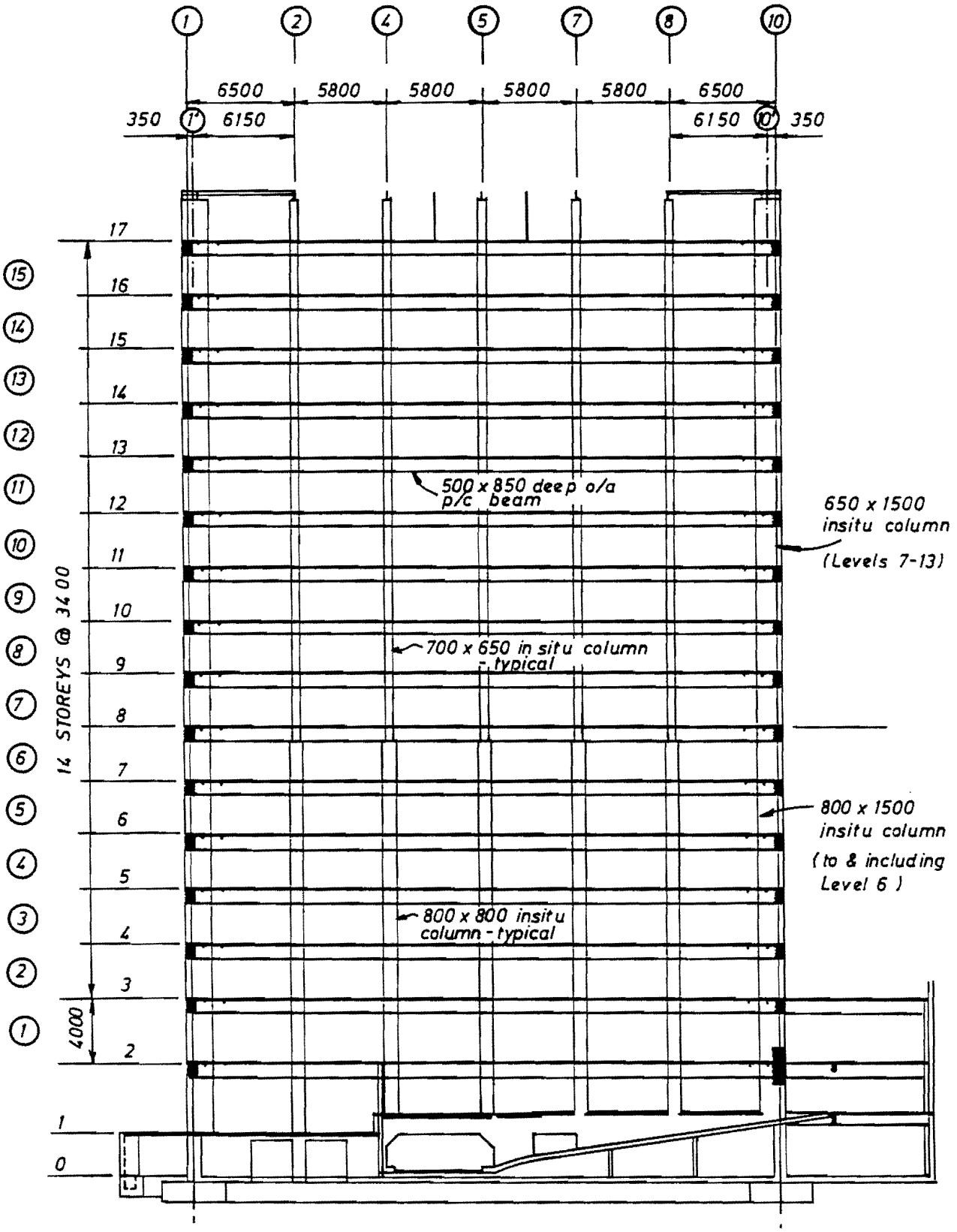

Clarendon Towers - Frame A, Elevation

Fig. D.3 Elevation of Frame A

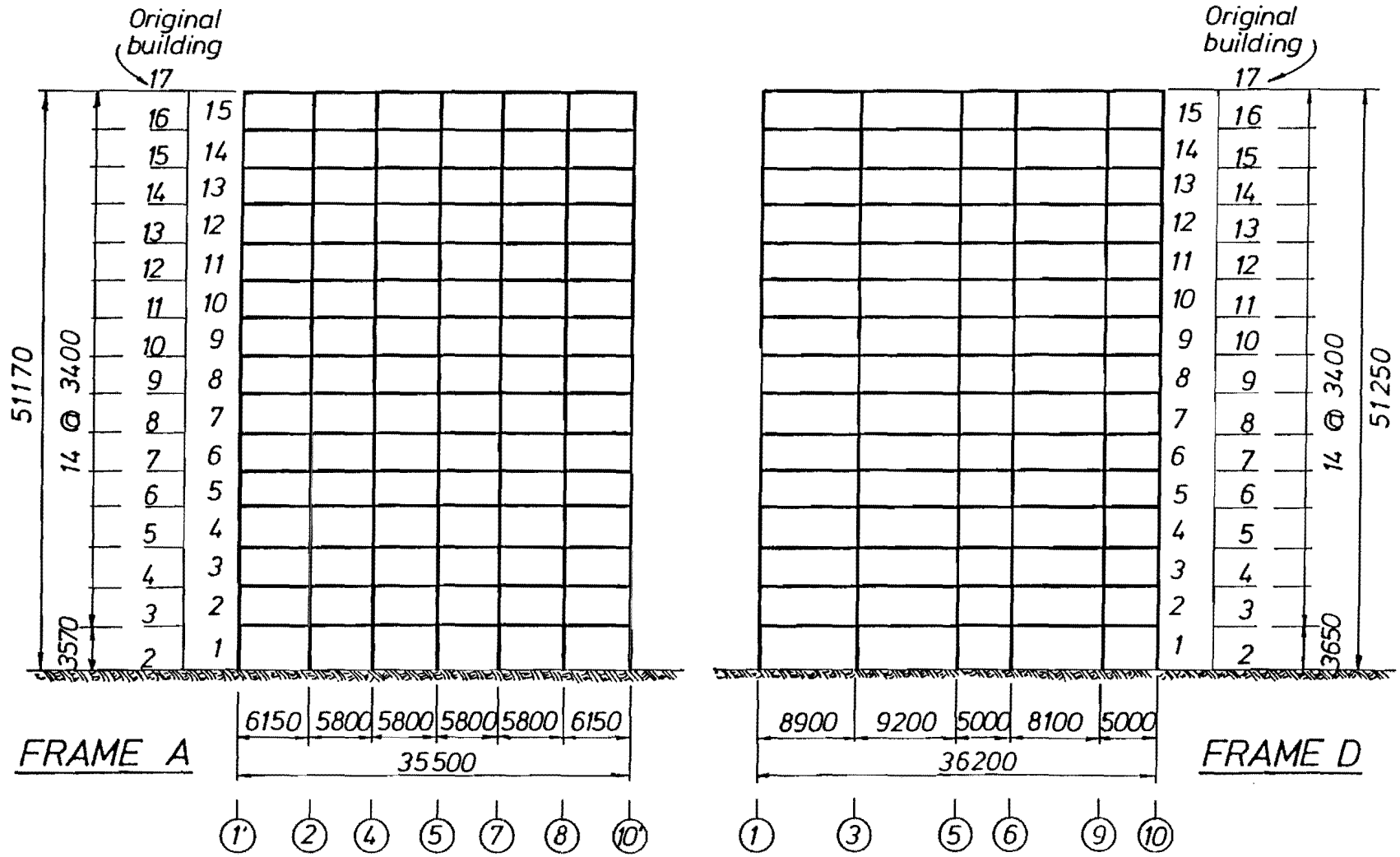

Fig. D.4 Analytic models for Frame A and D

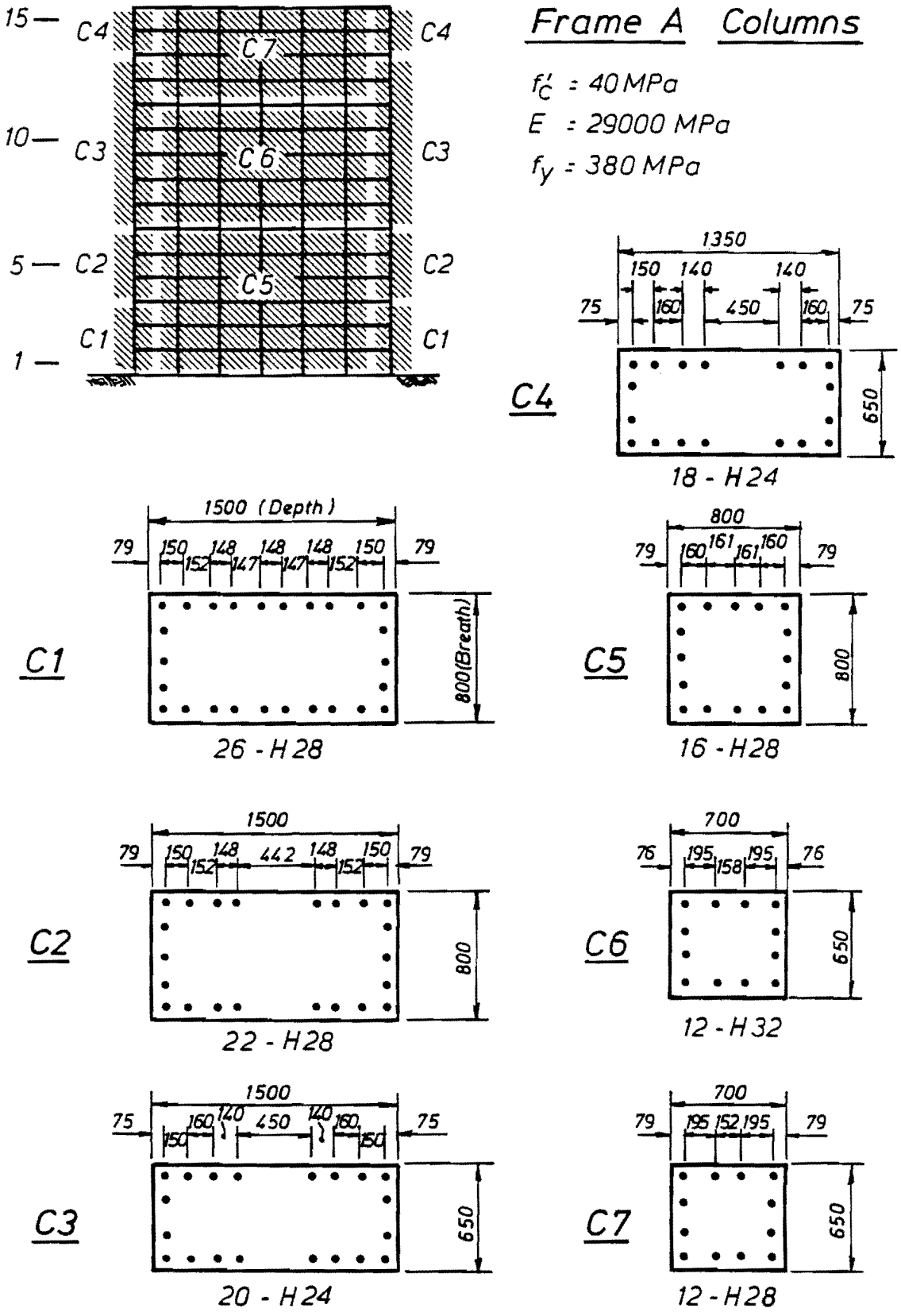

Fig. D.5 Details of the columns of Frame A

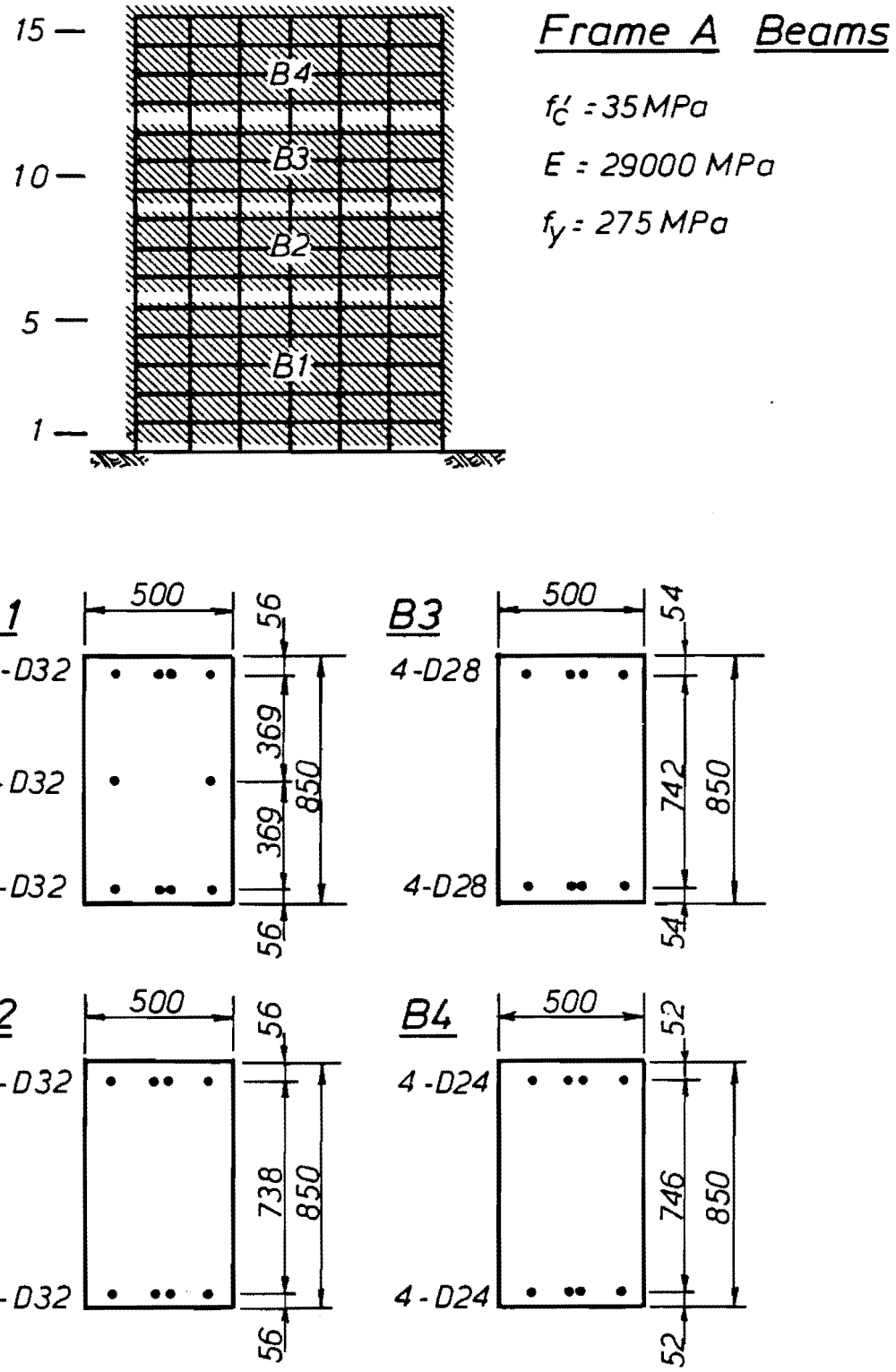

Fig. D.6 Details of the beams of Frame A

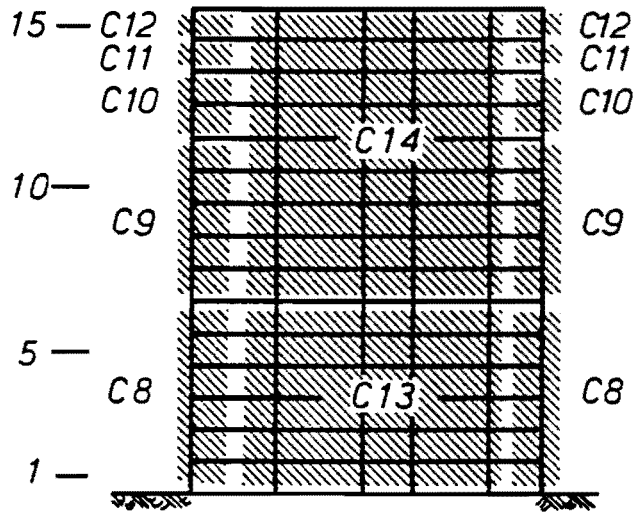

Frame D Columns

f'_c = 40 MPa

E = 29000 MPa

f_y = 380 MPa (H)
= 275 MPa (D)

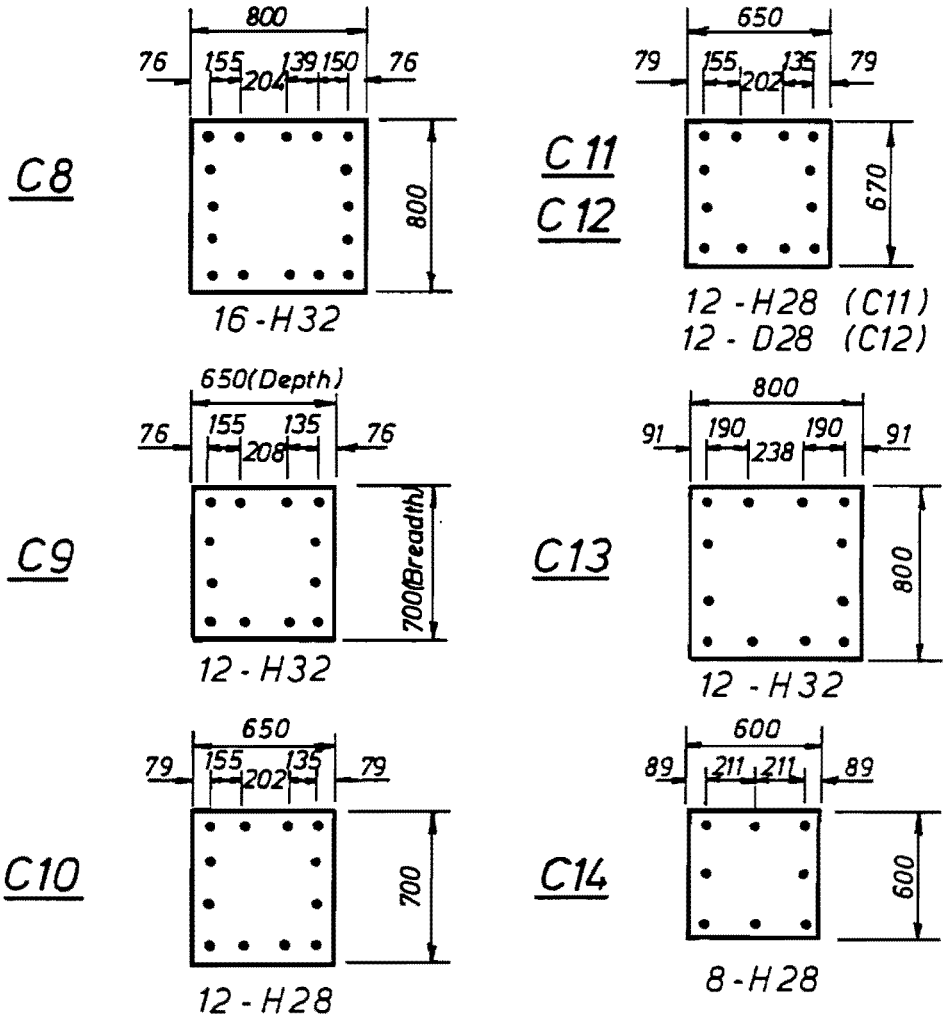

Fig. D.7 Details of the columns of Frame D

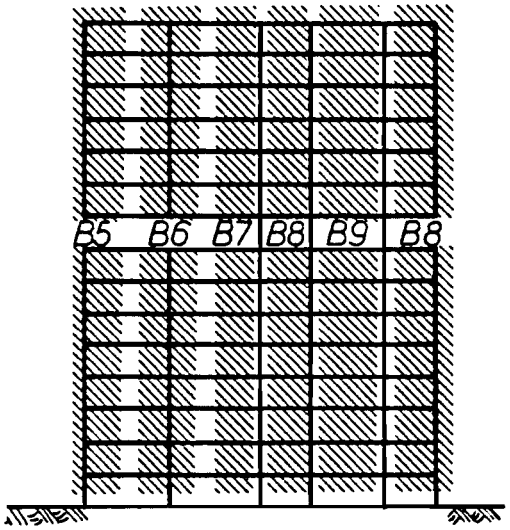

Frame D Beams

f'_c = 35 MPa

E = 29000 MPa

f_y = 380 MPa

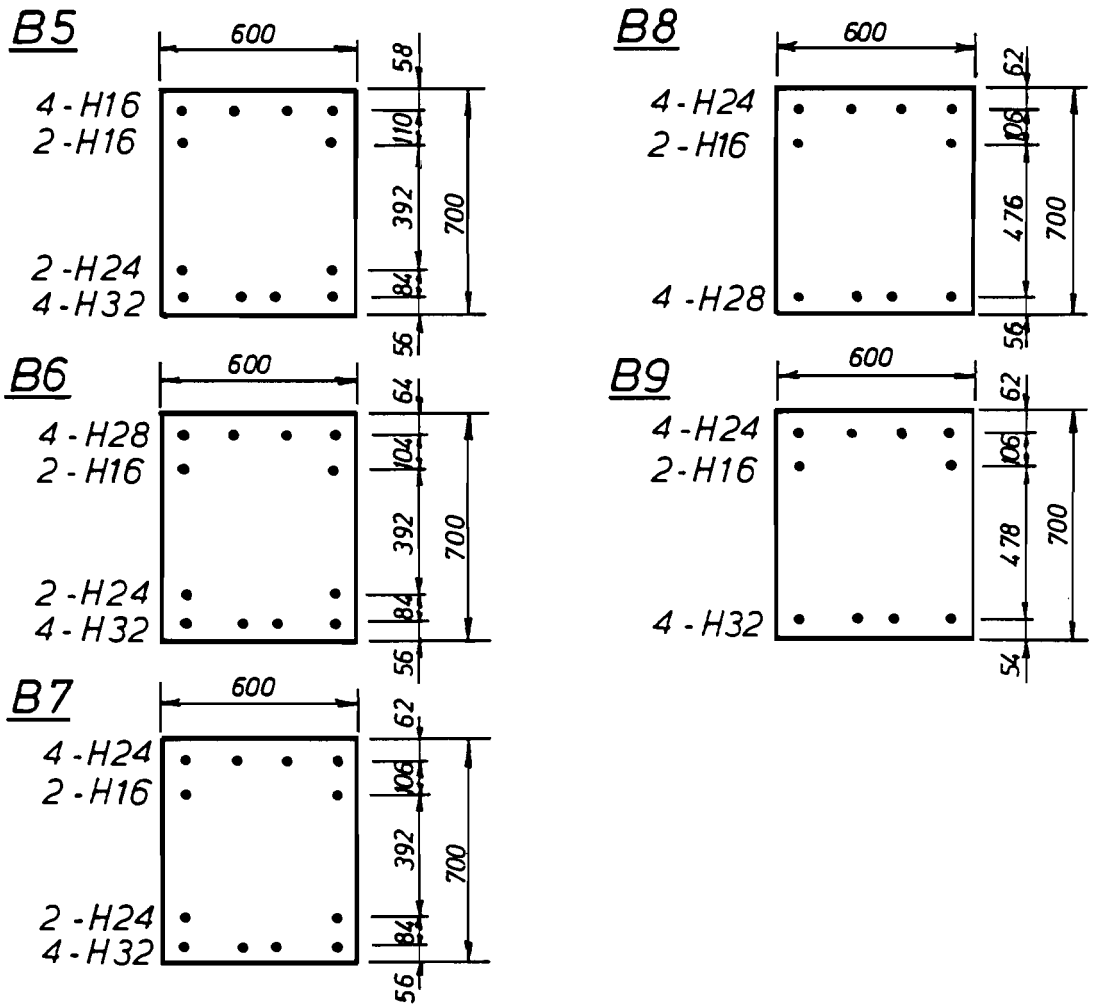

Fig. D.8 Details of the beams of Frame D

well as the material properties. Concrete strength for columns is 40 MPa and 35 MPa for beams. Specified yield strength of main bars for peripheral beams is 275 MPa and for other bars 380 MPa. These values were used in the analyses in Section 6.5 and 7.6.

The two approaches employed in estimating the storey characteristics for a spring-mass model were described in Appendix A. The storey characteristics for the frame A obtained by the two approaches are shown in Table D.1. Important details of calculating the initial stiffness k_i and yield shear strength V_{y_i} using Moto's approximation are summarised in Figs D.9-D.11. Contribution of the floor slabs was neglected.

Computing storey masses for Clarendon Towers is not as simple as shown in Appendix A. This is because the total mass is in this case assigned to frames of different stiffnesses. Hence, the problem is to find a way to estimate a tributary area for a frame during an earthquake excitation. A fundamental assumption engaged in the problem may be that a lateral displacement of any point of a floor slab is identical because the stiffness of slab for the relative displacement is considered very large. The assumption also enables us to pick up only one frame to estimate storey drifts for a direction of a building, rather than using all frames. In estimating a storey mass for a frame in practice, the assumption can be simplified as that each frame has the same fundamental period. Suppose each frame can be regarded as a S.D.O.F. system as shown in Fig.

Table D.1 Storey characteristics of Clarendon Towers

(1) Spring-mass model (A) (by a static analysis)

Storey	w_t (kN)	k (kN/mm)	α	V_y (kN)	C_{d_i}
15	2750	284	0.20	530	0.193
14	"	372	"	1000	0.182
13	2770	410	0.18	1320	0.160
12	"	429	"	1660	0.150
11	"	439	0.17	1940	0.140
10	"	446	"	2170	0.131
9	"	452	0.16	2380	0.123
8	"	462	"	2620	0.118
7	"	467	0.15	2780	0.112
6	2940	547	0.14	2960	0.106
5	"	552	"	3210	0.104
4	"	568	0.13	3400	0.101
3	"	596	0.14	3670	0.100
2	"	681	0.075	3910	0.099
1	3060	1250	0.089	4240	0.099

(2) Spring-mass model (B) (by a straightforward method)

Storey	w_t (kN)	k (kN/mm)	V_y (kN)	C_{d_i}
15	2750	483	474	0.172
14	"	"	916	0.167
13	2770	485	1330	0.161
12	"	"	1710	0.155
11	"	"	2050	0.148
10	"	"	2370	0.143
9	"	"	2660	0.137
8	"	"	2910	0.132
7	"	"	3130	0.126
6	2940	579	3320	0.119
5	"	"	3480	0.113
4	"	"	3610	0.107
3	"	"	3700	0.101
2	"	"	3770	0.095
1	3060	1577	3800	0.089

CALCULATION OF STOREY STIFFNESS (Frame A)

$$\frac{12 \cdot E}{h^2} = \frac{12 \times 29 (kN/mm)}{3400^2} = 3.01 \times 10^{-5} \ (kN/mm^4)$$

Storey Stiffness

STOREYS 14 & 15

$k_b = 4.16 \times 10^6 (mm^3)$, $k_b = 4.41 \times 10^6 (mm^3)$

$k_c = 39.2 \times 10^6 (mm^3)$	$k_c = 5.46 \times 10^6 (mm^3)$			$\bar{k} = \frac{2 \times 4.41}{5.46} = 1.62$	$\bar{k} = \frac{4.16+4.41}{5.46} = 1.57$	$\bar{k} = \frac{2 \times 4.16}{2 \times 39.2} = 0.106$
$D = 1.97 \times 10^6$	$D = 2.40 \times 10^6$	$D = 2.44 \times 10^6$	$D = 2.44 \times 10^6$	$D = 2.44 \times 10^6$	$D = 2.40 \times 10^6$	$D = \frac{0.106}{2+0.106} \times 39.2 \times 10^6 = 1.97 \times 10^6$

3400

$k_b = 4.16 \times 10^{-6}$, $k_b = 4.41 \times 10^6$

k = 483 kN/mm

STOREYS 7-13

$k_b = 4.16 \times 10^6 (mm^3)$, $k_b = 4.41 \times 10^6 (mm^3)$

$k_c = 53.8 \times 10^6 (mm^3)$	$k_c = 5.46 \times 10^6 (mm^3)$			$\bar{k} = \frac{2 \times 4.41}{5.46} = 1.62$	$\bar{k} = \frac{4.16+4.41}{5.46} = 1.57$	$\bar{k} = \frac{4.16}{53.8} = 0.077$
$D = 2.00 \times 10^6$	$D = 2.40 \times 10^6$	$D = 2.44 \times 10^6$	$D = 2.44 \times 10^6$	$D = 2.44 \times 10^6$	$D = 2.40 \times 10^6$	$D = 2.00 \times 10^6$

3400

k = 485 kN/mm

STOREYS 2-6

$k_b = 4.16 \times 10^6$, $k_b = 4.41 \times 10^6$

$k_c = 66.2 \times 10^6 (mm^3)$	$k_c = 10.0 \times 10^6 (mm^3)$			$\bar{k} = \frac{2 \times 4.41}{10.0} = 0.882$	$\bar{k} = \frac{4.16+4.41}{10.0} = 0.857$	$\bar{k} = \frac{4.16}{66.2} = 0.063$
$D = 2.02 \times 10^6$	$D = 3.00 \times 10^6$	$D = 3.06 \times 10^6$	$D = 3.06 \times 10^6$	$D = 3.06 \times 10^6$	$D = 3.00 \times 10^6$	$D = 2.02 \times 10^6$

3400

k = 579 kN/mm

STOREY 1

$$\frac{12 \cdot E}{h^2} = \frac{12 \times 29}{3570^2} = 2.73 \times 10^{-5} \ (kN/mm^4)$$

$k_b = 4.16 \times 10^6$, $k_b = 4.41 \times 10^6$

$k_c = 63.0 \times 10^6 (mm^3)$	$k_c = 9.56 \times 10^6 (mm^3)$			$\bar{k} = \frac{2 \times 4.41}{9.56} = 0.923$	$\bar{k} = \frac{4.16+4.41}{9.56} = 0.896$	$\bar{k} = \frac{4.16}{63.0} = 0.066$
$D = 17.3 \times 10^6$	$D = 4.61 \times 10^6$	$D = 4.65 \times 10^6$	$D = 4.65 \times 10^6$	$D = 4.65 \times 10^6$	$D = 4.61 \times 10^6$	$D = \frac{0.5+0.066}{2+0.066} \times 63.0 \times 10^6 = 17.3 \times 10^6$

3570

k = 1577 kN/mm

6150 | 5800 | " | " | 5800 | 6150

Fig. D.9 Calculation of initial storey stiffness (Frame A)

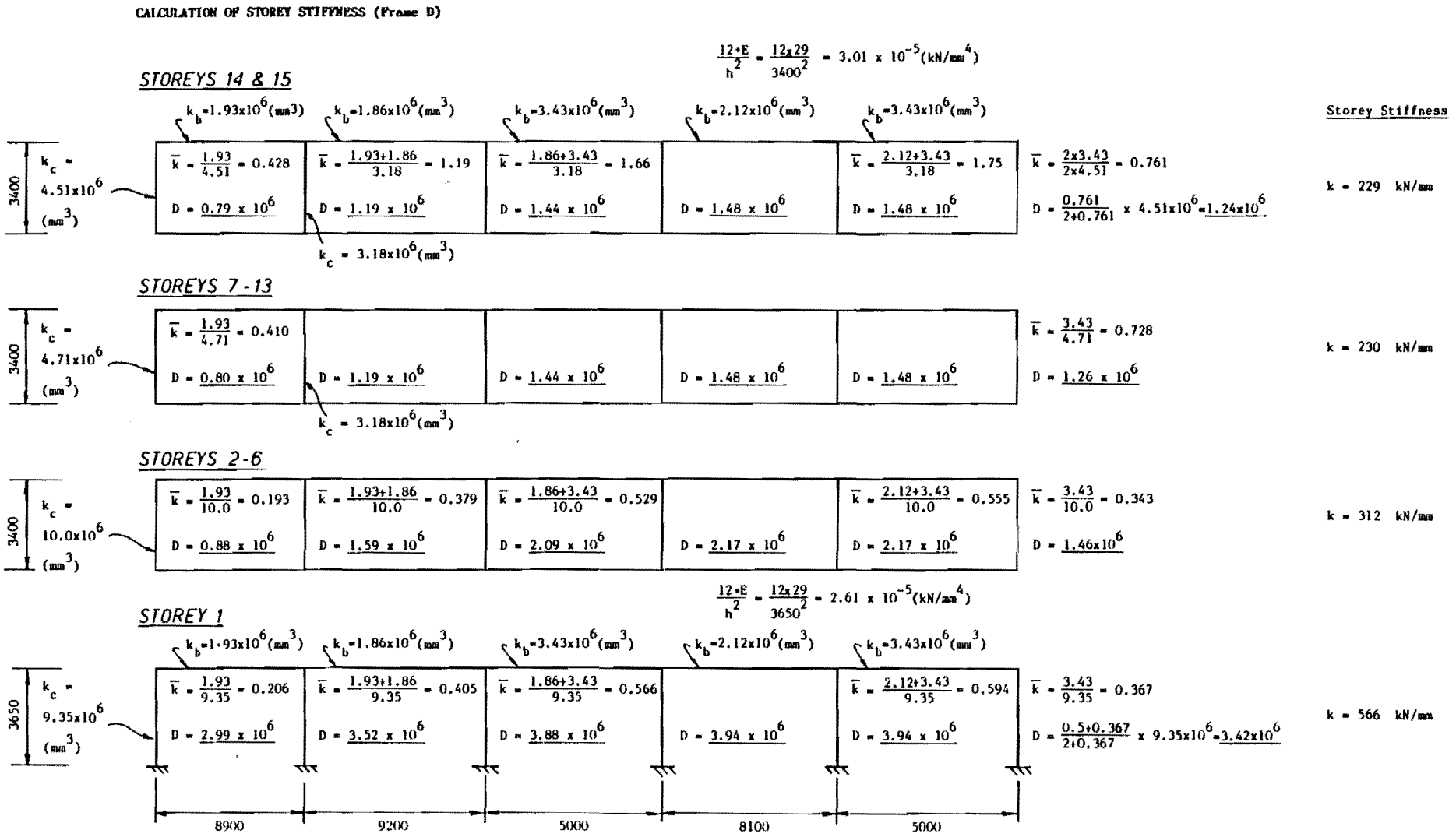

Fig. D.10 Calculation of initial storey stiffness (Frame D)

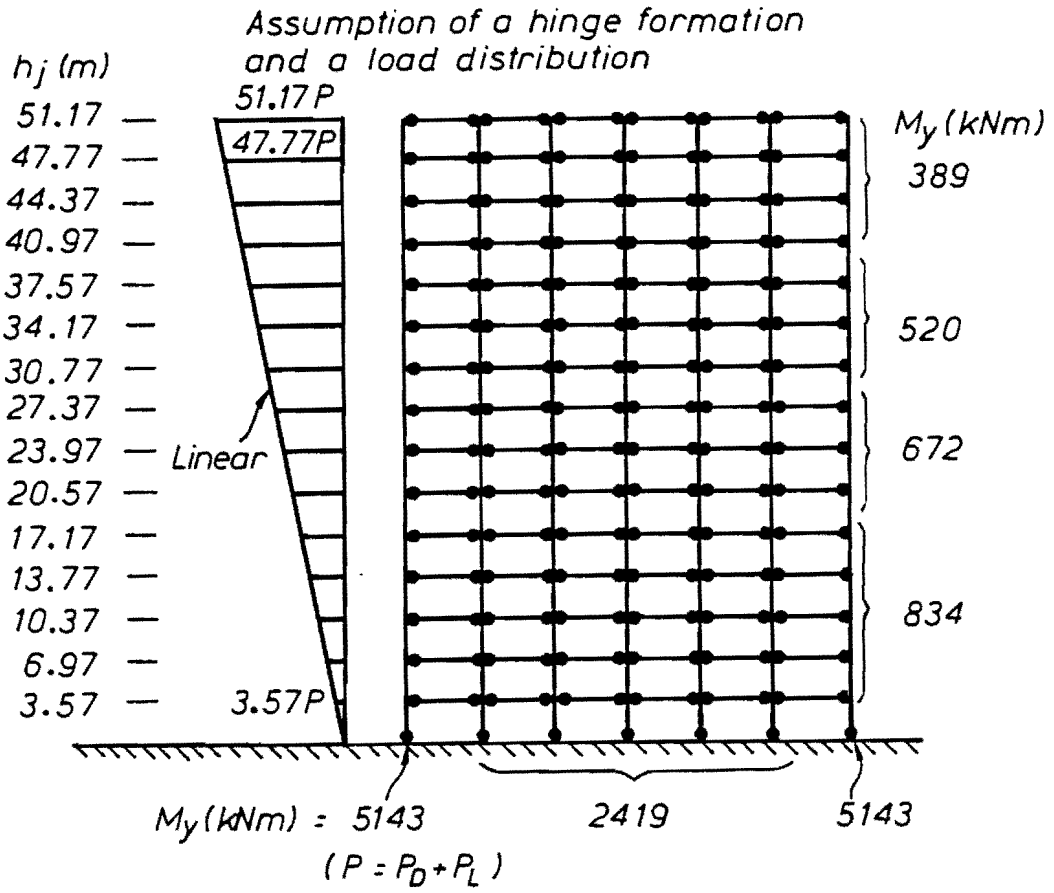

Storey	V_y (kN)	Storey	V_y (kN)
15	474	7	3131
14	916	6	3322
13	1327	5	3481
12	1706	4	3608
11	2054	3	3704
10	2371	2	3769
9	2656	1	3802
8	2909		

Fig. D.11 Calculation of yield storey strength (Frame A)

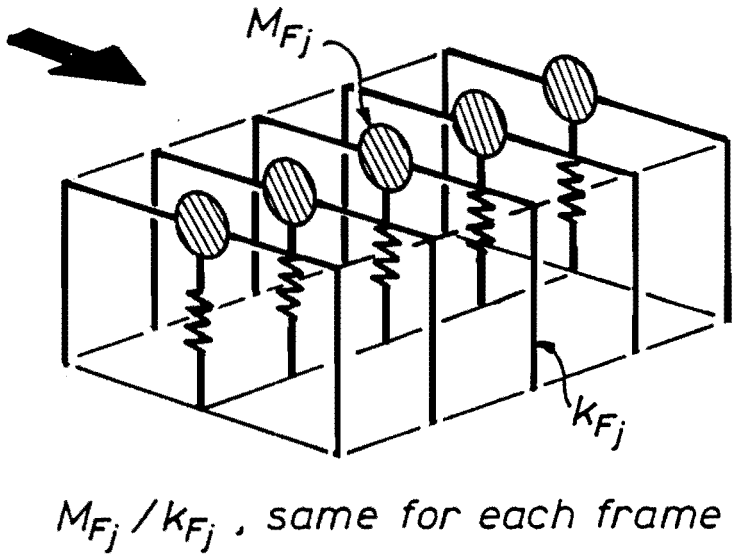

Fig. D.12 Analytic model in estimating storey mass

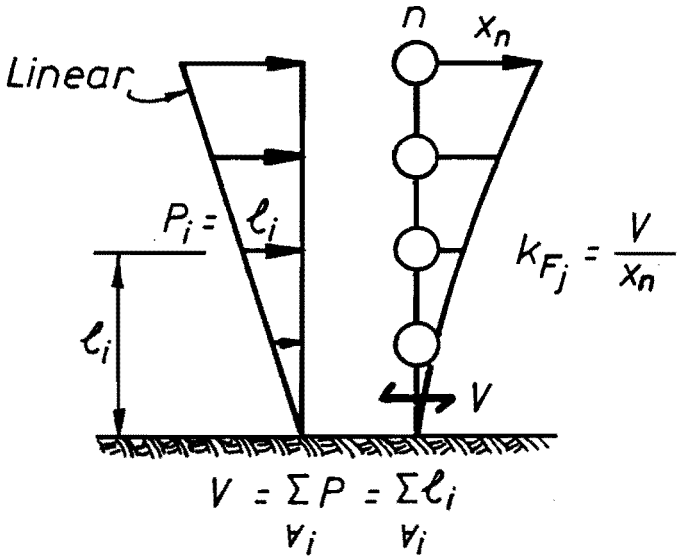

Fig. D.13 Assumptions for an initial stiffness of an entire frame

D.12. The period T can be given by:

$$T = 2\pi \sqrt{M_{F_j} / k_{F_j}} \tag{D.1}$$

where: M_{F_j} = mass of the frame j during an earthquake

k_{F_j} = stiffness of the frame j

When the ratio M_{F_j} / k_{F_j} for each frame is the same, the period becomes identical between the frames and a lateral displacement for each frame can be considered same. Thus, a mass of the frame j, M_{F_j} during an earthquake can be determined by:

$$M_{F_j} = \frac{M_T}{\sum_{1=1}^{m} k_{F_1}} \cdot k_{F_j} \tag{D.2}$$

in which:

m = the number of frames

M_T = total mass

Assuming an inverted triangular load distribution, a stiffness of the frame j, k_{F_j} can be calculated by (see Fig. D.13):

$$k_{F_j} = \frac{V}{x_n}$$

$$= \frac{\sum_{i=1}^{n} 1_{i,j}}{\sum_{i=1}^{n} \left(\sum_{x=1}^{n} (1_{x,j}) / k_{i,j} \right)} \tag{D.3}$$

where: V = shear force applied to the 1st storey

x_n = relative displacement at the top floor

from the basement

n = number of the storey

$l_{i,j}$ = height of the (i+1)th floor in the frame j

$k_{i,j}$ = ith storey stiffness of the frame j

By Eq. (D.3) the stiffnesses of frame A and D were calculated as shown in Table D.2 based on the spring-mass model (B). Frame A is about two times as stiff as frame D. Because the same result was obtained by a static analysis with the entire frame model, the weights of storeys of frame A for spring-mass models (A) and (B) are the same (see Table D.1). Details of obtaining the weight for frame A are shown in Table D.3. The dead loads for frame A and D were calculated, first (Table D.3 (1) and (2)). Secondly, other dead loads such as beams perpendicular to frame A and D, slabs and so on were computed, as shown in Table D.3(3). Total dead load for frame A was then obtained from Eqs (D.2) and (D.3). Finally, the total weight was calculated as 1.1 times the total dead load (see Table D.3(5)). The 10% of total dead load can be regarded as the total amount of live load.

Table D.2 Calculation of an initial stiffness of Frame A and D

Frame A					Frame D				
Storey	ℓ_i (m)	$\sum_{\ell=i}^{n} \ell_i$	k_i (kN/mm)	$\Sigma \ell_i / k_i$	Storey	ℓ_i (m)	$\sum_{\ell=i}^{n} \ell_i$	k_i (kN/mm)	$\Sigma \ell_i / k_i$
15	51.17	51.17	483	0.106	15	51.25	51.25	229	0.224
14	47.77	98.94	"	0.205	14	47.85	99.10	"	0.433
13	44.37	143.3	485	0.295	13	44.45	143.6	230	0.624
12	40.97	184.3	"	0.380	12	41.05	184.6	"	0.803
11	37.57	221.9	"	0.458	11	37.65	222.3	"	0.967
10	34.17	256.0	"	0.528	10	34.25	256.5	"	1.11
9	30.77	286.8	"	0.591	9	30.85	287.4	"	1.25
8	27.37	314.2	"	0.648	8	27.45	314.8	"	1.37
7	23.97	338.1	"	0.697	7	24.05	338.9	"	1.47
6	20.57	358.7	579	0.620	6	20.65	359.5	312	1.15
5	17.17	375.9	"	0.649	5	17.25	376.8	"	1.21
4	13.77	389.6	"	0.673	4	13.85	390.6	"	1.25
3	10.37	400.0	"	0.691	3	10.45	401.1	"	1.29
2	6.97	407.0	"	0.703	2	7.05	408.1	"	1.31
1	3.57	410.6	1577	0.260	1	3.65	411.8	566	0.728
Σ	410.6	-	-	7.504	Σ	411.8	-	-	15.19

$k_{F_A} = 410.6/7.504 = \underline{54.7 \text{ (kN/mm)}}$

$k_{F_D} = 411.8/15.19 = \underline{27.1 \text{ (kN/mm)}}$

Table D.3 Details of calculating the total weight for Frame A

(1) FRAME A (unit:kN)

Storey	Columns	Beams	Facade	(a) Total/Storey	(b)	(a)+(b)		1.1((a)+(b))
14,15	329	313	303	945	1552	2497		2750
7~13	344	311	"	958	1556	2514	x 1.1	2770
2~6	458	306	"	1067	1609	2676	=	2940
1	538	"	"	1147	1636	2783		3060

sub-total = 15078 (kN)

(2) FRAME D (unit:kN)

Storey	Columns	Beams	Total/Storey
14,15	188	335	523
7~13	192	"	527
2~6	313	325	638
1	369	"	694

sub-total = 8619 (kN)

(total dead load for Frame A during EQ) = 38755 (kN)

x 0.691

(total weight for Frame A during EQ) = 42650(kN)

(3) Others to divide into frame A & D

Storey	Columns*1	Beams*2	Slab	Facade*2	Total/Storey
14,15	179	190	1680	197	2246
7~13	185	"	"	"	2252
2~6	262	"	"	"	2329
1	308	182	"	"	2367

$$w_{F_A} = \frac{w_t}{k_{F_A}+k_{F_D}} \cdot k_{F_A}$$

$$= \frac{57965}{54.7+27.1} \cdot 54.7$$

$$= 38761 \text{ (kN)}$$

$$\frac{38761 - 15078}{34268} = 0.691$$

*1 (1) - (B), (C), (F) and (10) - (B),(C)

*2 Line (1) and (10)

sub-total = 34268 (kN) (0.684 from a static analysis)

(Total weight)/2 = 15078 + 8619 + 34268

= 57965 (kN)

REFERENCES

1. Ang, A.H-S., and Tang, W.H., Probability Concepts in Engineering Planning and Design, Vol. II, John Wiley and Sons, 1984.

2. Dooren, P. and Ridder, L., An Adaptive Algorithm for Numerical Integration over an N-Dimensional Cube, Journal of Computational and Applied Mathematics, Vol. 2, No. 3, 1976, pp207-217.

3. Genz, A.C. and Malik, A.A., Remarks on Algorithm 006: An Adaptive Algorithm for Numerical Integration over an N-Dimensional Rectangular Region, Journal of Computational and Applied Mathematics, Vol. 6, No. 4, 1980, pp295-302.

4. Hammersley, J.M. and Handscomb, D.C., Monte Carlo Methods, Methuen and Co. Limited, 1964.

5. Ayyub, B.M. and Haldar, A., Practical Structural Reliability Techniques, Journal of Structural Engineering, Vol. 110, No.8, August 1984, pp1707-1724.

6. Melchers, R.E., Monte-Carlo Methods for Structural Reliability Analyses, 10th Australasian Conference on the Mechanics of Structures and Materials, Univ. of Adelaide, Australia, 1986, pp7-12.

7. Dolinski, K., First-Order Second-Moment Approximation in Reliability of Structural Systems: Critical Review and Alternative Approach, Structural Safety, 1(1983), pp211-231.

8. Melchers, R.E. and Tang, L.K., Dominant Failure Modes in Stochastic Structural Systems, Structural Safety, 2(1984), pp127-143.

9. Tang, L.K. and Melchers, R.E., Reliability of Large Structural System, The 9th Australasian Conference on the Mechanics of Structures and materials, University of Sydney, 1984,pp295-300.

10. Murotsu, Y., Okada, H., Taguchi, K. et al., Automatic Generation of Stochastically Dominant Failure Modes of Frame Structures, Structural Safety, 2(1984), pp17-25.

11. Murotsu, Y., Okada, H.,Yonezawa, M. et al., Reliability Assessment of Redundant Structure, 3rd International Conference on Structural Safety and Reliability, pp315-329.

12. Moses, F., System Reliability Developments in Structural Engineering, Structural Safety, 1(1982), pp3-13.

13. Ang, A.H-S. and Ma, H-F., On the Reliability of Structural Systems, 3rd International Conference on Structural Safety and Reliability, pp295-314.

14. Ang, A.H-S. and Chaker, A.A., Analysis of Activity Networks under Uncertainty, Journal of the Engineering Mechanics Division, August 1975, pp373-387.

15. Ditlevsen, O., Narrow Reliability Bounds for Structural Systems, The Danish Center for Applied Mathematics and Mechanics, Report No. 145, October 1978, The Technical University of Denmark.

16. Bennett, R., Reliability Analysis of Frame Structures with Brittle Components, Structural Safety, 2(1985), pp281-290.

17. Bennett,R. and Ang, A.H-S., Formulations of Structural System Reliability, Journal of Engineering Mechanics, Vol. 112, No. 11, November 1986, pp1135-1151.

18. Frangopol, D.M., Influence of Load and Strength Correlation on the Performance of Metal Structures, Metal Structures Conference, 1985, Melbourne.

19. Frangopol, D.M., Sensitivity Studies in Reliability-Based Analysis of Redundant Structures, Structural Safety, 3(1985), pp13-22.

20. Vanmarcke, E.H., Matrix Formulation of Reliability Analysis and Reliability-Based Design, Comput. Struct., 13(1971), pp757-770.

21. Grimmelt, M.J. and Schuëller, G.I., Benchmark Study on Methods to Determine Collapse Failure Probabilities of Redundant Structures, Structural Safety, 1(1982/1983), pp93-106.

22. Melchers, R.E., Correlation Effects in the Reliability Analysis of Parallel Structures, The 8th Australasian Conference on the Mechanics of Structures and Materials, Newcastle, 1982, pp26-1 - 26-6.

23. Elms, D.G., Risk and Reality in Structural Engineering, Trans. N.Z.I.E., Vol. 7, No. 3/CE, Nov. 1980, pp93-108.

24. U.S. Nuclear Regulatory Commission, Reactor Safety Study: An Assessment of Accident Risks in U.S. Commercial Nuclear Power Plants, WASH-1400 (NUREG-75/014), 1975.

25. Pacific Gas and Electric Company, Analysis of the Risk to the Public from Possible Damage to the Diablo Canyon Nuclear Power Station from Seismic Events, U.S. NRC, Dockets No. 50-275-OL, 50-323-OL, 1977.

26. Commonwealth Edison Company, Zion Probabilistic Safety Study, Chicago, Illinois, 1981.

27. Smith, P.D., et al., Seismic Safety Margins Research Program (SSMRP); Phase I Final Report - Overview, NUREG/CR-2015, Vol. 1, 1981.

28. Kennedy, R.P. et al., Probabilistic Seismic Safety Study of an Existing Nuclear Power Plant, Nuclear Engineering and Design, Vol. 59, No. 2.

29. Gutenberg, B. and Richter,C., Frequency of Earthquakes in California, Bull. Seism. Soc. Amer., Vol. 34, 1944, pp185-188.

30. U.S. Department of Commerce/National Bureau of Standards, Development of a Probability Based Load Criterion for American National Standard A58, NBS Special Publication 577, 1980.

31. Siu, W.W.C., Parimi, S.R. and Lind, N.C., Practical Approach to Code Calibration, Journal of the Structural Division, July 1975, (ST7), pp1469-1479.

32. Ravindra, M.K. and Galambos, T.V., Load and Resistance Factor Design for Steel, Journal of the Structural Division, September 1978 (ST9), pp1337-1353.

33. Ang, A.H-S. and Cornell, C.A., Reliability Bases of Structural Safety and Design, Journal of the Structural Division, September 1974, (ST9), pp1755-1769.

34. Uniform Building Code, 1976 Ed., International Conference of Building Officials, Whittier, CA, 1976.

35. Algermissen, S.T. and Perkins, D.M., A Probabilistic Estimate of Maximum Acceleration in Rock in the Contiguous United States, U.S. Geological Survey Open File Report 76-416, 1976.

36. Committee on Reliability of Offshore Structures of the Committee on Structural Safety and Reliability of the Structural Division of ASCE, Application of Reliability Methods in Design and Analysis of Offshore Platforms, Journal of Structural Engineering ASCE, 1983, Vol. 109, No. 10, pp2265-2291.

37. Blockley, D.I., Predicting the Likelihood of Structural Accidents, Proc. Inst. Civ. Engineers, Part 2, 1975, 59, Dec., pp659-668.

38. Blockley, D.I., The Nature of Structural Design and Safety, Chapter 7, The Human Element, Ellis Horwood Limited, pp231-244.

39. Pugsley, A., The Prediction of Proneness to Structural Accidents, The Structural Engineer, June 1973, Vol. 51, No. 6,pp195-196.

40. Ellingwood, B., Design and Construction Error Effects on Structural Reliability, Journal of Structural Engineering, Vol. 113, No. 2, Feb. 1987, pp409-422.

41. Elms, D.G., Consistent Crudeness in Code Construction, 10th Australasian Conference on the Mechanics of Structures and Materials, Univ. of Adelaide, Australia, 1986, pp435-440.

42. Yamamoto, M. and Ang, A.H-S., Reliability Analysis of Braced Excavation, Structural Research Series, No. 497, Department of Civil Engineering, University of Illinois, Urbana, Ill, 1982.

43. Elms, D.G., Use of Fuzzy Sets in Developing Code Risk Factors, Civ. Engineering Syst., Vol. 1, June 1984, pp178-184.

44. Elms, D.G., The Principle of Consistent Crudeness, Proc. Workshop on Civil Engineering Applications of Fuzzy Sets, Purdue, Univ., 1985.

45. Wiggins, J.H., The Balanced Risk Concept: New Approach to Earthquake Building Codes, Civil Engineering - ASCE, Aug. 1972, pp55-59.

46. Starr, C., Social Benefit Versus Technological Risk, Science Am. Ass. Advancement Science, Vol. 165, Sept. 1969, pp1232-1238.

47. Elms, D.G., Reliability-Based Risk Factors, Bulletin of N.Z.N.S. for Earthquake Engineering, Vol. 13, No. 1, March 1980, pp3-13.

48. Ingles, O.G. and Saunders, J.R., The Concept of Engineering, Proc. 2nd Int. Conf. Applications of Statistics and Probability in Soil and Structural Engineering, Vol. II, Aachen., DGEG, 1975, pp119-129.

49. New Zealand Standard, Code of Practice for General Structural Design and Design Loadings for Buildings, NZS4203, 1984, Standards Association of NZ, Wellington.

50. New Zealand Standard, Code of Practice for the Design of Concrete Structures, NZS3101, Part 1, 1982, Standards Association of NZ, Wellington.

51. Paulay, T., Capacity Design of Reinforced Concrete Ductile Frames, Workshop on Earthquake-Resistant Reinforced Concrete Building Construction, Univ. of California, Berkeley, July 1977, pp1043-1075.

52. Paulay, T., Deterministic Design Procedure for Ductile Frames in Seismic Area, Reinforced Concrete Structures Subjected to Wind and Earthquake Forces, Publication SP-63, ACI, pp357-381.

53. Ogawa, S. and Elms, D.G., Probabilistic Analysis of a Reinforced Concrete Portal Frame, 10th Australasian Conference on the Mechanics of Structures and Materials, Univ. of Adelaide, Aug. 1986, pp75-80.

54. Elms, D.G., Pathological Limit State Functions, Proc. Ninth Aust. Conf. on the Mechanics of Structures and Materials, Sydney, Aust., Aug. 1984, pp306-310.

55. Turkstra, C.J., Theory of Structural Design Decisions, Solid Mechanics Study No. 2, Univ. of Waterloo, Waterloo, 1972.

56. Washa, G.W. and Wendt, K.F., Fifty Year Properties of Concrete, ACI Journal, Jan. 1975, pp20-28.

57. Law, A.M. and Kelton, W.D., Simulation, Modelling and Analysis, McGraw-Hill, New York, 1982.

58. Smith, W.D., Statistical Estimates of the Likelihood of Earthquake Shaking Throughout New Zealand, Bulletin of N.Z.N.S. for Earthquake Engineering, Vol. 9, No. 4, Dec. 1976, pp213-221.

59. Trifunac, M.D. and Brady, A.G., On the Correlation of Seismic Intensity Scales with the Peaks of Recorded Strong Ground Motion, Bulletin of the Seismological Society of America, Vol. 65, No. 1, Feb. 1975, pp139-162.

60. Murphy, J.R. and O'Brien, L.J., The Correlation of Peak Ground Acceleration Amplitude with Seismic Intensity and Other Physical Parameters, Bulletin of the Seismological Society of America, Vol. 67, No. 3, June 1977, pp877-915.

61. Clough, R.W. and Penzien, J., Dynamics of Structures, McGraw-Hill, New York, 1975.

62. Paulay, T., Personal Communication, 1987.

63. Berrill, J.B., Priestley, M.J.N. and Chapman, H.E., Design Earthquake Loading and Ductility Demand,Bulletin of the N.Z.N.S. for Earthquake Engineering, Vol. 13, No. 3, Sept. 1980, pp232-241.

64. Berrill, J.B., Priestley, M.J.N., and Peek, R., Further Comments on Seismic Design Loads for Bridges, Bulletin of the N.Z.N.S. for Earthquake Engineering, Vol. 14, No. 1, March 1981, pp3-11.

65. Iwan, W.D., Gates, N.C., Estimating Earthquake Response of Simple Hysteretic Structures, Journal of the Engineering Mechanics Division, ASCE, Vol. 105, No. EM3, June 1979, pp391-405.

66. Przemieniecki, J.S., Theory of Matrix Structural Analysis, McGraw-Hill, New York, 1968.

67. Banon, H., Biggs, J.H. and Irvine, H.M., Seismic Damage in Reinforced Concrete Frames, Journal of the Structural Division, ASCE, Vol. 107, No. ST9, Sept. 1981, pp1713-1729.

68. Banon, H. and Veneziano, D., Seismic Safety of Reinforced Concrete Members and Structures, Earthquake Engineering and Structural Dynamics, Vol. 10, 1982, pp179-193.

69. Meyer, C., Arzoumanidis, S.G. and Shinozuka, M., Earthquake Reliability of Reinforced Concrete Buildings, Proc. of the ASCE Symp. on Probabilistic Methods in Structural Eng., St Louis, Missouri, Oct. 1981, pp378-398.

70. Czarnecki, R.M. and Biggs, J.M., Earthquake Damage to Tall Buildings, Massachusetts Inst. of Tech., Structures Pub. No. 359, R73-8, Jan. 1973.

71. Akiyama, H., Earthquake-Resistant Limit-State Design for Building, University of Tokyo Press, 1985. (Translation from the Japanese Original "Kenchikubutsu no Taishin-Kyokugen Sekkei", University of Tokyo Press, 1980.)

72. Housner, G.W. and Jennings, P.C., The Capacity of Extreme Earthquake Motions to Damage Structures, Structural and Geotechnical Mechanics - A Volume Honouring N.W. Newmark, W.J. Hall, Prentice Hall, Englewood Cliffs, New Jersey, pp102-116, 1977.

73. Tanabashi, R., Studies on the Non-Linear Vibrations of Structures Subjected to Destructive Earthquakes, Proc. of 1st WCEE, 1956, pp6-1 - 6-16.

74. Housner, G.W., Limit Design of Structures to Resist Earthquakes, Proc. of 1st WCEE, 1956, pp5-1 - 5-13.

75. Bathe, K-J. and Wilson, E.L., Numerical Methods in Finite Element Analysis, Prentice-Hall, Englewood Cliffs, New Jersey, 1976.

76. Tajimi, H., Introduction to Structural Dynamics (in Japanese), Corona Publishing Co. Limited, 1965.

77. Crandall, S.H., Random Vibration (Volume 2), The M.I.T. Press, Cambridge, Massachusetts, 1963.

78. Robson, J.D., An Introduction to Random Vibration, Edinburgh at the University Press, 1963.

79. Vanmarcke, E.H., Random Fields: Analysis and Synthesis, The M.I.T. Press, Cambridge, Massachusetts.

80. Vanmarcke, E.H., Structural Response to Earthquakes, Seismic Risk and Engineering Decisions by Lomnitz, C. and Rosenblueth, E., Elsevier Scient. Pub. Co., 1976, pp287-337 (Chapter 8).

81. Rosenblueth, E., A Basis for Aseismic Design, Thesis, Univ. of Illinois, Urbana, 1951.

82. Ohsaki, Y., An Introduction of Spectral Analysis Subjected to Earthquake (in Japanese), Kajima Press, 1976.

83. Rice, S.O., Mathematical Analysis of Random Noise, Bell System Tech. J., Part I, Vol. 23, pp282-332, 1944; Part II, Vol. 24, pp46-156, 1945.

84. Umemura, H., Dynamic Seismic Design Method for Reinforced Concrete Structures (in Japanese), Gihoudo Press, 1973.

85. Carr, A.J., Ruaumoko, Computer Program Library, Department of Civil Engineering, University of Canterbury, New Zealand, 1986.

86. Muto, K., Seismic Analysis of Reinforced Concrete Buildings, World Conf. on Earthquake Eng., 1956.

87. Inoue, H. and Koyanagi, Y. et al.,Response Property of PWR Plant Embedded in Hard Rock, Part 1: Surrounding Ground Condition and Frequency Property (in Japanese), Proc. of the Annual Meeting of A.I.J., 1987.

88. Takahashi, I., Nakai, S. and Yoshida, K., Study on Earthquake Response Characteristics of Embedded Structures (in Japanese), Proc. of the Annual Meeting of A.I.J., 1987.

89. Berrill, J.B., Concepts from Seismology; 3. Source Models and Attenuation Models, Geomechanics 2 Handout, Univ. of Canterbury, New Zealand.

90. Kanamori, H. and Anderson, D.L., Theoretical Basis of Some Empirical Relations in Seismology, Bulletin of Seismological Soc. of America, Vol. 65, No. 5, Oct. 1975, pp1073-1095.

91. Shinozuka, M., Digital Simulation of Ground Accelerations, Proc. 5th WCEE, Rome, 1973.

92. Hou, S., Earthquake Simulation Models and Their Applications, M.I.T. Dep. Div. Eng. Rep. R68-17, 1968.

93. Idriss, I.H., Characteristics of Earthquake Ground Motion, Proc. ASCE Speciality Conf. on Earthquake Eng. and Soil Dynamics, 3, Pasadena, Ca., 1979, pp1151-1265.

94. Elms, D.G. and Silvester, D., Cost Effectiveness of Code Base Shear Requirements for Reinforced Concrete Frame Structures, Bulletin of N.Z.N.S. for Earthquake Eng., Vol. 11, No. 2, June 1978, pp85-93.

95. Silvester, D., Optimal Level for New Zealand Earthquake Code, Research Report 77/3, Dep. of Civil, Eng., Univ. of Canterbury, N.Z., Feb. 1977.

96. Gutenberg, B. and Richter, C.F., Earthquake Magnitude, Intensity, Energy and Acceleration, Bull. Seism. Soc. Am., Vol. 46, 1956, pp105-145.

97. Whitman, R.V., Biggs, J.M. et al., Methodology and Pilot Application, M.I.T. Dep. Civ. Eng. Res. Report, R74-15, April 1974.

98. Esteva, L. and Rosenblueth, E., Espectros de Temblores a Distancias Moderadas y Grandes, Bol. Soc. Mex. Ing. Sism., Vol. 2, No. 1, pp1-18.

99. Architectural Institute of Japan, Seismic Motions and Ground (in Japanese), 1983.

100. Hartzell, S., Analysis of the Bucharest Strong Ground Motion Record for the March 4, 1977 Romanian Earthquake, Bull. Seism. Soc. Am., Vol. 69, No. 2, April 1979, pp513-530.

101. Berrill, J.B., Personal Communication, 1987.

102. Walcott, R.I., New Zealand Earthquakes and Plate Tectonic Theory, Bull. New Zealand National Soc. for Earthquake Eng., Vol. 12, No. 3, June 1979, pp87-93.

103. Technical Institute of Shimizu Corporation, Application of SQC to Our Job (in Japanese), TQC D-Project, No. D-8203, 1982.

104. Ang. A.H-S. and Tang, W.H., Probability Concepts in Engineering Planning and Design, Vol. I, John Wiley and Sons, 1975.

105. Ingles, O.G., Safety in Civil Engineering - Its Perception and Promotion, UNICIV Report No. R-188, The University of New South Wales, Australia, July 1979.

106. Construction Industry Research and Information Association, Rationalisation of Safety and Serviceability Factors in Structural Codes, CIRIA Report 63, July 1977.

CLASSN:

A SIMPLIFIED PROCEDURE FOR ASSESSING FAILURE PROBABILITIES OF REINFORCED CONCRETE FRAME BUILDINGS UNDER EARTHQUAKE LOADING

S. OGAWA

ABSTRACT:
In order to develop a more rational structural code, a procedure is established for assessing failure probabilities of reinforced concrete frame buildings subjected to earthquake. The advanced First-Order Second-Moment method is used with the proposed performance function in terms of cumulative plastic strain energy.

Department of Civil Engineering, University of Canterbury, New Zealand, Doctor of Philosophy Thesis, 1988.